UNIVERSITEIT VAN PRETORIA
UNIVERSITY OF PRETORIA
YUNIBESITHI YA PRETORIA

Crystallographic and thermal investigation of coordination and ionic compounds of metal halides and 4-aminobenzoic acid and related molecules

By

Gerhard Ewout Overbeek

Thesis presented in partial fulfilment of the requirements for the degree of Masters of Science

at

The University of Pretoria

Department of Chemistry

Faculty of Natural and Agricultural Sciences

Supervisor: Dr Melanie Rademeyer

July 2011

Declaration

I declare that this dissertation, which I hereby submit for the degree of Master of Science at the University of Pretoria, is my own work and has not previously been submitted by me for a degree at another university. Where secondary material is used, this has been carefully acknowledged and referenced in accordance with university requirements. I am aware of university policy and implications regarding plagiarism.

Signature: ..... Date: .....

Acknowledgements

I would like to thank the following people for their invaluable support and assistance during the completion of this degree:

I would like to extend my sincere gratitude to my advisor, Dr. Melanie Rademeyer for the opportunity to conduct research under her supervision and for her valuable guidance, assistance and support throughout the course of this work.

I wish to express my appreciation to Dave Liles for his contribution to my crystallography experience.

I would like to thank Wiebke Grote, Linda Prinsloo and Dr. Jackie Nel for their significant contributions towards this research.

In addition, I would like to acknowledge the staff of the Department of Chemistry at the University of Pretoria for their support and encouragement.

I would like to express my deepest thanks to my family and closest friends for their love, spiritual and financial support.

Finally, Carolina. Your ever-present support and understanding has greatly motivated me over the past year, and for that, I am truly thankful.

List of Abbreviations

CSD	-	Cambridge Structural Database
DSC	-	Differential Scanning Calorimetry
CCD	-	Charged-Coupled-Device
NMR	-	Nuclear Magnetic Resonance
IR	-	Infrared
SCD	-	Single Crystal X-Ray Diffraction
PXRD	-	Powder X-Ray Diffraction
MOF	-	Metal Organic Frameworks
IRMOF	-	Iso-Reticular Metal Organic Framework
SBU	-	Secondary Building Units
Z	-	Number of Formula units in the unit cell
M_r	-	Molecular Mass
F_{hkl}	-	Structure Factor
α	-	Angle between b and c axis
β	-	Angle between a and c axis
γ	-	Angle between a and b axis
θ	-	Angle of incident X-ray beam

Conferences

40th South African Chemical Institute (SACI) National Convention and Federation of African Chemical Societies (FACS) meeting: A prelude event to the International Year of Chemistry:

University of the Witwatersrand, 16-21 January 2011
Poster Presentation: *4-Aminobenzoic Acid and related Ionic and Coordination Organic-Inorganic Compounds*

Publications

Rademeyer, M., Overbeek, G.E., Liles, D., Bis(4-aminobenzoic acid-κN)dichloridozinc(II). Acta Cryst. (**2010**). E66, m1634

Abstract

In organic-inorganic hybrid compounds an organic and an inorganic component are combined to form either a coordination or an ionic material. Relevant to the current study are hybrid materials composed of an organic part that contains one or more functional groups, for example amine, amide or carboxylic acid functional groups, and a metal halide inorganic portion. These functional materials display a range of interesting and desired properties, as evidenced from numerous literature reports on their properties.

In order to utilise these properties in applications, a detailed understanding of the way that the crystal structure influences the properties of a material is required. However, before this step can be achieved, it is necessary to obtain information on the structural trends of the materials, and to use the approach of crystal engineering to identify robust supramolecular synthons that may afford structural control and prediction.

The aim of the current study was to investigate the synthesis and crystal structures of hybrid materials, both ionic and coordination, composed of divalent transition metal halides and the organic components 4-aminobenzoic acid, 4-aminobenzamide and isonicotinic acid, and to identify the structural trends and crystal engineering synthons displayed by these materials. A secondary objective was the preliminary identification of properties exhibited by selected materials, in order to decide on the suitability of the materials for detailed future property investigations.

Part of the work describes the investigation of the structural characteristics of coordination materials prepared by the combination of the organic and inorganic components. Five novel crystal structures of coordination materials were determined, and these are compared with six related coordination structures reported in the literature. Two of the novel structures display interesting one-dimensional coordination polymers, one of which has never been reported previously in the literature.

The molecular and structural characteristics of both the novel and the literature coordination structures are presented in detail, and this discussion includes a description of the coordination geometry, the molecular geometry, packing trends, hydrogen bonding interactions and aromatic interactions. A comparison study across the three families of organic components in which the structural trends, hydrogen bonding interactions, aromatic interactions, ligand geometry and coordination modes are compared, is included. The results of the synthesis of the coordination materials by means of a mechanochemical method are presented, and the products afforded by this method are compared with those prepared via solution crystallisation. Finally, the results of preliminary studies of the thermal and electronic propertries of the materials are presented and interpreted.

The combination of the hybrid components as cations and anions to form ionic materials yielded nine novel structures, and these were compared with five related ionic structures reported in the literature. The novel structures include three polar structures that contain the 4-ammoniumbenzamide cation, and to our knowledge no structures containing this cation have ever been reported in the literature, hence a significant contribution to the structural knowledge of perhalometallate salts of 4-ammoniumbenzamide is made by this study. In addition two novel structures display interesting one-dimensional and two-dimensional polymeric anions, respectively, are reported.

The discussion of the novel and literature ionic structures includes a description of the molecular geometry of each of the components, the identification of packing trends, and an analysis of the hydrogen bonding and aromatic interactions occurring in the structures. The structures of all three families of organic components are compared, and trends in structural type, anion geometry, water inclusion, hydrogen bonding and functional group recognition are presented. In addition, a detailed analysis of robust crystal engineering synthons occurring in these structures is presented. Lastly the results of preliminary property investigations of the thermal and electronic properties of the materials are presented and discussed.

Table of Contents

List of Figures

List of Tables

List of Schematics

Designated Atom Colours

Oxygen

Nitrogen

Carbon

Hydrogen

Chapter 1

Introduction

Material Science

In recent years there has been a significant growth in the field of material science with focused interest in the functionality and properties of crystalline solids. The ways in which constituent molecules or ions arrange themselves in crystal structures regulate the structure which dictates the physical properties such as electrical, magnetic and catalytic properties (Antonio et al., 2001). Furthermore, there has been significant interest in framework structures with additional space that can accommodate guest molecules. These porous crystalline compounds could have numerous applications such as the capturing and storage of gases (hydrogen, carbon-dioxide) which may be used for fuel cells (Jacoby, 2008).

However, to bring about applications intended for crystalline solids, one needs to understand how to control crystal structure assembly in order to manage properties, which then ultimately results the ability to design materials with desired properties. One way of achieving this is the follow the approach described by the field of crystal engineering.

Crystal Engineering

"One of the continuing scandals in the physical sciences is that it remains in general impossible to predict the structure of even the simplest crystalline solids from a knowledge of their chemical composition"

(Maddox, 1998)

The field of crystal engineering aims to address the shortcomings in structure prediction and control through the experimental observation of crystal packing in a series of structures, and the identification of synthons and motifs based on non-covalent interactions to describe the supramolecular structure obtained.

Crystal engineering is the fundamental study of the packing of molecular or ionic constituents to produce crystalline solids that have desired physical and chemical properties (Desiraju, 1997). An understanding of the intermolecular forces acting between fragments brings attention to the collective properties generated by molecular aggregation as well as the relationship between these intermolecular forces and how they govern the assembly of distinct constituents in the molecular environment (Braga, 2003).

The term "crystal engineering" was originally introduced in an abstract by R. Pepinsky of the Pennsylvania State University in 1955 in which he suggested that cell dimensions and symmetries within his crystallized structures were "to a good extend controllable" (Braga, 2003). Gerhard Schmidt re-employed the term "crystal engineering" in 1971 when he realized that a proper theory of crystal packing was required by the systematic development of organic solid state chemistry (Desiraju, 1997).

Since then crystal engineering has become a rapidly expanding discipline where information on intermolecular interactions have been most reliably obtained through crystallography to understand the order of the atomic arrangement in the solid state. An understanding of the factors that dictate the arrangement of constituents would bring about an ability to control the ordering of fragments in structures.

The utilization of intermolecular interactions allows the assembly of molecular and ionic species into a desired structure through the engineering of a target network. These intermolecular forces include Coulombic attraction and repulsion forces between ionic constituents as well as van der Waals and hydrogen bonds between neutral or charged species (Braga, 2003). A blend of intermolecular forces allow for numerous possible combinations of constituents which now seem to become like "building blocks" or synthons that possesses their own unique set of properties which aggregate and organize according to these properties dictated by those intermolecular forces.

At first glance it would seem that chemical species in a crystal system can aggregate in an almost infinite number of ways, however recognizing and understanding the closest packing of molecular species by investigating trends one can observe how assembling is shape-controlled so as to minimize space and maximize density. By investigating the additional involvement of intermolecular interactions one can understand how a crystal network assembly is controlled. Therefore, development and purposeful design of novel materials that comprise particular physical properties can be aided by the knowledge and understanding of their chemical composition and their structural arrangement.

Supramolecular Chemistry

Supramolecular Chemistry is concerned with the domain beyond individual elements and molecular constituents and focuses on crystalline systems as a whole. It refers to assembly and spatial organization of crystal packing in terms of intermolecular interactions between molecular components (Desiraju, 1997), rather than the relationships between discrete atoms.

The production of supermolecules exists within the ability to bring together two or more molecules (supramolecular synthons) to produce a unique species (supermolecule) which possesses properties distinct from its molecular constituents (Scott, 2008). Investigation into distinctive forces that dictate the aggregation of molecules in the solid-state is a fundamental goal in the field of supramolecular chemistry as well as how to control and manipulate these forces (Loots, 2009). Crystal engineering is considered to be study of the information that develops and accumulates from such investigation which can then be implemented into the design and syntheses toward desired crystalline materials (Loots, 2009).

Therefore, one can consider that the study of supramolecular chemistry, when applied to crystalline solids, leads towards crystal engineering. In addition, communal viewpoints and objectives in supramolecular chemistry advanced the paradigm of modern crystal engineering to be the chemistry of periodical supermolecules (Braga, 2003).

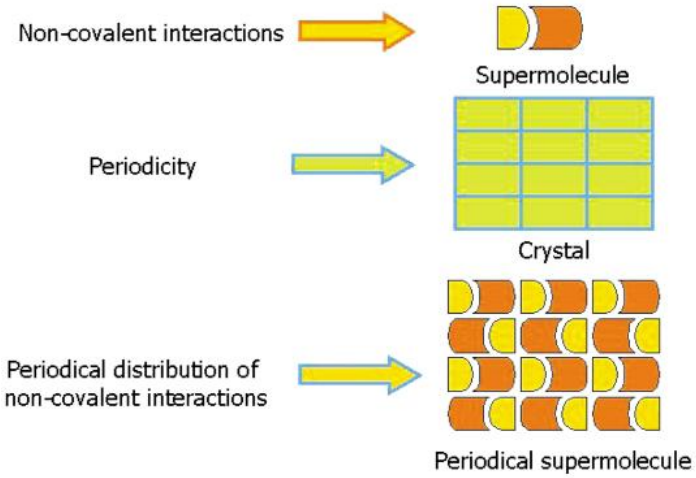

Figure 1.1: From supramolecular synthons to a periodical supermolecule. Compilation of the periodical distribution of non-covalent interaction of molecules or ionic building blocks to yield crystalline materials (Braga, 2003).

Supramolecular chemistry encompasses the study of non-covalent interactions , which include hydrogen bonds, halogen bonds, van der Waals interactions and ionic interactions. An understanding of the non-covalent bonds that dictate structure assemblage would give insight into the design of novel solids which would consist of desired functionality and properties (Desiraju, 1997).

Molecular Recognition

Molecular recognition is defined as "the energy and information involved in binding (with a purpose) and selection of substrate by a receptor (ligands with a purpose)" (Lehn, 1995)

Molecular recognition can be attributed to the interactions that manifest between molecules where non-bonding forces between molecules generate an ordered assembly of constituents into a crystal structure. Recognition between molecules essentially occurs due to the functional groups present on the molecules (Li, et al., 2007), and cause the assembly of a crystal structure to be restricted to a number of possible packing modes (Moulton et al., 2001).

Analogous to a lock and key, the mechanism of molecular recognition is restricted by specific orientations before interaction or matching between functional groups can occur. Recognition between and assembly of molecules essentially is controlled by the size, shape, orientation and extramolecular bonding capacity of discrete molecular constituents (Braga et al., 1998). The assembly of molecules in the solid state is largely dictated by the directional nature of intermolecular forces such as hydrogen bonds. Hydrogen bonds may be so strong that they have resemblance to covalent bonds while other hydrogen bonds are so weak that they are not easily distinguishable from van der Waals forces (Steiner, 2002).

The building blocks employed in this study, namely organic molecules or ions and metal halides (neutral or anionic) as discussed in a later section, have functional groups that have hydrogen bonding capabilities or modes of recognition that can theoretically combine in any order and sequence, to one another. For example, metal complex anions have hydrogen bond acceptor capabilities with no hydrogen donor capabilities (Adams et al., 2006), while the organic molecules under investigation have hydrogen-bond-donor and acceptor capabilities. The H_2O molecule may also be incorporated into the crystalline structure as crystallization is often carried out from water or water containing solvents, and thus cannot be excluded during recognition pattern investigations.

Different modes of recognition can arise as functional groups may, for example, have two potential hydrogen bond acceptors or modes where hydrogen bonding may manifest. The most prominent mode of recognition, whereby a hydrogen bond is formed between functional groups, will dictate the assembly of a molecular structure towards a minimal energy state. The initial and environmental variables may also have an underlying effect on the hydrogen bonding preferences and functional group recognition (Etter, 1990). Where a structure contains numerous types of functional groups capable of hydrogen bonding, a pattern of these bonds may be somewhat predictable if one considers that the strongest hydrogen-bond donor will most likely recognize and form hydrogen bonds with the strongest hydrogen bond acceptor (Etter, 1990). While investigations of hydrogen bonds between functional groups are considered, the metal-halide anion should not be excluded as non-covalent forces may exist between such units in a compound.

Intermolecular Interactions

At the heart of crystal engineering is intermolecular interactions. There exist interactions between molecules which determine how, and to what extent they join together and which dictate the arrangement and organization of molecular constituents within a structural framework. In addition to governing the structural design of molecular entities, intermolecular interactions are also responsible for the unique properties that solid-state materials exhibit (Knight, 2005). However, a good understanding of the nature of intermolecular interactions is essential in understanding the basic mechanisms that regulate molecular building blocks and controls solid-state assembly.

Typically, there are two categories in which chemical bonds can be classified into. Firstly, molecular interactions can be considered to be short-ranged (e.g. covalent), while intermolecular interactions are considered to be long-range interactions (Maitland, 1981). In addition to being electrostatic, these long range interactions are highly directional and occur between heteroatoms (Desiraju, 1996) which result in an overall attraction between molecules at specific distances where attractive forces dominate over repulsive electrostatic forces. There are a number of non-covalent interaction types that are important when considering interaction between molecular constituents and formation of solid-state materials, however none of these long-range forces are quite as prominent in the solid-state as the hydrogen bond (Loots, 2009).

Hydrogen Bonding

"The strong hydrogen bond is the master-key of molecular recognition, and full control of this interaction will lead to mastery of supramolecular chemistry in general"

Gautam R. Desiraju

The most recent IUPAC description of the hydrogen bond defines the hydrogen bond as an attractive interaction that occurs between a hydrogen atom from a molecule or molecular fragment X-H in which X is more electronegative than H, and an atom or group of atoms in the same or a different molecule, in which there is evidence of bond formation (Arunan et al., 2010).

Of these non-covalent bonding forces, the hydrogen bond could be considered to be the most important (Steiner, 2002) as it provides both directionality and strength (Braga et al., 1998). Furthermore, many physical properties that manifest in the crystalline form are as a result of the directing nature and stability of the hydrogen bond the solid state (Threlfall, 1995). These physical properties include optical properties, thermal stability, solubility, colour, conductivity, crystal habit and mechanical strength (Loots, 2009).

The critical role of the hydrogen bond is evident in biological processes, as it is the dominant force generating the binding processes of macromolecules to produce enzymes and proteins.

The classic definition of a hydrogen bond indicates that the hydrogen bond is electrostatic in nature, with a covalent bond between the hydrogen atom (having a partial positive charge) and an electronegative molecule or atom accompanied by an electrostatic interaction between the hydrogen atom and another electronegative species (Urbina, 2005). The donor atom (D) forms a covalent bond with the hydrogen atom (H) while the acceptor atom (A) forms an electrostatic interaction with the hydrogen atom.

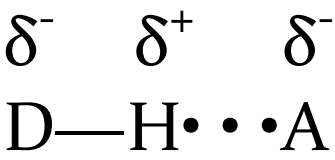

Figure 1.2: Electronegative and electropositive atoms associated with the hydrogen bond; with the hydrogen atom (H), the donor atom (D), and the acceptor atom (A).

The example above is that of a simple hydrogen bond existing between a single hydrogen bond donor and a single hydrogen bond accepter. However, hydrogen bonds may also be multi-centred, with more than one acceptor group being present. Types of hydrogen bonds exist (Figure 1.3), where a single hydrogen atom is shared between two hydrogen bond acceptors (bifurcated hydrogen bonds) or three (trifurcated) hydrogen bond acceptors (Aakeröy and Seddon, 1993).

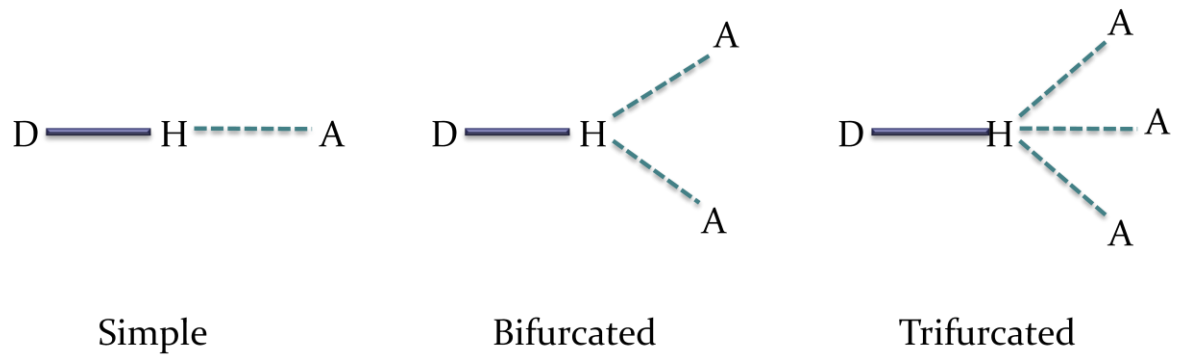

Figure 1.3: Simple and different modes of multi-centred hydrogen bonds.

The hydrogen-bond can be so strong that it resembles a covalent bond or it may be so weak that is resembles van der Waals interaction in strength (Steiner, 2002) and subsequently bond length would vary. Hydrogen bond strength is determined by electron density and electronegativity within the donating and acceptor groups. Directionality in hydrogen bonding is also important and is related to bond strength, however angles have a tendency to be linear and hence are favoured over bent geometries. The hydrogen bond D-H act like a proton donor and the acid/base properties of the donating and accepting groups gives the idea that the bond appears to be a proton transfer reaction (Steiner, 2002).

There are two important criteria when considering the formation of the hydrogen bond. Firstly the geometry involved in the hydrogen bond that encompasses distance as well as direction and secondly the energy associated with the bond (Hamilton, 1968).

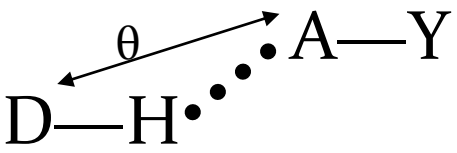

Figure 1.4: The angular dependency of the hydrogen bond, θ.

Figure 1.4 shows a simple example of a D-H···A hydrogen bond showing the angle θ, which tends towards linearity and typical values of angle θ range from 150°-180° (Desiraju, 1996). There have been a large number of studies on the hydrogen bond which produces an abundance of invaluable information regarding the geometric criteria that the hydrogen bond must adhere to.

The typical geometry of a hydrogen bond between a donor atom (D) and acceptor atom (A) (Figure 1.4) are related by the interatomic distances H···A and D···A as well as by the angle θ, shown in Figure, which indicate whether certain interactions are indeed hydrogen bonds (Desiraju, 1995).

As mentioned above, the length of the hydrogen bond is dependent on the electronegativities of the donating and accepting groups involved, which then influences bond strength. The H···A distance in an N—H···O hydrogen bond typically range between values of 1.80° to 2.00 Å, while values of 1.60 to 1.80 Å can be expected for the H···A distance in an O—H···O hydrogen bond (Desiraju, 1995, 1996).

A hydrogen bonded dimer is formed (Figure 1.5) when two identical molecules are linked together through hydrogen bonding to form a larger "molecule" that is held together by hydrogen bonds (Daintith, 2004). For example, in Figure 1.5 it is observed that the carboxylic acids functional groups form a dimer in which hydrogen bonds exist between the O of the C=O group and the H of the O-H group.

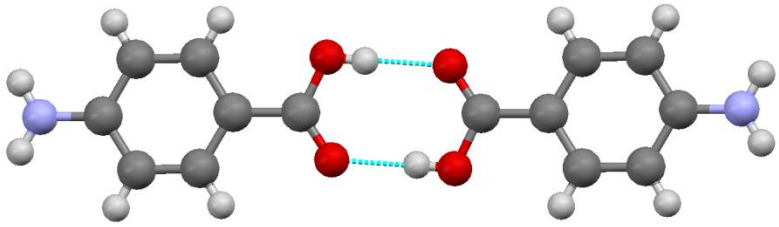

Figure 1.5: Formation of a carboxylic acid dimer between two 4-aminobenzoic acid molecules.

π-π Stacking

Another type of non-covalent interaction imperative to this study is π-π stacking, also known as aromatic interactions. Aromatic interactions are governed by electrostatic or van-der-Waals intermolecular forces which stabilizes π-π interactions between (Janiak, 2000).

Some of the attractive van-der-Waals interactions worth mentioning are the dipole-dipole (electrostatic) interactions (Figure 1.6a), which occurs between permanent and static charge distributions as well as the dipole-induced-dipole interactions (Figure 1.6b) and induced-dipole-induced-dipole interactions (Figure 1.6c).

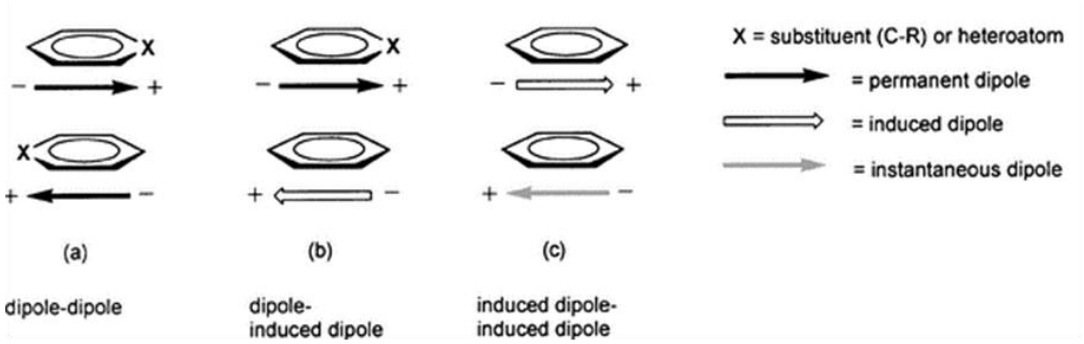

Figure 1.6: Illustration of electrostatic interactions between aromatic rings (Janiak, 2000).

The van-der-Waals interactions mentioned are inherently attractive in nature and the intensity of the attractive force rapidly dissipates with distance. Pauli repulsion occurs at short distances (Figure 1.7), when electron clouds start to overlap and the electron shells repel one another.

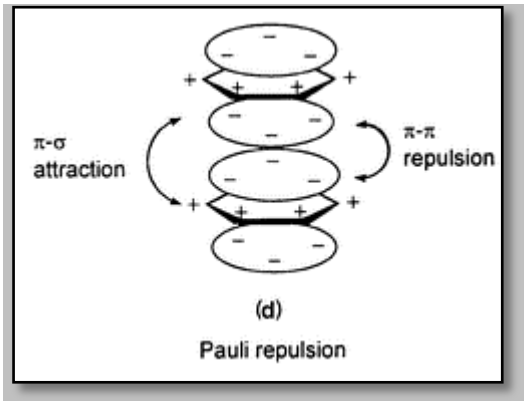

Figure 1.7: Competitive Pauli repulsion and electrostatic attraction forces (Janiak, 2000).

Several modes of stacking in which aromatic rings can organise exist. These stacking arrangements are the result of competition between electrostatic attraction and repulsion forces that result from the partially negative π-orbitals and partially positive σ-orbitals.

Figure 1.8 below illustrates the different packing geometries possible for aromatic rings. The modes of stacking include a parallel face-to-face stacked arrangement or a parallel slipped arrangement or a point-to-face (T-shaped) arrangement.

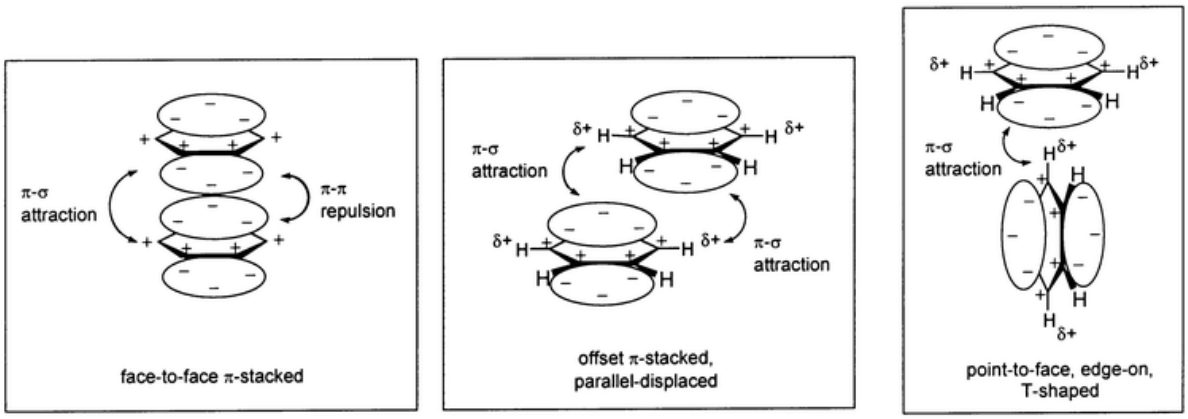

Figure 1.8: Illustration of the different modes of stacking of aromatic rings (Janiak, 2000).

Stacking is most commonly, offset or slipped parallel packing, as π-π repulsion dominates over π-σ attraction forces in face to face packing. However in offset stacked and T-shaped geometry π-σ attraction forces dominate. The angle of the ring normal and the vector moving through the ring centroids form, generally, an angle of around 20° (Janiak, 2000). The point in the centre of the aromatic ring is called the centroid, and distances between centroids (centroid-to-centroid distance) are usually around or shorter than 3.8 Å (Janiak, 2000).

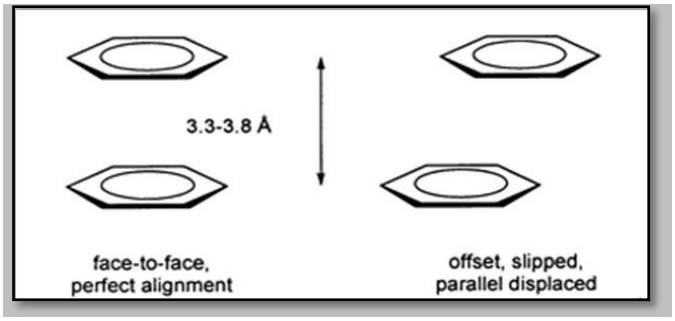

Figure 1.9: Distances and angles between aromatic centroids (Janiak, 2000).

Aromatic rings that contain nitrogen hetero atoms will typically conform towards an offset stacking of the rings as a result of the reduction of electrons in the π system which reduces the Pauli repulsion forces acting between the rings (Janiak, 2000). In the same way, when a functional group on the aromatic ring is an electrophilic substituent, π-electron density in the ring decreases and stacking is promoted. Aromatic electrophilic substituents include amines (Ar-NH_2) and acids (Ar-COOH) (Solomons and Fryhle, 2004).

Halogen bond

The unique chemical nature of the halogen bond (XB) provide additional tools in crystal engineering, and are widely exploited due to the ability of the halogen atom to act as an elecrophilic species and non-covalently bond to an acceptor atom. The halogen bond can be utilized to influence supramolecular structures as it crucially dictates architectural packing and produces unique properties (Bertani, et al., 2010). The halogen bond is of particular interest to this study as metal-halide salts (MX_2) are employed during synthesis.

The non-covalent halogen bond, however less familiar, is similar to that of the hydrogen bond as it is an intermolecular interaction that provides directionality in crystal design (Minguez, et al., 2005). The halogen bond has the interaction form D—X···Y, where X is the electrophilic halogen atom (Lewis acid) and D is any atom, group or molecule that donates the halogen and Y is the acceptor atom (Lewis Base) (Bertani, et al., 2010). Inorganic halogens (M-X) are directional nucleophiles that have well defined geometries, the angle M-X···Y being close to 180° (Politzer, et al., 2006), whereas the geometries of hydrogen bonds vary in series (linear, bifurcated) (Minguez, et al., 2005).

The four halogens capable of acting as electrophiles and that partakes in halogen bonding include iodine, bromine and chlorine and with iodine generally forming the strongest interactions (Politzer, et al., 2006).

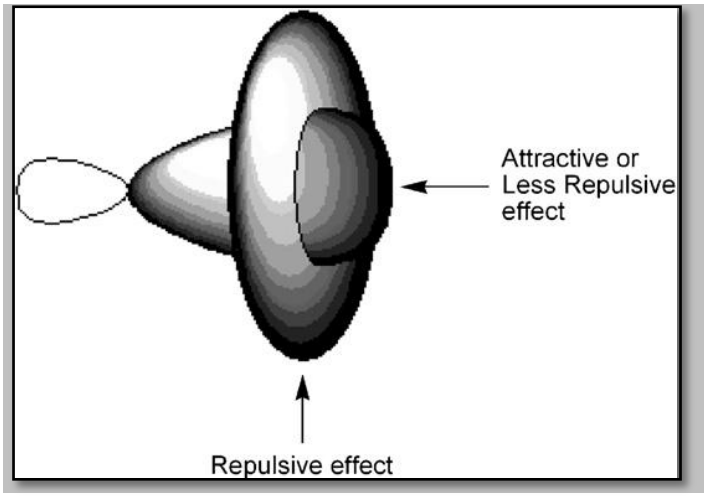

Figure 1.10: Schematic representation of the electrostatic potential in covalently bound Cl, Br and I atoms (Bertani, et al., 2010)

Studies done by Brinck et al. (1992), suggest that halogen atoms bonded to less electronegative atoms show electrostatic potential (Figure 1.10) with positive potential qualities on the side opposite the covalently bound atom consequently allowing attractive and repulsive interactions to develop. Halogen atoms bonded to a transition metal can behave as electron donor moieties in the formation of hydrogen bonds (Bertani, et al., 2010).

Polymorphism

Polymorphism is the occurrence of chemical compounds with equal compositions, but that exist in different physical forms, i.e. variations in their crystal structures (Daintith, 2004). The possibility of at least two distinct polymorphs for PABA exists in the solid crystalline phase due to different arrangements that molecules can adopt in a crystal lattice, resulting in packing polymorphism (Gracin and Rasmuson, 2004). Additionally, conformation polymorphism occurs as a result of flexible species that can adopt different conformations in the crystal lattice and generate different structures (Batten, 2009).

The materials under investigation in the current study can, theoretically, exibit polymorphism, and these different solid crystalline phases often vary in solid-state properties, for example stability, crystal shape, density and dissolution rate (Gracin and Rasmuson, 2004), which may result in different network assembly.

Given that variations in the network occur, even though the same building blocks are utilized and the molecular formulas are identical, the term “supramolecular isomerism” was created to describe this type of polymorphism (Moulton and Zaworotko, 2001). Additional influences on crystal network assembly and crystal structure comes from the variation of different solvents used which may result in structural polymorphs.

Numerous examples of suitable organic molecules exist that exhibit different polymorphic forms and are well documented. 4-Aminobenzoic (PABA) is one such organic building block which is utilized in the current study, and it shows two polymorphic forms. The first polymorphic form that PABA displays is the commercially available α-polymorph, which crystallizes in the form of long needles of a fibrous nature, the second β-polymorph crystallizes as prismatic crystals (Gracin and Rasmuson, 2004).

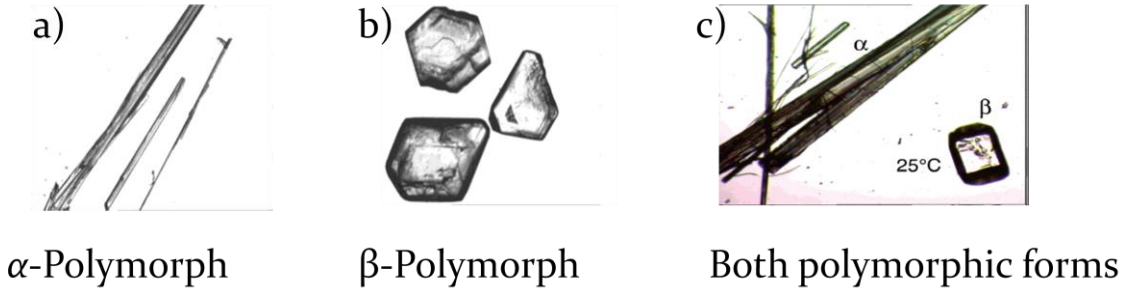

Figure 1.11: Illustration of (a) the fibrous needle crystals, (b) and the prismatic crystals of the a- and b-polymorphs of PABA. (c) Crystals of both polymorphs at 25°C (Gracin and Rasmuson, 2004).

PABA has two enantiotropic polymorphic forms and their thermal stability causes each system to be metastable at particular temperatures. The transition from one form to the other occurs at 25°C, below which the β-polymorph is stable. In addition, certain solvents may influence and favour the formation of a particular form, for instance the formation of dimers between the carboxylic acid groups of the α-polymorph will be kinetically favoured especially in less polar solvents (Gracin and Rasmuson, 2004).

Metal Organic Frameworks (MOF)

A solid crystalline structure with a highly ordered molecular arrangement, where strong bonding and linking between constituent units of metal ions and organic molecules provides a robust structure framework, which is geometrically well defined, can be considered to satisfy the term metal organic framework (MOF) (Roswell, et al., 2004). Thus, organic components act as linkers between metal atoms in a MOF. This class of solid state materials includes metal and organic coordination polymers that extend into multidimensional systems (Cheetham, 2006).

The graph below shows the increase in the number of reported metal-organic framework (MOF) structures in the Cambridge Structural Database (CSD) in recent years and the inset indicates the natural log of the number of structures over the last three decades (Long et al., 2009).

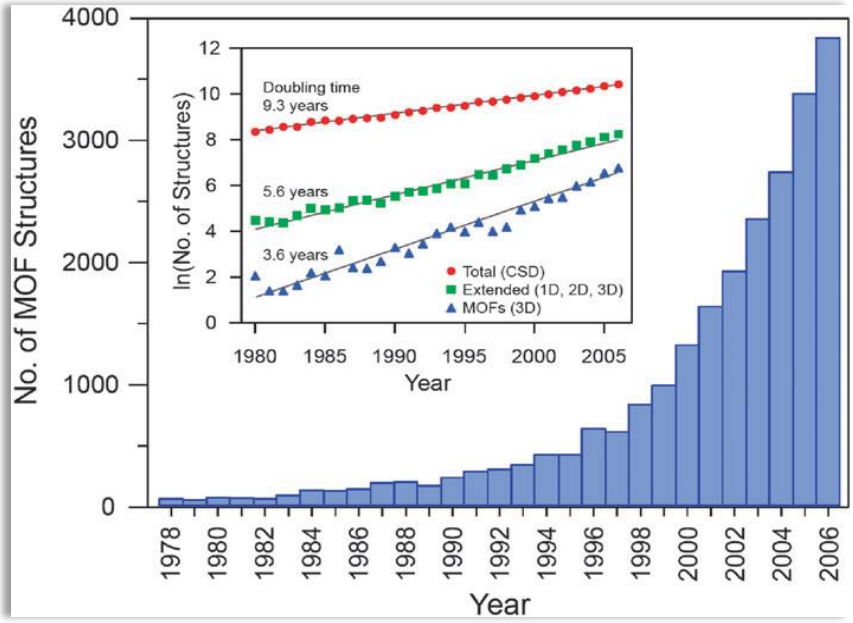

Figure 1.12: Exponential growth in reported MOF structures in the Cambridge Structural Database (Long et al., 2009).

Linking metal ions and rigid organic molecules can form multidimensional structures which provide characteristic properties, such as porosity, surface areas that dictate inclusion of guest molecules, and the optical and magnetic properties of the compound (Roswel, et al., 2004). Synthesis of crystalline solids under customized controlled conditions allows the molecular building blocks to organize in such a way that control of physical and chemical properties is possible (Roswel, et al., 2004).

In recent years there has been a considerable increase in research regarding the applications of these MOF compounds. One of the most prominent features that MOF compounds posses is the ability to accommodate larger molecules within the pore cavities. Fields in which such technologies can be exploited include petrochemistry, gas and solvent storage, catalysis and selective separation due to these solids high thermal stability and inorganic porous surfaces (Férey, 2008).

MOF compounds are generated by the combination of secondary building units (SBU) and the particular arrangement of such SBU's linked by organic ligands (linkers) produce rigid pores. Commonly, SBU's are classified as inorganic clusters that can accommodate and link with a particular number of linear organic ligands, which are generally carboxylic acid containing ligands (Batten, 2009).

The organic ligand typically coordinates to the metal via the carboxylate functional group and produces the inorganic-carboxylate cluster (secondary building unit) and furthermore, the SBU's can be linked together by organic ligands (linkers). This introduces the opportunity to employ various linkers with a range of different lengths, shapes and even aromaticity (Figure 1.13) to effect the pore size, shape and chemical nature of the MOF (Batten, 2009).

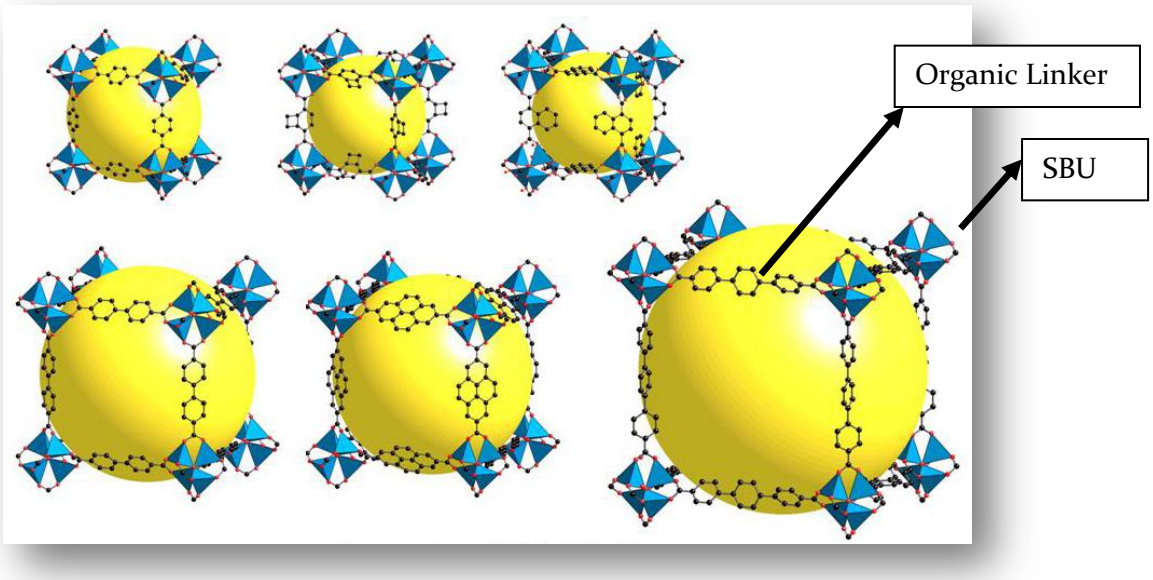

Figure 1.13: Representation of IRMOF's, (Iso-Reticular Metal-Organic Framework), showing the increase in pore volume (highlighted in yellow) with increasing size of the linear linking ligand (Eddaoudi, et al., 2002).

This provides the prospect to tune, amongst other properties, pore size, as illustrated by the work done on the design of an isoreticular series (IRMOF) (Eddaoudi, et al., 2002), using carboxylate ligands of varying length to increase the physical dimensions of the pores (Figure 1.13. This tuneable quality paves the way forward for the safe storage and transport of gases as the solid adsorbent can accommodate gases like hydrogen, methane and carbon dioxide at low gas pressures (Batten, 2009).

It should be noted that there exist a classification of these all encompassing materials based on the dimensionality of the considered frameworks.

		Dimensionality of Inorganic Constituent			
Dimensionality of Organic Constituent		**0**	**1**	**2**	**3**
	0	Molecular Complexes	Hybrid Inorganic Chains	Hybrid Inorganic Layers	3-D Inorganic Hybrids
	1	Chain Coordination Polymers	Mixed Inorganic-Organic Layers	Mixed Inorganic-Organic 3-D Framework	
	2	Layered Coordination Polymer	Mixed Inorganic-Organic 3-D Framework		
	3	3-D Coordination Polymer			

Table 1.1: Classification of hybrid materials and coordination compounds based on their dimensionality (Cheetham, 2006).

Aspects of the current study

Hybrid Compounds

Organic-inorganic hybrid materials consist of inorganic and organic moieties that self-assemble by means of covalent and intermolecular interactions to produce highly ordered nano-composite structures. The term "hybrid" arises from the combination of organic and inorganic parts. Two distinct types of hybrid compounds are relevant to the current study, namely coordination and ionic hybrid compounds. The classification is based on the mode of interaction between the constituents from which the material is prepared.

The aim of the current project is to study both ionic and coordination organic-inorganic hybrid materials, in which metal halide inorganic parts are combined with the organic parts 4-aminobenzoic acid, 4-aminobenzamide and isonicotinic acid. The introduction of halides provides bridging capabilities between metal centres and thus a convenient method of connecting transition metals and expanding the dimensionality, while organic ligands impart a greater variation in the coordination framework and/or hydrogen bonding network.

Further advantages innate to halides are their relatively short and rigid nature of bonding providing highly ordered crystalline solids (Batten, et al., 2009). The metal ion chosen can produce geometries ranging from square-planar, tetragonal, prismatic and octahedral allowing for a great extend of design.

The type of material formed through the combination of the two parts can be controlled by changing the synthetic conditions. When combined in acidic medium protonation of the organic component may occur to form a cation, and additional halogeno ligands coordinate to the metal atom to form a perhalometallate anion, $M_pX_q^{n-}$, where the metal atom is indicated by M and the X represents the halogen atom, resulting in an ionic compound. In the absence of an acid the organic component coordinates to the metal atom, while some of the halogeno ligands remain coordinated to the metal atom to form a neutral molecule.

The organic component, metal atom and halide atom will be varied systematically to test the effect of a change in one of these parameters on the structure and non-covalent interactions.

Inorganic Constituent

Extensive work on transition metals have been done in this study, due to both their ability to compliantly form coordination polymers (discussed later) and due to their range of physical and chemical properties including geometric, magnetic and electronic, which are well reported in the literature.

The transition metals that are used in the current study are the first row transition metals Zn, Cd, Hg, Cu, Mn and Co. Metals employed in the synthesis are used in their halide-salt form (chloride, bromide or iodide salt) and provide versatility as to the coordination geometry of the metal atom. The employment of transition metals for the synthesis of coordination and ionic compounds hold numerous advantages due to their kinetic lability, thermal stability, ease of use and widespread availability.

Additional properties of these metals include luminescence, conductivity and, for certain metals, a native magnetic disposition. They also demonstrate a predictive nature of their coordination geometries which makes them excellent applicants towards functional design and synthesis of these compounds (Batten, 2009). Metal atoms can direct network topology and can be used to target specific coordination geometries (Batten, 2009).

The type of perhalometallate anion (in ionic compounds) or metal halide coordination layer (in coordination compounds) that is formed depends on the specific metal and halide atoms selected, and the templating effect of the organic part. The metal coordination number may vary, and in the ionic compounds the anion may be zero dimensional and isolated, or one or two-dimensional and extend through the structure, resulting in interesting, anisotropic properties including semi-conduction. Metal halide starting materials include CuX_2, ZnX_2, CdX_2, HgX_2, CoX_2 and MnX_2, where X = Cl, Br or I.

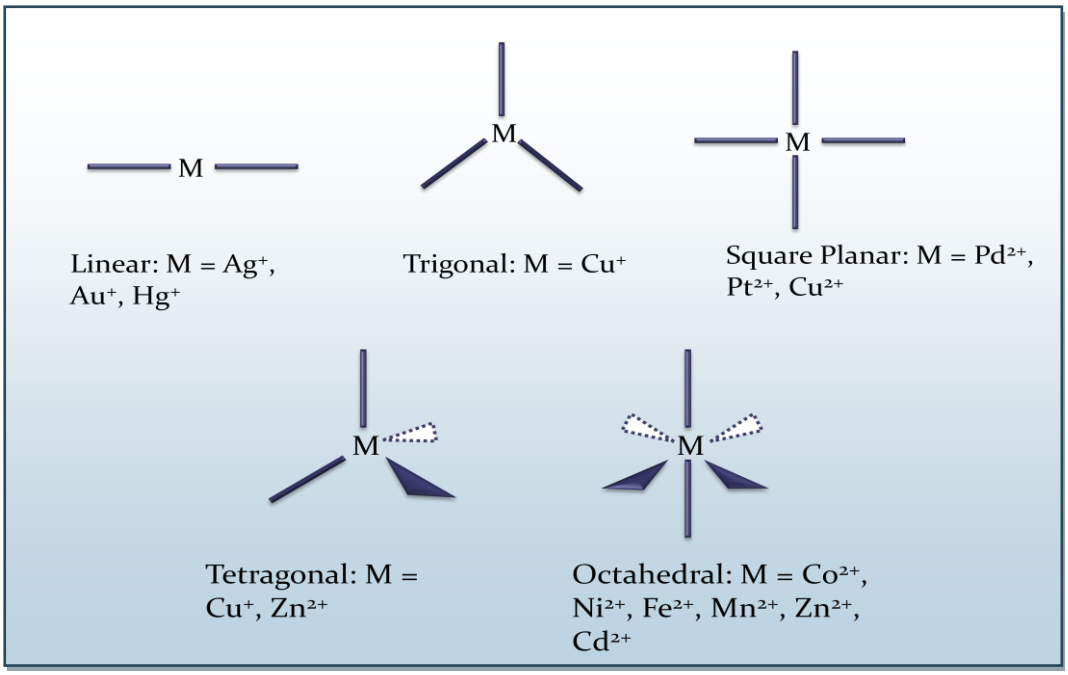

Figure 1.14: Illustration of some of the common transition metals and their general coordination geometries (Batten, 2009).

Organic Constituent

The organic component can be varied to produce and incorporate specific functionalities, for instance, number of hydrogen bonding sites, hydrophilic nature and steric hindrance (Batten, 2009). When selecting the organic cations consideration into their specific functionalities is taken, as selected candidates offer variation in bond strength, hydrogen bonding sites and steric bulk. The incorporation of organic cations that are aromatic in nature provides the basis for strong intermolecular interaction (e.g. π-π stacking) and contribute towards the layering of organic molecules and dictate the packing of the structure (Batten, 2009).

In addition to the usage of bridging ligands, the dimensionality of the structure may controlled through the employment of multifunctional organic constituents, where the bridging ligands connect metals and produce coordination chains or polymers (Batten, et al., 2009).

Materials: Organic components selected for this study

The organic components employed in the current study all contain two functional groups, which are changed in a systematic fashion according to the principles of crystal engineering, and are shown below:

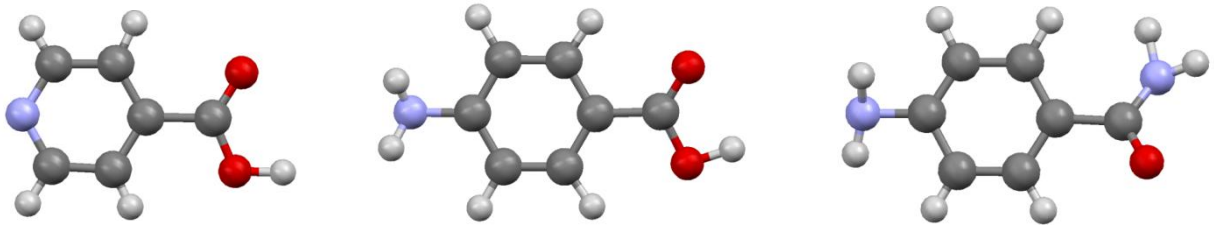

(a) **(b)** **(c)**

Figure 1.15: (a) Isonicotinic acid (b) 4-Aminobenzoic acid (c) 4-Aminobenzamide.

The organic molecules selected for this study were chosen for their rigidity, and capacity to form strong intermolecular interactions. The particular organic components employed in this study contain amide (R-$CONH_2$), carboxylic acid (R-COOH), amine (R-NH_2) and pyridine functional groups. Due to the presence of more than one functional group in each molecule, more than one potential protonation (in the case of ionic materials) or coordination (in the case of coordination materials) site is available in these organic components.

The advantage of using organic molecules with multiple functional groups is their capacity to not only interact with the inorganic anion through hydrogen bonds (in ionic materials) or coordination (in coordination materials), but to also have functional groups free to interact with the environment. Hence, the organic constituents, in addition, interact with each other through hydrogen bonds and Van der Waals interactions between available functional groups, and typically forms, with a few exceptions, layers of organic molecules.

The ability to form π-π interactions between the aromatic rings of organic molecules promotes packing of organic layers. The organic parts show a systematic change with respect to their functional groups. In the isonicotinic acid molecule a pyridine nitrogen atom as well as a carboxylic acid group is available for protonation or coordination. In going from the isonicotinic acid molecule to the 4-aminobenzoic acid molecule, the N atom is moved from inside the aromatic ring to an amine substituent on the aromatic ring while the carboxylic acid functional group is retained.

The 4-aminobenzamide molecule is related to the 4-aminobenzoic acid molecule in that is possesses an amide group where the 4-aminobenzamide molecule has a carboxylic acid group. Both the amide and carboxylic acid groups have two potential coordination sites and one hydrogen bonding acceptor site, but the amide group has increased hydrogen bonding capability through the NH_2 group compared to the OH moiety of the carboxylic acid functional group.

Carboxylic acid-containing ligands demonstrate notable practicality when it comes to integration into coordination polymers and due to the large range of such ligands available and the strong bonds that can be formed make them feasible candidates (Batten, et al., 2009). They may coordinate to a metal either in a monodentate or bidentate manner (Reynolds et al., 2003) as illustrated in Figure 1.16. The ability of the carboxylate ligand to undergo bidentate coordination makes it possible for the functional group to act as a bridging ligand connecting metals and produce inorganic chains (Batten, et al., 2009).

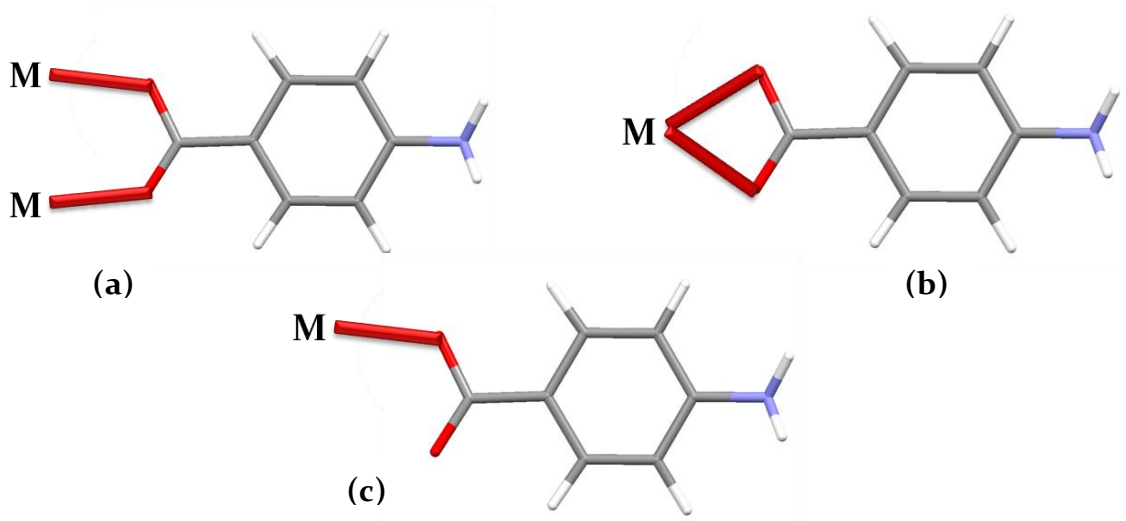

Figure 1.16: Illustration showing potential coordination possibilities of the carboxylate group (a) show coordination bridging two metal atoms and (b) shows the bidentate coordination to a single metal atom and (c) shows the monodentate coordination to a metal atom.

In addition to this mode of bonding, the group can also covalently bond to a two metal centres and bridge them producing a one-dimentional inorganic chain (Nandhini, et al., 2002). For this reason, organic constituents possesing the carboxylate group proves to be very popular in the design and synthesis of coordination polymers.

The carboxylic acid group can act as a hydrogen bonding donor or acceptor, or both. The amide functional group can theoretically coordinate to a metal atom through either the O or N atom, or can potentially form a bridge between two metal atoms as shown in Figure 1.17. Amides are weak bases and are expected to be protonated only in strongly acidic conditions.

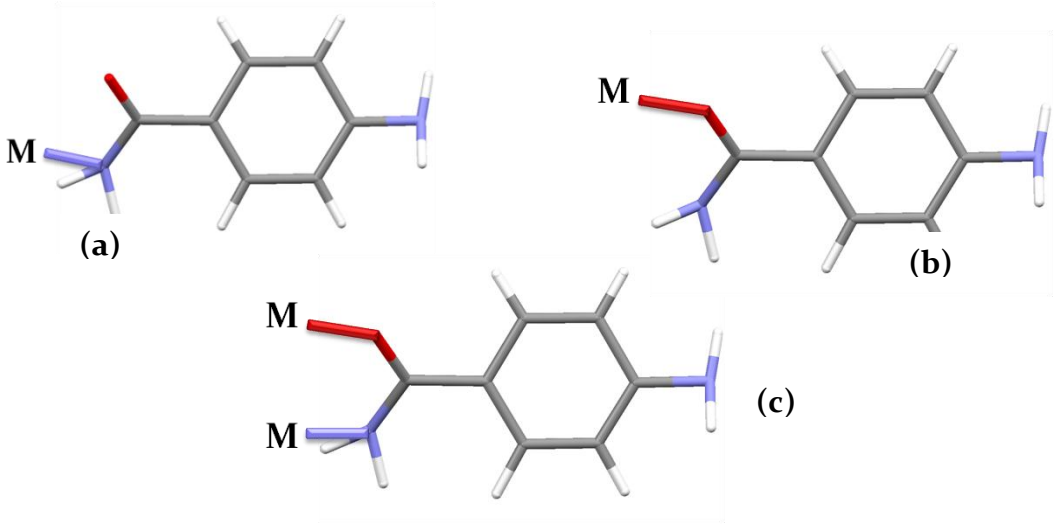

Figure 1.17: Figure showing potential coordination possibilities of the amide group; (a) shows coordination via the N atom and (b) shows coordination via the O atom to a metal atom while (c) shows coordination via both the N and O atoms to form a bridge between metal atoms.

The amine nitrogen atom as well as the pyridine nitrogen atom are basic and can be protonated (in ionic materials) to form $R\text{-}NH_3^+$ or $R\text{-}NH^+$ respectively or coordinate to a metal atom (in coordination materials), and can also participate in hydrogen bonding.

In all the cations employed the two functional groups are 180° apart at terminal ends of the molecule. In the case of the isonicotinic acid molecule, the 4-aminobenzoic acid molecule and the 4-aminobenzamide molecule the functional groups are linked by an aromatic group resulting in a fairly rigid molecules, but rotation of the functional groups relative to the aromatic group is possible.

Zwitter-Ion

Zwitter ionic compounds have both positive and negative electrical charges on the same compound that are produced as a result of an internal neutralization reaction (Daintith, 2004). The term is restricted to compounds that have the opposite charges occurring on non-adjacent atoms within the compound, and are also sometimes referred to "inner salts" or dipolar ions (McNaught and Wilkinson, 1997).

Amino acids can occur in their zwitter ionic form under neutral conditions with their functional groups producing an overall net charge of zero. These species have both a basic amine group and an acidic carboxylic acid group, that cause the transfer of a proton from the carboxyl group to the amino group in a internal neutralization reaction.

Subsequently, many amino acids demonstrate properties that are distinctive to ionic compounds, for example, high melting points and solubility in water (Daintith, 2004). In an aqueous solution a proton (H^+) transfers from the carboxyl group to the amino group and produces an ion with a negative charge and a positive charge (Figure 1.18) while the net charge of the species is zero (Clark, 2004).

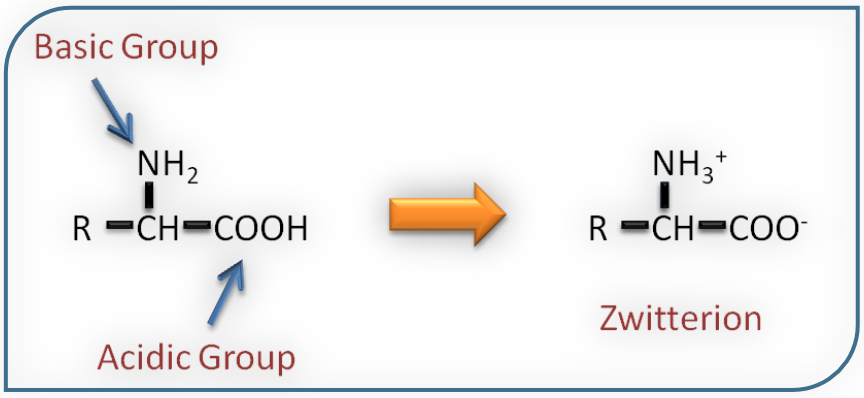

Figure 1.18: The intermolecular transfer of a proton under neutral aqueous conditions. (From Clark, 2004).

Depending on the acidity of the solution, the formation of either the cationic species (NH_3^+), by decreasing the pH, or the anionic species (COO^-), by increasing the pH, will be favoured (Figure 1.19). In an aqueous solution however, the zwitter ion interacts with the water molecules (which can act as either a base or an acid). The favoured direction of the reactions will be determined by the chemical nature of the "R" group (Clark, 2004).

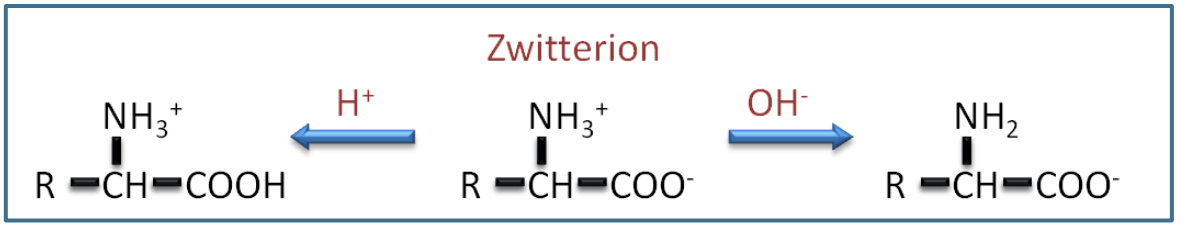

Figure 1.19: Illustration showing the effect of pH on the zwitterion. At low pH the formation of the positive ion is promoted, while high pH promotes the negative ion.

In the same manner, zwitterions occur among other types of organic molecules (zwitterionic amino-based molecules), where the amine group is attached to a carbon not adjacent to the carboxylate group (α-carbon), but separated by two or more carbons (Mercier, 2004).

Since amine and carboxylic acid containing molecules are employed in this study, it should be noted that the possibility exist that a zwitterionic form of these constituents may be produced in solution, as different synthetic conditions could, such as pH, could promote its formation.

Structure Dimensionality

The dimensionality of a hybrid compound can be determined by the metal-halide bonding mode, or the metal-organic ligand bonding scheme, whereby such bonds need to be covalent bonds exclusively.

Inorganic ligands like halogeno ligands are able to covalently bond to a metal centre and bridge to another metal due to its dative bonding capabilities. This bridging may occur in both the ionic and coordination materials to form an inorganic polymer which comprises metal atoms that coordinate to inorganic ligands to form coordination bridges, and this results in one-, two and even three dimensional structures.

The expansion and dimensionality of the inorganic polymer is dependent on both the bridging capabilities of the halide as well as the type of metal and its geometry. Different dimensionalities of the inorganic polymer can be targeted due to the coordination geometries of selected metals. The metal ion chosen can produce geometries ranging from square-planar, tetragonal, prismatic and octahedral allowing for a great extend of design.

Dimensionality in Ionic materials

In ionic materials of the type under investigation, the bridging of metal atoms by halogeno ligands can result in block-like perhalometallate anions, one-dimensional perhalometallate chain anions, two-dimensional perhalometallate sheet anions or even three-dimensional perhalometallate anions, with examples illustrated below.

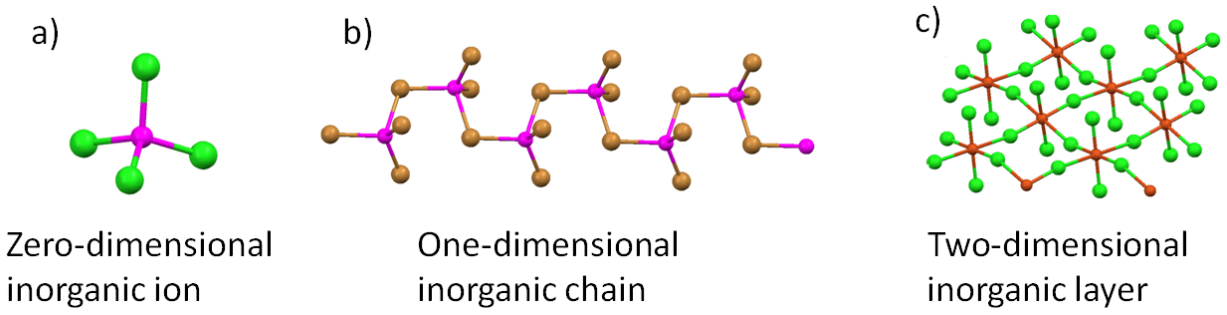

Figure 1.20: (a) Isolated 0-D inorganic ion, (b) 1-D inorganic chain, (c) 2-D inorganic layer.

In these perhalometallate anions, the halogeno ligands can act as hydrogen bond acceptor sites on the anions (Brammer et al., 2001).

Dimensionality in Coordination Materials

The bridging of metal atoms by halogeno ligands also occur in coordination materials of the type under investigation. This results in a coordination polymer, which may be one- or two dimensional. Additionally, greater variation of coordination polymer framework design can be achieved through the intentional selection of particular organic ligands (Batten, et al., 2009). Shown in Figure 1.21 is the varying dimensionality that coordination polymers can adopt when coordinated to a bridging ligand. Such variations are as a result of metals selected and the coordination geometry of the metal centres.

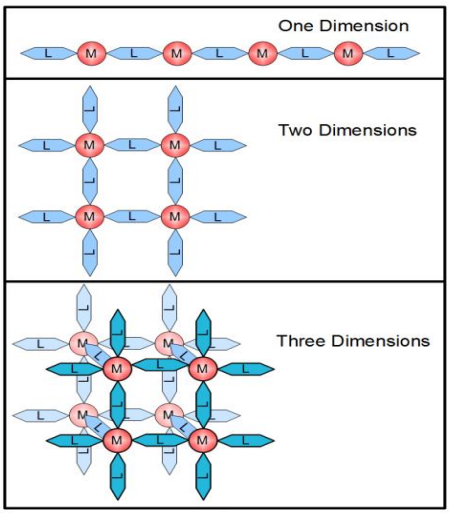

Figure 1.21: Schematic representation of the dimensionality of coordination polymers containing bridging ligands and 2, 4 and 6 coordinated metal centres (Public Domain Wiki Accessed online: http://upload.wikimedia.org/wikipedia/commons/4/4b/Dimensionalityand Coordination.png).

Relevant to the current study, further linking of one- or two-dimensional polymers through coordinated organic ligands may occur. The bridging of metal atoms through halogeno and organic ligands is another possibility which should be kept in mind. Figure 1.22 illustrates a number of bridging possibilities in coordination materials.

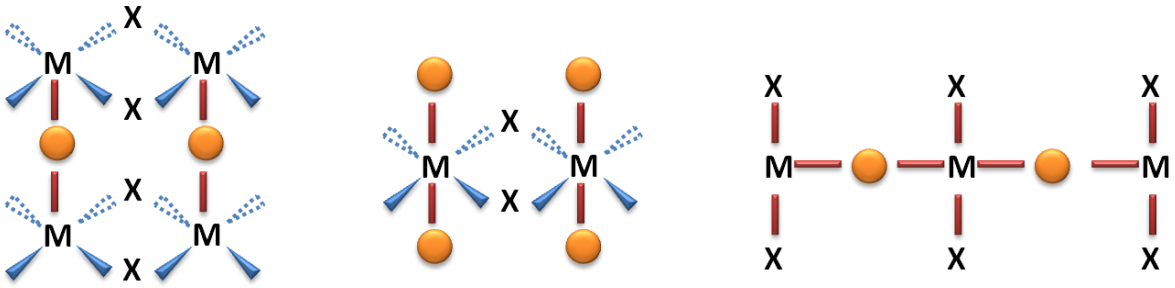

Figure 1.22: Schematic representation of the possible permutations of coordination polymers containing multi-functional ligands. The yellow circle represents the multifunctional organic ligand.

Figure 1.23, 1.24 and 1.25 below illustrate examples from the literature that demonstrate coordination and bridging via both halogeno and organic ligands.

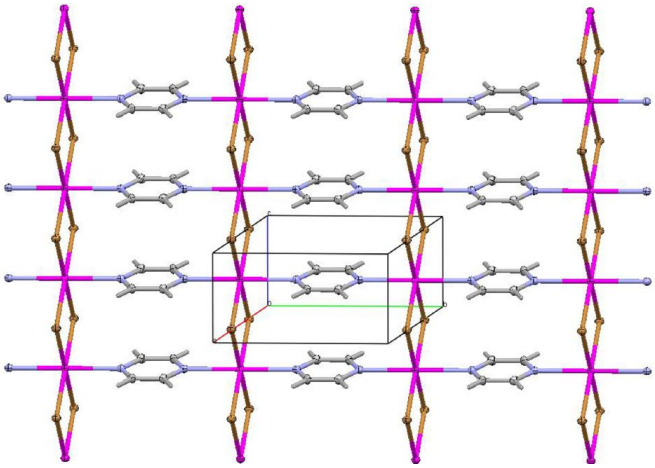

Figure 1.23: Illustration of inorganic chains linked via organic ligands that are positioned on the axial positions of the octahedra (Bell, et al., 2000).

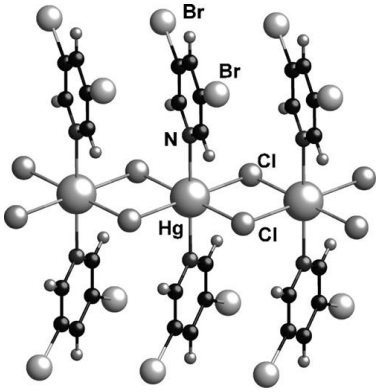

Figure 1.24: Illustration of an inorganic chain, where the organic ligands are positioned on the axial positions on the octahedra (Hu, et al., 2007).

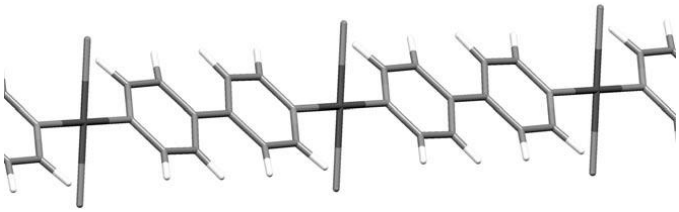

Figure 1.25: Illustration of an organic-inorganic chain whereby the metal centres are linked via multifunctional organic ligands (Englert, 2010).

Hybrid Compounds

Hybrid structures show interesting structural modes, combining organic and inorganic constituents to produce new properties and functional materials, which include membranes, catalysts and sensors, also photovoltaic cells, microelectronic and micro-optical and photonic components, as well as in therapeutic targeting, imaging with controlled release properties (Sanchez, et al., 2005). Other investigations have produced possible applications in organic optoelectronics as well as for the use in electroluminescent (EL) devices (Wang, et al., 2007).

With the introduction of the field of "organic-inorganic electronics" arose simple and inexpensive synthetic techniques towards ionic crystalline hybrids with desired electronic properties (Mitzi et al., 2001). These hybrid materials show semi-conducting properties as they form multilayered inorganic sheets alternating with insulating organic layers to generate quantum well structures. The band gap value can be controlled via the interactions of the organic unit on the inorganic sheets through steric influences and intermolecular interactions (Mitzi, 2004).

Additional application and fields being actively investigated include molecular self-assembly in nanotechnology as well as catalysis, chemical separation, optics and electronics (Dugald et al., 2005). However, to bring about applications intended for crystalline solids, one needs to understand how to control crystal structure assembly in order to manage their properties, which then ultimately results in desired properties.

Ionic Hybrid Compounds

Ionic hybrid compounds relevant to the current study (also called ionic materials) consist of inorganic perhalometallate anions and organic cationic components that are intimately arranged by a series of non-covalent and ionic interactions at the nanoscale (Sanchez, et al., 2005). This ionic structure provides an opportunity to combine the chemical and physical properties of the organic and inorganic constituents within a single crystalline structure. The ionic materials are of great interest in materials science because they often retain the desired properties of both the organic and the inorganic component, giving a material whose properties are often superior to that of their individual constituents (Mitzi, 2000). The combination of the components may also produce new unique characteristic properties (Mitzi, 2000).

These hybrid structures have exceptional stability that stem from non-covalent interactions present in the system. Included in this range of interactions are charge assisted hydrogen bonds between cationic organic species and inorganic species in the inorganic layer. Additionally, weak van der Waals forces between organic components, and stronger ionic and covalent interactions amongst the metal halide in the inorganic sheet contribute towards the stability of the structure (Mitzi, 2000).

Organic species that are commonly used in these materials contain one or more functional groups that are able to interact ionically with perhalometallate anions through strong hydrogen bonds (Mitzi, 2001). Protonation of the organic molecules produce cations that serve as hydrogen bond donors to inorganic anions and then organize into extended one, two or three dimensional structures (Brammer et al., 2001).

Properties and Applications of Ionic Hybrid Materials

Ionic hybrid compounds provide the opportunity to integrate useful characteristics of both organic and inorganic constituents into a single composite (Mitzi et al., 2001). Many technological opportuinities have developed from this prospect as exemplified in Figure 1.26 below which shows an example of one such an electronic device that is based on an organic–inorganic perovskite material.

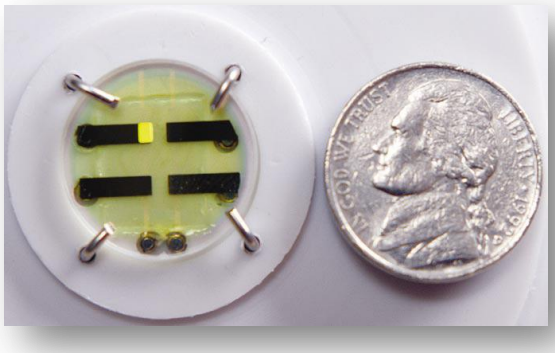

Figure 1.26: Organic-Inorganic Light Emitting Diode. A nickel coin is presented to provide scale for size comparison (Mitzi et al., 2001).

A large number of studies have been carried out towards the synthesis of hybrid organic-inorganic materials that demonstrate semi-conducting and optical properties. The search for electronic devices includes computing devices, displays, sensors and solar cells that are not only easily synthesized but are also low-cost (Mitzi, 2004).

Work done by Kouselas and colleagues (Kouselas et al., 1996) in connection with electronic band-gap calculations produced successful results which corresponded to experimental data in the study of PbI- and PbBr-containing hybrid compounds. An investigation into a family of organic-inorganic hybrid tin iodide perovskite semiconductors whereby experimental excitation energies correlated with calculated band gaps was done by Knutson and Martin (2005). Their findings demonstrated that variations in the Sn-I-Sn angles was the primary influence on the tuning of the band gap, while the bonding distance Sn-I also contributed significantly (Knutson and Martin, 2005).

A study done by Xu and Mitzi (2003), wherein a tin containing organic-inorganic hybrid compound was produced, offered a new solution processable perovskite material that showed potential semi-conductive properties. Their investigation suggested that the excitation peak associated with the band gap was influenced by the dimensionality of the Sn-I framework (Xu and Mitzi, 2003).

Analogous to the above mentioned study, two new semi-conducting hybrid compounds were produced by Xu and colleagues (2003) which showed that steric distortions notably influenced the Sn-I-Sn angles which had a significant effect on the experimental excitation peaks. In the same way, Mitzi and co-workers (2001) observed that subtle structural modifications generated by the type of organic cation employed, altered the Sn-I-Sn angle and was the primary cause of the shift in observed optical properties.

Organic-inorganic salts demonstrate optical properties which have been extensively studied and can be used for light-emitting diodes and as channels of thin-film field-effect transistors. A study done by Papavassilou and co-workers (2000) on PbI-containing hybrid compounds demonstated the optical absorpsion, photoluminescence and photoconductivity of these compounds (Papavassilou et al., 2000).

Coordination Hybrid Compounds

The field of material science, over the past few decades, has produced a crescendo of solids which are described as compounds containing metal ions linked by molecular species. This collection of newfangled compounds has been termed metal-organic frameworks, coordination polymers and hybrid organic-inorganic materials. This variety of terms however, has many similarities in definition and carries with them an overlap in description (Rowsell, et al., 2004).

Distinctions however can be made to differentiate between terms and elucidate seemingly nebulous definitions. Prominent features based on composition and the mode of interaction between constituent species making up the compound are used to obtain particular distinctions as each term carries with it a characteristic connotation relating to the compound it encompasses (Rowsell, et al., 2004).

The term coordination compound is defined as a neutral molecule or ion (the so called ligand) that bonds to a central metallic atom by coordinative covalent bonds. The Oxford Dictionary of Chemistry (Daintith, 2004) describes a coordination bond simply as a compound in which coordinate bonds are formed. Coordination compounds then, are discrete coordination complexes whereby no dimensionality of either the organic or inorganic constituent exists.

In the current study the materials formed by the coordination of the organic component to the metal halide component was studied (also called coordination materials). All of the ligands employed possess more than one possible coordination site, and may also potentially coordinate through more than one coordination site.

When coordination occurs though only one functional group, the uncoordinated functional groups typically participates in the formation of non-covalent interactions in the structure.

An interplay of effects exist in the coordination bond connecting the ligand and metal centre, and for this reason, additional tools in crystal engineering towards organic-inorganic hybrid materials are made available (Braga, et al., 1998), for example the hydrogen bonding capability of a ligand may be altered through coordination to a metal atom. Bonding mode preference however, due to nature and characteristics of the ligand, can be influenced, subsequently extending the hydrogen bonding capacity between acceptor and donor groups on the nanoscale.

Metal ions that are linked via coordination ligands which expand into an infinite array are regarded as coordination polymers. An important discriminatory factor that separates coordination polymers from hybrid compounds is that the coordination net must be defined by coordination bonds exclusively, while discrete molecular species that are linked by hydrogen bonds only is considered to be coordination complexes (Batten, et al., 2009).

Properties and Applications of Coordination Hybrid Materials

The well-ordered structures that result from the self assembly of organic molecules have limited conducting properties unless metal centres are incorporated into the structures forming hybrid coordination polymers (Welte et al., 2009). A study conducted by Amo-Ochoa and co-workers (2009) produced two Ni(II) containing one-dimensional coordination polymers (Figure 1.27) in which conducting characteristics of the materials were confirmed through electrical measurements (Figure 1.28).

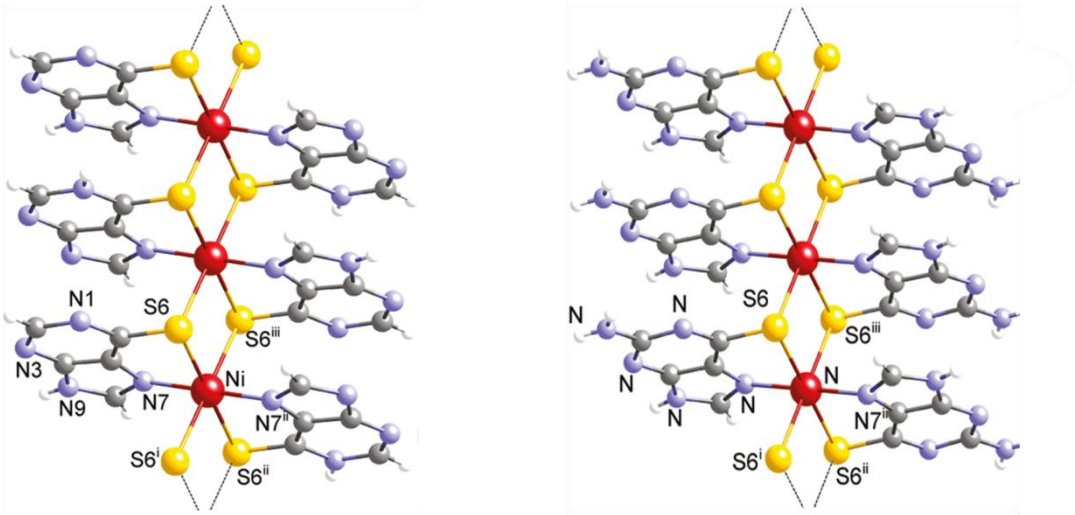

Figure 1.27: Fragment of the polymeric chain and crystal packing of the Ni(II) containing coordination polymers (Amo-Ochoa, et al., 2009).

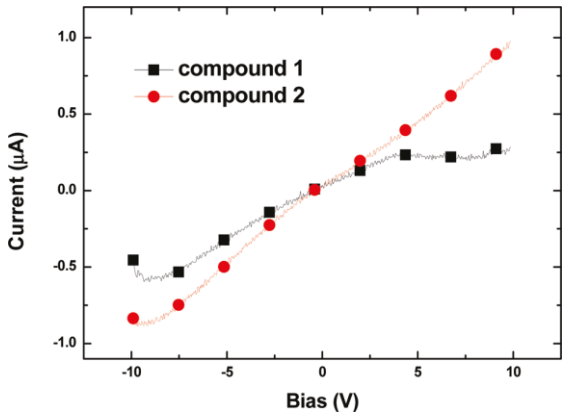

Figure 1.28: Two probe electrical measurements for both N(II) containing coordination compounds at 300 K. (Amo-Ochoa, et al., 2009).

The electrical conductivity measurements were carried out using two probe DC analysis and compounds was observed to show ohmic behaviour. The conductivity values however, are considered to be underestimated due to the crystal-electrode electrical contacts and the conductivity values are higher compared to other similar coordination polymers reported in the literature (Amo-Ochoa, et al., 2009).

Investigations done by Welte and colleagues (2009) on Pt(II) containing coordination polymers, included their electrical characterization by means of gold evaporated electrodes.

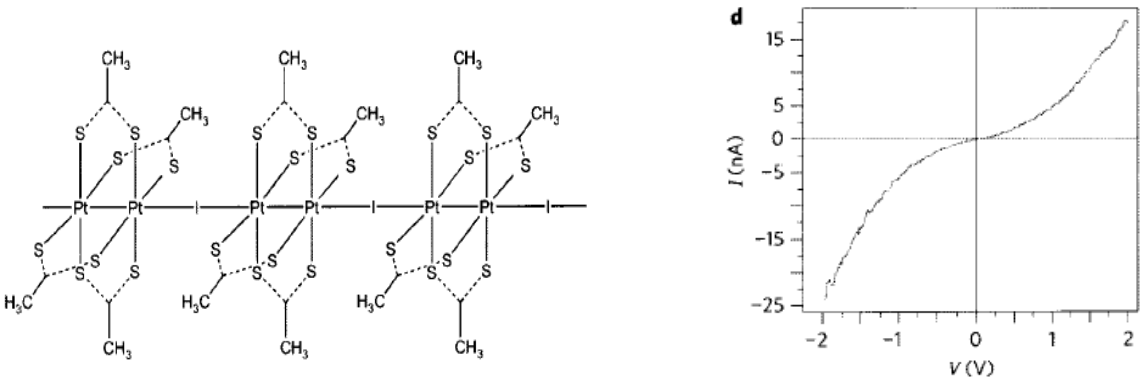

Figure 1.29: (a) Fragment of the polymeric chain of the Pt(II) containing coordination polymer and (b) the current vs. voltage characteristic taken by contacting the polymeric material via the gold electrode.

Work done by Knorr and co-workers (2010) on the luminescent properties of Cu(I) containing coordination polymers showed that the solid-state luminescence spectra of the polymers exhibited intense halide-to-metal charge-transfer emissions. Hybrid coordination compounds exhibit magnetic properties and are the centre of interest for many studies and investigations. These investigations focus on the study of molecular and bulk magnetism which are analyzed in relation to the geometries of the structures (Herringer, et al., 2010). A study done by Herringer and colleagues (2010) showed how a family of Cu(II) containing organic-inorganic polymers exhibit antiferromagnetic interactions.

Specific Aspects of this Study

Problem Identification:

At present we cannot predict the structure and properties of a material, in this case novel metal halide- and organic cation-containing ionic and coordination compounds. Related compounds have been shown to have interesting properties, and also applications, and the development of improved materials is vital for technological advancements, however this requires structural control.

The principles of crystal engineering can be used to assist in understanding fundamentally how the constituents and non-covalent interactions dictate the crystal packing in a structure. This can be achieved by systematically varying different components making up the compounds (in this case the organic part, metal and halide atoms), and noting the effect of the change on the structure, non-covalent interactions and thermal properties. In addition, global structural trends can be identified which would assist in structure prediction.

Overall, such a study would make a large contribution to the prediction and understanding of the material's structure and its properties, and finally would, in the long term, allow for the identification of potential applications of the materials.

Research Aims and Objectives

1. Synthesis of coordination compounds/polymers/networks: A systematic synthesis of a number of families of coordination polymers/networks will be performed. In these families three variables will be changed systematically, namely metal atom, halide atom and organic part. Metal halide starting materials will include CuX_2, ZnX_2, CdX_2, HgX_2, CoX_2 and MnX_2, where X = Cl, Br or I. The dimensionality of the network is expected to be dependent on the coordination ability of the organic part, the number and position of its functional groups and the identity of the metal atom.

2. Synthesis of ionic organic-inorganic hybrids: A number of families of organic-inorganic hybrids will be synthesised. The same organic and inorganic components used for the coordination system will be employed. Note that the addition of an acid, HX, allows for the formation of an ionic compound through the protonation of a functional group on the organic component.

3. Crystallization of materials: Both coordination and ionic hybrid compounds will be crystallized under different environmental conditions with the aim of obtaining good quality single crystals for X-ray diffraction studies, and to investigate the existence of polymorphism in these systems.

4. Structural characterisation using single crystal X-ray diffraction: Single crystal X-ray diffraction (SCD) studies will be performed on good quality single crystals of both systems, to obtain their single crystal structures.

5. Mechanochemical synthesis: Selected materials will be synthesised mechanochemically, and the product will be compared to that obtained from solution crystallization through the use of powder XRD.

6. Analysis of non-covalent interactions: Single crystal structures will be analysed in terms of non-covalent interactions which occur in the structures. Hydrogen bonding and aromatic interactions between functional groups will be studied, and crystals engineering synthons identified.

7. Preliminary Investigation of thermal and thermal behaviour properties of materials: Differential scanning calorimetry (DSC) will be used to investigate any solid-solid phase transitions, melting and decomposition.

8. Preliminary investigation of the electronic properties of selected materials: Examination by means of a two probe direct current (DC) electrical conductivity measurements. Observing the regression from current vs. potential applied over a crystal will provide insight into the electronic nature as well as semi-conducting behaviour of such materials.

Potential Outcomes

The relationships between the material composition and structural characteristics will be determined and structural trends identified. Crystal structures will be analysed in terms of their non-covalent interactions and robust synthons will be identified.

Chapter 2

Experimental Techniques

Synthesis

The organic and inorganic components discussed in Chapter 1 were combined under different experimental conditions to prepare the corresponding ionic and coordination materials. Table 2.1 is a matrix of all the compounds that can be obtained through different combinations of organic components, metal atoms and halogen atoms.

All of the compounds in this matrix were synthesised, but good quality single crystal structures could not be obtained for all the materials in the matrix. Combinations that were successfully analysed by single crystal X-ray diffraction (SCD) are indicated by a red star. Selected materials for which single crystal structures could not be obtained were studied using powder X-ray diffraction (PXRD), but this could only be done for the samples that were not hygroscopic, or that did not react with the aluminium sample holder used in the powder diffraction experiment.

Table 2.1: Matrix of SCD and PXRD analysis of successfully synthesized compounds.

Component	Isonicotinic Acid 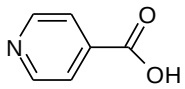		4-Aminobenzoic acid 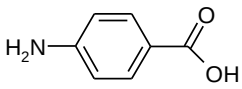		4-Aminobenzamide 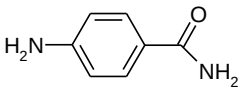	
	Ionic	Coordination	Ionic	Coordination	Ionic	Coordination
$ZnCl_2$	-	✦	★ 1:1	✦ ★ 1:1	✦ ★ 1:1	✦
$ZnBr_2$	-	✦	★ 2:1	✦	★ 1:2	✦
$CuCl_2$	✦	✦	-	✦ ★ 1:1	✦	✦
$CuBr_2$	✦	✦	-	-	✦	-
$CdCl_2$	-	★ 1:2	-	-	-	-
$CdBr_2$	-	-	★ 1:2	-	★ 1:2	-
CdI_2	-	-	-	-	-	-
$HgCl_2$	-	-	-	★ 2:1	★ 2:1	-
$HgBr_2$	★ 2:1	-	-	★ 2:1	★ 2:1	-
HgI_2	-	-	-	-	-	-
$MnCl_2$	-	✦	✦	✦	-	-
$MnBr_2$	✦	✦ ★ 2:1	✦	✦	-	✦

Keys to table:

PXRD: ✦ Stoichiometric ratios are indicated in Tables 3.11 to 3.13 and Tables 4.20 to 4.22.

SCD: ★ Stoichiometric ratio indicated (Metal halide : Organic Species)

Solution Synthesis and Crystallization

Crystals for both the ionic and the coordination compounds were obtained through slow evaporation at standard pressure and room temperature. The general method required that all starting materials be dissolved in a suitable solvent in the case of the coordination compounds, and in a diluted acid (0.5 M) in the case of the ionic compounds, however some samples were dissolved in a mixture of solvents to in order to facilitate specific solubility and in some cases promote slower or faster evaporation. Other solutions were subjected to sonication and short periods of heating if solutes remained undissolved.

A complete set of tables, indicating the stoichiometry of the ratio of organic component to inorganic component, are given in the Appendix (Table A1 to A3).

Synthesis of coordination compounds

Different stoichiometric ratios between the inorganic and organic components were employed in the synthesis of the coordination compounds to investigate the effect that this would have on the material obtained and the structural characteristics of the material. Reactants used included the organic molecules 4-aminobenzoic acid, 4-aminobenzamide, isonicotinic acid and the metal salts $ZnCl_2$, $ZnBr_2$, $CuCl_2$, $CuBr_2$, $HgCl_2$, $HgBr_2$, $CdCl_2$, and $CdBr_2$. Each organic component was combined with a single metal salt according to a specific stoichiometric ratio. Mixed compounds containing more than one organic or inorganic component were not considered.

Table A1 in the Appendix lists the stoichiometric ratio's of the metal halide to organic components used in the synthesis of the coordination compounds. In addition the masses of each of the components are given in this table.

All the coordination compounds were prepared using a solution synthesis technique, while a select number were also prepared by a mechanochemical grinding process. In the solution technique the reactants are weighed off according to their stoichiometric ratios and then dissolved in either chloroform, methanol, ethanol or distilled water in a glass beaker. Solutions are then stirred and placed on a heating plate until fully dissolved and then removed and left at room temperature, open to the atmosphere, to cool down, and allowing the solution to evaporate and crystallization to occur. The crystallization process typically takes a couple of days. Details on the mechanochemical synthesis are provided below.

Additionally, another method of synthesis is also employed, which is a slight modification of the previously mentioned technique. This method necessitates the addition of a few drops of an acid that may or may not correspond to the metal halide. This is done to promote the dissolution of starting materials and to investigate the effects that pH has on the synthesis of hybrid coordination compounds.

Synthesis of ionic compounds

The ionic compounds were also prepared via a solution technique, but in this method the salt of the organic part was first prepared via the reaction of the organic molecule with a mineral acid HX. Table A2 and A3 in the Appendix lists the stoichiometric ratios and masses of metal halides and organic salts employed.

The synthetic technique of organic-inorganic hybrid compounds followed a two-step approach. Firstly the organic material is dissolved either in, chloroform, methanol, ethanol or distilled water whereupon a stoichiometric excess of acid is added (typically a 1.5 excess), employing either hydrochloric acid (32%) or hydrobromic acid (55%). The solution is then allowed to evaporate resulting in the precipitation of the organic salt.

Finally, the salts obtained from the previous step is combined with a particular metal salt in different stoiciometric ratios, whereupon the mixture is either ground (see section on mechanochemical synthesis below) or dissolved in distilled water and subjected to stirring with a magnetic stirrer bar to make certain that a homogeneous solution is obtained and to promote dissolution of the starting materials. For the majority of crystallizations, the halogen in the acid corresponded to the halogen of the metal salt, however various combinations of halides were also considered to investigate the occurrence of a solid solution in the crystalline composite. Crystallization then commenced upon cooling in open air at room temperature. An example of the chemical reactions occurring in the two synthetic steps are given below for an amine organic component.

- $R\text{-}NH_2 + HX \Rightarrow R\text{-}NH_3^+X^-$ (Salt)
- $R\text{-}NH_3^+X^- + MX_2 \Rightarrow R\text{-}NH_3^+MX_4^{2-}$ (Hybrid compound)

Mechanochemical Synthesis

In a society where there is an ever increasing awareness of the environmental impact of hazardous substances being produced it is the responsibility of any modern scientists to investigate and utilize alternative "green chemistry" methodologies. Mechanochemistry is concerned with the exclusion of solvents from usual synthetic approaches and development of cleaner more energy efficient technologies (Garay et al., 2007).

Grinding as a method can be utilized to investigate the efficiency of solvent free synthesis of metal complexes and hybrids. The mechanical energy that is supplied during grinding causes an endothermic reaction to occur within the mixture of crystalline solids. As the solids heat up, particle size is significantly reduced, subsequently increasing the surface area and particles are allowed to collide and react in the melted phase (Trask, et al., 2005).

There exist ball mills which are programmable and needs no physical effort and are used for systematically studying of this field (Garay et al., 2007). In this study however, grinding of the combined solid components was done with an agate mortar and pestle. Characterization of mechanochemical products is not possible with single crystal X-ray diffraction, as the size of ground crystals arising from this reaction are on the order of a couple of microns in diameter, hence there samples are typically studied by powder X-ray diffraction. This technique can provide information on the degree to which reactants participated in the reaction and to confirm whether the product had formed. Schematic 2.1 illustrates the process of grinding, and in this reaction a colour change indicates that a reaction has occurred.

Schematic 2.1: Making crystals from crystals.

When employing the mechanochemical method, however, the energy introduced in the reaction can favour the formation of a different polymorph or compound compared to that formed from solution synthesis. This occurrence can be identified by comparing the calculated powder pattern of a single crystal structure prepared via solution synthesis with the experimental powder pattern of the mechanochemical product.

In the solvent drop grinding method a few drops or minimum amount of solvent is added to the mixture and then subjected to mechanical grinding. The solvent may assists in and accelerate the reaction process. In addition to acting as a catalyst, including solvents into grinding synthesis increases the degree of freedom of the molecules and allows species to distribute homogeneously and collide more frequently (Chadwick, et al., 2007).

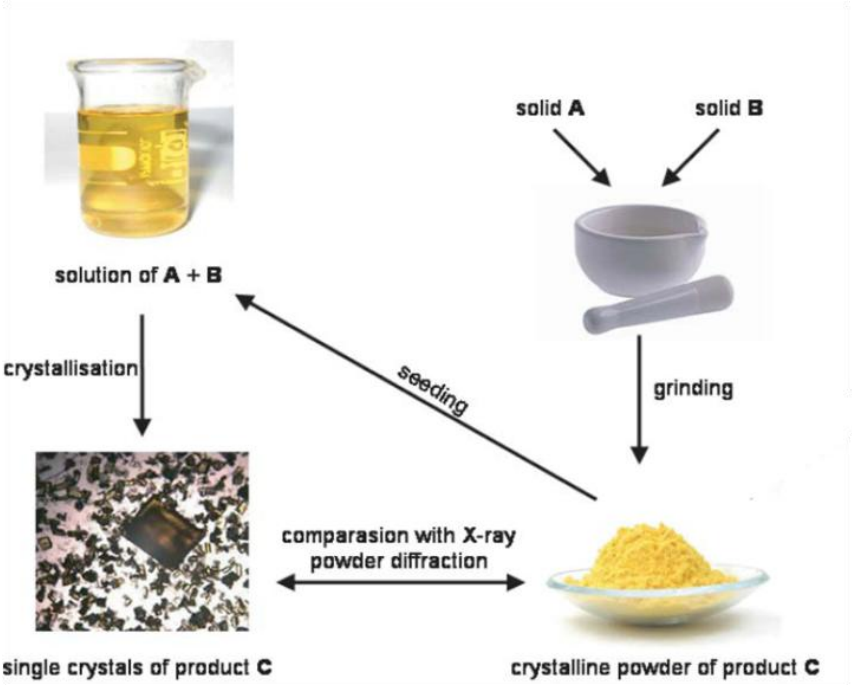

Schematic 2.2: Schematic representation of the solid–solid processes and the strategy to obtain single crystals by re-crystallisation via seeding (Braga et al., 2006).

The diagram above illustrates the techniques and strategies that can be utilized when mechanochemical methods are employed. Single crystals, of a particular polymorph, may be obtained by means of re-crystallizing the solid grinding product in a 1 pot solution, where further analysis and comparison between products can be carried out by means of PXRD.

In addition to crystallization from solution, a selected number of materials were also prepared by the mechanochemical route in order to confirm that the same materials are obtained through solution crystallization and grinding.

Structural Investigation

X-Ray Crystallography

The advancement of the instrumental techniques that are employed for structural determination has allowed for the rapid collection of crystal diffraction data. This development is exemplified by the number of structures in the Cambridge Structural Database, which recently passed the 500,000 milestone of structures submitted (Accessed online, 2011). Moreover, an exponential growth in the number of publications that report crystal structures has been observed and in addition, in many studies the packing arrangements and molecular interactions are fundamentally examined. This contributes knowledge to the field of crystal engineering.

One of the most prominent and routinely used characterization techniques used today is the determination of a material's crystal structure. By using non-destructive X-ray radiation to establish the atomic arrangement of the molecules in a three dimensions within a crystal system allows for the determination of a solid's structural configuration and provides fundamental information relating to the compound's chemical formula and the nature of the interactions (Atkins et al., 2006).

X-rays form part of the electromagnetic spectrum, and have short wavelengths in the order of 0.1-100Å. These high energy waves originate when electrons collide with a metal. As the electrons are ejected from the metal, valence electrons, from higher energy states, move down to lower levels causing the emission of X-rays (Atkins, et al., 2006). In X-ray crystallography X-ray beams are generated in tubes that consist of a heated tungsten filament that produces electrons which are then accelerated towards a metal anode that emits X-rays. The X-ray beam is directed towards a target material and interacts with the electrons in the crystal lattice of that material, causing the x-rays to scatter (Atkins, et al., 2006).

The wavelengths of X-rays, as postulated by Max von Laue, are comparable to the separation between the atoms of the crystal lattices and when passed through a crystalline structure will undergo diffraction and subsequently result in constructive and destructive interferences (Atkins, et al., 2006). Scattering of X-rays upon interactions with electrons within the atoms will follow an ordered direction since these atoms have a highly structured arrangement consequently resulting in interference maxima and minima.

Fundamentally based on Bragg's law, this technique allows for the determination of atomic positions in the unit cell of a crystal. It relates the angle between planes in the crystalline structure to the wavelength of the electromagnetic radiation.

$$\lambda = 2d_{hkl}\sin\theta$$

Bragg's law: Stipulates what conditions are required in order for diffraction to take place.

Where n: is the number of complete waves ;

θ: (Bragg's angle) is the compliment of the angle of incident ray and scattering plane

d_{hkl} : is the distance between layers of atoms or ions

λ: is wavelength of the electromagnetic radiation

(Daintith, 2004)

Only when the atoms lie in parallel planes and the space between them are constant is Bragg's law satisfied and constructive interference can occur. Therefore, under certain conditions, the radiation scattered from the electrons will be in phase. The reflections that occur once a crystal structure is subjected to a beam of X-rays can be measured and these diffracted intensities provide information on the crystal structure. The size and shape of the unit cell determines the positions of the reflections. The distribution of the electron density in the unit cell determines the intensity of the reflection.

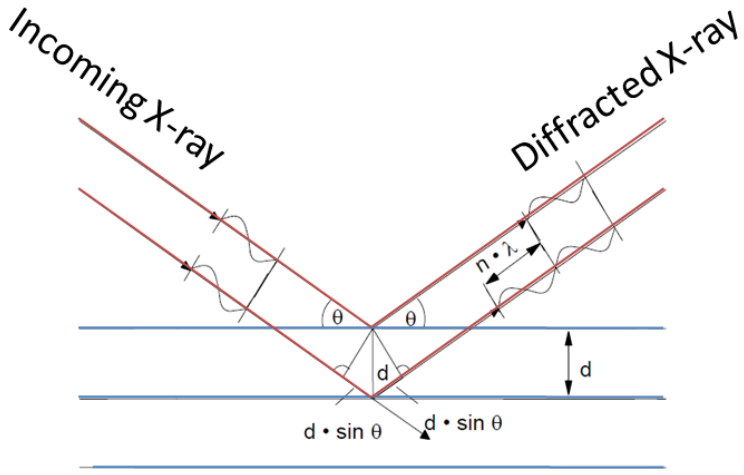

Schematic 2.3: Illustrating the Miller planes of a crystal lattice.

Since X-rays are diffracted by electrons surrounding each atom in the unit cell, better scattering will imply more electrons. The atomic scattering factor f_i is the related to the amount of scattering that is produced by a specific atom in the unit cell and is characteristic to that atom since scattering increases with atomic number, Z.

The structure factor F_{hkl} describes each *hkl* reflection and each *hkl* reflection beam is the sum of all the beams reflected from all the atoms in a particular direction.

$$F_{hkl} = |F_{hkl}| \exp(i\phi_{hkl}) = \sum_{j=1}^{N} f_j \exp 2\pi i(hx_j + ky_y + lz_j)$$

Single-Crystal Diffraction (SCD)

A single X-ray diffractometer can be used to determine the three dimensional arrangement of molecules of ions in crystalline materials. This technique allows for non-destructive analysis and is arguably the most user friendly method to characterize and determine the precise position of atoms in the unit cell. As a required condition, the crystals harvested should not have any physical limitations. Single crystals that are optically clear were selected in this study to ensure good reflection data so that when the X-ray beam passes through the crystal no structural defects could affect the scattering.

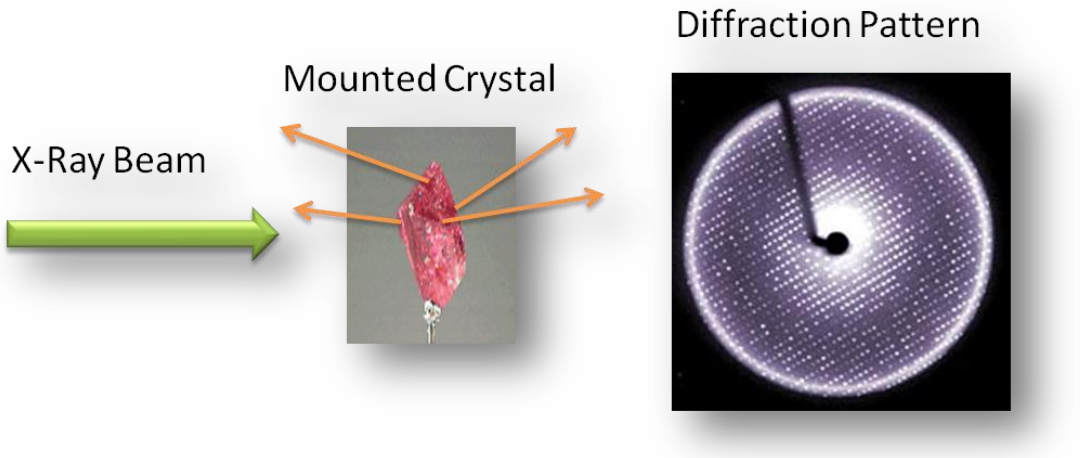

Schematic 2.4: Diagram illustrating the X-ray beam bombarding a mounted crystal. Reflection data is then captured with a CCD(Charged-Coupled-Device) area-detector (Jeffrey, 2006).

Before crystals are analyzed they need to be of one phase and be a specific size (0.1-0.5mm in each dimension) to be suitable for SCD. Crystals are then mounted on a glass fibre employing glue, and placed on the head of the goniometer and subjected to an intense beam of X-rays while diffracted X-rays are measured by means of a CCD area-detector

In this study single crystal X-ray diffraction analysis was done on a Bruker (Siemens) P4 CCD diffractometer using graphite monochromated Mo-Kα radiation at 20°C at the University of Pretoria. Data was collected using SMART software (Bruker, 2001), while cell refinement and data reduction was done using SAINT software (Bruker, 2001)

Structures of all novel compounds were solved by using SHELXS-97 (Sheldrick, 2008) and refined with SHELXL-97 (Sheldrick, 2008), as part of the program WinGX, version 1.80.03 (Farrugia, 1999). Analysis of the structural features was done using the Mercury software package (Macrae, at al., 2008) whereby additional information could be obtained of the non-covalent bonds such as the hydrogen-bonds and short contacts that allowed for structural expansion and packing investigation.

Powder X-Ray Diffraction (PXRD)

This analytical technique allows for swift phase identification of crystalline solids, provided that the powder diffraction pattern can be compared to a relevant pattern. Powder diffraction patterns can yield useful on information unit cell dimensions of a structure through indexing of the diffraction pattern (Dutrow, 2009). Each powder diffraction pattern pattern is characteristic of a compound. Additional applications include the determination of the purity of the sample and identification of specific polymorphs within the sample. The analytical method of powder XRD provides qualitative means of sample analysis whereby a set of scattered X-ray spots is condensed into a one dimensional representation of intensity versus the angle θ.

Powder samples obtained from the grinding process in this study were analyzed using this technique. Data was collected on a PANalytical X'Pert Pro powder diffractometer with an X'Celerator detector and variable divergence-and receiving slits with Fe filtered Co-Kα radiation. Phases were identified using X'Pert Highscore plus software. Further investigation of analyzed data was then done on the programs PowderCell, (Version2.4) (Kraus and Nolze, 2000) and Fityk, (Wojdyr, 2010).

Powder XRD analysis of the samples provides a way of determining whether the synthesis of the compounds using mechanosynthetic methods was successful. By comparison to the reactants' powder patterns, one can superimpose the patterns and see whether overlap is present and also see whether a novel compound (product) is present by comparing the peak list of the respective reactants. The material that is sampled for PXRD analysis is different to that used for SCD since a single crystal is not required for analyses, therefore a bulk amount of the sample in powder form can be used. Hence a representative sample is analysed, giving the complete picture of the sample.

Another useful application of the powder patterns obtained is to compare the calculated powder pattern from a known single crystal structure to that of a novel compound and observe whether there is an overlap in the peaks. This would indicate whether the two compounds are isostructural as would be indicated by overlap of their unique peaks or "fingerprints". Alternative polymorphs can also manifest as different methodologies present different variables such as kinetic energy being supplied during grinding, and this would be evident from powder XRD patterns.

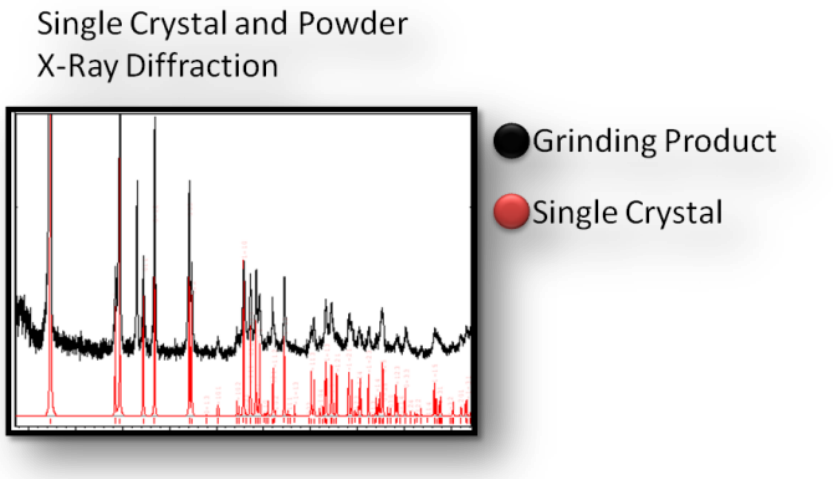

Figure 2.1: The XRD pattern of a powder product and calculated powder pattern from a single crystal structure which can be used to compare grinding products with single crystals obtained from solution and also to investigate possible polymorphs.

Cambridge Structural Database (CSD)

The investigation of individual structures has relatively limited significance unless comparable studies of similar structures can be done. A comprehensive survey of a large number of structures produces invaluable findings that provide assistance when it comes to the study of novel compounds. The Cambridge Structural Database has a collection of over 500,000 compounds (Accessed online, 2011), and in addition can provide essential statistical data on the structures of the compounds. Analysis of the qualitative geometric attributes (bonding schemes, distances and angles) of CSD structures allow for the comprehensive evaluation of structural features that novel compounds may contain.

Extensive searches were performed to find all the structures appearing in the CSD that are relevant and related to the current study. This added to the number of structures available for comparison, and also assisted in the identification of structural trends. The February (2011) update of the CSD (version 5.32) was employed for this step.

Property Investigations

In addition to the study of the structural characteristics of the materials, preliminary property investigations were performed. This was done to roughly gauge the properties of these types of materials, including their thermal stability and electronic properties. Only selected materials were tested in this manner, with the aim of identifying the types of properties displayed by the materials, and to decide whether future investigations into this will be worthwhile.

Analytical techniques are imperative to the property determination and characterization of organic-inorganic hybrid compounds. Techniques such as differential scanning calorimetry (DSC), photoluminescense measurements and two probe DC electrical measurements were employed to highlight the general properties of selected materials, with an eye on the identification of properties to study in future detailed structure-property relationships investigations.

Thermal Analysis

The objective of caloric analysis is to measure the heat exchange in a system to study the changes occurring in a materials with an increase or decrease in temperature. Heat exchange is connected with a heat flow that causes differences in the local temperature in the system (Höhne et al., 1996). As a material undergoes chemical reaction, or a phase transition, physical transitions processes occur that are intimately linked with the generation or consumption of heat, which are investigated by calorimetric methods (Höhne et al., 1996). Caloric measurements have been utilized for more than two centuries to investigate the thermodynamic properties of materials (Höhne et al., 1996).

Differential Scanning Calorimetry

Differential Scanning Calorimetry (DSC) measurements involve the measurement of the energy transferred as heat to or from a sample as the temperature is systematically increased, allowing the enthalpy changes due to thermal decomposition or phase transition processes to be studied. The technique is also used for chemical analysis and for the investigation of the products that form as a result heating a substance (Daintith, 2004).

The term “differential” refers to the fact that, during analysis, any physical and chemical changes that the sample undergoes is compared to a reference material that remains chemically and physically inert. In addition, the term “scanning” is used here to indicate that temperature of the sample and reference material is systematically increased over a specific range (Atkins and de Paula, 2006). In DSC, both the sample and reference material are heated simultaneously and are maintained at equal temperatures throughout the scan. As separate power supplies are used to electrically heat the sample and reference material, the difference in the amount of power supplied can be recorded against the furnace temperature (Atkins et al., 2006).

Thermally induced changes in the sample are indicated as deviations from the DSC baseline depending on whether there is an increase or decrease in the power supplied to the sample. Deviations from the baseline can be positive or negative which indicate endotherms or exotherms respectively. When an endothermic reaction or transition has occurred it is indicated by a positive deviation from the baseline while an exothermic reaction is indicated by a negative deviation (Atkins et al., 2006). Endothermic events are indicative of melting, sublimation, solid-solid transition, desolvation or chemical reactions. Exothermic events are indicative of crystallization, solid-solid transitions, decomposition or chemical reactions (Rawlinson, 2006). DSC analysis was carried out using a Mettler Toledo DSC1 STAR^e System under a N_2 gas purge and by utilizing STAR^e Software (version 9.20).

However, even though the thermal analysis of the compounds was a major aim of this study, this step had to be terminated prematurely due to the nature of the samples investigated. Corrosive acid vapours are released from the ionic materials on heating, and even some of the coordination materials reacted with the aluminium sample holders employed. Hence, a detailed understanding of the thermal properties and decomposition of the materials could not be obtained. Preliminary DSC results are presented in Chapters 3 and 4 for the coordination and ionic materials respectively.

Electronic Conductance

When considering a single atom, electrons occur in discrete energy levels, however when a large number of atomic orbital exist in a solid, such as a crystal, an overlap of their orbitals give rise to a continuous band of energy levels that are separated by energy gaps (Atkins, et al., 2006). For example, in a crystal structure, electrons are held together in a lattice and are influenced by a number of surrounding nuclei forming bands which represents a large number of allowed quantum states and it is the outermost electrons that form the valence band which has the highest energy (Daintith, 2004).

The electronic properties that are found in crystalline compounds originate from the band structure. In order for electrons to move through the solid, they have to change from a lower quantum state (valence band) to a higher allowed quantum state (unoccupied conduction band) in order for conduction to occur (Daintith, 2004). Between the valence band and the conduction band lies the band gap which electrons must overcome, and once the electrons are elevated to the conduction band they have a high degree of freedom.

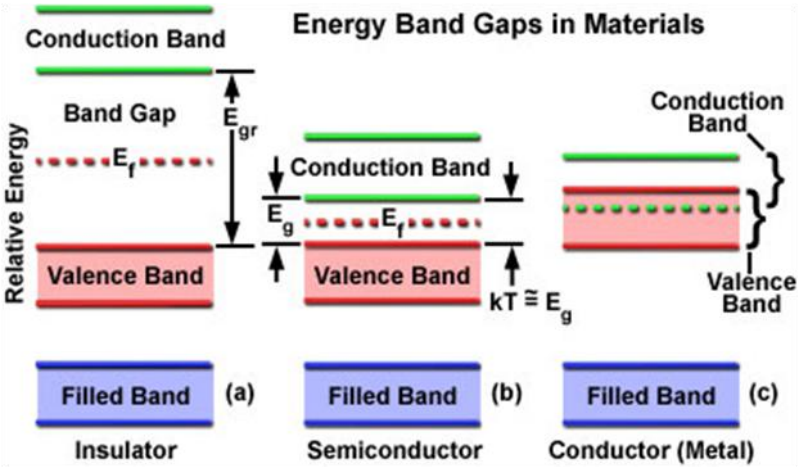

Schematic 2.5: Energy band gaps in (a) insulators, (b) semiconductors and (c) conductors, ("Diode Lasers", Accessed Online, 2011: http://micro.magnet.fsu.edu/primer/java/lasers/diodelasers/index.html).

Schematic 2.5 illustrates the different relative sizes of the band gap for an insulator, a semi-conductor and a metallic conductor ("Diode Lasers", Accessed Online, 2011). In the case of conducting materials (c) the valence and conductor band overlap, providing vacant states, while in an insulating material (a) the valence and conductor band are separated by a large band gap of forbidden states and the electrons subsequently do not have enough energy to be excited to the conduction band. A semiconductor (b) has its valence and conduction band separated by a narrow band gap and allows electrons to move into the empty orbitals of the conduction band upon enough energy contribution via thermal agitation.

The electronic conducting property of every material is intimately related to and can be expressed by its band gap and the energy of the band gap. The band gap energy can be expressed by the variable E(g) in eV in addition the thermal excitation energy is expressed by kT and the HOMO energy (Fermi energy) as E(f) ("Diode Lasers", Accessed Online, 2011). In addition, the structure of the material determines the way in which orbitals overlap to form the band structure, and as a result have a large influence on the electronic properties of a material.

The electronic conductivity of selected materials prepared in this study was investigated. In this experiment a single crystal of good quality was glued to a glass microscope slide. Silver paste was applied over opposite faces of the crystals, and allowed to dry overnight. A two-probe DC instrument, in the absence of light, was used to electrically characterize the crystals. Electrodes were placed on the silver contacts, on both sides of the crystal. A potential was then applied over the crystal, which increased over time, and the current was measured at each potential. A plot of potential current (I) versus potential difference (V) is obtained in this experiment. The characteristics of the current-potential plot give an indication of the electronic behaviour of the crystal. Figure 2.2a below illustrates the current-voltage curve for an ohmic material, where the curve is linear, and the slope gives the resistance of the conductor and Figure 2.2b shows the non-linear current-voltage curve that is indicative of a semi-conducting material (Serway, 1990). Hence, the category of electronic behaviour of the material can be deduced from this experiment.

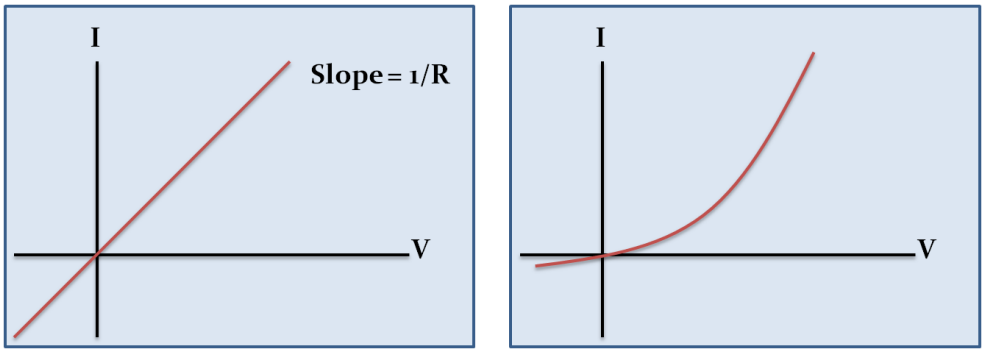

Figure 2.2: (a) The current-voltage curve for an ohmic material and (b) the current-voltage curve for a semi-conducting diode (Serway, 1990).

However, certain limitations were encountered which may cause the measured current values to be underestimated. The silver paste employed for the investigation is not the most favourable material, as silver electrodes have an ability to form complexes with halides, which as a result, can restrict the potential range accessible to these electrodes and inhibit measurements over the crystal-electrode contacts (Haddad and Jackson, 1990).

Photoluminescence

In recent years intense interest has developed regarding the luminescent properties of coordination polymers and metal-organic frameworks. The phenomenon of luminescence is brought on by the re-emission of radiation that arises from the electronic transition caused by a previous photoexcitation process, from an exited state to the ground state (Atkins et al., 2006). This process is divided into two categories, firstly fluorescence which is the rapid radiative decay with some energy dissipation and secondly, phosphorescence which is luminescence that continues after photoexcitation (Batten et al., 2009). The particular mechanism involved with fluorescence is that of radiative decay from an excited state that has the same multiplicity as the ground state and that such transition is spin-allowed. Phosphorescence however, is radiative decay from a state that has a different multiplicity from the ground state and the transition is spin forbidden (Atkins et al., 2006).

Organic-inorganic coordination polymers may accommodate organic ligands, otherwise known as “antenna ligands” that can absorb radiation and transfer the excitation energy to the metal ion, thus sensitizing the metal emission. This photoexcitation process is otherwise known as ligand-to-metal charge transfer (LMCT) and additionally the reverse process is also possible whereby the charge is transferred to the ligand (MLCT) (Batten et al., 2009). Numerous transition metal containing coordination polymers have been widely investigated as they offer more thermal stability compared to the ligand on its own. Commonly, photo-physical properties are exhibited by d-metals at room temperatures and they also have the potential to couple emission properties with ligands. Examples of such metal ions include Zn(II), Cd(II), Cu(I) and Ag(I) (Batten et al., 2009).

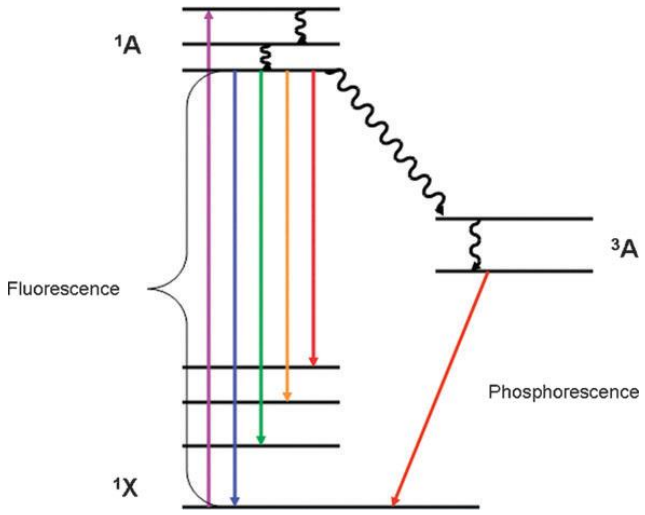

Schematic 2.6: Jablonski diagram illustrating the electronic states of an organic linker involved in luminescence phenomena (Allendorf, et al., 2009).

Excitation of the organic molecule (Schematic 2.6) occurs through the singlet–singlet transition and the subsequent emission then commonly occurs from the lowest singlet excited state (^{1}A). Alternatively, phosphorescence occurs due to the non-radiative transfer of energy to lower lying states via linker-based triplet state (^{3}A) (Allendorf, et al., 2009).

The organic molecule plays an important role in the luminescence of MOF structures as it can function as an antenna ligand that partakes in energy transfer towards the metal (Allendorf, et al., 2009). Many inorganic polymers that contain carboxylate ligands have display strong fluorescence emission resulting from ligand-to-metal charge transfer (LMCT) (Batten et al., 2009). The combination of organic ligands and transition-metal ions to produce coordination polymers is an effective technique to produce new materials that show potential applications as light-emitting diodes (LED's) (Janaik, 2003)

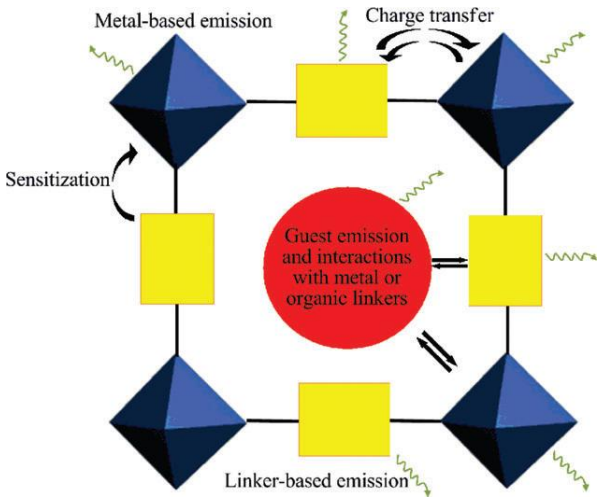

Figure 2.3: Illustration of possible emissions of a porous MOF structure (Allendorf, et al., 2009).

MOF compounds also show luminescence behaviour, exemplified by the comprehensive reports in the literature and the amount of research that has been carried out towards luminescent MOF application. Figure 2.3 illustrates the general modes whereby luminescence can be generated in MOF's and include direct emission from the organic linker or due to a charge transfer from such linkers to the metal-clusters as well as from transition-metal ions with unpaired electrons (Allendorf, et al., 2009)

The pores featured in MOF structures allow for the inclusion of luminescent guest molecules and in addition, π-π interaction between certain organic linkers and guest molecules can generate excited complexes (Allendorf, et al., 2009). The photophysical properties of organic luminescent groups have been widely studied and consequently, organic linkers have been employed in MOF structures and are typically conjugated organic compounds. These linkers are able to absorb radiation in the UV and visible regions and emission follows directly from the linker or a charge can be transferred to a coordinated metal (Allendorf, et al., 2009).

In a luminescent material electrons in their excited state undergo radiative recombination and the band gap of an inorganic layer is closely associated with the excitation state (Xu, 2003). The difference between excitation and emission maxima of an absorbing species is known as the Stokes shift and represents the electronic overlap of the ground and excited state (Allendorf, et al., 2009).

Materials that demonstrate luminescence is characteristic to compounds that show semi-conducting behavior. When a photon has an energy that is greater than that of the energy associated with the band gap of the material, it is possible for the photon to be absorbed and an electron will then be able to cross the forbidden energy gap and be excited from the valence band up to the conduction band (photoexcitation)(Heiman, 2004).

The electron has a surplus of energy, which it loses as it falls back to the valence band, which is converted to a luminescent photon that is emitted from the material (photoluminescence). The energy that is associated with the emmited photon is a direct measure of the band gap energy, E_g, of the material (Heiman, 2004).

In this study the photoluminescence spectrum of one material was measured at room temperature, employing a Jobin Yvon Horiba TX64000 Raman Spectrometer, in order to obtain the broad category of electronic behaviour of the material.

Chapter 3

Coordination Compounds

Structures relevant and related to those under investigation in the current study can easily be located and accessed by employing the search facilities of the CSD and exploring recent literature. This process not only aids in increasing the number of structures available for comparison, but also prevents duplication of structures already reported.

The structural investigation of relevant compounds in the CSD allows for the most important structural aspects to be determined and other possible combinations of organic and inorganic aggregation may be studied. In addition, packing trends in crystal structures and crystal engineering synthons and motifs can be identified. A thorough literature survey provides the opportunity to study the single crystal structures of a family of materials which give an indication of structural trends and motifs, and the role of non-covalent interactions like hydrogen bonding in the structure.

Extensive studies on hybrid coordination compounds and polymers have been reported in the literature, with a vast number of papers focusing on compounds and polymers containing metals such as Cd, Cu, Zn, Hg as well as Mn.

One of the most interesting aspects of coordination compounds formed between metal halides and organic ligands is the wide spectrum of bridging modes occurring between the metal atoms through halogeno bridging ligands, and this is a central theme in many literature reports. The dynamics and driving force involved with the formation of halide-bridged polymers of divalent metals result in different permutations produced by the connectivity of building units.

Depending on the type of bridging, zero, one or two dimensional metal halogeno sections may be present. Additional linking of the inorganic parts through organic linkers can further increase the dimensionality of the structure. Divalent transition metals that produce halide-bridged polymers have numerous modes in which they organize and can be categorized based on the structural features of their connectivity. Scheme 3.1 below shows the most prevalent metal coordination geometries with at least one bridging halide that exist in one-dimensional inorganic polymers (Englert, 2010).

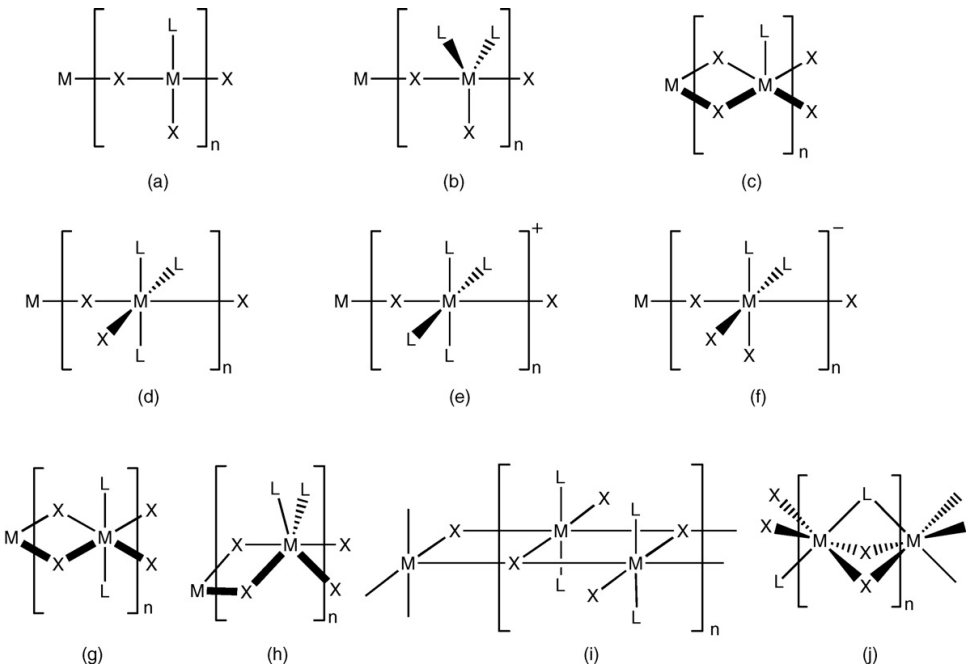

Schematic 3.1: Most prevalent metal coordination geometries in one-dimensional inorganic polymers (Englert, 2010).

In scheme 3.1a an example of a tetra-coordinated anion can be observed which is formed by a corner-sharing tetrahedron, while Scheme 3.1b shows a fivefold metal coordination geometry and is shown to exist in either a square-pyramidal or a trigonal-bipyramidal corner-sharing polyhedral and Scheme 3.1c shows the occurrence of an in edge-sharing tetragonal pyramid geometry (Englert, 2010).

The most prevalent of geometries encountered, in bridging metal halides, is the hexa-coordination (Scheme 3.1d-f), where a single ligand bridges two metal centres. Various degrees of ligand substitution may be present in this polymer as shown in schemes 3.1d-f. Additionally, octahedral coordination chains exist where these geometries are linked through edge sharing (Scheme 3.1g-i) or through face sharing, (Scheme 3.1j) where the stoichiometry results in the presence of two bridging halides and a neutral bridging ligand (Englert, 2010).

Extensive work and investigation done by Morsali and Masoomi (2009) provided a review of all the reported coordination polymers of mercury(II) and mercury halide coordination polymers over the last two decades. Due to the possible applications of polymeric mercury compounds, their investigation focused on the varying coordination numbers and donor binding capabilities of mercury.

Englert (2010) reviewed the structures and properties of halide-bridge polymers containing divalent metals and a range of ligands, and focused extensively on the dimensionality of the polymers. Metal atom coordination geometries ranging from four to six are covered, as well as different types of bridging modes. In addition to one-dimensional chain polymers, the review also considers polymers that are further linked via halide bridges or organic ligands to from two dimensional structures.

Coordination structures that contain the group 12 transition metals Cd and Hg tend to form low-coordinate linear or other distorted coordination polymers due to the d^{10} configuration and its associated flexible coordination environment. This phenomenon consequently allows the structures to adopt various geometries ranging from tetrahedral to octahedral and extreme distortions thereof (Morsali and Masoomi, 2009). In addition, the particular lability associated with these d^{10} metals allows any formation of coordination bonds to be reversible, subsequently enabling ligands and metal ions to rearrange during the organization and packing of the crystal structure (Morsali and Masoomi, 2009). The employment of Cd and Hg in coordination polymer synthesis allows network structures to adopt highly ordered arrangements as these metals have extensive capacities for various types of architectures.

Zinc(II)-halogeno Coordination Compounds

In zinc-halogeno coordination compounds the formation of a mononuclear tetrahedral complex is prevalent (Hu and Englert, 2003) and Zn(II) halide-bridged inorganic polymers rarely occur (Englert, 2010). Zinc structures that contain halide-bridging ligands usually have approximately symmetric M-X-M bridges and predictable M···M distances allowing for the formation of stable hybrid structures which make them suitable building blocks for crystal engineering (Hu, et al., 2007).

Zinc coordination structures generally adopt a tetrahedral geometry with significant distortions thereof, irrespective of the nature of the organic ligand that coordinates to the zinc atom. Figure 3.1 below shows a wave-like Zn(II) containing one-dimensional coordination polymer, where the zinc atom has a tetrahedral geometry and coordinates to two terminal chloro ligands and two organic ligands which bridge neighbouring zinc units (Zhang, et al., 2008).

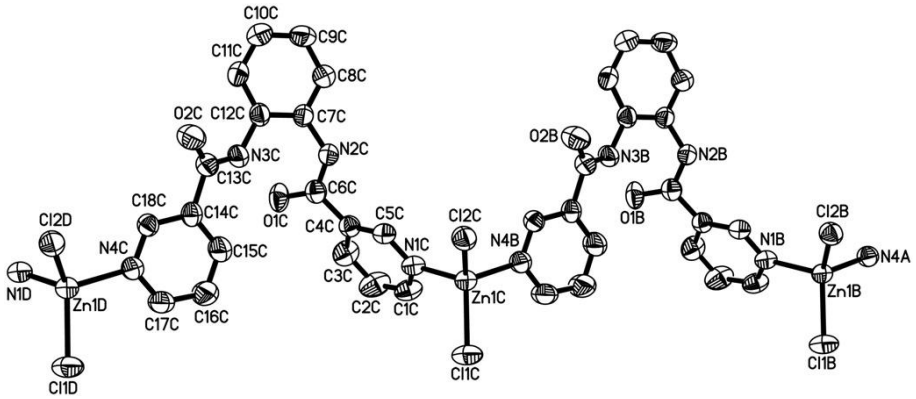

Figure 3.1: A one-dimensional Zn(II) containing coordination polymer (Zhang, et al., 2008).

Cadmium (II) –halogeno coordination complexes and polymers

The crystal structure of $CdCl_2$ follows a cubic close packed arrangement where the cadmium ions fills one-half the octahedral voids and are surrounded and coordinated to three chloro ligands and three Cd metal centres (Chandrasekhar and Senapati, 2010).

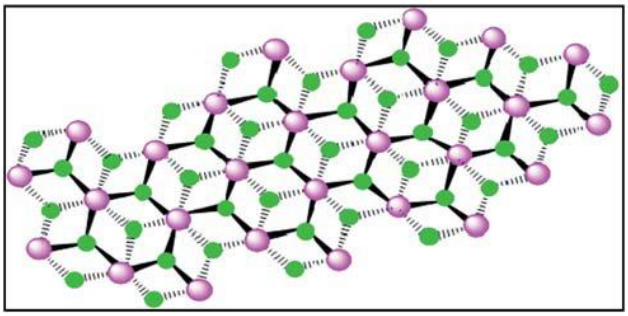

Figure 3.2: The layered structure of $CdCl_2$ (Cd and Cl atoms indicated by pink and green colours respectively, (Chandrasekhar and Senapati, 2010).

$CdCl_2$ has a layered structure (Douglas, et al., 1994) and is the model structure that is adopted by many other metal halide solids. These metal salts include MnCl2, FeCl2, CoCl2, NiCl2, MgCl2 and ZnBr2 (Wells, 1975 and Wyckoff, 1960).

Extensive work has been done by Chandrasekhar and Senapati to observe whether the structural motifs that exist in the solid-state CdCl2 structure could be stabilized by the introduction of an organic ligand during synthesis. What was observed from their research is that by introducing multi-site coordination ligands, containing aromatic rings, molecular ligand-stabilized inorganic solid state structures could be synthesized. Their investigation lead to the formation of two structurally different one-dimensional coordination polymers (Figure 3.3) stabilized by organic ligand interactions.

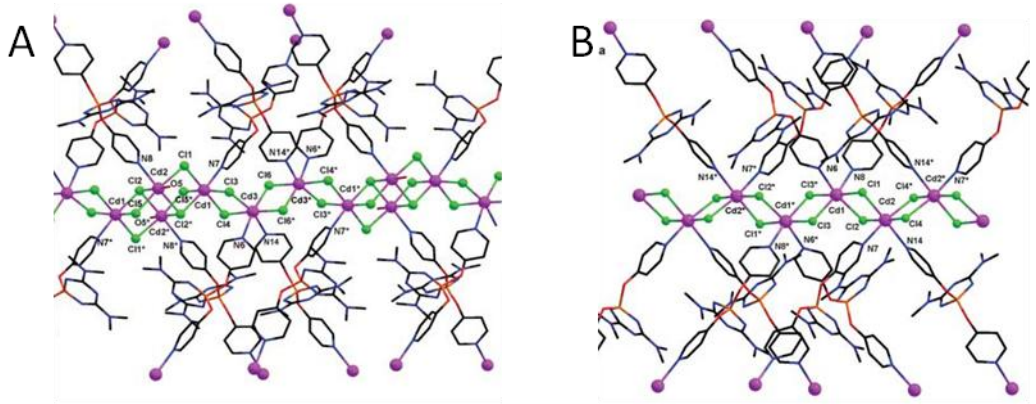

Figure 3.3: The two distinct one-dimensional $CdCl_2$ inorganic chains (Chandrasekhar and Senapati, 2010).

In the same way, Cd(II) coordination polymers were synthesisized by varying the halide component (Cl, Br, I) and by using halogen substituted organic ligands (Hu et al, 2003). This study, carried out by Hu and co-workers, presented the formation of 15 different Cd(II)-halogeno chain polymers. The majority of the coordination polymers reported exhibited a six coordinated cadmium metal atom with four bridging halide ligands in the equatorial positions and two pyridine ligands in the axial positions (Hu, et al., 2003).

Inorganic-organic Mercury(II) Coordination Complexes and Polymers:

The most prominent coordination number of mercury(II) is four and the most frequently occurring one-dimensional motifs that mercury(II)-halide coordination polymers show are linear chains, zig-zag chains, double chains, ladder-like chains, and when zig-zag chains get intertwined, helix chains (Morsali and Masoomi, 2009).

A study by Morsali and Masoomi (2009) reported details on numerous mercury(II) polymers of varying dimensionalities and insight into the effect of the coordination numbers of mercury. One of most interesting and noteworthy details of their investigation was the examination of numerous mercury containing coordination polymers having multiple mercury(II) metal centres with more than one coordination number.

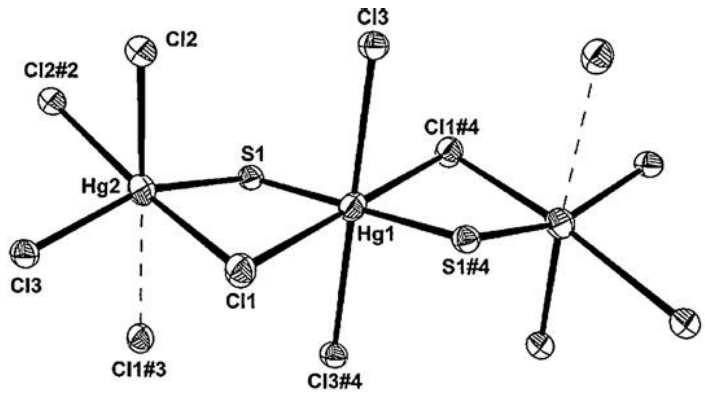

Figure 3.4: Visual representation illustrating the coordination mode of the two crystallographically different mercury atoms (Fleischer, et al., 2006).

Figure 3.4 above illustrates an example of a compound that has more than one mercury centre with different coordination modes. The one mercury atom has a slightly distorted ochtahedral geometry while the other mercury centre has a 5+1 coordination mode containing an elongated Hg···Cl contact with a highly distorted (pseudo)-octahedral geometry.

Studies done on one-dimensional polymers containing halogen bridged divalent mercury atoms by Hu and co-workers suggest that the bonding distances between a mercury and a halogen ligand (Hg···X) are variable and cover the range of covalent bonds and van der Waals interactions. Information from the study suggest that the size of the ligand is not exclusively the determining factor for the structure type adopted as exemplified by both pseudo-octahedral Hg(II) coordination and five-coordinated mercury from the study (Hu, et al., 2007)

Structural investigation of related coordination compounds

An investigation of known structures in the literature that are pertinent to this study was performed to ensure that significant relevant information would be obtained so that discussion and comparison with the novel compounds would be done with an insightful approach. The Cambridge Structural Database was utilized to see which structures, of the family of considered building blocks employed in this study, were known and published. A total number of six relevant structures were located in the literature. A concise overview of the family of compounds relevant to this study is given along with an analysis of their structures.

The literature structures will be labelled alphabetically employing uppercase letters. A reference guide listing the different labels and the compounds they refer to is provided within the dissertation. Literature compounds can be distinguished by their CSD reference codes.

Please note that the terms “compound X” and “structure X” are used interchangeably in the discussion. The hydrogen bonding distances quoted refer to the distance between the hydrogen bond donor and hydrogen bond accepter unless stated otherwise.

Table 3.1: Crystallographic data of reported literature compounds containing 4-Aminobenzoic acid and Isonicotinic acid:

Compound	A	B	C	D	E	F
Empirical Formula	$(C_7H_7O_2N)_2CdCl_2$	$C_7H_8O_3NCdCl_3$	$C_7H_8O_3NCdBr$	$(C_7H_7O_2N)_2CdI_2$	$C_6H_5O_2NCuCl$	$(C_6H_5O_2N)_2PdCl_2$
M_r(g/mol)	457.58	301.99	346.45	-	223.90	423.52
Crystal system	Triclinic	Orthorhombic	Monoclinic	Monoclinic	-	Triclinic
Space group	$P\bar{1}$	*P*bca	$P2_1/c$	C_2/c	$P2_1/c$	$P\bar{1}$
Z	2	8	4	4	2	1
a/Å	6.362 (3)	8.7606 (3)	6.4357(2)	15.8720(2)	14.097(8)	3.9554(2)
b/Å	7.512 (3)	10.6930 (3)	7.2533(3)	4.5115(1)	3.747(1)	7.4830(4)
c/Å	17.258 (8)	19.7616 (7)	19.7258(6)	25.0187(7)	14.251(7)	12.5456(7)
α/°	94.55 (4)	90.00	90.00	90.00	90.00	75.625(3)
β/°	96.81 (5)	90.00	90.890(2)	97.474(2)	101.34(4)	88.898(3)
γ/°	104.59 (4)	90.00	90.00	90.00	90.00	80.313(3)
V (Å^3)	787.421 (1)	1851.21	920.69	1776.28	738.063	354.475
F(ooo)	-	1168	656	1192	-	208
D_c (g cm^{-3})	-	2.167	2.499	2.395	-	1.984
μ (mm^{-1})	-	2.619	6.683	4.724	-	1.701
R-Factor (%)	2.5	3.48	5.39	4.53	6.0	2.38
Diffractometer	Enraf-Nonius CAD-4	Siemens Smart CCD	Siemens Smart CCD	Siemens Smart CCD	Nicolet R3m	Nonius Kappa-CCD
T (k)	295	293	293	293	-	295
λ(Mo Kα) (Å)	0.5608	0.71073	0.71073	0.71073	0.71069	0.71073
Reflections collected	5771	5826	2833	2852	-	3711
Unique reflections	-	1646	1596	1555	990	1251
Parameters	-	119	119	106	100	-
R[F^2>2σ(F^2)]	-	0.0348	0.0539	0.0453	0.060	0.0238
wR(F^2)	0.027	0.1056	0.1413	0.1206	0.068	0.0582
Δp_{max} & Δp_{min} (e Å^{-3})	0.635 and -0.533	0.863 and -0.639	1.276 and -1.453	1.143 and -1.043	0.62 and -0.67	0.3522 and -0.3118

$R=\sum||F_0|-|F_c||/\sum|F_c|$
$wR=[\sum w(F^2_0-F^2_c)^2/\sum w(F^2_0)$

4-Aminobenzoic acid containing structures

A total number of four coordination compounds of metal halides and 4-aminobenzoic acid have been reported in the literature, and they are discussed in further detail below.

A: catena(bis(p-aminobenzoic acid-N)-bis(μ2-chloro)-cadmium(II)) (Le Fur and Masse, 1996), (CSD Refcode: TEHVIL)

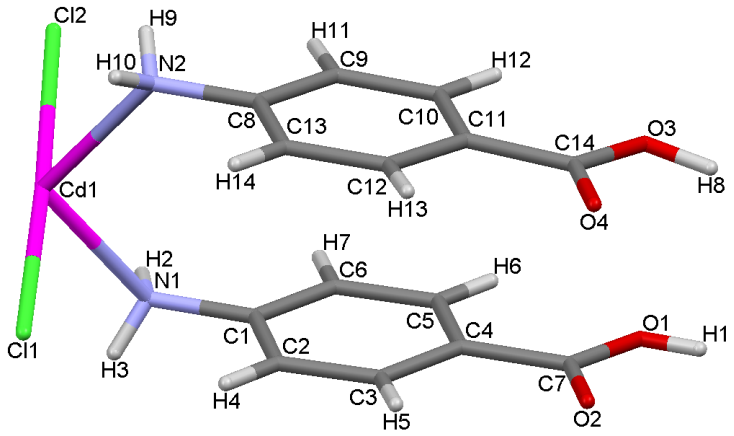

Figure 3.5: Asymmetric unit of compound A:

The asymmetric unit of structure A is illustrated in Figure 3.5, and consists of a cadmium atom, which is coordinated to two chloro ligands as well as to two 4-aminobenzoic acid constituents through the nitrogen atom on the amine group of the organic ligand, in a cis conformation. The pair of aromatic rings of the organic ligands lie parallel to one another in an offset arrangement.

In the structure four chloro ligands and two 4-aminobenzoic acid ligands are coordinated to the central cadmium metal, which has a distorted octahedral geometry. Each pair of bridging chloro ligands is shared between a neighbouring cadmium atom. The bridging chloro ligands exhibit two shorter and two longer metal-halogen bonds. The shorter metal-halogen bonds (2.729 Å and 2.567 Å) could represent electron sharing covalent bonds while the longer bonds (2.613 Å and 2.600 Å) are probably electron pair donating bonds. The nitrogen atom on the organic molecule has a distorted tetrahedral geometry and shows a large bonding distance towards the coordinated carbon atom at 1.42 Å (Le Fur and Masse, 1996). The carboxylic acid functional groups on the 4-aminobenzoic acid molecule lie in the same plane as the aromatic ring.

A one-dimensional inorganic chain of edge sharing octahedra is formed, through pairs of bridging chloro ligands along the a-axis. As a result of cis edge sharing the inorganic chain

follows a zig-zag pattern. In this manner a one-dimensional coordination polymer is formed by means of the bridging halogeno ligands, as shown in Figure 3.6.

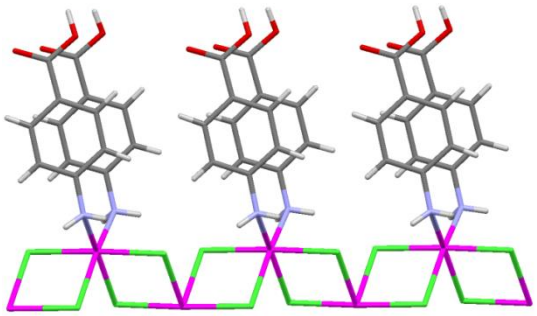

Figure 3.6: Expansion viewed along the b-axis.

The one-dimensional polymers pack to form a layered structure consisting of organic bi-layers alternating with inorganic layers. The organic bi-layer is comprised of two layers of organic ligands while the inorganic layer contains the metal and halogen atom, as illustrated in Figure 3.7.

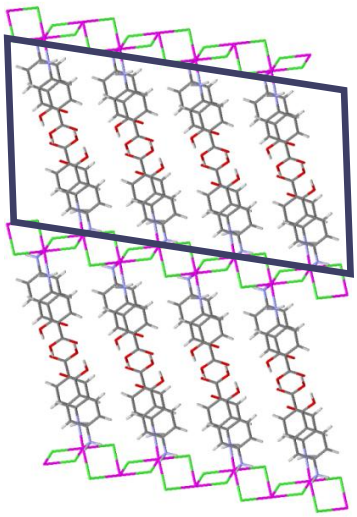

Figure 3.7: Packing of structure A, viewed along the b-axis. The superimposed block highlights the organic bi-layer.

There exist hydrogen bonds between carboxylic groups, O—H···O at distances of 2.608 Å and 2.630 Å for each of the ligands respectively, to form carboxylic acid hydrogen bonded dimers. These dimers link the organic ligands in the organic bi-layer. Hydrogen bonding also occurs in the inorganic layer, between one hydrogen atom on the amine group and a chloro ligand, as well as between the chloro ligand and a hydrogen atom on the aromatic ring of the 4-aminobenzoic acid moiety. The hydrogen bond network maintains the packing cohesion betwee neighbouring layers to form a two-dimensional hydrogen bonded sheet of coordination polymers.

Pairs of aromatic rings lie in planes which are parallel to one another and the distances between their centroids are 3.722 Å. Their stacking is offset π-stacked, which promotes π-σ

attraction. Polarization occurs due to the decrease in electron density of the aromatic rings because of the electron withdrawing capacity of the carboxylic functional groups, subsequently the π-π repulsion between rings also decreases and there is more π-σ attraction.

***B: catena-[(μ₂-chloro)-(μ₂-4-aminobenzoato)-aqua-cadmium(II)], (Wang, et al., 2002), (CSD Refcode:* WUQGOE)**

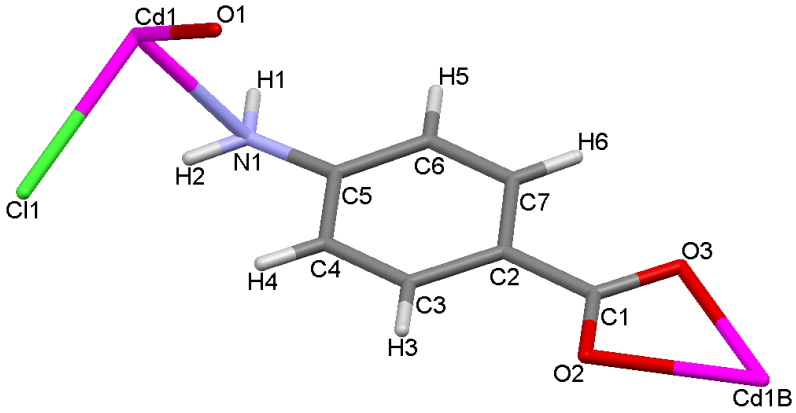

Figure 3.8: Asymmetric Unit of compound I:

The main difference between literature structure A, and the current structure is that in the current structure both ends of the 4-aminobenzoic acid ligand are coordinated, while in the previous structure only the amine end of the molecule is coordinated. This impacts on the dimensionality of the resulting structure, and was achieved through deprotonation of the carboxylic acid functional group, employing NaOH to extract the carboxylic acid proton, to form a carboxylate group through which additional coordination occurs.

In the asymmetric unit a single deprotonated 4-aminobenzoic acid constituent is coordinated to a cadmium atom via a lone pair on the nitrogen atom of the amine group. The functional groups of the organic constituents lie on the same plane as the aromatic ring resulting in a planar geometry for the organic ligand. Additionally the cadmium atom coordinates to a μ₂-chloro ligand and a neutral water (aquo) ligand resulting in an octahedral geometry. The ligands that make up the equatorial plane of the cadmium octahedron are the two carboxylate oxygen atoms, the nitrogen atom and the water molecule, while the two bridging chloro ligands are positioned in the apical positions (Wang, et al., 2002).

The chloro ligands act as μ₂-bridges and subsequently form an infinite one-dimensional inorganic chain. The mode in which the organic unit is coordinated to the cadmium atom alternates successively between coordination via the nitrogen atom and the carboxylate group (Figure 3.9). This gives rise to an inorganic chain having trans cadmium octahedra while the carboxylate end of the ligand coordinates to a different cadmium atom.

Two chloro ligands are coordinated to the cadmium metal atom and act as a bridging ligands between adjacent cadmium atoms, at distances (Cd—Cl) 2.58 Å and 2.65 Å respectively, and bridge with an angle (Cl—Cd—Cl) of 171.13°.

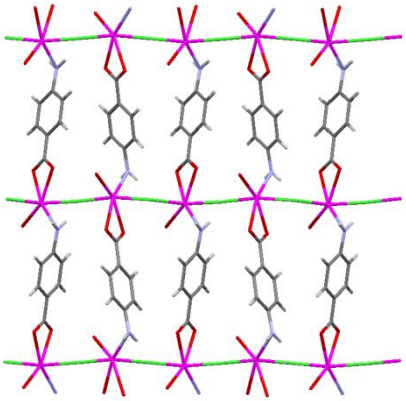

Figure 3.9: Expansion of asymmetric unit viewed along the b-axis.

There is no indication of π-π interactions between the aromatic rings, as the distances between their centroids far exceed the expected interaction distance. Expansion of the unit cell shows the bridging of cadmium metal atoms via chloro ligands which consequently produces an infinite one-dimensional inorganic chain. Additionally, bridging between inorganic chains occur via the multifunctional organic units. The unique mode of coordination that occurs between both the nitrogen atom and carboxylate ogygen atoms provide an organic bridge beween inorganic chains to give a coordination structure with a two-dimensional geometry. Unlike the organic bi-layer observed in structure A, structure B forms a single organic layer as a result of coordination occurring on both sides of the ligand.

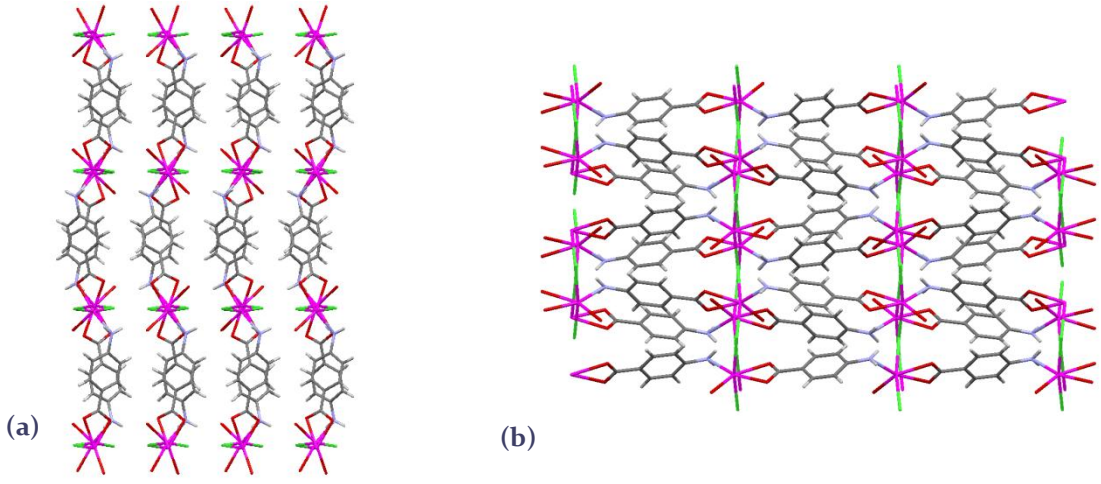

Figure 3.10: Packing of structure B viewed along the (a) a-axis and (b) b-axis.

There exist hydrogen bonds between the water (aquo) ligand and the oxygen atoms of the carboxylate group, at distances of 2.776 Å and 2.773 Å. Hydrogen bonding is present between the hydrogen atom on the nitrogen atom and the chloro ligand with a distance of 3.186 Å as well as between the hydrogen atom on the nitrogen and oxygen of the carboxylic group, at a distance of 2.969 Å.

***C: catena-[(μ_2-Bromo)-(μ_2-4-aminobenzoato)-aqua-cadmium(II)], (Wang, et al., 2002), (CSD Refcode:* WUQGUK)**

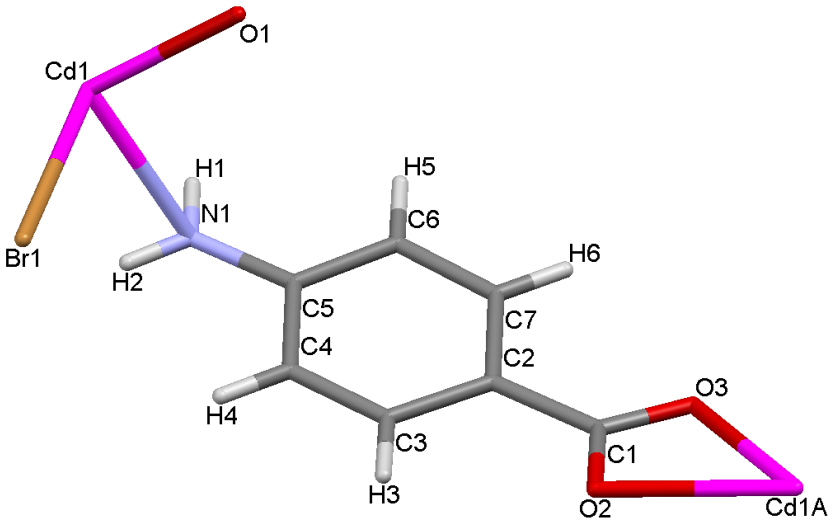

Figure 3.11: Asymmetric Unit of compound C:

This structure differs from structures A and B in that both ends of the ligand is coordinated, as observed in structure B, through deprotonation of the carboxylic group, but in addition further linkage occurs through halogeno ligands to form what can essentially be viewed as a three-dimensional coordination network.

The asymmetric unit consists of a cadmium atom that is coordinated to the nitrogen atom of the amine functional group as well as to the carboxylate group of another ligand. Additionally a water molecule is coordinated to the cadmium atom as well as a bridging bromo ligand. This bridging bromo ligand was not present in literature structure B reported previously.

In the structure two bridging bromo ligands are bonded to the cadmium metal atom at distances of 2.787 Å and 2.830 Å. The two coordinated chelating carboxylate oxygen atoms are bonded to the cadmium atom at distances of 2.393 Å and 2.413 Å while the coordinated nitrogen atom is bonded at a distance of 2.353 Å from the cadmium metal atom. The aquo ligand has a bonding distance of 2.236 Å to the cadmium atom. The octahedral geometry of the cadmium atom is greatly distorted; still the bridging bromo ligands form a four membered ring with the cadmium metal atoms. The distance between neighbouring metal centres (Cd—Cd) is 3.795 Å.

The unique mode of coordination that occurs between both the nitrogen atom and carboxylate oxygen atoms provide an organic bridge between inorganic units. Note that a one-dimensional inorganic polymer of the type observed in structure B is not present in the current structure. Instead the bridging that occurs through the bromo ligands results in isolated inorganic units which terminate due to the cis position of the bromo μ_2-bridges.

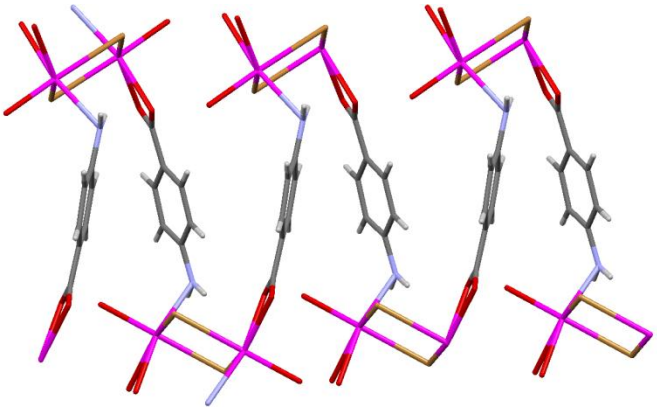

Figure 3.12: Expansion of asymmetric unit viewed along the a-axis.

The organic constituent has many similarities to that of the previously discussed organic ligand. However, there are some important differences that are observed which undoubtedly contributes to the variation seen in the molecular geometry of the present compound.

The amine functional group is observed to be planar to the aromatic ring, however the carboxylate group is rotated with respect to the ring. This rotation arises from the coordination bond that exists between the carboxylate oxygen atoms and the cadmium metal and since the metal geometry is highly distorted it conforms the carboxylate to a rotated position. This rotation is not present in structure B and is probably due to the additional bridging through the bromo ligand which requires distortion of the ligand.

Similar to the previous structure, it is observed that there are no π-π interactions between the aromatic rings, since the aromatic rings lie in planes that are not parallel to one another and because their centroid-to-centroid distances are too large.

The isolated inorganic unit consist of two cadmium metal centres that are octahedrally coordinated and bridged through two edge sharing bromo ligands forming a four membered ring with the cadmium metal atoms. Each cadmium has a distorted octahedral geometry and the equatorial plain of the octahedron is generated by the by the two carboxylate oxygen atoms, a nitrogen atom and a bromo ligand while the axial positions are occupied by a water oxygen atom and the other bromo ligand (Wang, et al., 2002).

Expansion of the unit cell shows how the bromo ligands produce an interconnection of neighbouring cadmium octahedra which forms a three-dimensional structure. The multifunctional organic unit connects cadmium metals through the nitrogen atom and carboxylate group simultaneously and subsequently generates an organic layer.

The coordination mode of the organic unit is similar to the previously discussed compound (B); however the layer that is generated by the inorganic constituent is different owning to the cis orientation of the bromo ligands (Wang, et al., 2002). Hydrogen bonding links the terminal inorganic chains to yield a two-dimensional layer of discrete inorganic chains which alternates with the organic layer.

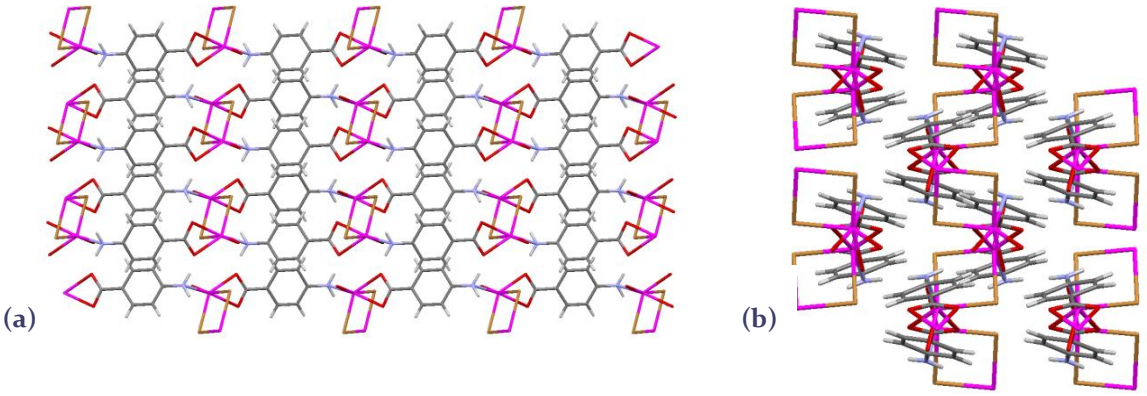

Figure 3.13: Packing of structure C viewed along the (a) b-axis and (b) c-axis.

It is of some significance to include the weak inter-layer Cd···Br interaction (3.798 Å) that exist between different inorganic units as it plays an important role in consolidating the architectural arrangement of the crystal structure. This interaction extends the two-dimensional layers into a three dimensional structure (Wang, et al., 2002).

There exist two hydrogen bonds between the water ligand and an oxygen atom of two different carboxylic functional groups (O—H···O) at distance of 2.716 Å and 2.818 Å. Additionally a hydrogen bond between the amine group and a bromo ligand (N—H···Br) at a distance of 3.375 Å exists. Also, between the amine and carboxylic acid oxygen atom a hydrogen bond occurs (N—H···O) at a distance 3.050 Å (Wang, et al., 2002).

***D: di-iodo-bis(4-aminobenzoic-acid-N)-cadmium(II), (Wang, et al., 2002), (CSD Refcode:* WUQHAR)**

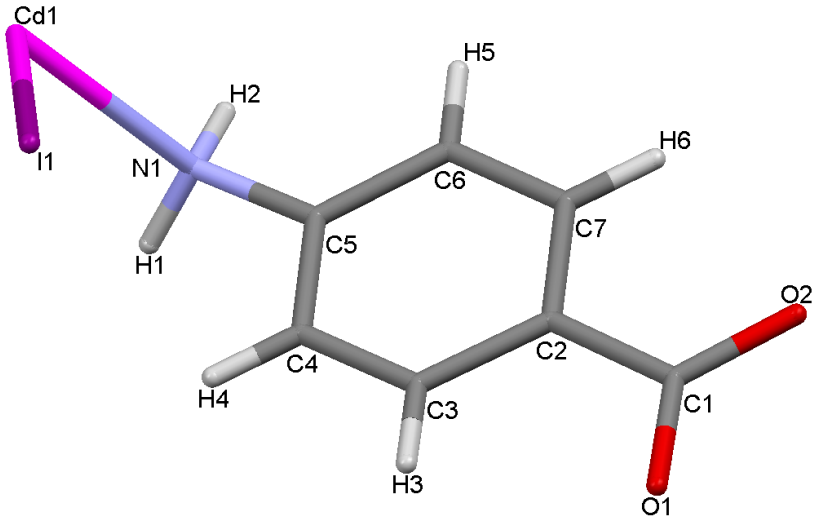

Figure 3.14: Asymmetric Unit of compound D:

The asymmetric unit consists of a cadmium metal atom that is coordinated to an iodo ligand and a 4-aminobenzoic acid molecule through the nitrogen atom of the amine functional group. The molecule lies on a two-fold rotation axis, and the rest of the molecule is generated by symmetry. It should be noted that the hydrogen atom could not be placed on the carboxylic acid group.

In the structure two iodo ligands are coordinated to the cadmium atom at a Cd—I distance of 2.828 Å while the nitrogen atom of the amine group coordinates to the cadmium atom at a Cd—N distance of 2.348 Å. The tetrahedral geometry of the metal atom is highly distorted, with the iodo ligands forming an I—Cd—I angle of 95.12 ° while the nitrogen atoms forms an N-Cd-N angle of 148.83 °. The aromatic rings of the organic constituents lie in planes which make an intersecting angle of 83.41 ° with one another.

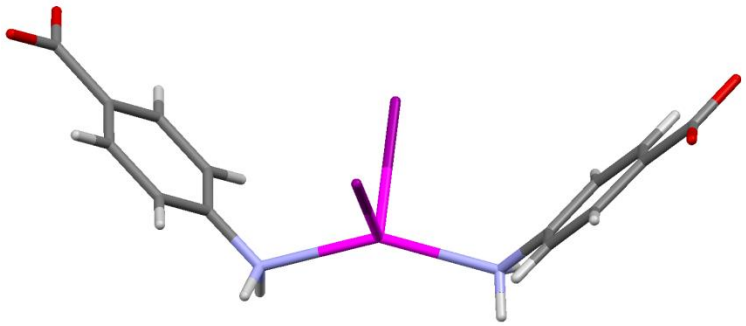

Figure 3.15: Molecular geometry of compound D.

The carboxylic acid and amine functional groups are observed to be planar to the benzene ring resulting in a planar ligand. The nitrogen atom coordinates to the cadmium atom in a tetrahedral fashion while the carboxylate group forms a hydrogen bonded dimer with a neighbouring organic unit and subsequently forms an organic bi-layer. The aromatic rings on the organic components, that are non-covalently bonded to one another lie in the same plane. Additionally they also lie parallel to those benzene rings that make up the organic bi-layer.

The parallel packing of the organic layers fixes the coordinated inorganic unit and contributes largely to their packing orientation. A one-dimensional row of discrete inorganic units are produced and it is observed that the isolated tetrahedral units are all orientated in the same direction in a row, but they alternate in orientation in neighbouring inorganic rows.

Formally the coordination molecules are viewed as being isolated, and there are no bridging iodo ligands between consecutive metal atoms. However, all the isolated tetrahedral complexes are oriented in the same direction, as can be seen in Figure 3.16. The iodo ligand's inability to bond to neighbouring cadmium metal centres is exemplified by the large distance between two of the iodo ligands and the cadmium atom, which is equal to 3.337 Å. However, this weak interaction may still influence the packing and orientation of the discrete units. Hydrogen bonds link neighbouring isolated complexes through N-H...I hydrogen bonds at a distance 3.141 Å to form a hydrogen-bonded ribbon.

There exist hydrogen bonds between the oxygen atoms of the carboxylic groups (O—H···O) at a distance of 2.631 Å. These interactions link these hydrogen bonded ribbons into two-dimensional hydrogen bonded sheets. This produces an organic bi-layer that alternates successively with an inorganic layer.

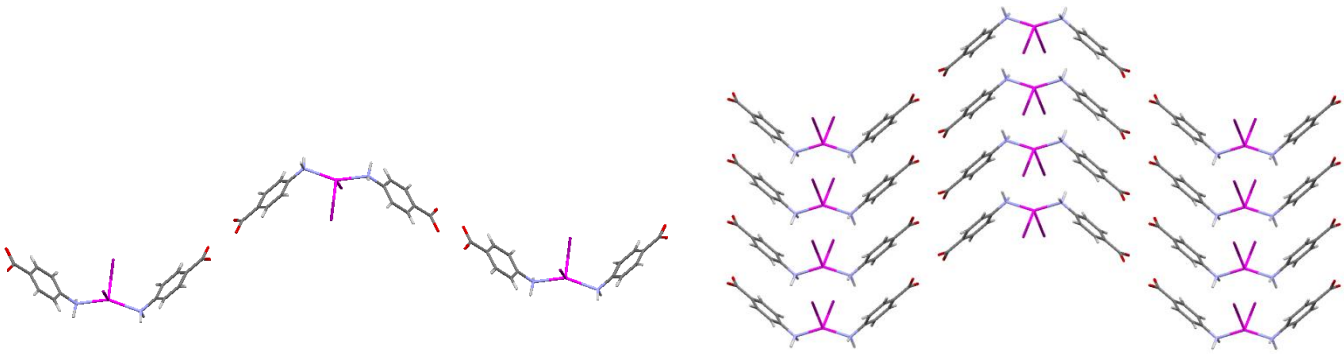

Figure 3.16: Expansion of the molecular geometry of compound D.

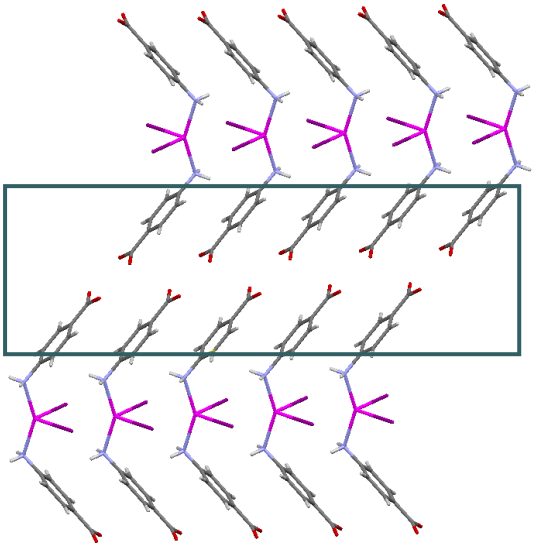

Figure 3.17: Packing of structure D, viewed along the a-axis. The organic bi-layer is highlights by the superimposed block.

The aromatic rings of the organic constituents lie in planes that are parallel to one another; however there are no direct overlaps between the rings. The distance between the centre of parallel rings are 4.648 Å (centroid-to-centroid distance). It is observed that the parallel displacement between the aromatic rings is large, which causes π-π repulsion to decrease, however π-σ attraction now competes more strongly with the weaker repulsion force.

Isonicotinic acid containing structures

Two structures were identified from the literature that contains metal halide components combined with the isonicotinic acid ligand. The structural features of these compounds are discussed below.

E: catena((μ$_3$-chloro)-(isonicotinic acid-N)-copper(I)), (Goher and Mak, 1985), (CSD Refcode: DENLUD)

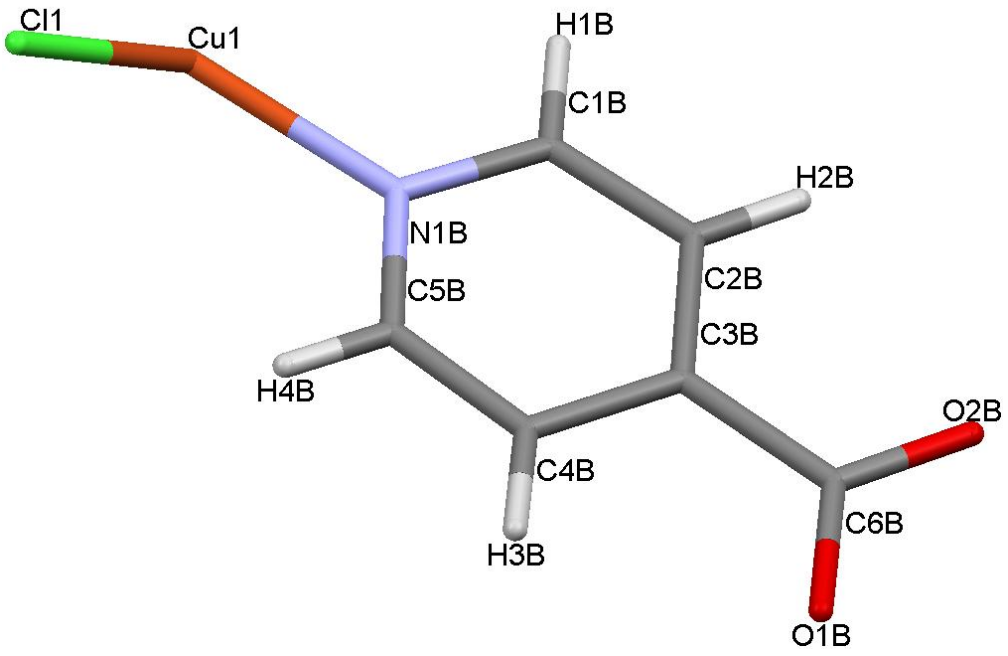

Figure 3.18: Asymmetric Unit of compound E:

The asymmetric unit consists of the isonicotinic acid organic unit that is coordinated to a copper atom via the pyridine nitrogen atom. Furthermore, the metal centre coordinates to a chloro ligand. The authors could not place the hydrogen atoms on the carboxylic acid functional group.

The copper metal centre has an approximately tetrahedral geometry and covalently bonds to three chloro ligands and coordinates to the nitrogen atom of the isonicotinic acid ligand. The metal centres are connected to neighbouring units via three bridging chloro ligands. The edge sharing Cu_2Cl_2 units form parallelograms that connect neighbouring inorganic units with the shortest (Cu—Cl) bond at 2.316(3) Å and the longest at 2.488(3) Å which establishes the link between metal centres (Goher and Mak, 1985). Twisting between discrete inorganic Cu_2Cl_2 units in the polymeric chain can be described by the dihedral angle that is generated between them (Cu···Cl···Cu) at 67.7° (Goher and Mak, 1985).

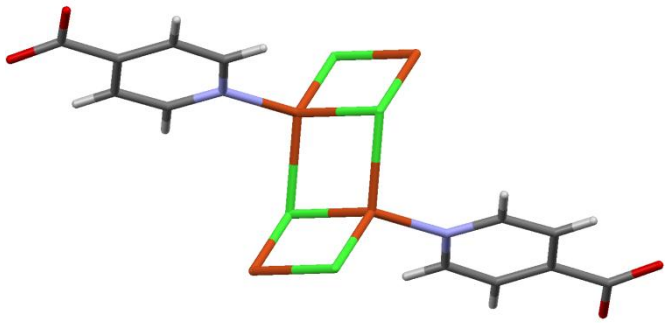

Figure 3.19: Molecular geometry of compound E.

A one-dimensional inorganic ribbon is produced as a result of the edge sharing of Cu_2Cl_2 units (Figure 3.19). The translation of the inorganic units (which are centrosymmetric,) along the b-axis generates the polymeric chain which alternates sequentially with the organic layer (Goher and Mak, 1985). The carboxylic acid groups lie planar to the aromatic ring and form carboxylic acid hydrogen bonded dimers, consequently producing organic bi-layers.

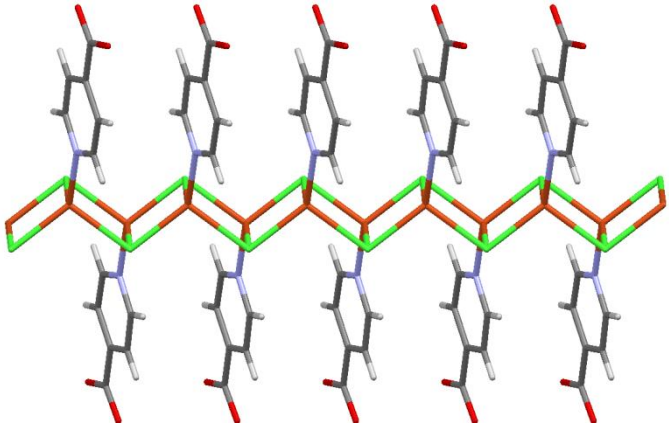

Figure 3.20: Expansion of the asymmetric unit, viewed along the a-axis.

Figure 3.20 above illustrates how the aromatic rings of the isonicotinic acid units lie parallel to one another. The distance between their centroids, 3.747 Å, is indicative of $\pi - \pi$ interactions which account for the organized stacking formation.

Figure 3.21 shows the hydrogen bonding dimers connecting the organic units forming the bi-layer. The organic units are bonded, via their nitrogen lone pairs, to metal centres and the hydrogen bonding dimers connect neighbouring coordination polymers.

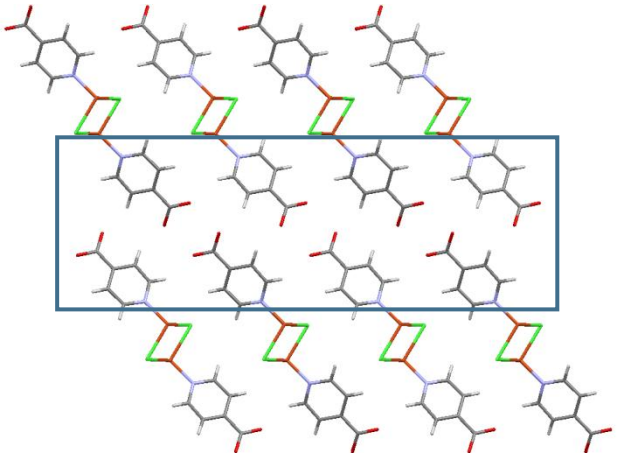

Figure 3.21: Packing of structure E, viewed along the b-axis.

***F: trans-dichloro-bis(pyridine-4-carboxylic acid-N)-palladium(II), (Qin. Et, al., 2002), (CSD Refcode:* CIJBOM01)**

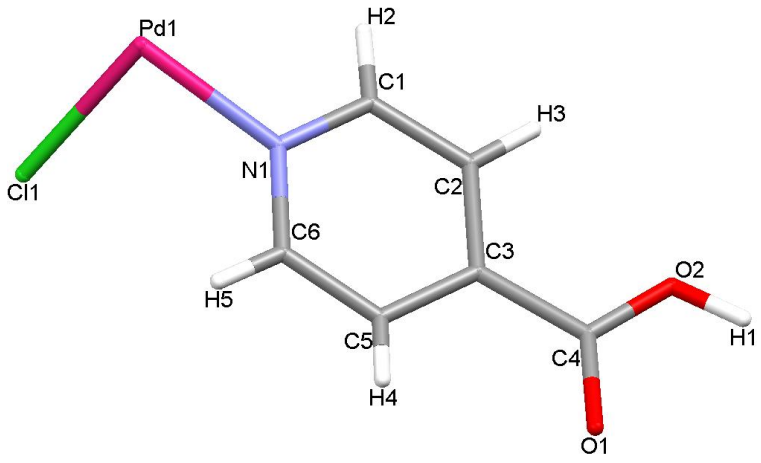

Figure 3.22: Asymmetric Unit of compound F:

The asymmetric unit consists of an isonicotinic acid organic unit that is coordinated to a palladium atom via a lone pair on the nitrogen atom. Furthermore, the metal centre coordinates to a chloro ligand. The palladium atom is positioned on a centre of inversion, and the rest of the molecule is generated by the symmetry operator (-x, -y, -z).

The palladium metal centre has a square planar geometry and covalently bonds to two chloro ligands and coordinates to two nitrogen atoms from the isonicotinic acid units. The angle between nitrogen atoms formed by the metal centre (Cl···Pd···Cl) is exactly 180°, and the angle that the chloro ligand makes with the covalently bonded nitrogen atom (Cl···Pd···N) is 90.47°.

The two halogeno ligands have the same bonding distances to the palladium atom (Pd—Cl) at 2.305 Å. The dihedral angle between the palladium geometrical plane and the approximate plane of the coordinated aromatic units is 57.47°. The carboxylic acid group is observed to lie in same plane as the aromatic ring.

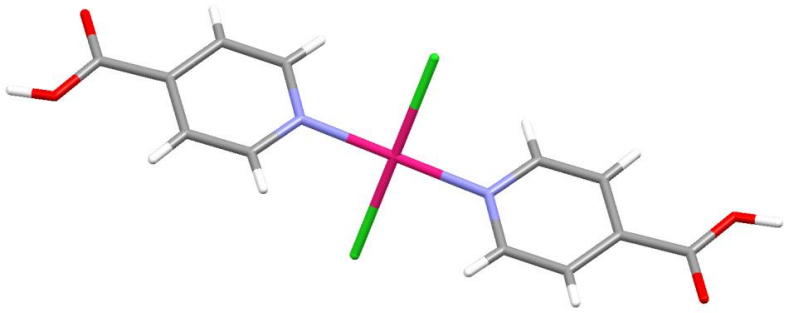

Figure 3.23: Molecular geometry of compound F.

There are no chloro ligands that bridge neighbouring metal centres and subsequently the discrete coordination molecules are present. The distance between coordinated chloro ligands and neighbouring palladium atoms (Pd—Cl···Pd) is 3.452 Å and the halogeno ligand fails to bridge the metal centres as a result of the size of the chloro ligand.

Neighbouring isolated molecules are linked through the hydrogen bonding interactions involving their carboxylic acid functional groups on the isonicotinic acid moiety and and consequently form hydrogen bonded ribbons. The hydrogen bonding distances associated with the dimer is 1.709 Å.

Isolated molecules pack in layers, to form a structure which consists of alternating inorganic layers consisting of the metal atom and halide atoms, and an organic bi-layer which contains the isonicotinic acid moiety. Further expansion of the unit cell shows hydrogen bonded ribbons adopting a wave-like structure once translated along the b-axis (Figure 3.25).

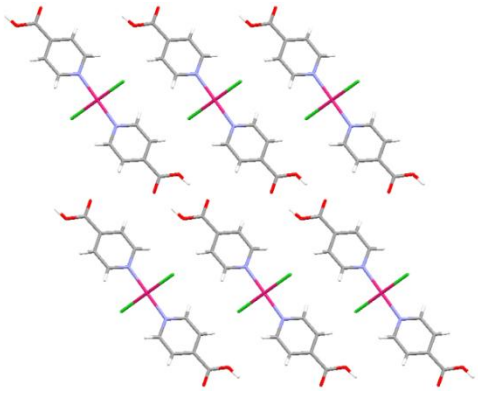

Figure 3.24: Expansion of the asymmetric unit, viewed along the a-axis.

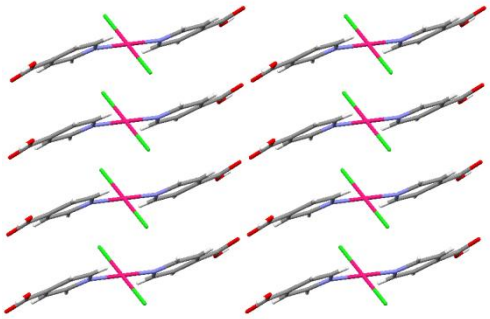

Figure 3.25: Expansion of the asymmetric unit, viewed along the b-axis.

The aromatic rings of isonicotinic acid units lie in planes that are approximately parallel to one another and are stacked in a slightly offset orientation. The distance between their centroids (3.955 Å) is too large to indicate substantial $\pi - \pi$ interactions, however their parallel displacement promotes the occurrence of π-σ attraction as their packing arrangement would suggest. The carboxylic acid groups form dimers connecting discrete inorganic units and consequently forming organic bi-layers.

4-Aminobenzamide containing structures:

There was no coordination structures found in the CSD containing 4-aminobenzamide. This provided an opportunity to employ this multifunctional organic constituent within the synthesis of organic-inorganic coordination compounds.

Results

Structural investigation of novel compounds:

Crystals obtained in the current investigation were analyzed by SCD and the crystal structures obtained were solved using direct methods. A set of tables are given below to indicate which structures determined in this study are novel (highlighted in bold) and which have been published previously in the literature and CSD. Novel structures are indicated by Roman numerals while literature compounds are labelled alphabetically using uppercase letters. Key characteristics are included, for novel compounds, in the table as well as the reference code obtained from the Cambridge Structural Database. Tables indicate the metal atom as well as the halogen atom used as the starting components for each organic molecule employed. Crystallographic information files (CIF) of all the novel structures are included on the accompanying CD.

Table 3.2: 4-Aminobenzoic Acid.

Metal	Cl	Br	I
Zn	**I: Novel Structure (Tetrahedral coordination unit)**	-	-
Cd	A: TEHVIL (Le Fur and Masse, 1996) B: WUQGOE (Wang, et al., 2002)	C: WUQGUK (Wang, et al., 2002)	D: WUQHAR (Wang, et al., 2002)
Hg	**II: Novel structure (Square Planar coordination unit)**	**IV: Novel structure (Octahedral coordination unit)**	-
Cu	**III: Novel structure (Square planar coordination unit)**	-	-

Table 3.3: Isonicotinic Acid.

Metal	Cl	Br
Cu	E: DENLUD (Goher and Mak, 1996)	XUXZOF01 (Mateo-Marti, et al., 2008)
Pd	F: CIJBOM01 (Qin, et al., 2002)	-
Mn	-	**V: Novel structure (Octahedral coordination unit)**

Table 3.4: Crystallographic data of novel compounds containing 4-Aminobenzoic acid or Isonicotinic acid:

Compound	I	II	III	IV	V
Empirical Formula	$C_7H_7O_2NZnCl$	$C_7H_7O_2NHgCl$	$C_7H_7O_2NCuCl_2$	$C_7H_7O_2NHgBr$	$C_6H_7O_3NMnBr_3$
M_r(g/mol)	410.54	373.18	271.58	472.23	460.98
Crystal system	Monoclinic	Monoclinic	Triclinic	Triclinic	Monoclinic
Space group	*C*2/c	*C*2/c	$P\bar{1}$	$P\bar{1}$	*C*2/c
Z	4	4	1	1	4
a/Å	30.646(2)	31.519(2)	4.6473(5)	4.1601(8)	7.6684(6)
b/Å	4.7248(3)	4.6476(3)	5.9582(7)	7.3828(1)	20.2919(2)
c/Å	11.6157(8)	11.7386(8)	14.0364(2)	14.413(3)	12.7616(1)
α/°	90.00	90.00	86.716(2)	100.368(3)	90.00
β/°	97.0890(1)	97.7930(1)	88.515(2)	98.167(3)	99.7590(1)
γ/°	90.00	90.00	88.297(2)	93.426(3)	90.00
V (Å³)	1669.05	1703.68	387.738	429.367	1957.05
F(ooo)	832	676	135	213	892
D_c (g cm^{-3})	1.634	1.455	1.16	1.83	1.57
μ (mm^{-1})	1.81	9.17	1.73	8.220	4.77
R-Factor (%)	2.9	2.9	3.9	7.1	3.4
Diffractometer	Siemens P4 Bruker 1k CCD	Siemens P4 Bruker 1k CCD	Siemens P4 Bruker 1k CCD	Siemens P4 Bruker 1k CCD	Siemens P4 Bruker 1k CCD
T (k)	293	293	293	293	293
λ(Mo Kα) (Å)	0.71073	0.71073	0.71073	0.71073	0.71073
Reflections collected	4246	4333	2093	2217	3946
Unique reflections	1571	1606	1404	1522	1790
Parameters	105	123	151	106	147
R[F²>2σ(F²)]	0.029	0.029	0.038	0.071	0.034
wR(F²)	0.079	0.076	0.113	0.184	0.090
Δp_{max} & Δp_{min} (e Å^{-3})	0.33 and -0.30	0.52 and -1.08	0.5 and -0.38	4.96 and -2.51	0.94 and -0.83

$R=\sum||F_0|-|F_c||)/\sum|F_c|$
$wR=[\sum w(F^2_0-F^2_c)^2/\sum w(F^2_0)$

Novel 4-Aminobenzoic acid containing structures

A total of four 4-aminobenzoic acid containing structures were synthesized and yielded suitable crystals for SCD. The structural features of these compounds are discussed below.

I: bis(4-aminobenzoato -N)- dichlorozinc(II)

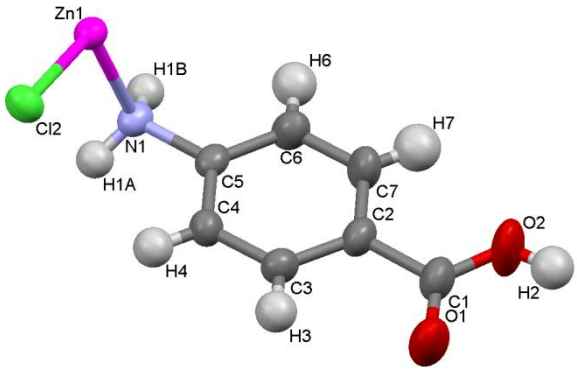

Figure 3.26: Asymmetric unit of compound I: Ellipsoids are drawn at the 50% probability level.

A detailed investigation of this novel compound has been written up and published (Rademeyer, et al., 2010) by our research group. An electronic copy of the article is included on the supplementary CD. It should be noted that for this structure, and all other structures, the choice of which oxygen atom on the carboxylic acid group is protonated was established by locating the hydrogen atom in the difference map.

The asymmetric unit of I is illustrated in Figure 3.26, and consists of a zinc atom which is coordinated to the organic unit via the nitrogen atom on the amine functional group. The nitrogen atom has a tetrahedral geometry and is observed to be planar, along with the trans carboxylic acid group, to the aromatic ring. The unit cell contains four asymmetric units. The zinc atom lies on a two-fold rotation axis, and the rest of the molecule is generated by this symmetry operation, as illustrated in Figure 3.27 below.

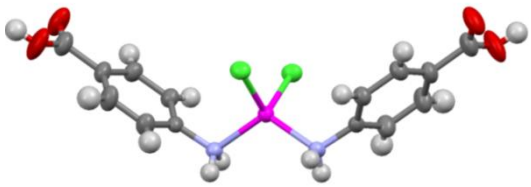

Figure 3.27: Molecular geometry of compound I.

The zinc atom is tetrahedrally coordinated to two chloro ligands, and two organic ligands. The bond distances between the two chloro ligands and zinc atom (Zn1—Cl2) are 2.245(5) Å while the distance between the nitrogen atoms and the zinc atom (Zn1—N1) are also equal at 2.058(2) Å.

The tetrahedral geometry of zinc atom is slightly distorted with a Cl2—Zn1—Cl2 angle of 109.08(5)° while the nitrogen atoms form an angle (N1—Zn1—N1) of 114.97(5)° with the metal centre.

The molecular packing results in a structure that consists of alternating organic and inorganic layers. The organic layer is comprised of two separate layers of organic ligands, effectively forming an organic bi-layer, while the inorganic layer contains the metal and halogen atoms. The layers extend parallel to the bc-plane.

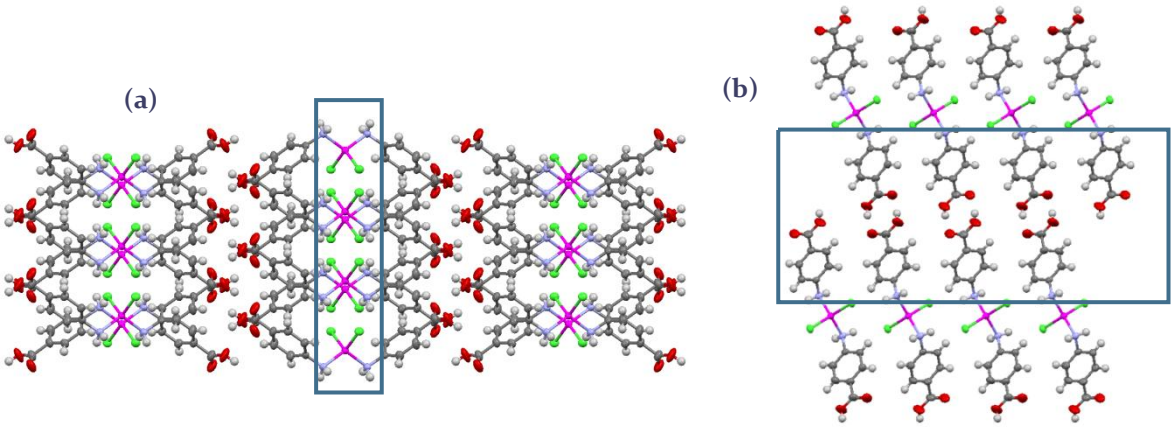

Figure 3.28: (a) Expansion viewed along the c-axis and (b) along the b-axis. The inorganic and organic bi-layers are indicated within the blocks.

The coordinated chloro ligands fail to bridge neighbouring zinc atoms by reason of the relative small size of the ligand, even though the molecules have the correct orientation for bridging by two ligands to occur. This observation is exemplified by the large distances between the terminal chloro ligand and neighbouring zinc atom (Zn1—Cl2···Zn1), where the Cl··· Zn distance is 3.879 Å.

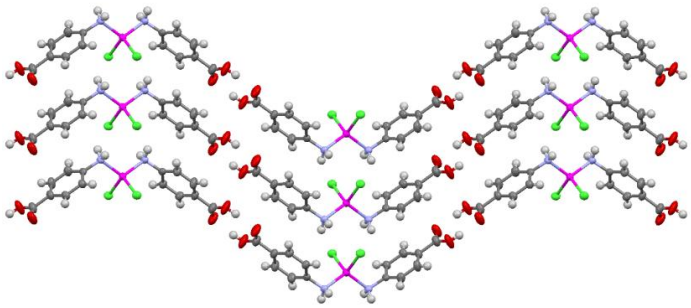

Figure 3.29: Expansion viewed along the c-axis.

In the inorganic layer a hydrogen bonding interaction is present between the nitrogen atom of the amine group and a chloro ligand (N1—H1A···Cl2) at a distance of 2.64(2) Å. As a result of the aromatic rings lying parallel to one another, π-π interactions fix the coordinated inorganic units at a particular distance from one another.

The aromatic rings on the organic components lie in parallel planes. Additionally they also lie parallel to those benzene rings that make up the organic bi-layer and neighbouring bi-layers alternate in their orientation. The parallel packing of the organic ligands in the organic layers fixes the discrete inorganic unit and contributes to their packing orientation. As a result of the aromatic rings lying parallel to one another, π-π interactions fix the coordinated inorganic units particular distance from one another.

Further expansion produces inorganic layers composed of discrete units that organize into a two-dimensional grid to produce an inorganic sheet. The organic constituents are connected via hydrogen bonds between their carboxylic acid functional groups. This produces an organic bi-layer that alternates successively with an inorganic layer (Figure 3.28).

There exist hydrogen bonds between the oxygen atoms of the carboxylic groups (O2—H1···O1) at a distance of 2.609(3) Å (Table 3.5). Additionally between the nitrogen atom of the amine and a chloro ligand (N1—H1A···Cl2) at a distance 3.5028(2) Å and (N1—H1B···Cl2) at a distance 3.3978(2) Å H-bonds exist.

Table 3.5: Hydrogen-bond geometry of structure I, (Å, °).

Compound I				
D—H···A	***D—H***	***H···A***	***D···A***	***D—H···A***
O2—H1···O1 [i]	0.80	1.82	2.609(3)	170
N1—H1A···Cl2 [ii]	0.90	2.64	3.5028(2)	162
N1—H1B···Cl2 [iii]	0.90	2.60	3.3978(2)	148

Symmetry codes: (i) –x +3/2, -y +3/2, -z + 2; (ii) –x +1, -y, -z + 2; (iii) –x +1, y – 1, -z +3/2.

The aromatic rings of the organic constituents lie in planes that are parallel to one another, however there is no direct overlap between the rings and they have a slipped parallel arrangement. The distance between the centre of the parallel rings are 4.725 Å (centroid-to-centroid distance).

II: bis(4-aminobenzoato -N)- dichloromercury(II))

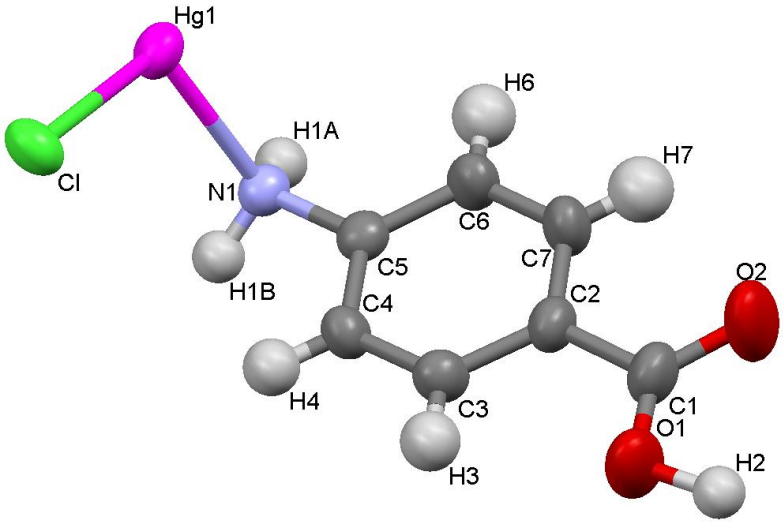

Figure 3.30: Asymmetric unit of compound II: Ellipsoids are drawn at the 50% probability level.

The asymmetric unit consists of a mercury metal centre that coordinates to the organic unit via the nitrogen atom from the amine functional group. The nitrogen atom has a tetrahedral geometry and is observed to be planar, along with the trans carboxylic acid group, to the aromatic ring. It is observed that the unit cell is generated by 4 asymmetric units.

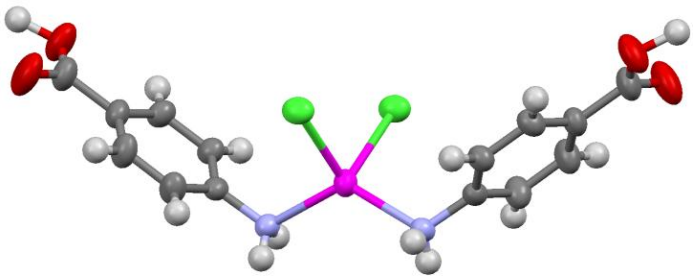

Figure 3.31: Molecular geometry of compound II.

It is observed that compound II is isostructural to compound I. The mercury atom adopts a tetrahedral geometry that coordinates to two chloro ligands and to two organic ligands. The bonding distances between the coordinated chloro ligands and the metal centre (Hg1—Cl) are 2.5052(37) Å, while the distances between the nitrogen atoms and the mercury atom (Hg—N) are also equal at 2.2585(37) Å. The chloro ligands produce an angle (Cl—Hg—Cl) of 98.25(4)° with the metal centre, while the angle formed by the nitrogen atoms (N—Hg—N) is 127.44(16)°, consequently causing the mercury tetrahedral geometry to be distorted. The aromatic rings of the two ligands lie on planes that intersect one another.

The nitrogen atom of the amine group coordinates to the mercury atom while the carboxylic acid in the trans position, and forms a dimer with a neighbouring organic unit (Figure 3.32).

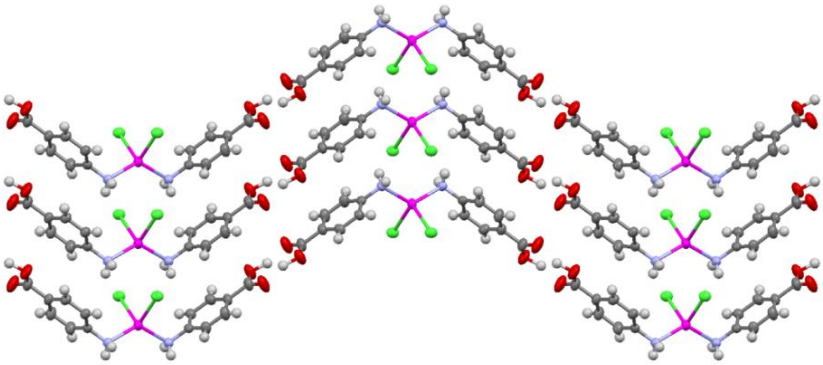

Figure 3.32: Expansion viewed along the c-axis.

The aromatic rings on the organic components lie in parallel planes. Each hydrogen bonded chain follows a wave-like structure due to the dihedral angle that is formed between intersecting organic planes. The parallel packing of the organic layers fixes the discrete inorganic unit and contributes to their packing orientation.

In the image of the previously discussed structure, it is observed that the coordinated chloro ligand fails to bridge neighbouring mercury. The distances between the coordinated Cl ligand and a neighbouring mercury metal atom (Hg—Cl···Hg) is observed to be 3.555 Å. This distance can be observed to be smaller than that of the previous zinc structure. As a result, the aromatic rings that lie parallel to one another, have shorter distances between them and subsequently their π-π interactions increases.

Further expansion produces inorganic layers composed of discrete units that organize into a two-dimensional grid to produce an inorganic sheet. The organic constituents are connected via hydrogen bonds between their carboxylic acid functional groups. This produces an organic bi-layer that alternates successively with an inorganic layer (Figure 3.33).

The packing, viewed along the *b*-axis clearly indicates the bi-layer of the organic constituent, alternating with the inorganic layer. The orientation of the mercury tetrahedron alternates in successive inorganic layers, which can be observed when viewed down the c-axis.

(a)

(b)

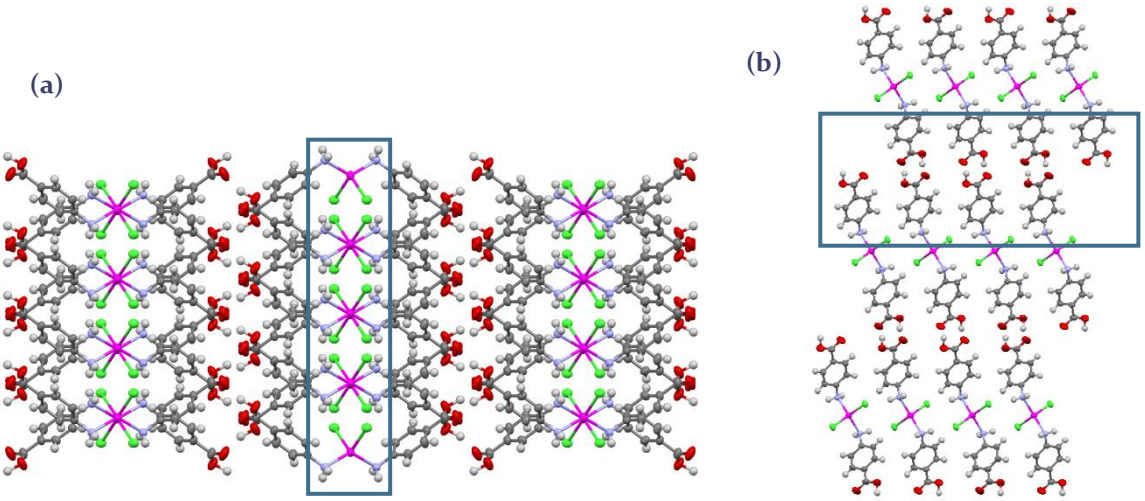

Figure 3.33: Packing of structure viewed along the (a) c-axis and (b) along the b-axis. The inorganic and organic bi-layers are shown within the blocks.

There exist hydrogen bonds between the oxygen atoms of the carboxylic groups (O2—H1···O1) at a distance of 2.600(5) Å (Table 3.6). Additionally two hydrogen-bonds exist between the nitrogen atom of the amine group and the chloro ligands at distances (N1—H1A···Cl) 3.407(3) Å and (N1—H1B···Cl) 3.344(3) Å.

Table 3.6: Hydrogen-bond geometry of structure II, (Å, °).

Compound II				
D*—*H*···*A	***D*—*H***	***H*···*A***	***D*···*A***	***D*—*H*···*A***
N1—H1A···Cl [i]	0.90	2.52	3.407(3)	168.3
N1—H1B···Cl [ii]	0.90	2.63	3.344(3)	136.8
O2—H1···O1 [iii]	0.82	1.79	2.600(5)	169.4

Symmetry codes: (i) –x +1, -y, -z + 2; (ii) –x +1, y -1, -z + 3/2; (iii) –x + 3/2-y +3/2, -z + 2.

The aromatic rings of the organic constituents lie in planes that are parallel to one another and the orientation of the planes alternate in organic bi-layers. However, there is no direct overlap between the rings and it is observed that they have a slipped parallel arrangement. The distance between the centres of parallel rings (centroid-to-centroid distance) is 4.648 Å.

III: bis(4-aminobenzoato -N)-dichlorocopper(II))

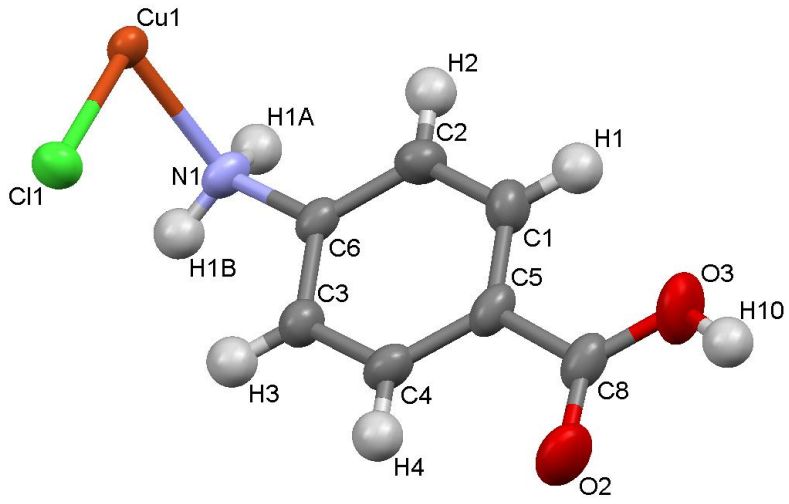

Figure 3.34: Asymmetric unit of compound III: Ellipsoids are drawn at the 50% probability level.

The asymmetric unit consists of a copper metal centre that coordinates to a chloro ligand and to the organic unit via the nitrogen atom from the amine functional group. The nitrogen atom has a tetrahedral geometry and is observed to be planar, along with the trans carboxylic acid group, to the aromatic ring. The copper atom is positioned on a centre of inversion, and the rest of the molecule is generated by the symmetry operator (-x, -y, -z). By expanding the asymmetric unit, via short contacts, it is observed that the unit cell is generated by only one asymmetric unit.

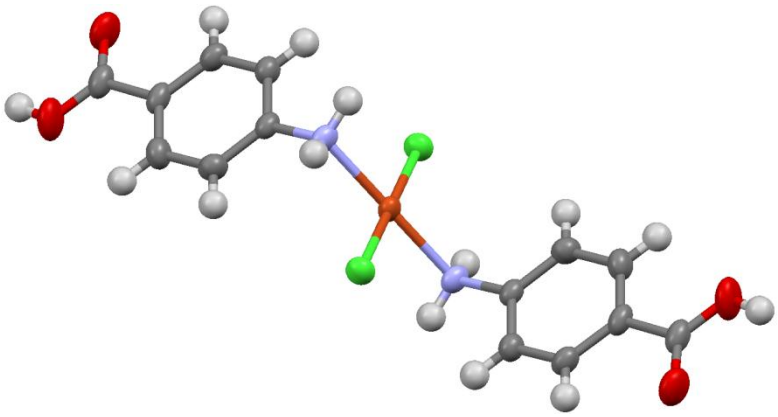

Figure 3.35: Molecular geometry of compound III.

The copper atom adopts a square planar geometry and coordinates to two chloro ligands and two organic ligands. The bonding distance between the metal centre and the chloro ligands (Cu1—Cl2) are equal at 2.2514(7) Å and the coordination distance between the nitrogen atoms and the metal centre (Cu1—N1) are 2.0361(28) Å and are also equivalent.

The angles that are produced between the nitrogen atom and the chloro ligands (N—Cu—Cl) on the geometrical plane are 88.60° and 91.40°. The aromatic rings, situated on the organic ligands, lie on parallel planes and therefore have no dihedral angle. They do however form an intersecting angle of 69.37 °with the geometrical plane of the metal coordination sphere.

Analogous to the previously described structure, a nitrogen from the amine coordinates to the copper coordination sphere while the carboxylic group forms a hydrogen bonded dimer with neighbouring organic units, however due to the square planar geometry of the copper atom, a stepwise organic-inorganic polymeric chain is generated (Figure 3.36).

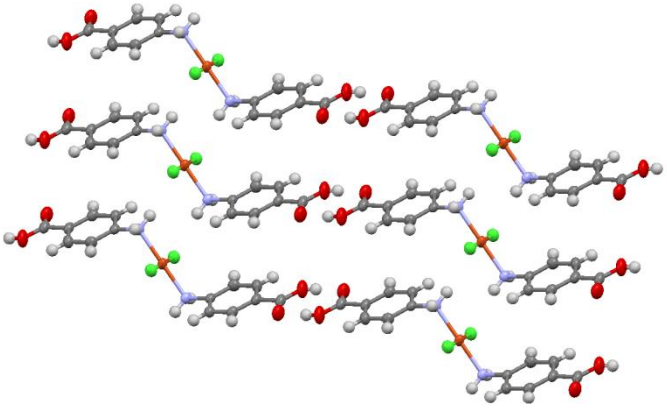

Figure 3.36: Expansion of the coordination sphere.

The aromatic rings on the organic components lie in parallel planes. The parallel packing of the organic layers fixes the discrete inorganic unit and contributes to their packing arrangement. The copper atom coordination units do not covalent bonds to one another. The units do however form a, hydrogen bonded, two-dimensional sheet consisting of isolated inorganic units orientated along the ab-plane.

Due to the relatively small size of the ligands, it is observed once again that the coordinated chloro ligand fails to bridge neighbouring copper atoms. The distances between the coordinated chloro ligands and a neighbouring copper atoms (Cu—Cl···Cu) is observed to be 3.549 Å. However, the arrangement of discrete inorganic units to form a polymeric chain would suggest the possibility of an electrostatic potential occurring between coordinated chloro ligands and neighbouring copper atoms, as proposed by Brinck et al. (1992).

Expansion of the unit cell produces inorganic chains composed of discrete units along both the a-axis and b-axis which then organize into a two-dimensional grid to produce an inorganic sheet. The organic constituents are connected via hydrogen bonds between their carboxylic acid functional groups. This produces an organic bi-layer that alternates successively with an inorganic layer (Figure 3.37).

The packing, viewed along the a-axis clearly indicates the bi-layer of the organic constituent, alternating with the single isolated inorganic layer. The expansion of the inorganic layer consisting of inorganic units can be observed when viewed along both the a-axis and b-axis.

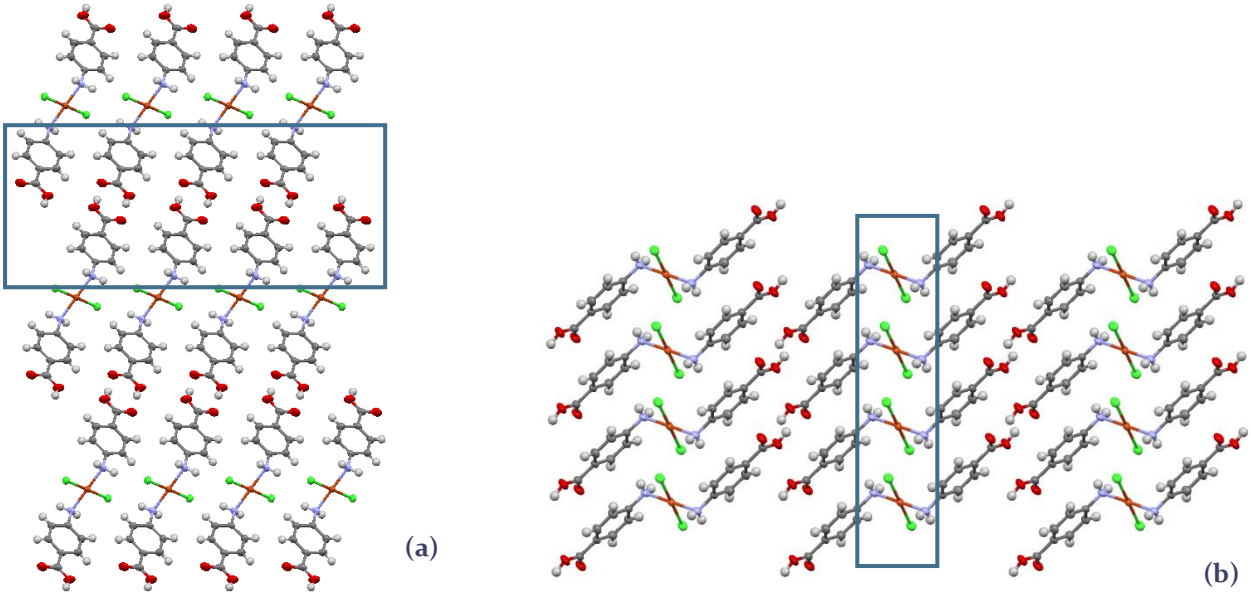

Figure 3.37: Packing of structure viewed along the (a) a-axis and (b) along the b-axis. The inorganic layer and organic bi-layers are shown within the blocks.

Between the carboxylate groups dimers are formed, and the hydrogen bond associated with this interaction (O1—H1···O2) has a length of 2.615(3) Å (Table 3.7). Additionally a hydrogen bonds exists between the nitrogen atom of the amine group and the chloro ligand at a distance (N1—H1B···Cl2) 3.488(3) Å.

Table 3.7: Hydrogen-bond geometry of structure III, (Å, °).

Compound III				
D*—*H*···*A	***D*—*H***	***H*···*A***	***D*···*A***	***D*—*H*···*A***
O1—H1···O2 [i]	0.763(2)	1.861(2)	2.615(3)	1.69.8(2)
N1—H1B···Cl2 [ii]	0.90	2.60	3.488(3)	170.7

Symmetry codes: (i) –x + 3, -y +1, -z - 1; (ii) x, y + 1, z.

The aromatic rings of the organic constituents lie in planes that are parallel to one another and the distance between these planes is 3.37 Å. There is no direct overlap between the rings and there exist an extreme slipped displacement. The distance between the centre of parallel rings is equal to 4.646 Å (centroid-to-centroid distance). The angle produced by the ring normal and the vector through the ring centre is 48.1° which is far beyond the general angle of 20° expected for these types of π-π interactions.

IV: catena-(bis(μ₂-bromo)-bis(4-aminobenzoato)-mercury(II))

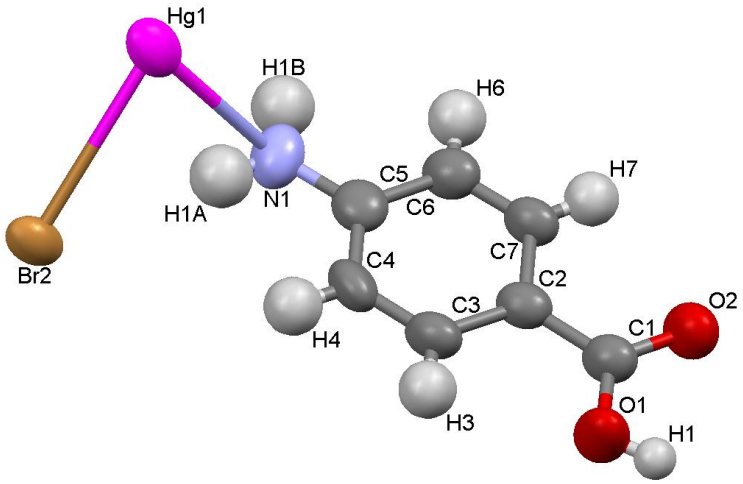

Figure 3.38: Asymmetric unit of compound IV: Ellipsoids are drawn at the 50% probability level.

The asymmetric unit of compound IV is illustrated in Figure 3.38 and consist of a mercury atom that coordinates to a bromo ligand and to an organic unit via the nitrogen atom. The nitrogen atom on the amine functional group has a distorted tetrahedral geometry, and it observed that the amine group lies parallel with the aromatic ring and the trans carboxylic acid group. The unit cell comprises one asymmetric unit.

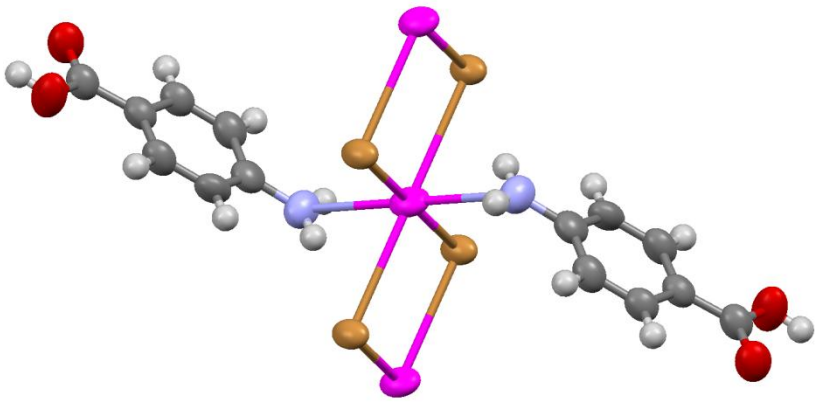

Figure 3.39: Molecular geometry of compound IV.

The mercury atom coordinates to two four μ_2-bromo ligands in the equatorial positions, and to two 4-aminobenzoic acid ligands atoms at the axial positions to produce an octahedral geometry. The bonding distance between the mercury atom and the bromo ligands is equivalent for each trans bromo pair lying on the equatorial plane. These distances (Hg—Br) are 2.4520(9) Å and 3.259 Å, with the latter distance illustrating extreme elongation.

The difference in bond lengths are consequential of the bromo ligands forming both electron sharing covalent bonds and electron pair donating bonds within the octahedron. The bonding distance, representing the coordination between the mercury atom and the equatorial nitrogen atoms (Hg1—N1), is equivalent at 2.824 Å. The octahedron is distorted, axially by 75.09° relative to the equatorial plane and equatorially, the angle generated by the bromo ligands, is 87.59°. The aromatic rings, situated on the organic ligands, lie on parallel planes. They do however form an intersecting angle of 56.60° with the equatorial plane of the mercury octahedron (Figure 3.40).

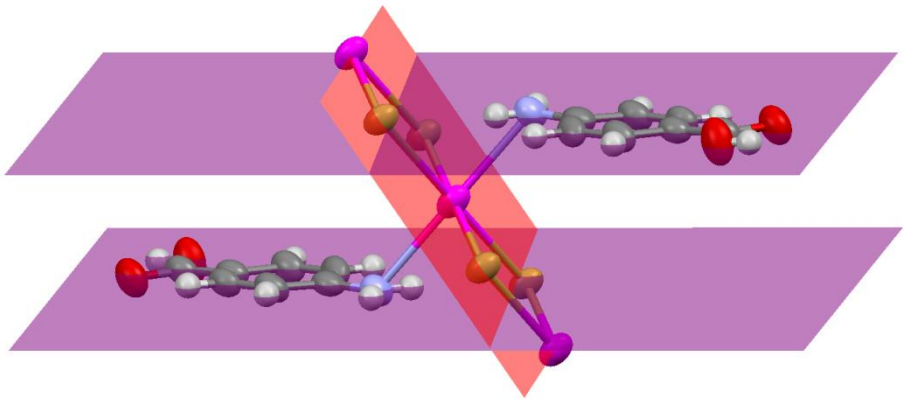

Figure 3.40: Illustration of the planes, from which the intersecting angle can be determined.

Expanding the octahedron produces a one-dimensional polymeric chain along the b-axis (Figure 3.41) where edge sharing of ligands occur via the equatorial bridging polymeric bromo ligands. The distance between neighbouring metal centres is 4.160 Å and these atoms form four membered rings with the bromo ligands.

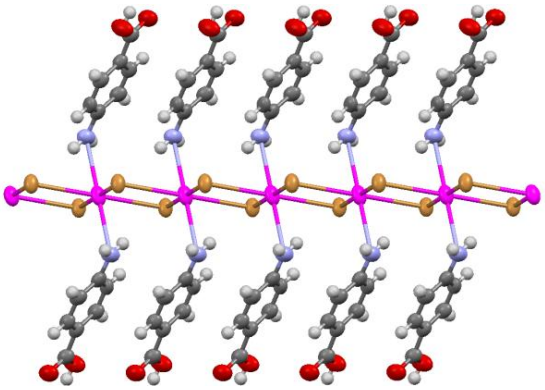

Figure 3.41: Expansion of the coordination sphere.

Similar to the structures describes previously, the amine group coordinates to the mercury atom via lone pairs while the carboxylic acid group produces hydrogen bonded dimers with neighbouring organic units which consequently forms the organic bi-layers (Figure 3.42). This intermolecular interaction connects neighbouring inorganic layers that alternate, successively, with the organic bi-layer, and link polymers.

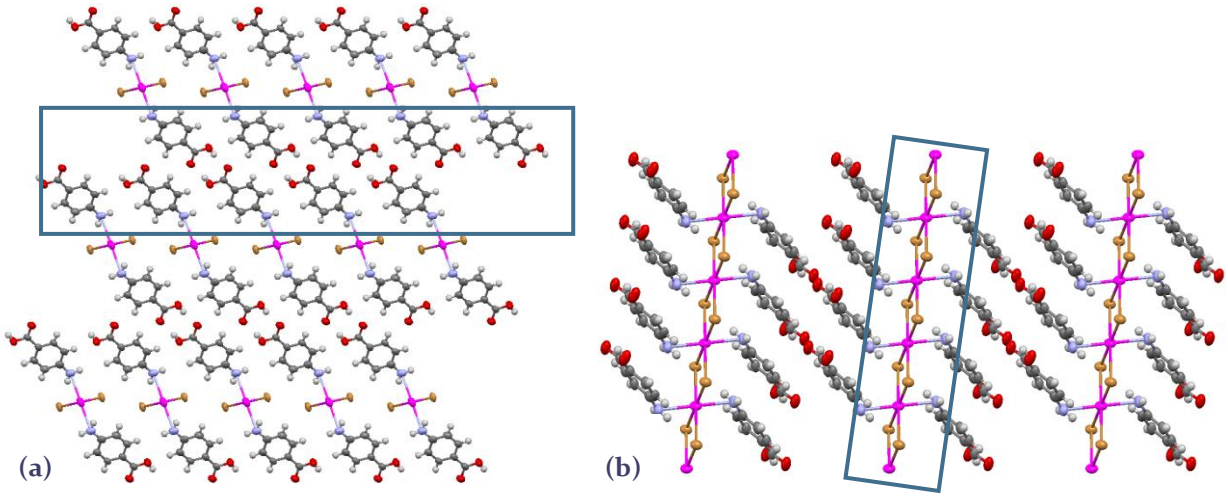

Figure 3.42: Packing of structure viewed along the (a) a-axis and (a) along the b-axis. The inorganic layer and organic bi-layers are shown within the blocks.

The packing observed in the structure along the c-axis, illustrates how further expansion of the unit cell produces inorganic chains that organize into a two-dimensional grid to produce an inorganic sheet that consist of discrete chains. Figure 3.43 further illustrates how this inorganic grid alternates with an organic layer of coordinated organic constituents.

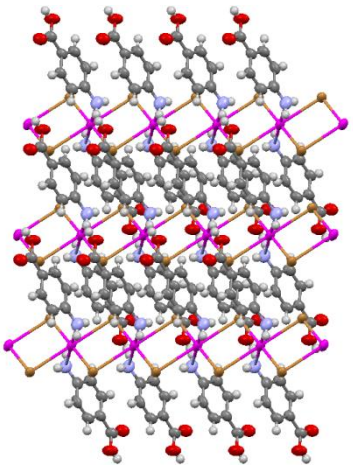

Figure 3.43: Packing of structure viewed along the c-axis.

Between the carboxylic acids, hydrogen-bonds exist that produce hydrogen bonded dimers and the hydrogen bonding associated with this interaction (O1—H1···O2) has a distance of 2.628(1) Å (Table 3.8). A hydrogen bond occurs between a nitrogen atom and a bromo ligand (N1—H1A···Br2) at 3.687(9) Å.

Table 3.8: Hydrogen-bond geometry of structure IV, (Å, °).

Compound IV				
D*—*H*···*A	***D*—*H***	***H*···*A***	***D*···*A***	***D*—*H*···*A***
O1—H1···O2 [i]	0.82	1.83	2.628(1)	165.8
N1—H1A···Br2 [ii]	0.86	2.83	3.687(9)	176.8

Symmetry codes: (i) –x + 3, -y + 3, -z + 1; (ii) x - 1, y, z.

The aromatic rings of the organic constituents lie in planes that are parallel to one another and the distance between these planes is 3.470 Å. There is no direct overlap between the rings and it is observed that there exists an extreme slipped displacement which is analogous to previous structures. The distance between the centre of parallel rings are 4.160 Å (centroid-to-centroid distance). The angle produced by the ring normal and the vector through the ring centre is 35.20° which is larger than the general angle of 20° expected for these types of π-π interactions.

Novel Isonicotinic acid containing structures

A novel isonicotinic acid containing compound was synthesized and yielded a suitable crystal for SCD, and its structural features are discussed below.

V: bis(μ-isonicotinoato) tetrakis[μ-bromomanganate(II) dibromo]

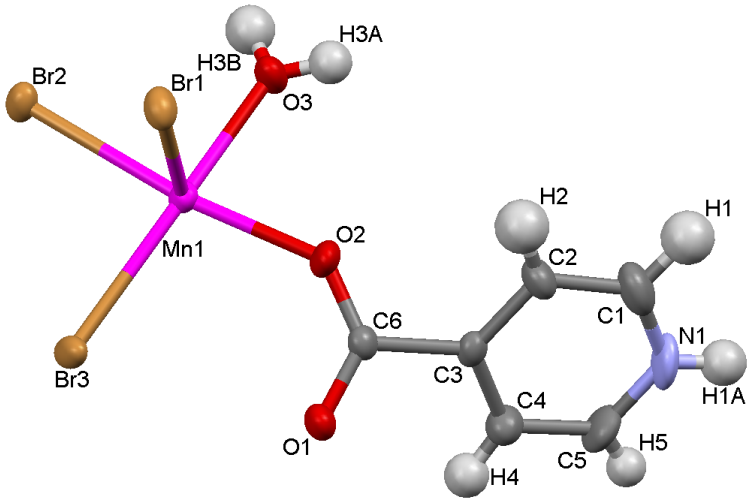

Figure 3.44: Asymmetric unit of compound V: Ellipsoids are drawn at the 50% probability level.

The asymmetric unit is shown in Figure 3.44 and consist of a manganese atom that coordinates to three bromo ligands and a water molecule as well as to an organic ligand via one of the oxygen atoms of the carboxylate group. The pyridine nitrogen atom is protonated. The carboxylate group does not lie parallel with the plane generated by the aromatic ring and is rotated by 42.79 ° with respect to this plane. The unit cell comprises four asymmetric units.

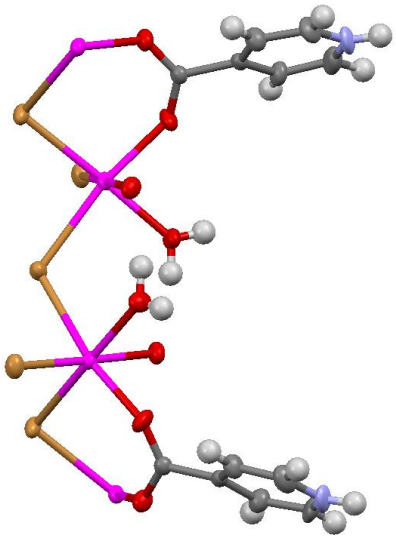

Figure 3.45: Molecular geometry of compound V.

The manganese atom adopts a distorted octahedral geometry. The equatorial positions of the octahedron are occupied by the two bridging bromo ligands and two oxygen atoms; one from the water molecule and and one from carboxylate group. The axial positions of the octahedron are occupied by a terminal bromo ligand and an oxygen atom of a carboxylate group belonging to a different organic unit.

The bonding distances between the metal centre and the μ_2-bromo ligands are (Mn1—Br2) 2.7248(6) Å and (Mn1—Br3) 2.6798(7) Å. The oxygen atoms on the equatorial positions have coordination distances of (Mn—O3) 2.1809(31) Å and (Mn—O2) 2.1568(28) Å. On the axial positions coordination distances of (Mn—O1) 2.2126(26) Å and (Mn—Br1) 2.6673(7) Å are observed.

The two bridging bromo ligands occur on special positions, with a site occupying factor of 0.5. Bridging of neighbouring manganese atoms occurs through one μ_2-bromo ligand and two bidentate carboxylate oxygen groups consequently forming an edge sharing octahedron. The coordinated carboxylate group however only bridges neighbouring metal centres and its bidentate capacity generates a six-membered ring. Pairs of neighbouring metal atoms are bridged by two carboxylate groups and one bromo ligand. This observation is exemplified by the distance between neighbouring manganese atoms, which alternate between 4.047 Å and 4.580 Å.

The former distance represents those metal centres that have both a bridging bromo ligand and a carboxylate bridging mode while the latter distance characterizes those metal centres that only have a single bridging bromo ligand connecting them. The bridging between neighbouring metals via the oxygen atoms of the bidentate carboxylate fixes the distance between the metal atoms and conform shorter spaces between them.

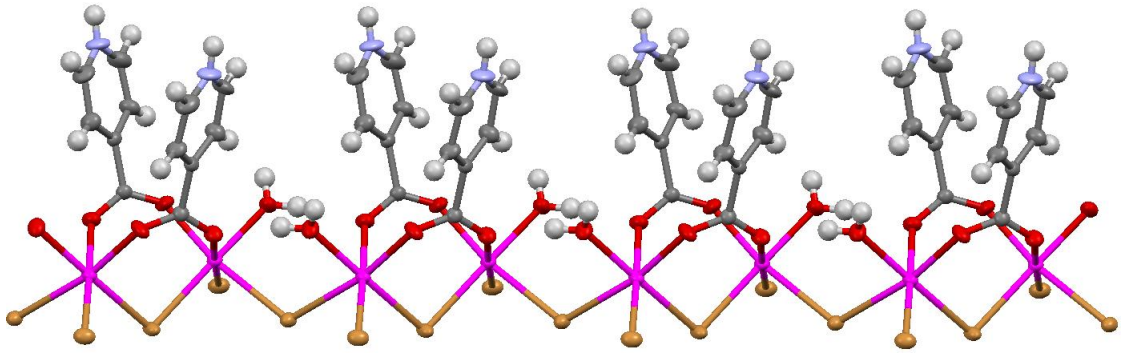

Figure 3.46: Expansion of the asymmetric unit viewed along the c-axis.

To our knowledge, this type of one-dimensional polymer has never been reported for any combination of organic ligand, metal atom or halogeno ligand.

Figure 13.46 illustrates how expansion of the octahedron produces a one-dimensional polymeric chain along the c-axis. In addition to the aqua ligands, the isonicotinato ligands are also positioned cis relative to the inorganic polymer, while all the bromo ligands, shared or terminal, are cis and positioned on the opposite side of the polymer.

The carboxylate group is observed to have an angular offset to the plane through the aromatic ring of the organic ligand and the ligand is rotated by an angle of 42.31° with respect to the coordinating functional group. This may be due to competitive non-covalent intermolecular interactions that occur firstly as a result of π-π stacking between neighbouring organic rings and secondly through hydrogen bonding that occurs between functional groups. These hydrogen bonds occur between the hydrogen atom of the pyridine group and a bromo ligand situated on an opposing inorganic chain. It appears as if hydrogen bonding overcomes π-π stacking which then evidently constrains the ligands and causes the organic rings to lie in non-parallel planes and in addition increases the distances between their centroids to a distance of 4.368 Å.

The packing, along the c-axis, observed in structure IV is illustrated in Figure 3.47. It is observed that the carboxylate group coordinates to the manganese atom via the oxygen atoms while the protonated nitrogen atom in the trans position generates hydrogen bonds with terminal bromo ligands that are coordinated on the neighbouring inorganic chain which consequently produces a single organic layer. This intermolecular interaction connects neighbouring inorganic sections that alternate successively with the organic layer.

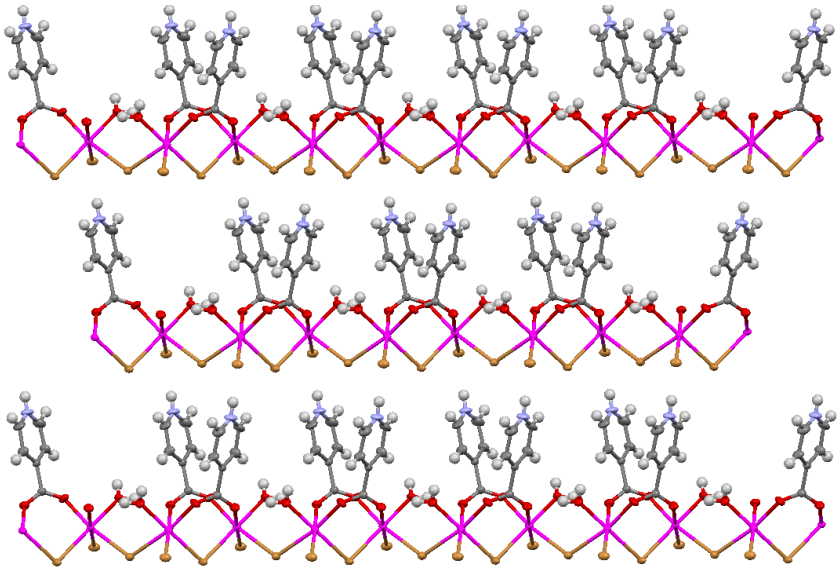

Figure 3.47: Packing of structure viewed along the c-axis.

It is observed that the inorganic polymers lie parallel to one another (Figure 3.47) and as result constrains organic layers to be formed in parallel succession.

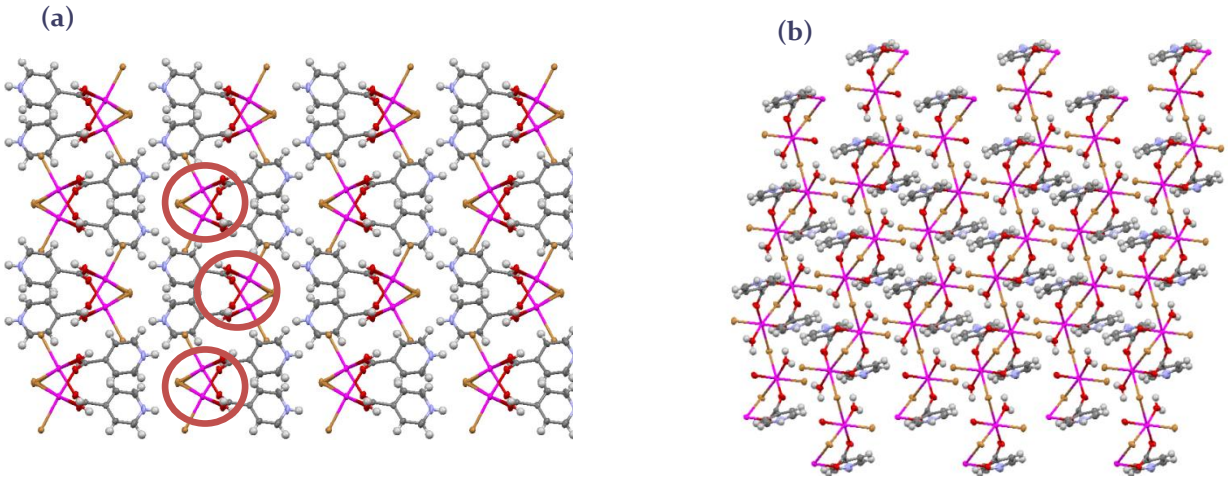

Figure 3.48: Packing of structure viewed along the (a) a-axis and (b) b-axis. Inorganic polymers are indicated by the circles.

Hydrogen bonding parameters are listed in Table 3.9. There exists intramolecular hydrogen bonds within the inorganic chain between one of the hydrogen atoms on the water ligand and an oxygen atom on a bridging carboxylic acid group (O3—H3B···O1) at a distance of 2.810(4) Å. Hydrogen bonding also exists between neighbouring inorganic chains, where the hydrogen atom on the water ligand interacts with a bromo ligand from another inorganic chain (O3—H3A···Br1) at a distance of 3.350(3) Å. Additionally between the protonated nitrogen atom of the pyridinium group and the coordinated bromo ligand (N1—H1A···Br1) a hydrogen bond occurs at a distance of 3.286(4) Å

Table 3.9: Hydrogen-bond geometry of structure V, (Å, °).

Compound V				
D*—*H*···*A	***D*—*H***	***H*···*A***	***D*···*H***	***D*—*H*···*A***
O3—H3A···Br1 [i]	0.82(6)	2.55(6)	3.350(3)	165(5)
O3—H3B···O1 [ii]	0.85(6)	1.96(6)	2.810(4)	172(5)
N1—H1A···Br1 [iii]	0.82(6)	2.53(6)	3.286(4)	153(4)

Symmetry codes: (i) –x + 1/2-y + 1/2, -z + 2; (ii) x - 1, y, z; (iii) x + 1/2, y + 1/2, z.

The aromatic rings of the organic ligands lie in planes that are not parallel to one another and are observed to be present in pairs. Gaps are observed to exist between pairs of aromatic rings. The distances between the centroids of the aromatic rings are 4.368 Å which is not indicative of aromatic interactions. The ring normal and the vector through the ring centroids produce an angle of 21.23° which indicate that the rings don't overlap and are displaced in a parallel fashion.

Comparison Study

This section aims to compare the structural features and trends in the novel coordination hybrid structures, and to compare these features with those of the literature structures where relevant. Isostructurality parameters between structures are determined by using ISOV software package (Fabian and Kalman, 1999). The degree of similarity between isostructural structures can be expepressed by employing the isostructurality parameters reported by the ISOV software package (Fabian and Kalman, 1999). The parameter I(v) gives an indication of the correspondence of atom positions of isostructural compounds. The higher the I(v) value reported, the better the correspondence between structures.

4-Aminobenzoic acid containing structures

The 4-aminobenzoic acid containing coordination compounds, I (Figure 3.49a) and II (Figure 3.50a) have monoclinic crystal systems and have equivalent $C2_1/c$ space groups. Compound I has a tetrahedral geometry which is generally the observed geometry for zinc metal atoms and compound II has a tetrahedral mercury metal atom which is also a common geometry for mercury atoms. It is observed that compound I and II are isostructural with I(v)=83.0. Compound IV (Figure 3.50b) has a triclinic crystal system and a $P1$ space group and comprises a mercury atom demonstrating an octahedral coordination geometry. Compound D (Figure 3.49b) has a tetrahedral geometry and crystallises in the monoclinic crystal system and exhibits the $C2_1/c$ space group but is not isostructural to compound I or II.

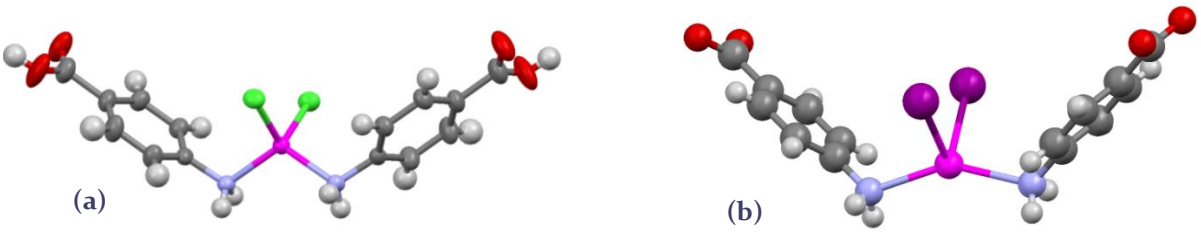

Figure 3.49: Molecular units of (a) compound I: di-chloro-bis(4-aminobenzoic-acid-N)-zinc(II) and (b) compound D: : di-iodo-bis(4-aminobenzoic-acid-N)-cadmium(II) , (Wang, et al., 2002).

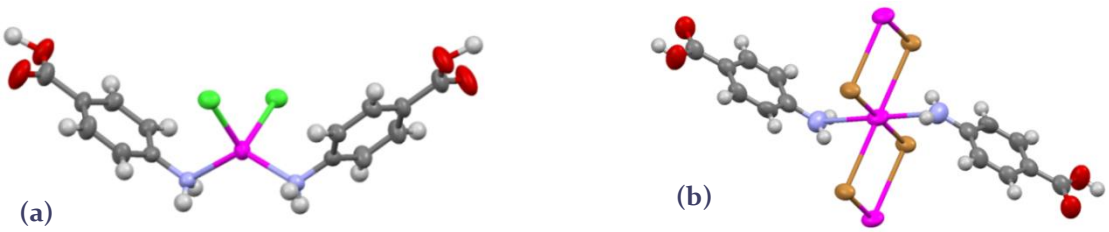

Figure 3.50: Molecular units of (a) compound II: di-chloro-bis-(4-Aminobenzoic acid-N)-mercurate(II)) and (b) compound IV: catena-(bis(μ2-bromo)-bis(4-Aminobenzoicacid)-mercury(II)).

The unit cell parameters of the four structures are listed in Table 3.10:

Table 3.10: Unit cell parameters of the selected 4-aminobenzoic acid containing coordination compounds (Isostructural compounds I and II are here shown in blue).

Compound	Space Group	a(Å)	bÅ	cÅ	α/°	β/°	γ/°	I(v)
I	*C*2/c	30.646(2)	4.7248(3)	11.6157(8)	90.00	97.0890(10)	90.00	83.0
II	*C*2/c	31.519(2)	4.6476(3)	11.7386(8)	90.00	97.7930(10)	90.00	
IV	*P*$\bar{1}$	4.1601(8)	7.3828(14)	14.413(3)	100.368(3)	98.167(3)	93.426(3)	-
D	*C*2/c	15.8720(2)	4.5115(1)	25.0187(7)	90.00	97.474(2)	90.00	-

Figures 3.51 to 3.52 illustrate the packing of the molecular units in one-dimension. In all the structures the aromatic planes of the ligands in a specific organic layer are parallel. In the tetrahedrally coordinated structures D, I and II organic layers alternate in their orientation, but they adopt the same parallel orientation in the octahedrally coordinated structure IV.

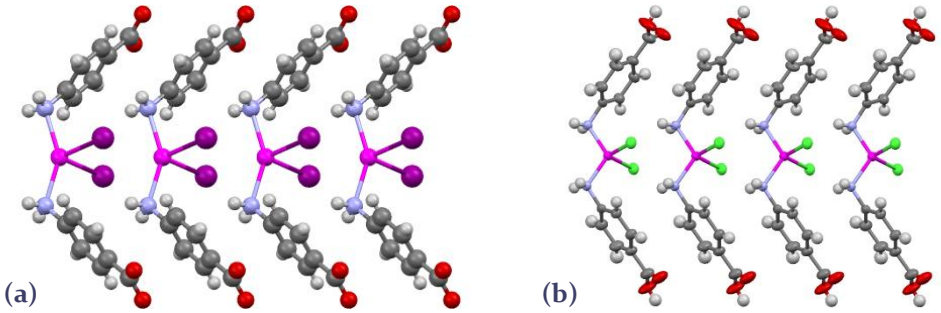

Figure 3.51: Expansion of the molecular units of compound (a), D and (b), I.

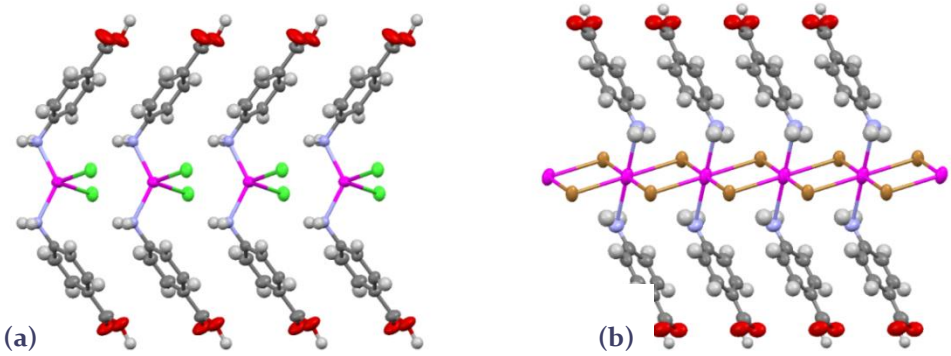

Figure 3.52: Expansion of the molecular units of compound (a), II and (b), IV.

The distances that exist between the metal atom and the coordinated halide (M—X) are observed to be (Cd—I) 2.828 Å, (Zn—Cl) 2.245 Å and (Hg—Cl) 2.505 Å for compounds D, I and II respectively. The distances that occur between coordinated halogeno ligands and neighbouring metal atoms (M···X) are measured to be (Cd···I) 3.337 Å, (Zn···Cl) 3.879 Å and (Hg···Cl) 3.556 Å. It is noticed that the large iodo ligand has the largest M—X coordination distance, and as a result forms the shortest non-covalent bond M···X between neighbouring units.

The aromatic rings are tilted relative to the inorganic layer. This can be attributed to the tetrahedral geometry of the sp^3 nitrogen atom, and the need to accommodate the hydrogen atoms on the nitrogen atom. It was noted in the literature and in this study that ligands such as pyridine, are perpendicular to the inorganic layer due to the sp^2 hybridisation of the N atom.

The observed coordination distances that occur between the metal atom and halogen ligand (Hg—Br) of compound IV is 3.260(1) Å 2.452(9) Å and as a result, the coordinated bromo ligand is able to covalently bridge neighbouring units. The aromatic rings on the coordinated organic ligand are observed to tilt away from the perpendicular plane relative to the inorganic chain and produce an intersecting angle of 48.74°. Unlike the former compounds, structure IV has its trans organic ligands orientated in opposite directions.

Figures 3.53 and 354 illustrate the packing observed in the structures and it is observed that all the considered structures exhibit hydrogen bonded dimers between carboxylic acid groups that produce organic bi-layers and as a result form two-dimensional hydrogen bonded inorganic-organic sheets.

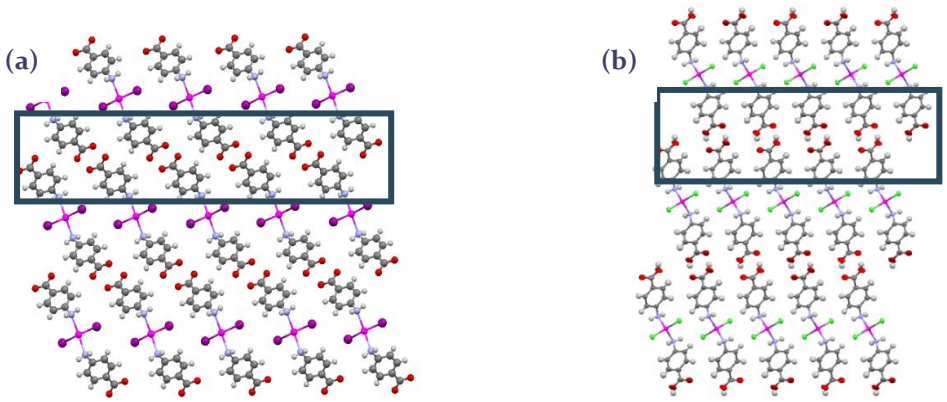

Figure 3.53: Packing of compound (a) D and (b) I viewed along the b-axis. The organic bi-layers are shown within the blocks.

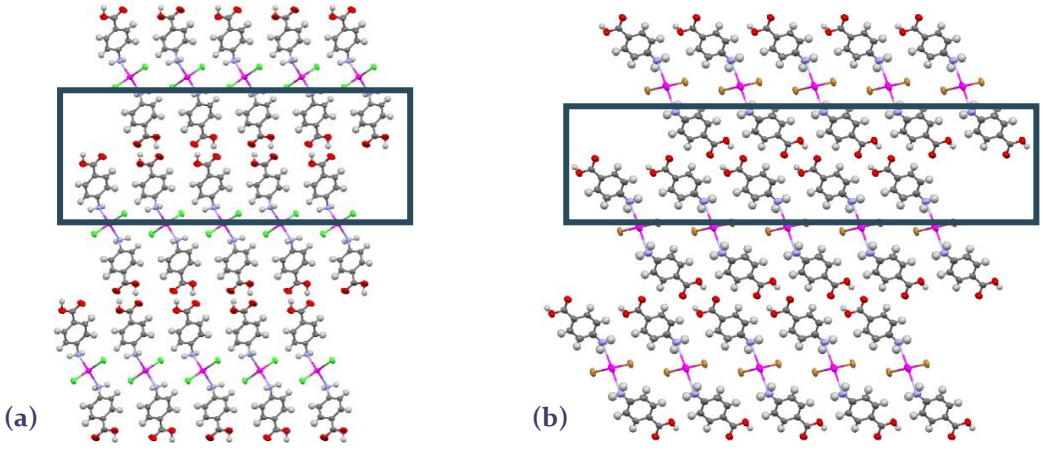

Figure 3.54: Packing of compound (a) II viewed along the b-axis and (b) IV viewed along the a-axis. The organic bi-layers are shown within the blocks.

Despite the similarities observed in the molecular expansion as well as packing of the 2-dimensional sheet, the structures differ in three-dimensional packing, except for structures I and II, as shown in Figure 3.55 and 3.56 below:

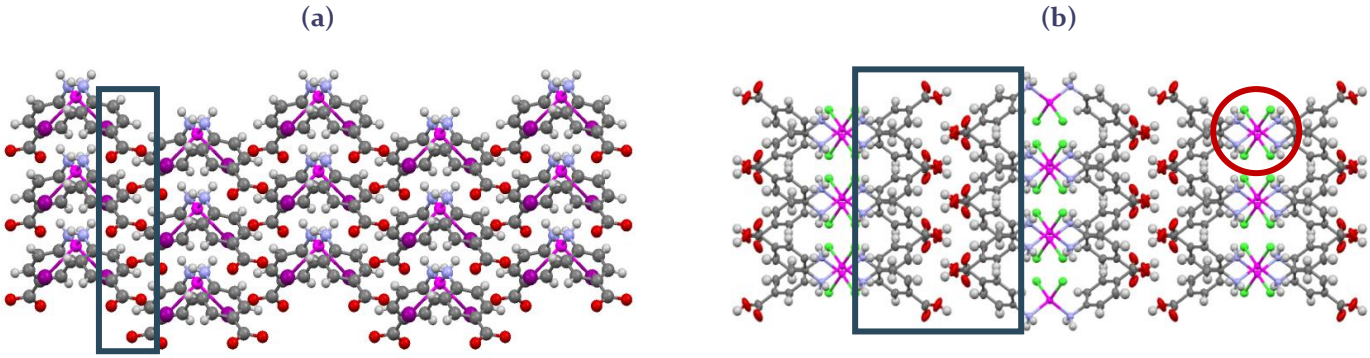

Figure 3.55: Packing of compound (a), D and (b), I viewed along the c-axis. The single organic and organic bi-layers are shown within the blocks. Inorganic units are shown within the circle.

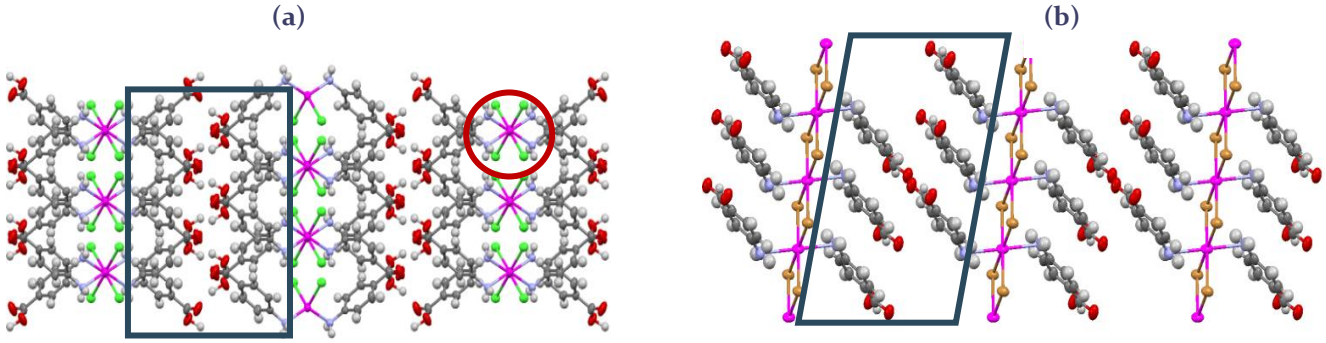

Figure 3.56: Packing of compound (a), II viewed along the c-axis and (b), IV viewed along the b-axis. The organic bi-layers are shown within the blocks. Inorganic units are shown within the circle.

Structure D, has an organic layer that alternates with the inorganic layer while structures I, II and IV have organic bi-layers that alternate with the inorganic layers. The discrete inorganic polymers in structures I and II are observed to lie parallel and expand along the c-axis and as a result form two-dimensional inorganic sheets.

The aromatic rings of all the structures are stacked in a slipped parallel displacement. The centroid-to-centroid distances are measured to be 4.512 Å, 4.725 Å, 4.648 Å and 4.160 Å for compound D, I, II and IV respectively. It appears that the inorganic component has a templating effect on the rings. The shortest centroid-to-centroid distances between the rings (4.160 Å) belongs to structure IV which consists of an inorganic polymer. The rings are observed to have a small displacement in their stacked arrangement and short distances between their centroids.

Crystal packing comparison across families

Structures of compound F and III crystallize in triclinic crystal systems and have equivalent *P*1 space groups. The palladium metal has a square planar geometry (compound F) and is similar to the square planar geometry observed for the copper metal in compound III. The structures however, have different organic ligands coordinated to the metal centres. Structure F has two isonicotinic acid ligands that coordinates through the ring sp^2 nitrogen, trans, to the palladium metal. Structure III has two 4-aminobenzoic acid ligands that coordinate through the sp^3 nitrogen from the amine, trans to the copper atom.

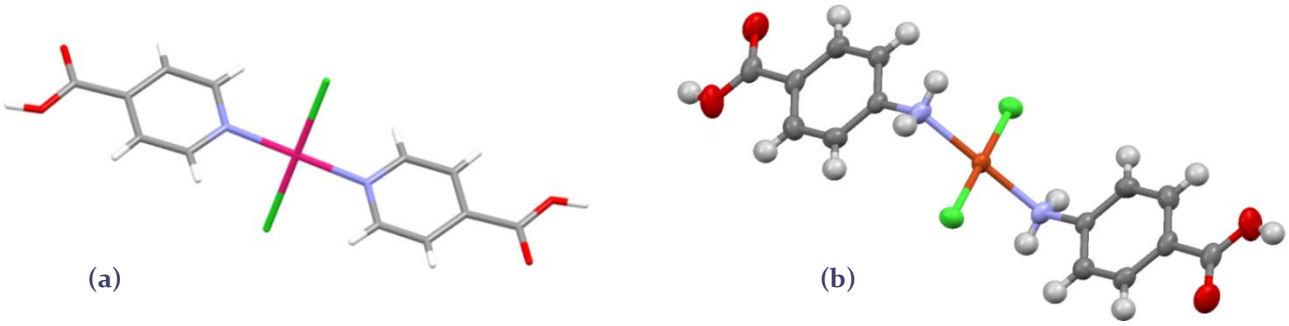

Figure 3.57: Molecular units of (a) compound F: trans-Dichloro-bis(pyridine-4-carboxylic acid-N)-palladium(II), (Qin. Et, al., 2002) and (b) compound III: di-chloro-bis-(4-Aminobenzoic acid-N)-copper(II)).

The organic ligands of structure F are observed to coordinate in a linear fashion to the palladium atom and maintain a planar geometry relative to the aromatic rings. The amine groups on the 4-aminobenzoic acid ligands maintain a tetrahedral geometry, and as a result, the aromatic rings lie on parallel planes, but not in the same plane as the $CuCl_2$ unit.

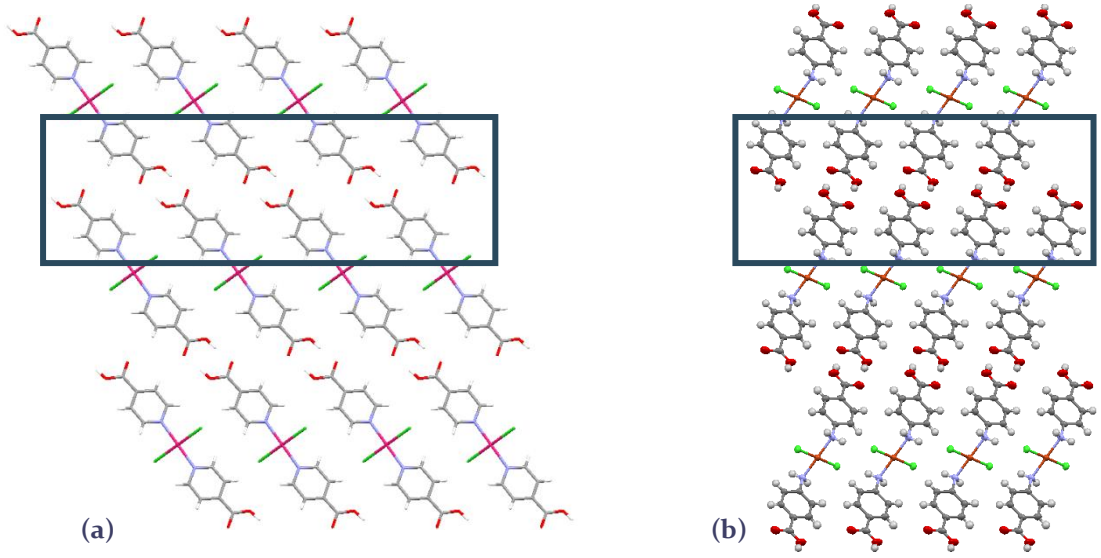

Figure 3.58: Packing of compound (a), F and (b), III viewed along the a-axis. The organic bi-layers are shown within the blocks.

Figure 3.58 illustrate the packing of F and III along the a-axis. It is observed that both structures form hydrogen bonded dimers that connect neighbouring coordination units and as a result, organic bi-layers are produced. Within both structures layers, consisting of coordinated molecules, are generated that comprises discrete coordination units.

In Figure 3.59 below, the packing of structure F and III are shown. It is observed that structure F forms a wave-like, hydrogen bonded chain while in structure III, a stepwise organic-inorganic chain is generated. The organic bi-layers can also be observed in this packing arrangement and are observed to alternate, in succession, with the inorganic layers.

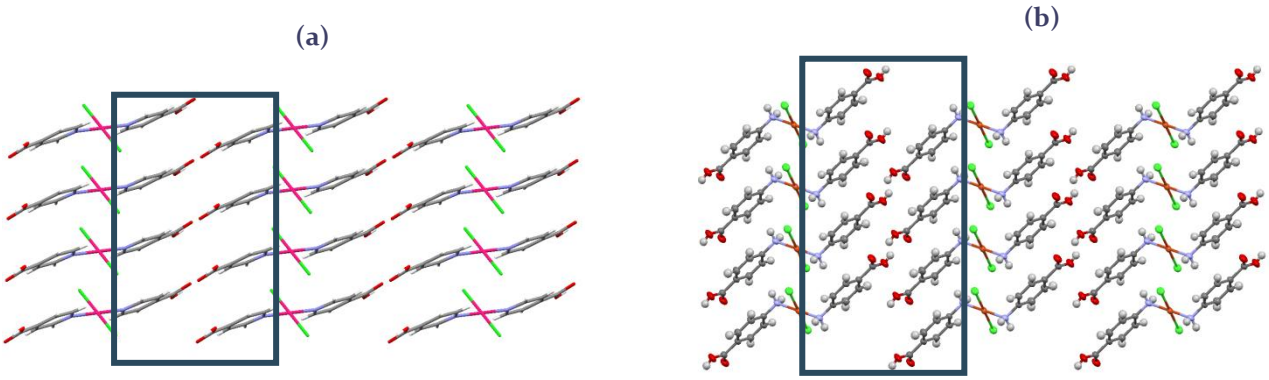

Figure 3.59: Packing of compound (a), F and (b), III viewed along the b-axis. The organic bi-layers are shown within the blocks.

In both the structures, the aromatic rings are observed to lie in planes that are parallel to one another. The stacking of the rings in structure F are slightly offset and have centroid-to-centroid distances of 3.955 Å, while in structure III they exist in extreme parallel displacement and have centroid-to-centroid distances of 4.646 Å.

The structure of the novel compound V is compared to a similar structure found in the literature (catena((μ$_3$-trimethylammoniumacetato)-tetrakis(m2-chloro)-aqua-di-manganese) with CSD reference code YARVUI. Albeit dissimilar organic ligands, the literature structure also comprises a one-dimensional inorganic chain made up of coordinated manganese octahedra.

Structure YARVUI (Figure 3.60(a)), has a $P2_1/n$ space group and structure V (Figure 3.60(b)) has a $C2/c$ space group, however both belong to the monoclinic crystal system. Structure YARVUI comprises manganese octahedra that are connected by bridging chloro ligands and via carboxylic groups of betaine to generate an infinite bond chain along the c-axis (Schreuer and Haussuhl, 1993). Structure V is made up out of manganese octahedra that are connected to neighbouring units via bridging bromo ligands and via carboxylic groups of isonicotinic acid to form an infinite chain along the a-axis. Instructure YARVUI, each carboxylate group bridges three metal atoms, while only two are bridged in structure V.

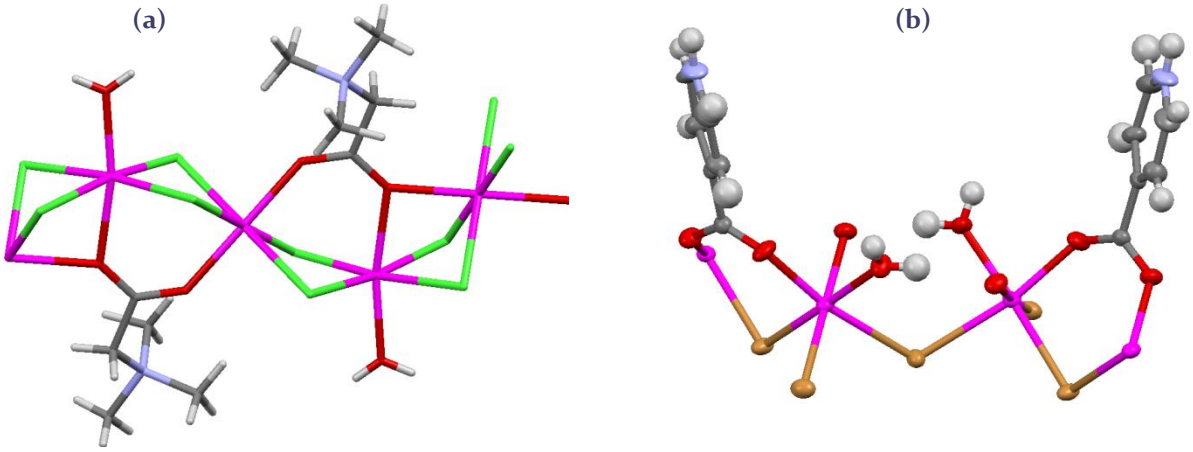

Figure 3.60: Molecular geometry of (a) structure YARVUI: (Schreuer and Haussuhl, 1993) and (b) structure V.

The octahedra in structure YARVUI are connected via edge sharing and face sharing while structure V demonstrate connection via common edges only. The isonicotinato and water ligands in structure V are positioned cis, relative to the inorganic chain while in structure YARVUI the betaine and water ligands are coordinated trans, relative to the inorganic chain. In the same way, all the bromo ligands, shared or terminal are positioned cis on the chain of structure V. The bridging chloro ligands of YARVUI are all shared and are coordinated on the equatorial positions of the octahedral.

Figure 3.61 below illustrates the relative position of the organic ligands to the inorganic polymer.

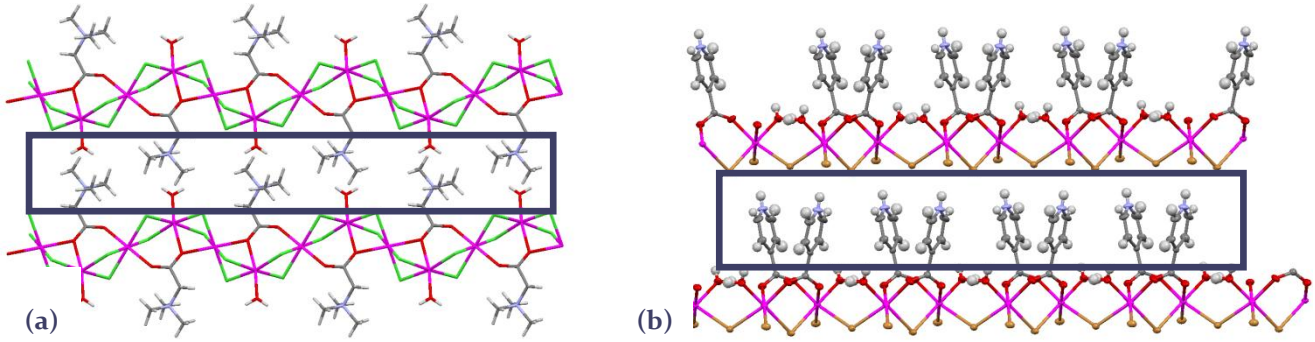

Figure 3.61: Expansion of structure (a) YARVUI viewed along the a-axis and structure (b) V, viewed along the c-axis.

Figure 3.62 shows the packing of the structures along the a-axis, for structure YARVUI, and along the c-axis, for structure V. It is observed that in both structures the inorganic polymers lie parallel to one another and as result constrains organic layers to be formed in parallel succession.

It is observed that both inorganic structures exhibit inorganic polymers that pack in a parallel fashion (Figure 3.62), however each discrete polymer, when viewed along the a-axis, for structure V and c-axis, for structure YARVUI, undergoes periodic displacement relative to the b-axis and a-axis respectively.

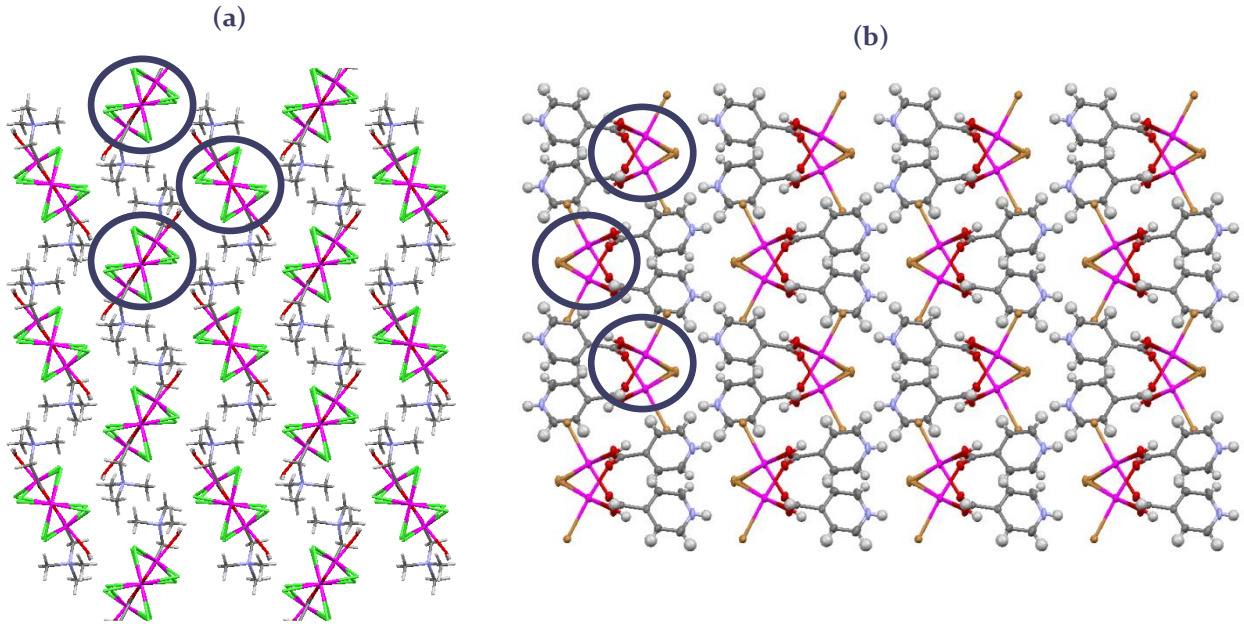

Figure 3.62: Structure V, viewed along the a-axis and structure YARVUI, viewed along the c-axis.

Coordination mode

In all the 4-aminocarboxylic acid structures coordination occurs through the amine group, while the carboxylic acid functional group participates in hydrogen bonding. However, in the isonicotinic acid containing structure V, coordination occurs through a carboxylate functional group. This can be explained by the formation of an isonicotinic acid zwitterion in solution, whereby the proton of the carboxylic acid group is transferred to the pyridine nitrogen atom, as illustrated below:

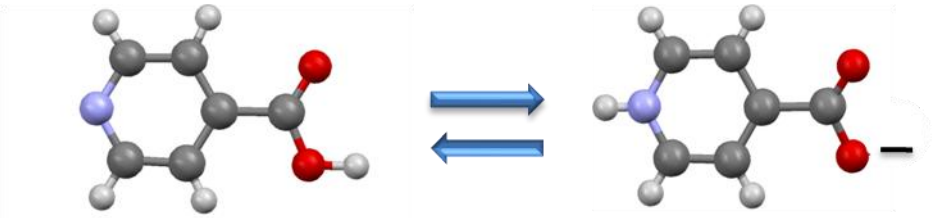

Figure 3.63: Zwitterionic form of isonicotinic acid.

This is a spontaneous process, and if the equilibrium shifts to the right, the species available for coordination would preferentially coordinate through the carboxylate functional group. The question as to why zwitterion is formed in the case of the isonicotinic acid molecule, but not in the case of the 4-aminobenzoic acid molecule can be answered by considering the basicity of the two nitrogen atoms. In general, pyridine nitrogen atoms are stronger bases than amine nitrogen atoms, hence the formation of the zwitterion in a solution of the isonicotinic acid molecules occurs, but this does not happen in a solution of 4-aminobenzoic acid molecules.

Ligand Geometry

It is observed that all the organic ligands of the 4-aminobenzoic acid containing coordination compounds demonstrate a planar geometry, however the isonicotinic acid containing compound (structure V) does not exhibit a planar ligand geometry. In structure V the carboxylate group has an angular offset to the plane of the aromatic ring and rotates by an angle of 42.31°.

Aromatic Interactions

In the 4-aminobenzoic acid and isonicotinic acid containing coordination structures, the aromatic planes of the ligands in an organic layer are parallel, and exhibit a slipped stacking. Centroid-to-centroid distances range from 4.160 Å to 4.725 Å, which are not indicative of aromatic interactions, as the expected centroid-to-centroid are usually around 3.8 Å (Janiak, 2000).

Hydrogen bonding

The formation of carboxylic acid dimers is a common structural motif in all the 4-aminobenzoic acid containing coordination compounds. Hydrogen bonds typically also occur between the nitrogen atom of the coordinated amine group and halogeno ligands and/or water molecules (if present). Zero-, one- or two-dimensional hydrogen bonds occur in the coordination structures, as illustrated below for the novel 4-aminobenzoic acid coordination compounds.

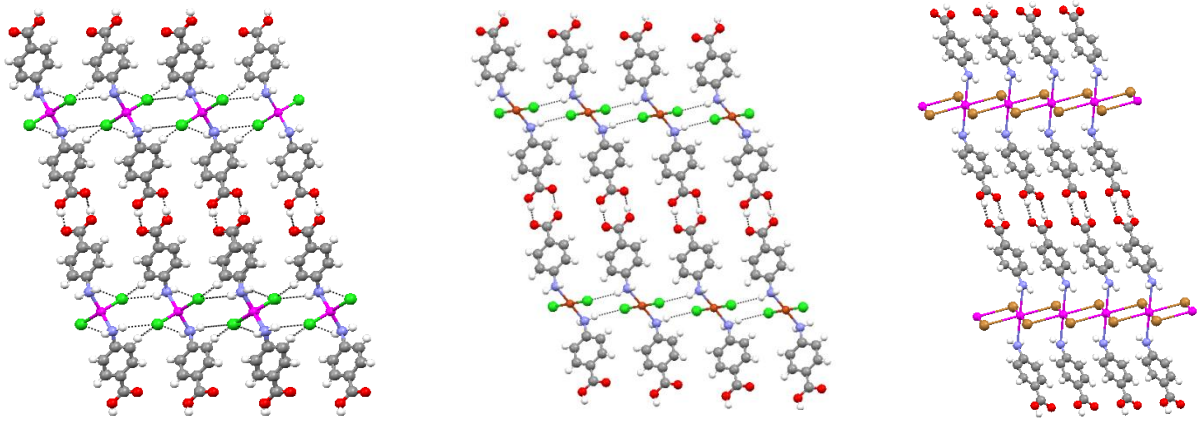

(a) (b) (c)

Figure 3.64: Hydrogen bonding interactions in novel coordination compounds of 4-aminobenzoic acid (a) structure I (also representative of structure II due to isostructurality) (b) structure III (c) structure IV.

Powder X-Ray Diffraction

In order to determine if the coordination materials obtained through solution synthesis techniques, and characterised via single crystal X-ray diffraction, may be obtained through mechanochemical synthesis, via grinding of the organic and the inorganic component, the powder X-ray diffraction patterns of the products obtained in the grinding experiments were analysed via powder X-ray diffraction. The experimental powder patterns were compared with the powder pattern calculated from the single crystal structure, and the results are given below. Note that the mechanochemical preparation of only a few selected combinations of organic and inorganic components was studied, and the results are given below.

Mechanochemical preparation of compound I: di-chloro-bis(4-aminobenzoic-acid-N)-zinc(II)

The crystal structure of compound I was discussed previously, and the molecular geometry is shown in Figure 3.65.

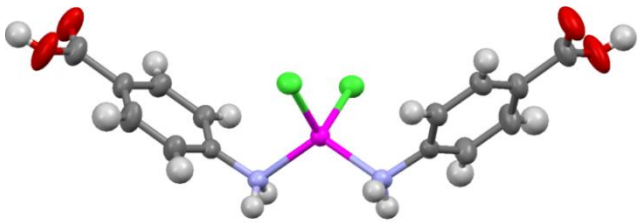

Figure 3.65: Molecular geometry of compound I.

Figure 3.66 shows the superposition of the experimental powder X-ray diffraction pattern obtained for a sample of I prepared by the mechanochemical preparation, and the powder X-ray diffraction pattern calculated from the single crystal structure of compound 1.

The large degree of peak overlap confirms that the mechanochemical preparation of I was successful, and that the compound can be prepared without the use of a solvent through the grinding of the organic and inorganic components.

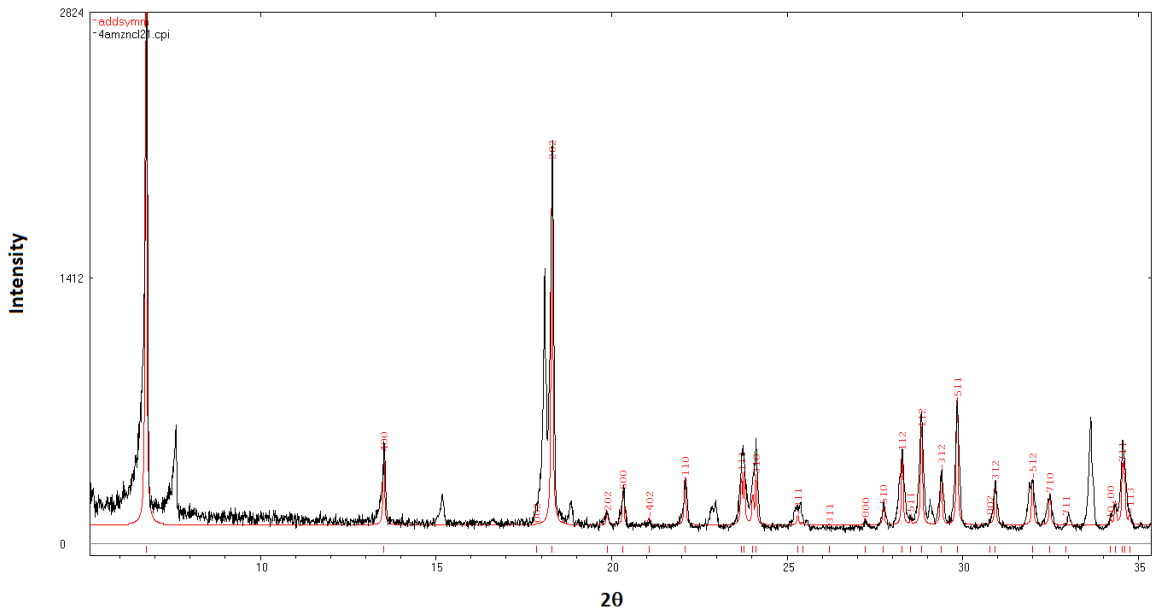

Figure 3.66: Superposition of calculated powder diffraction pattern (red) and experimental powder diffraction pattern of compound I.

Mechanochemical preparation of compound II: di-chloro-bis-(4-aminobenzoic acid-N)-mercurate(II))

Figure 3.67 X shows the molecular geometry observed in structure II, as discussed earlier.

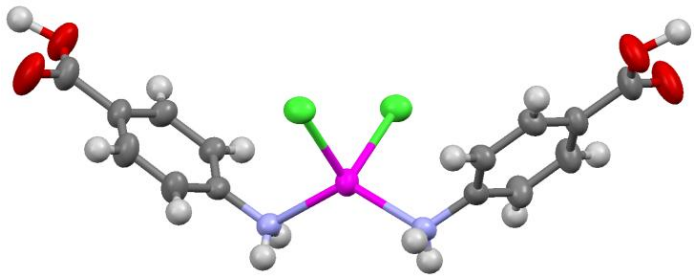

Figure 3.67: Molecular geometry of compound II.

The experimental powder diffraction pattern of the product prepared by the grinding of the two components is superimposed on the powder diffraction pattern calculated from the single crystal structure of compound II in Figure 3.68.

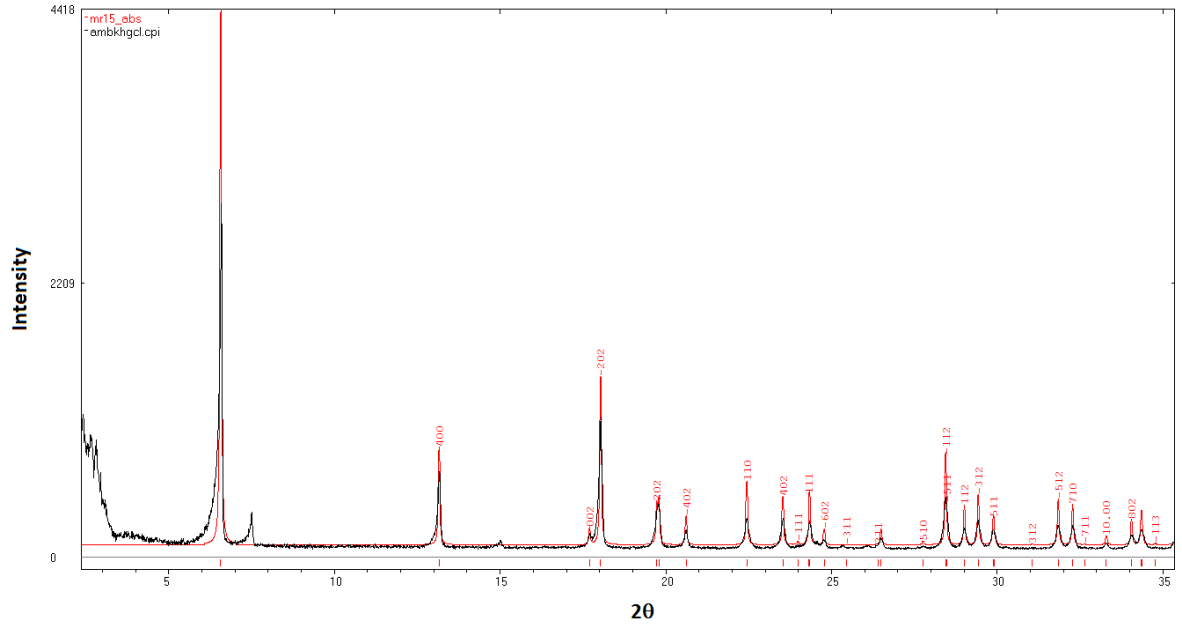

Figure 3.68: Superposition of calculated powder diffraction pattern (red) and experimental powder diffraction pattern of compound II.

The successful preparation of compound II via mechanochemical synthesis is confirmed by the matching of the experimental powder pattern and the powder pattern calculated from the single crystal structure.

Mechanochemical preparation of compound III: di-chloro-bis-(4-aminobenzoic acid-N)-copper(II))

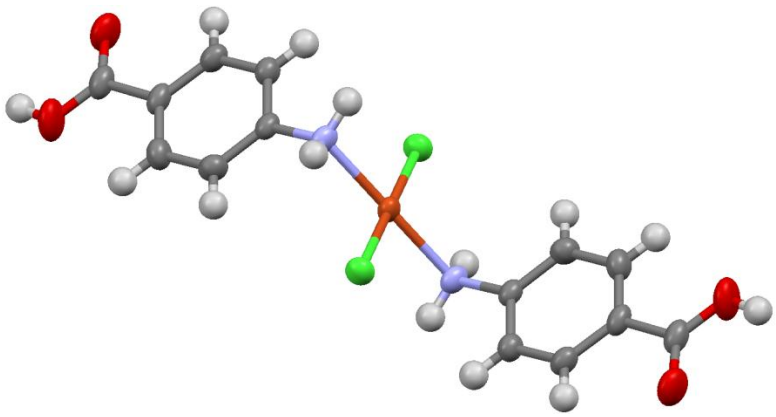

Figure 3.69: Molecular geometry of compound III.

As discussed previously, compound III displays a square planar coordination geometry around the central copper atom, as shown in Figure 3.69. Compound III was also prepared using a solid-state mechanochemical technique as can be seen from the matching of experimental and calculated powder diffraction patterns, illustrated in Figure 3.70.

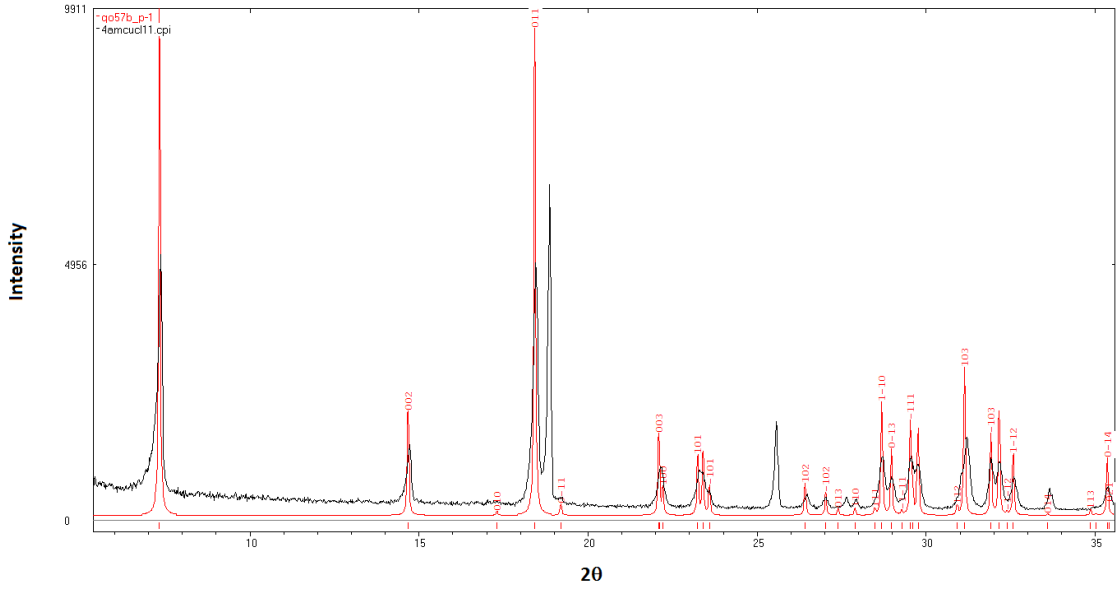

Figure 3.70: Superposition of calculated powder diffraction pattern (red) and experimental powder diffraction pattern of compound III.

Mechanochemical preparation of compound IV: catena-(bis(μ2-bromo)-bis(4-aminobenzoicacid)-mercury(II))

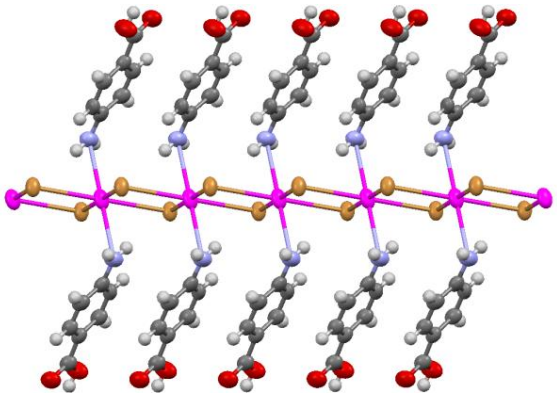

Figure 3.71: Geometry of compound IV.

As shown in Figure 3.71, compound IV displays a one-dimensional polymeric structure. The agreement between the powder X-ray diffraction pattern obtained experimentally from a mechanochemically prepared sample, and the powder pattern calculated from the single crystal structure of compound IV conforms the successful solid state preparation of compound IV.

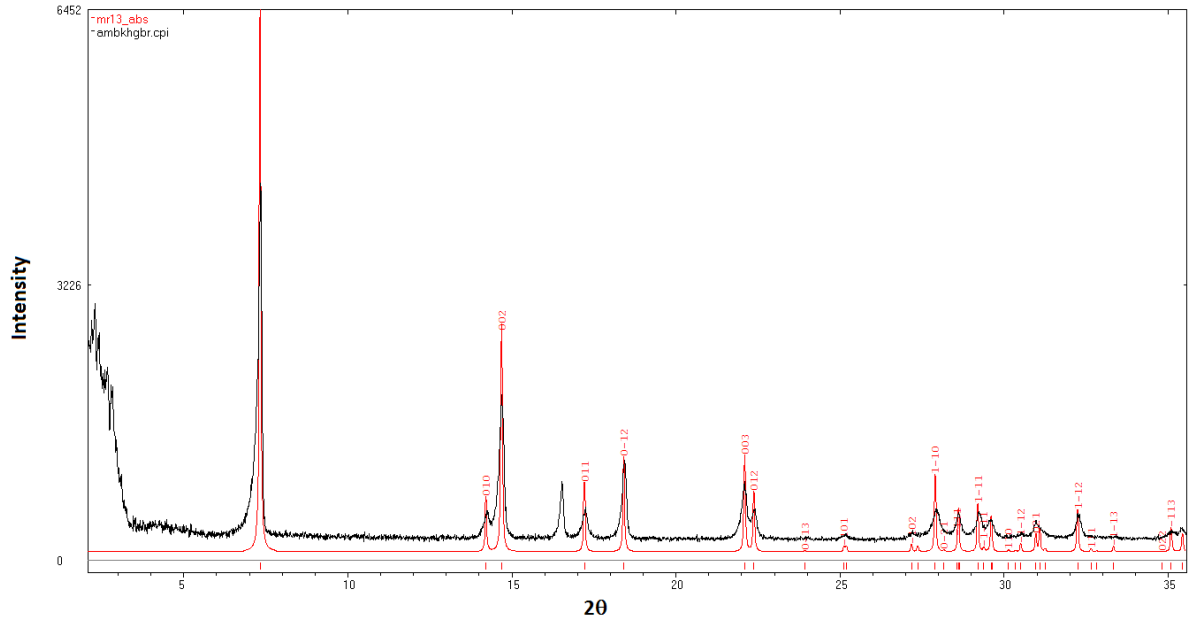

Figure 3.72: Superposition of calculated powder diffraction pattern (red) and experimental powder diffraction pattern of compound IV.

Even though the 4-aminobenzoic acid compounds above were prepared successfully, the not all of the other samples prepared mechanochemically yielded the same form as observed in the single crystal structure studies. For example, the isonicotinic acid coordination compound V as obtained via solution crystallization techniques could not be prepared via griding of the components. A possible reason is the fact that coordinated water molecules are present in the single crystal structure, but these were not available duting the grinding experiment. It is clear from Figure 3.73 that the experimental powder X-ray diffraction pattern obtained from the product of the grinding experiment and the powder X-ray diffraction pattern calculated from the single crystal structure do not match.

Within all of the above reported diffraction patterns (compound I, II, III and IV) there are diffraction peaks that do not overlap with the calculated powder pattern. The source of these peaks may be attributed to reagents within the sample or the presence of other products.

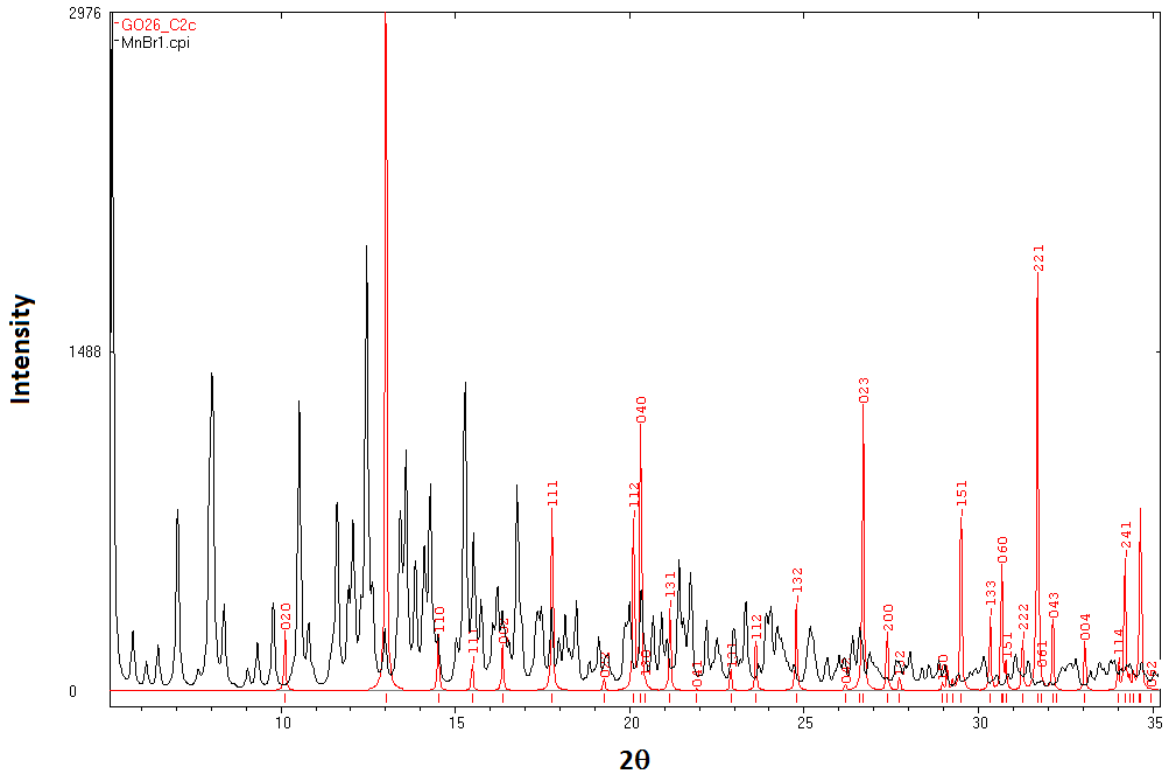

Figure 3.73: Superposition of calculated powder diffraction pattern (red) and experimental powder diffraction pattern of compound V.

Tables 3.11 to 3.13 summarise the outcome of the rest of the solid-state grinding experiments. The comparison that is made shows whether a new product was formed, or whether finger prints of either the organic or inorganic reagent could be observed in the experimental diffraction pattern. The powder diffraction patterns are not shown here – they are included in electronic format on the CD.

Table 3.11: PXRD analysis of products obtained during grinding synthesis of isonicotinic acid containing coordination compounds (Ratio: Organic Molecule : Metal Halide).

Reactants		PXRD Analysis		
Metal-halide	**Ratio**	**Organic Molecule**	**Metal-halide**	**Product**
$MnCl_2$	1:1	-	-	X
$MnCl_2$	1:2	-	-	X
$MnCl_2$	2:1	-	-	X
$MnBr_2$	1:1	-	X	X
$MnBr_2$	1:2	X	X	-
$MnBr_2$	2:1	X	-	X
$CuBr_2$	1:1	-	X	X
$CuBr_2$	1:2	-	X	X
$CuBr_2$	2:1	X	X	-
$CuCl_2$	1:1	-	X	X
$CuCl_2$	1:2	X	X	-
$CuCl_2$	2:1	X	X	-
$ZnCl_2$	1:1	-	-	X
$ZnCl_2$	2:1	-	-	X
$ZnBr_2$	1:1	-	-	X
$ZnBr_2$	2:1	-	-	X

Table 3.12: PXRD analysis of products obtained during grinding synthesis of 4-aminobenzoic acid containing coordination compounds (Ratio: Organic Molecule : Metal Halide).

Reactants		PXRD Analysis		
Metal-halide	**Ratio**	**Organic Molecule**	**Metal-halide**	**Product**
$MnCl_2$	1:1	-	-	X
$MnCl_2$	2:1	X	-	X
$MnBr_2$	1:1	-	-	X
$MnBr_2$	2:1	-	-	X
$CuBr_2$	1:2	X	X	-
$CuCl_2$	1:2	-	X	X
$ZnBr_2$	1:2	-	-	X
$ZnCl_2$	1:2	-	-	X

Table 3.13: PXRD analysis of products obtained during grinding synthesis of 4-aminobenzoic acid containing coordination compounds (Ratio: Organic Molecule: Metal Halide).

Reactants		PXRD Analysis		
Metal-halide	**Ratio**	**Organic Molecule**	**Metal-halide**	**Product**
$MnCl_2$	1:1	-	-	X
$MnCl_2$	1:2	-	-	X
$MnCl_2$	2:1	-	-	X
$MnBr_2$	1:1	X	X	-
$MnBr_2$	1:2	X	X	-
$MnBr_2$	2:1	X	X	-
$CuBr_2$	1:1	-	X	-
$CuBr_2$	1:2	X	X	-
$CuBr_2$	2:1	X	X	-
$CuCl_2$	1:1	-	-	X
$CuCl_2$	1:2	-	X	X
$CuCl_2$	2:1	-	-	X
$ZnCl_2$	1:1	-	-	X
$ZnCl_2$	2:1	X	-	X
$ZnBr_2$	1:1	-	-	X
$ZnBr_2$	2:1	-	-	X

As can be observed in Tables 3.11 to 3.13, in some grinding experiments the reagents did not react, and both the powder patterns of the reagents were observed. Another possible scenario is the formation of a product, with no evidence of any remaining reagents, but the experimental diffraction pattern does not correspond to any of the powder diffraction patterns calculated from the single crystal structures. In certain grinding experiments a new product was formed, but some of the starting materials remained.

Only structures I – IV above were prepared successfully via mechanochemical synthesis, and their products corresponded to known single crystal structures. The structural characteristics of the other grinding products could not be determined, but this will fall under future work to be done.

Preliminary Property Investigations of Coordination Compounds

Thermal Analysis

As mentioned previously, the thermal analysis investigation of the compounds was not completed due to instrumental problems related to the corrosive nature of the materials. Preliminary DSC results are discussed below.

The hybrid samples that were used for DSC analysis were crystals obtained from solution synthesis, which may or may not have been suitable for SCD.

Figure 3.73 below shows the DSC scans of the organic starting reagents 4-aminobenzoic acid, 4-aminobenzamide and isonicotinic acid. The DSC scans of the pure inorganic metal halides could not be determined due to the fact that many are hygroscopic, as well as the fact that they react with with the aluminium sample pans employed in the DSC studies.

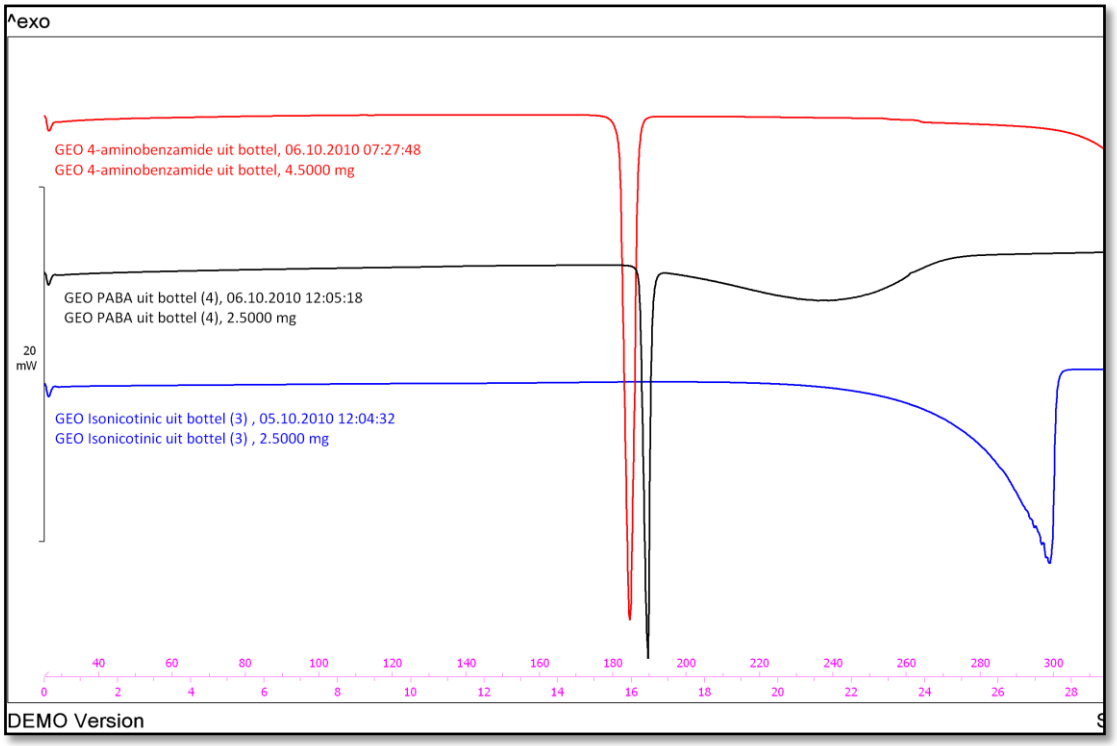

Figure 3.73: DSC scan of the organic molecules used in the synthesis of coordination compounds. Red curve: 4-aminobenzamide; black curve: 4-aminobenzoic acid; blue curve: isonicotinic acid.

The 4-aminobenzamide scan indicates an endothermic peak corresponding to melting at 184°C while the 4-aminobenzoic acid scan exhibits an endothermic peak indicating melting at 190°C. The isonicotinic acid scan shows a broad asymmetric melting endothermic peak at 298°C.

Due to the problems experienced with regards to the DSC studies, the full range of coordination compounds could not by studied by this technique. A selected number of preliminary results are discussed below, and all of the obtained DSC results are given in the Appendix.

Figure 3.74 below illustrates the DSC scans of the coordination compounds of 4-aminobenzoic acid and the three zinc metal halides. Firstly, by comparison with the DSC scan of pure 4-aminobenzoic acid (black scan), it is evident that novel coordination products were formed since their DSC scans differ from that of the pure organic reagent.

The DSC scan of the $ZnCl_2$ analogue is different from the bottom scans, and show only a small thermal event around 210°C. This structure determined by single crystal X-ray diffraction, and was discussed previously.

The single crystal structures of the $ZnBr_2$ and ZnI_2 combinations with 4-aminobenzoic acid were not determined in the current study, but from the similarity of their DSC scans (blue and green scans) it can be expected that they exhibit similar structures, and may even be isostructural, and that their structures are probably different from that of the $ZnCl_2$ compound. Their DSC scans show two overlapping peaks, that are similar in shape for the two materials, with the thermal event occurring at a slightly lower temperature for the ZnI_2 analogue.

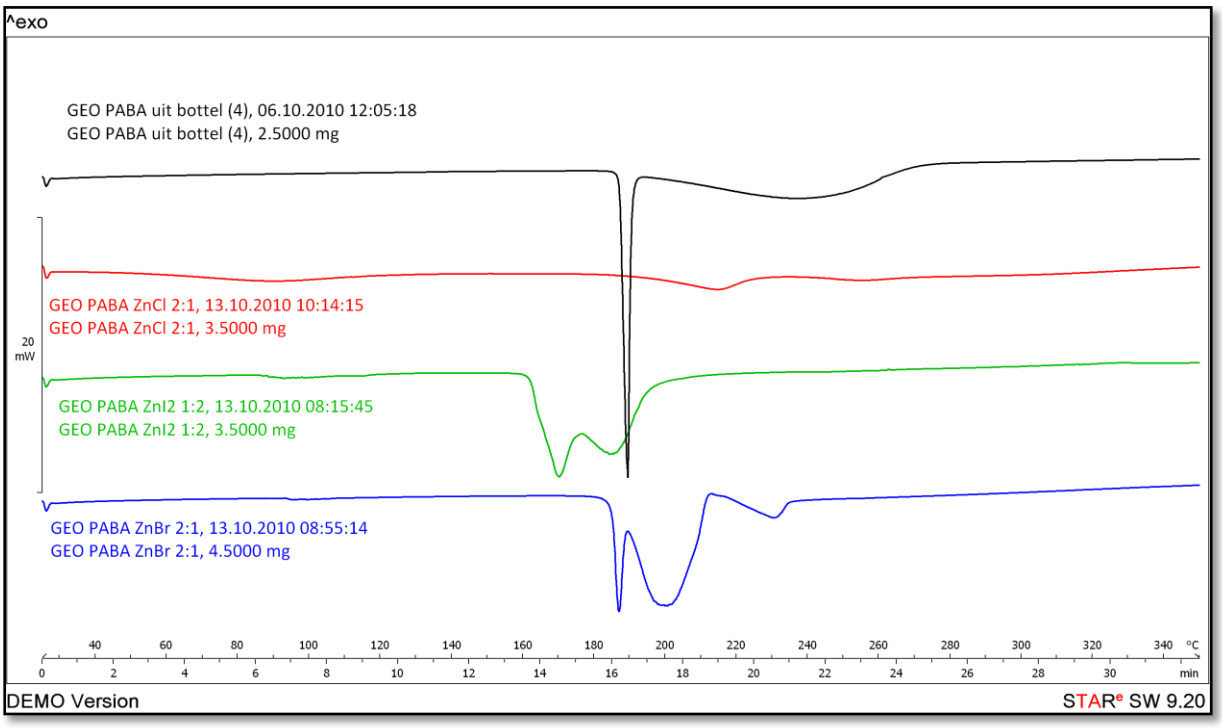

Figure 3.74: DSC scan of 4-aminobenzamide acid (black), 4-aminobenzoic acid + $ZnCl_2$ (2:1) (red), 4-aminobenzoic acid + ZnI_2 (1:2) (green), 4-aminobenzoic acid + $ZnBr_2$ (2:1) (blue).

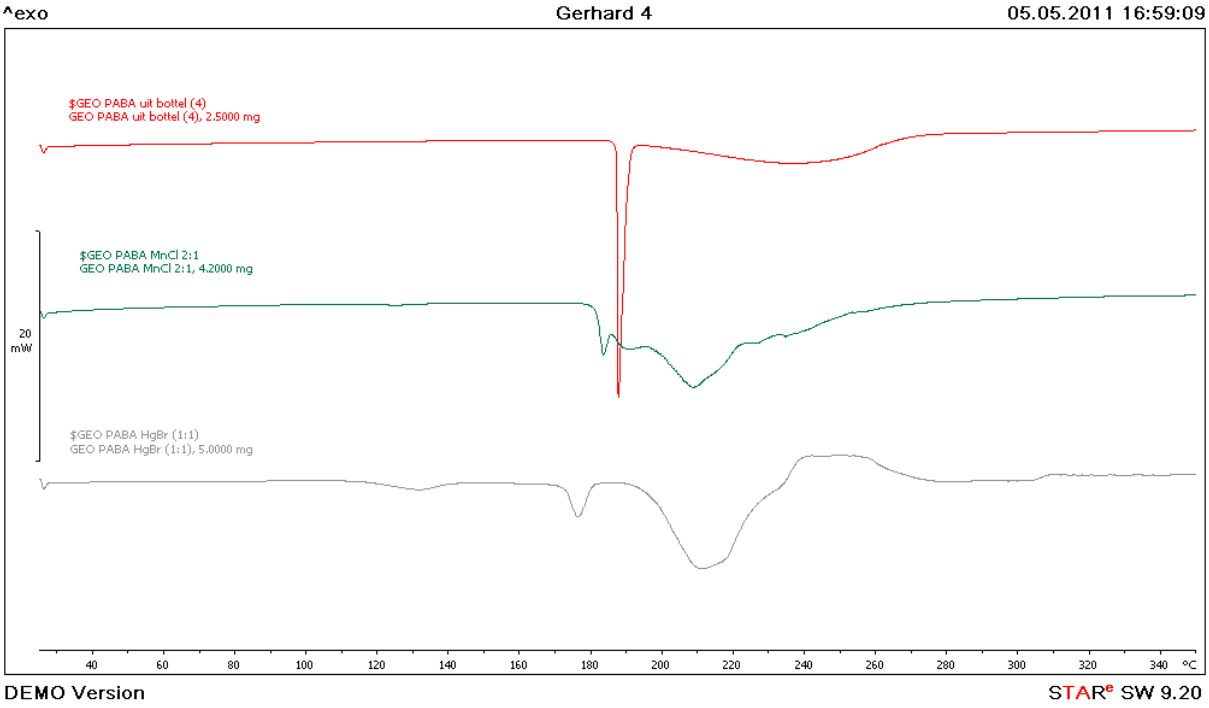

Figure 3.75: DSC scan of 4-aminobenzoic acid (red), 4-aminobenzoic acid + $MnCl_2$ (green), 4-aminobenzoic acid + $HgBr_2$ (blue).

The DSC scan of crystals of the structure IV (combination of 4-aminobenzoic acid and $HgBr_2$) is shown in Figure 3.75. It was observed that the DSC scan of the coordination compound prepared by the combination of 4-aminobenzoic acid and $MnCl_2$ is similar to that of compound IV. The single crystals of the 4-aminobenzoic acid and $MnCl_2$ combination was not of good enough quality to allow for the single crystal structure determination, but based on the similarity in the DSC scans, it can be expected that the structures may be similar. This prediction is further supported by the fact that $MnCl_2$ coordination compounds are often polymeric and is comparable with the $HgBr_2$ compound which is also polymeric.

In conclusion, despite the fact that a number of problems were experienced with regards to the investigation of the thermal behaviour of the compounds, and the fact that the study could not be completed due to these problems, structural predictions could be made based on the similarity of the DSC scans of compounds of known structure and the DSC scans of compounds of which the solution crystallised crystals are not suitable for single crystal structure determination.

Electronic conductance

As a preliminary study, electrical conductivity measurements were carried out using two probe DC analysis on the compound IV (Figure 3.76). The aim of this study was to identify if the material showed potentially interesting electronic properties, and if future studies of these properties are viable. It was observed from the shape of the current-potential curve that compound IV shows semi-conducting behaviour. Please see Figure 3.38 on page 82 for the asymmetric unit of compound IV.

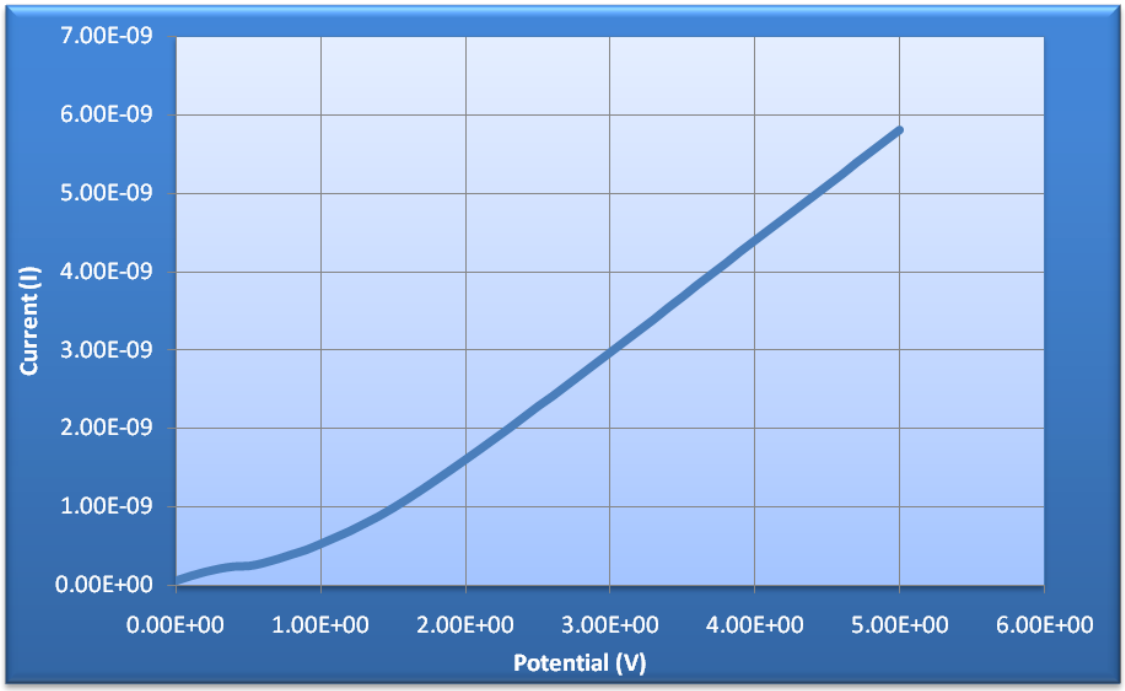

Figure 3.76: Two probe DC scan of compound IV:

The value of the measured current is observed to be lower than that observed for the studies carried out by Amo-Ochoa and co-workers (2009) and Welte and colleagues (2009) on the conductivity of related hybrid coordination compounds. Analogous to their reasoning, the measured current values may be underestimated due to the potential problems related to crystal-electrode electrical contacts.

Chapter 4

Ionic Hybrid Compounds

Introduction

Literature Review on Ionic Materials

A literature review on ionic structures relevant to the current study is given below. The first section of the literature review deals with general aspects of perhalometallate salts of organic cations containing different functional groups, but is by no means exhaustive. The aim is to highlight important aspects of these structures. The second part of this literature review focuses exclusively on the structural aspects of compounds identified in the CSD as relevant to the current study.

General aspects:

Structures containing simple arylammonium or alkylammonium cations combined with perhalometallate anions are wide-spread in the literature and the CSD, but this is not the case for structures that combine perhalometallate anions with more complex organic cations, cations that contain functional groups other than the ammonium group, or for cations that contain more than one functional group.

A structure that is commonly encountered is related to the perovskite mineral structure. It often forms when n-alkylammonium cations are combined with perhalometallate anions, and is discussed in more detail below.

The Perovskite Structure

The mineral structure of perovskite ($CaTiO_3$), in its principle form, is assumed by many compounds and establishes the prototype for numerous crystal structures, particularly oxides with stoichiometries AMX_3 (Atkins, et al., 2006). Having an ideal cubic structure, the perovskite arrangement consists of a large cation (A) which is surrounded by twelve anions (X) and forms the primary close-packed layers while a corner-sharing cation (M) is located in the octahedral holes which are produced by the six surrounding anions. The individual charge on cations A and B need not be definite, however their collective valence must be equivalent to 6 as to balance out X^{2-} in the formula AMX_3 (Klein, 2002).

Expanding the perovskite unit cell reveals an extended three-dimensional network of corner-sharing octahedron layers (Figure 4.1) where a divalent metal halide (MX_6) forms a corner-sharing octahedral. The size of the 12-fold coordination holes among the octahedron is controlled by the size of the cation.

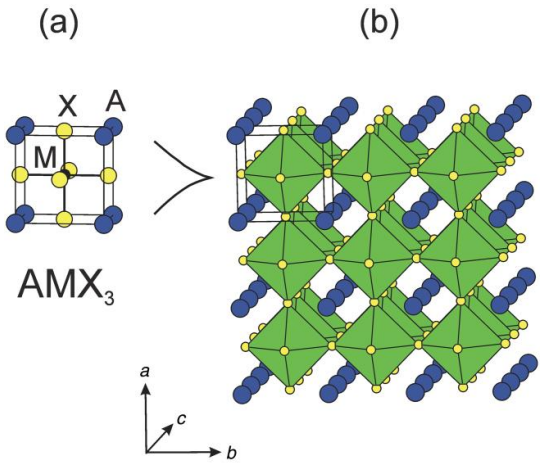

Schematic 4.1: (a) The ideal structure of the AMX_3 perovskite unit cell, (b) View of the structure as it is extended in three dimensions (Mitzi, 2000).

Substitution of the cation A in the mineral perovskite structure by a larger organic cation gives a related hybrid perovskite structure. The most simplistic form of a layered perovskite structure consists of a layer of corner sharing octahedral metal halides MX_4^{2-}, which successively alternates with either a cationic organic bi-layer or a monolayer. The presence of either a monofunctional or bifunctional cation will be the determining factor that controls the occurrence of either an organic-monolayer or bi-layer. Depicted in Figure 4.2(a) is an example of a monoamaonium organic cation (RNH_3^+) that forms a bi-layer while Figure 4.2(b) shows a diammonium organic cation ($^+NH_3RNH_3^+$) that forms a mono-layer (Mitzi, 2000).

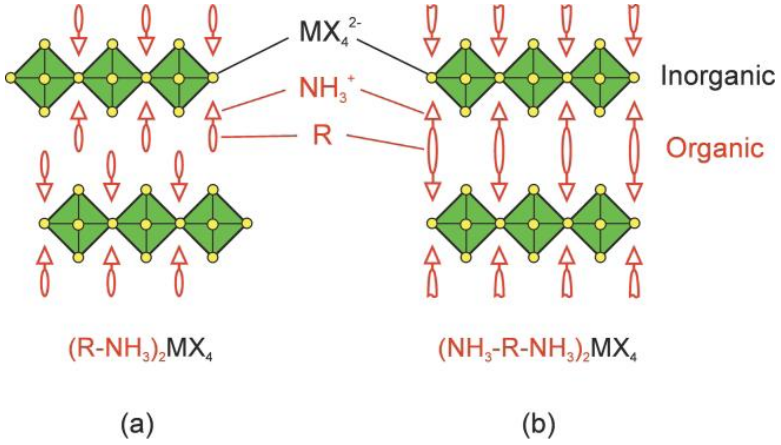

Schematic 4.2: Schematic representation of a single layered perovskite with (a), monoammonium (RNH_3^+) or (b) diammonium ($^+NH_3RNH_3^+$) organic cation (Mitzi, 2000).

Pervading through the literature are numerous examples of hybrid compounds that adopt the layered perovskite structure. This provides an opportunity towards the functional integration of useful organic cations and inorganic anions within a single nanocomposite structure and in addition, provides an opportunity to combine distinct characteristics and to produce unique electronic, magnetic and optical properties (Mitzi, 2000).

There is an opportunity for the introduction of more complex organic molecules into the rigid layered perovskite structure, with further interest surrounding oligomer-containing organic-inorganic perovskites. An oligomer is a molecule that consists of a few identical molecules that are joined together (Ramanathan, 2005). As a result of the inorganic framework's templating effect and influence on the orientation of the cations, significant outcomes with regard to electrical and optical properties of the organic layers may follow. This observable fact is exemplified by the effect that the type of oligomer and its orientation within organic layer has on the mobility of the channel layer in organic thin-film transistors (OTFT's) (Mitzi, 2000).

Further research towards the semi-conducting behaviour of multifunctional hybrid perovskite compounds have been done and comprehensive research into how perovskite layers can be used as semi-conducting channels in thin-film field effect transistors (TFT's) (Mitzi et al., 2001). Recent investigation into the use of zwitterionic amino based molecules have attracted attention as bifunctional organic species that are able to orientate and fix the perovskite layer via the cationic ammonium part and be able to, via the carboxylate anionic part, act as ligands to complex metal atoms (Marcier, et al., 2004).Mitzi and co-workers have published a large amount of work on perhalometallate structures (Mitzi, et al., 1999; Mitzi, 2000; Mitzi, 2001; Mitzi, et al., 1999). In these papers issues related to the templating effect of the cation on the perhalometallate anion and vice versa are addressed, structures containing more than one organic cation are investigated, and the steric interactions between the organic and inorganic layers, as well as the incorporation of a chromophoric organic cation into an ionic perhalometallate structure are studied.

A number of research groups have also published research focussed on studying the properties of ionic hybrids, often with the approach of understanding how the crystal structure influences the properties of the materials. Examples include the study of the semi-conducting properties of ionic hybrids (Mitzi, 2004), electroluminescence (Mitzi, et al., 2002), optical properties and superconductivity (Drichko, et al., 2004). The electronic properties of a range of ionic hybrids were studied by Mitzi (Mitzi, 2004), and he also demonstrated the use of the ionic material (H_2AEQT) $PbBr_4$ in the construction of an organic-inorganic light emitting diode (Mitzi et al., 2001). The tunability of the band gap of certain perovskite hybrids was illustrated by Knutson et al., (2005).

Another group that has done extensive work on the ionic hybrid materials, following a crystal engineering approach, is the research group of Orpen (Orpen and Angeloni, 2001; Orpen et al., 2010). They have done careful studies to ascertain the effect of a small change in organic component on the overall structure as well as the crystal engineering synthons. In addition they have investigated the role of a change in metal component of the perhalometallate anion on the structure. The release of HCl, and the conversion from an ionic structure to a coordination structure at a temperature above room temperature has been demonstrated by the group of Orpen. It was illustrated by the group of Brammer that this process is reversible, and that HCl uptake occurs when the coordination compound is exposed to the gas (Brammer et al., 2010; Brammer et al., 2011). These groups also investigated the mechanochemical preparation of ionic hybrid materials extensively (Orpen, et al., 2010; Adams, et al., 2010; Brammer et al., 2010).

A number of review papers focussing on the ionic hybrids have been published in the literature. These include, among others, a review on the structural diversity and crystal engineering aspects of iodometallate hybrids (Mercier, et al., 2009), a review paper by Arnby and colleagues (Arnby, et al., 2004) which highlighted the crystal engineering aspects of structures containing halocuprate perahlometallate anions, and a paper by Kumar and co-workers (Kumar, et al., 2005) investigated the robustness of a common halocuprate synthons. The dimensionality of the hydrogen bonding network formed in a range of ionic hybrid salts was studied by Adams and colleagues (Adams, et al., 2006).

Specific structures relevant to the current study

As done in the previous chapter for the coordination compounds, an search was carried out to find ionic hybrid compounds in the literature that are relevant to the current study. The utilization of the CSD and the study of recent scientific literature provided for the location and examination of relevant compounds that comprise both cationic and anionic species that are related to the families of ionic materials investigated in this study.

A total of five crystal structures that are related to the ionic materials under investigation were found in the CSD. These include crystal structures containing protonated 4-aminobenzoic acid or isonicotinic acid with perhalometallate fragments relevant to this study. Additionally, a search of protonated 4-aminobenzamide salts containing metal halide anionic fragments revealed that no such structures had been recorded in the Cambridge Structural Database. This provided an opportunity to employ valuable multi-functional cations that hitherto had remained under-exploited.

Of the organic molecules selected for this synthesis, perhalometallate structures of isonicotinic acid is the most prevalently recorded in the literature, with four structures reported in the CSD. The utilization of the multi-functional isonicotinic acid in ionic complexes provides an opportunity to integrate the fluorescence properties of the organic molecule with the photophysical and photochemical properties of the metal (Liu and Yuan, 2005). Work done by Angeloni and Orpen on ionic tetrachloroplatinate salts incorporating N-protonated isonicotinic acid demonstrated the formation of hydrogen bonded one-dimensional ribbons and two-dimensional networks (Angeloni and Orpen, 2001).

At this stage a word on the systematic naming system employed for protonated cations is in order. Protonation of a neutral isonicotinic acid molecule yields a 4-carboxypyridinium cation, while protonation of a neutral 4-aminobenzoic acid molecule gives a 4-carboxyanilinium cation, while protonation of a 4-aminobenzamide molecule produces a 4-ammoniumbenzamide cation.

The crystallographic parameters of the ionic hybrid structures located in the literature are listed in Table 4.1. Note that the literature structures will be labelled using uppercase letters following the same system that was introduced in Chapter 3. For a specific structure Y the terms compound Y and structure Y will be used interchangeably.

Table 4.1: Crystallographic data of literature compounds containing 4-carboxyanilinium and 4-carboxypyridinium cations and perhalometallate anions:

Compound	G	H	I	J	K
Empirical Formula	$2(C_7H_8O_2N)^+[CdCl_4(H_2O)]^{2-}$	$2(C_6H_6O_2N)^+[CuCl_4]^{2-}\cdot H_2O$	$2(C_6H_6O_2N)^+[PtCl_4]^{2-}\cdot H_2O$	$2(C_6H_6O_2N)^+[PdCl_4]^{2-}\cdot H_2O$	$2(C_6H_5O_2N)^+[PtCl_4]^{2-}$
M_r(g/mol)	283.26	489.61	507.19	532.4	583.11
Crystal system	Monoclinic	Triclinic	Triclinic	Triclinic	Triclinic
Space group	$P2_1/c$	$P\bar{1}$	$P\bar{1}$	$P\bar{1}$	$P\bar{1}$
Z	2	1	1	1	1
a/Å	12.0794(1)	7.038(4)	6.9551(1)	6.9942(2)	7.1544(1)
b/Å	5.8333(5)	8.510(5)	8.5188(1)	8.5052(2)	7.5492(2)
c/Å	14.8963(1)	8.868(4)	8.9795(1)	8.9252(1)	8.2906(2)
α/°	90.00	86.17(5)	86.462(1)	85.754(2)	90.43(3)
β/°	100.376(1)	74.51(4)	73.017(9)	73.059(2)	114.88(3)
γ/°	90.00	65.69(4)	66.472(1)	66.135(1)	92.75(3)
V (Å^3)	1032.47	465.894	465.61	463.886	405.56
F(000)	564	247	-	-	-
D_c (g cm^{-3})	1.822	1.745	-	-	-
μ (mm^{-1})	1.608	1.776	8.139	1.609	9.327
R-Factor (%)	2.45	0.5	1.9	2.23	1.95
Diffractometer	Siemens Smart CCD	CAD-4 Diffractometer	-	Bruker-AXS CCD	Bruker-AXS CCD
T (k)	293	293	173	-	
λ(Mo Kα) (Å)	0.71073	0.7107	-	0.71073	0.71073
Reflections collected	2995	1094	-	4927	4651
Unique reflections	1825	-	2114	2105	1853
Parameters	165	144	-	-	-
$R[F^2>2\sigma(F^2)]$	0.0245	0.0503	-	0.022	0.020
$wR(F^2)$	0.0713	0.1352	-	-	-
Δp_{max} & Δp_{min} (e Å^{-3})	0.388 and - 0.718	--	-	-	-

$R=\sum||F_0|-|F_c||/\sum|F_c|$
$wR=[\sum w(F^2_0-F^2_c)^2/\sum w(F^2_0)$

Structural investigation of related ionic compounds

A number of literature structures important to the current investigation are discussed below. Their main structural features are highlighted to allow for the comparison with novel structures determined in the current investigation, and for the identification of structural trends.

4-Carboxyanilinium and perhalometallate containing structures

A single structure containing a protonated 4-aminobenzoic acid molecule, also known as a 4-ammoniobenzoic acid ion, has been reported in the literature, and its structural characteristics are discussed below.

G: bis(4-carboxyanilinium) trans-diaquatetrachlorocadmate, (Wang et al., 2002), (CSD Refcode: WUGHIZ)

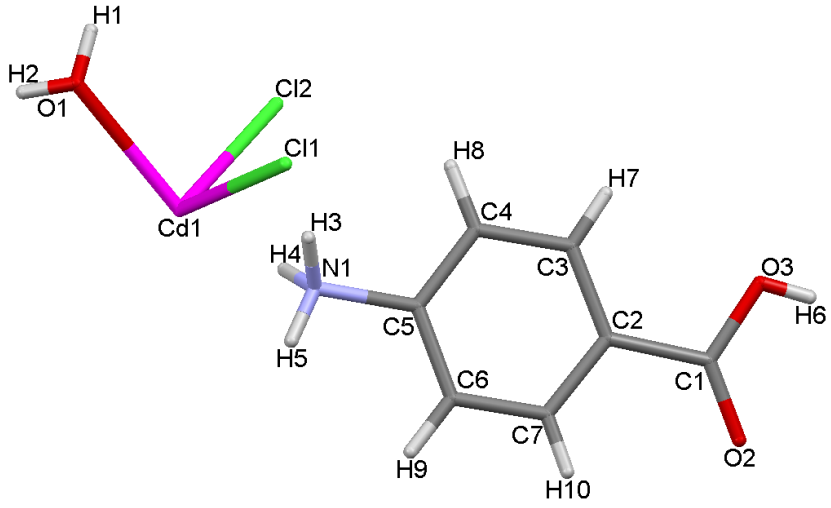

Figure 4.3: Asymmetric Unit of compound G:

The asymmetric unit of compound G is shown in Figure 4.3, and consists of a carboxyanilinium cation and a cadmium atom that coordinates to two chloro ligands and to the oxygen atom of a water molecule. The protonated nitrogen atom has a tetrahedral geometry and lies parallel to the plane of the aromatic ring while the carboxylic acid group makes a dihedral angle of 3.47° with respect to the aromatic plane. The metal atom is located on an inversion centre, with the symmetry operator generating the rest of the inorganic anion, as illustrated in Figure 4.4. The unit cell comprises two asymmetric units.

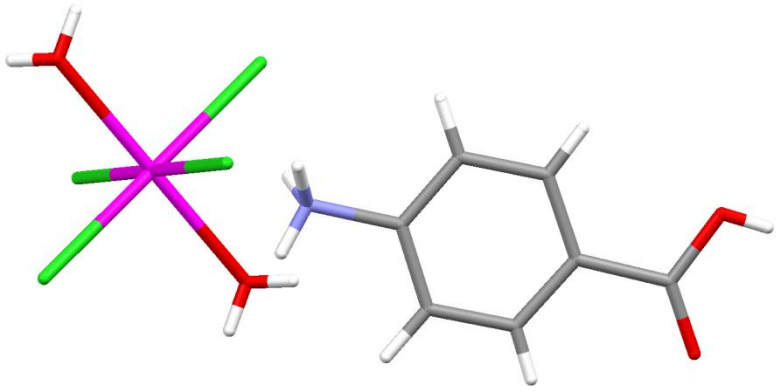

Figure 4.4: Molecular geometry of compound G:

The complex is composed of a 4-carboxyanilinium cation and a perhalometallate anion that consists of an octahedral cadmium metal atom that coordinates to four chloro ligands and two water (aquo) ligands through the oxygen atoms.

Figure 4.4 illustrates the discrete, inorganic $[(CdCl_4(H_2O)_2]^{2-}$ anion that consists of four coplanar chloro ligands that coordinate to the cadmium atom and which lie in the equatorial plane. Additionally, two water molecules coordinate via their oxygen atoms and are situated at the axial positions. The four coordinated chloro ligands lie in the same plane at distances (Cd—Cl) of 2.570 Å and 2.569 Å respectively from the cadmium atom. The square planar geometry produced by the chloro ligands is slightly distorted. The distortion is illustrated by the angles that are generated between chloro ligands and the cadmium atom (Cl-Cd-Cl) with values of 93.10° and 86.90°. In the case of a perfect square planar geometry these angles would be equal to 90°. The coordinated oxygen atoms from the water molecules lie a distance 2.364 Å from the cadmium atom (Cd—O), with the O-Cd-O angle equal to 180° due to the presence of the inversion centre.

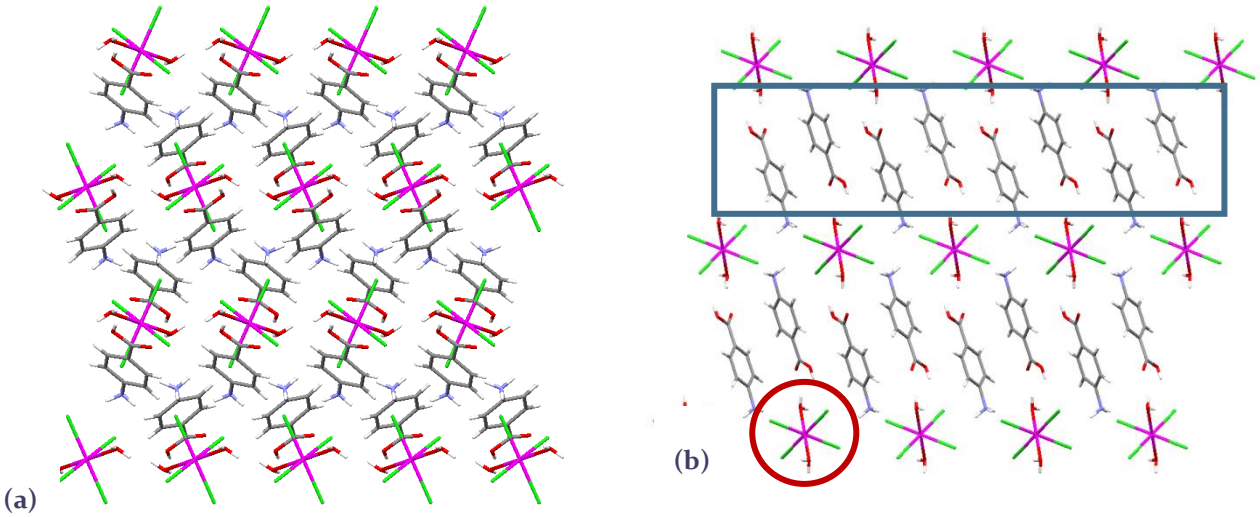

Figure 4.5: Packing of structure G viewed along the (a) a-axis and (b) b-axis. An isolated inorganic anion is circled and the organic layer is shown in the block.

It is observed (Figure 4.5(a) and (b)) that translation of the unit cell forms a layered structure. This structure contains alternating organic and inorganic layers. The isolated carboxyanilinium cations comprise the organic layer, while the inorganic anions form the inorganic layers. The ammonium group penetrate the inorganic layer, and interacts with the anions through hydrogen bonding. In addition, the carboxylic acid group of the organic cations interact with the inorganic anions through hydrogen bonding. In the organic layer cations alternate in their relative orientation when viewed along the c-axis, as illustrated in Figure 4.6 below.

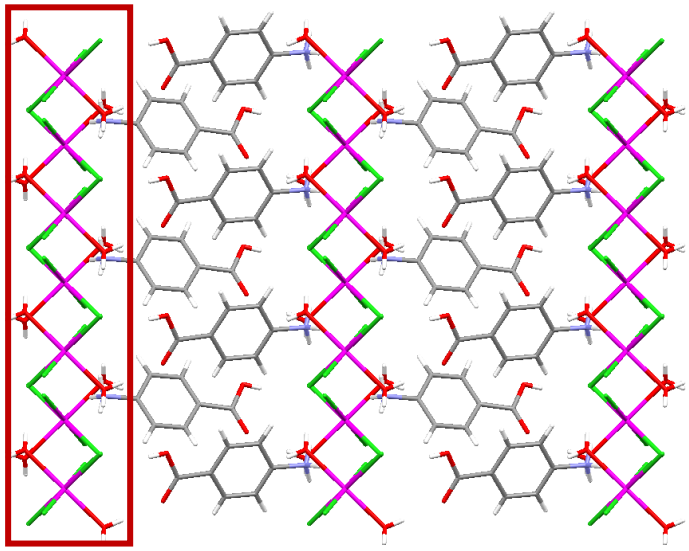

Figure 4.6: Packing of structure viewed along the c-axis. The inorganic layer is shown in the block.

Extensive intermolecular hydrogen bonding occurs in this structure, which link the organic and inorganic building blocks and as a result form alternating layers. The nitrogen atom on the ammonium group is surrounded and linked to three chloro ligands via hydrogen bonds at distances 3.228 Å, 3.233 Å and 3.193 Å. Additionally the carboxylic acid functional group forms a hydrogen bond with a chloro ligand (O-H...Cl) with a distance of 3.032 Å while the oxygen on the carboxylic group forms a hydrogen bond with a coordinated water molecule (O-H...O) with a distance of 1.985 Å. Between the nitrogen atom of the ammonium group and a coordinated water molecule a hydrogen bond with a distance of 2.990 Å occurs.

4-Carboxypyridinium and perhalometallate containing structures

A total of four structures comprising protonated isonicotinic acid cations (i.e. 4-carboxypyridinium cations) and perhalometallate anions have been reported in the literature, and their main structural features are discussed below.

H: bis(4-carboxypyridinium) tetrachlorocuprate dihydrate, (Kumar, et al., 2005), (CSD Refcode: PAQLOJ)

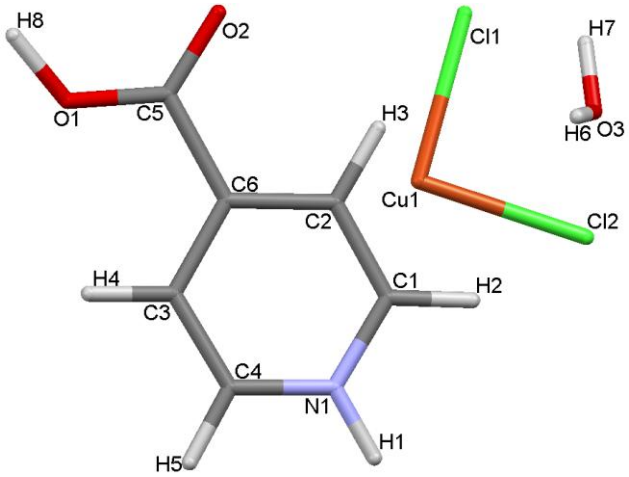

Figure 4.7: Asymmetric Unit of compound H:

Figure 4.8 shows the asymmetric unit of compound H which consists of a 4-carboxypyridinium cation that is protonated on the pyridine ring nitrogen atom and a copper atom that coordinates to two chloro ligands. In addition, a neutral water molecule also forms part of the asymmetric unit. The carboxylic acid functional group makes a dihedral angle of 8.15° with the aromatic plane. The metal atom lies on an inversion centre, which generates the rest of the anion. The unit cell consists of two asymmetric units.

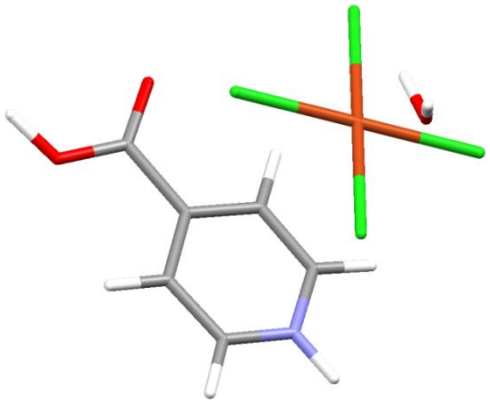

Figure 4.8: Molecular geometry of compound H.

The perhalometallate anion consists of a copper atom that has a square planar geometry and coordinates to four chloro ligands that lie on the same plane. The chloro ligands have bonding distances (Cu—Cl) of 2.266 Å and 2.236 Å, and make angles (Cl—Cu— Cl) of 90.55° and 89.45° with respect to the metal atom, resulting in a slight distortion in the square planar geometry of the anion.

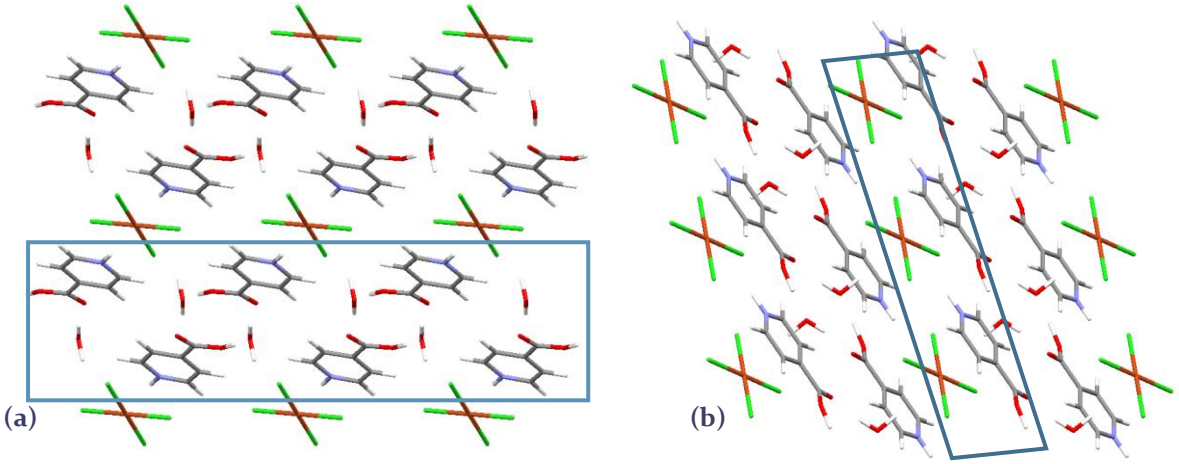

Figure 4.9: Packing of structure H viewed along the (a) a-axis and (b) b-axis. The organic bi-layer and inorganic layer is illustrated within the blocks.

A layered structure, which consists of alternating organic and inorganic layers, is formed. The organic cation comprises the organic bi-layer, while the inorganic anions form the inorganic layer. The inorganic anions, when viewed along the a-axis (Figure 4.9), are observed to lie in parallel succession with organic bi-layers and similarly, when viewed along the b-axis, discrete inorganic anions can be seen to lie parallel and packing in two-dimensional layers.

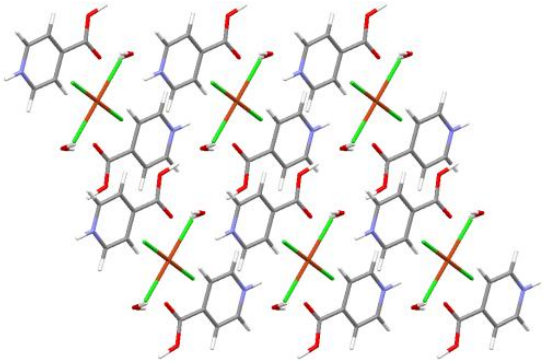

Figure 4.10: Packing of structure H viewed along the c-axis.

It is observed that there exist no direct interactions between the discrete perhalometallate anions. Extensive intermolecular hydrogen bonding occurs in this structure, which links the organic and inorganic building blocks so that they aggregate to form alternating layers. A strong charge-assisted, bifurcated hydrogen bonding interaction is present between the pyridine nitrogen atom and the inorganic unit. Hydrogen bonding between the nitrogen atom on the 4-carboxypyridinium cation and two chloro ligands occur at distances of (N—H···Cl) 2.33 Å and 2.42 Å and make angles (N—H···Cl) of 141° and 134°.

It is observed that the carboxylic acid functional group of the isonicotinic acid moiety does not form the habitual cyclic hydrogen bonded dimer, instead neutral water molecules act as bridging units between neighbouring 4-carboxypyridinium cations. Hydrogen bonding distances are (O—H···O) 2.667 Å and 2.616 Å while two coordinated chloro ligands also act as hydrogen bonding acceptor atoms (O—H···Cl) with H-bonding distances of 2.622 Å and2.392 Å (Kumar, et al., 2005). The resulting one-dimensional hydrogen bonded ribbon is illustrated in Figure 4.11. The solvate water molecules play a significant role in the stabilization of the crystal structure as they also form hydrogen bonds with the coordinated chloro atom of the anion moieties (Kumar, et al., 2005). The significance of the water molecule, and it's involvement in the organization and arrangement of both organic and inorganic constituents in the structure, is exemplified by the number of intermolecular interactions that it partakes in.

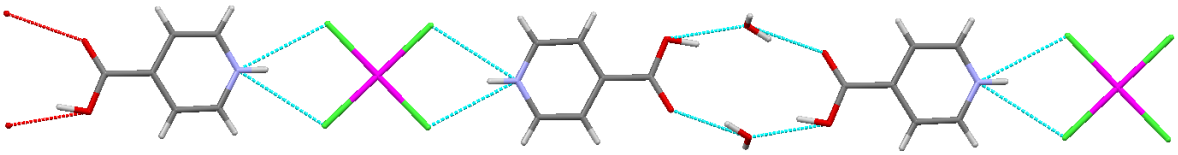

Figure 4.11: One-dimensional, hydrogen bonded organic-inorganic ribbon.

I: bis(4-carboxypyridinium) tetrachloroplatinate dihydrate, (Angeloni and Orpen, 2001), (CSD Refcode: QIDLIY)

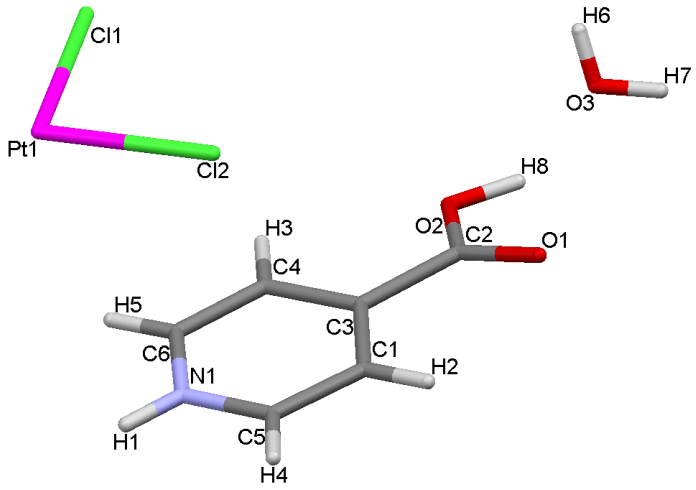

Figure 4.12: Asymmetric Unit of compound I:

Structure I is isostructural to structure H reported above, and will be discussed briefly. As shown in Figure 4.12, the asymmetric unit of compound I consists of a 4-carboxypyridinium cation, with protonation occurring on the pyridine ring nitrogen atom of the isonicotinic acid molecule, and a platinum atom that is coordinated to two chloro ligands. Comparable to the previously discussed structure, a neutral solvate water molecule is also present in the asymmetric unit.

The carboxylic acid functional group makes a dihedral angle of 10.39° with the aromatic plane. The metal atom is located on an inversion centre, and the rest of the inorganic anion is generated by the symmetry operator. The unit cell contains two asymmetric units.

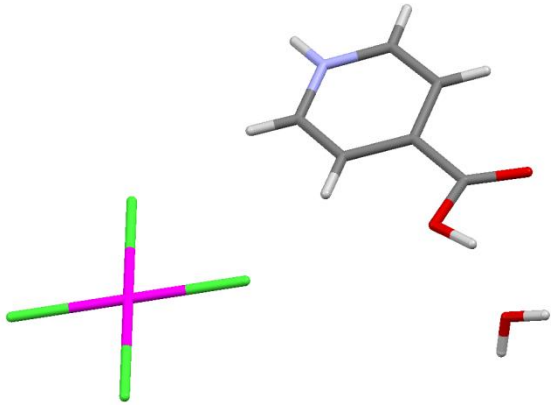

Figure 4.13: Molecular geometry of compound I.

The perhalometallate anion consists of a platinum atom that coordinates to four chloro ligands and has a slightly distorted square planar geometry. The chloro ligands have bonding distances (Pt—Cl) of 2.310 Å and 2.308 Å and make angles (Cl—Cu— Cl) of 90.33° and 89.67° with respect to the metal atom producing a slight distortion in the square planar geometry.

Similar to the previous structure, expansion of the molecular sphere demonstrates how the platinum tetrachloro anions pack to form an inorganic layer composed of discrete constituents while the protonated nitrogen atom of the cation demonstrates bifurcated hydrogen bonding with the anionic moiety.

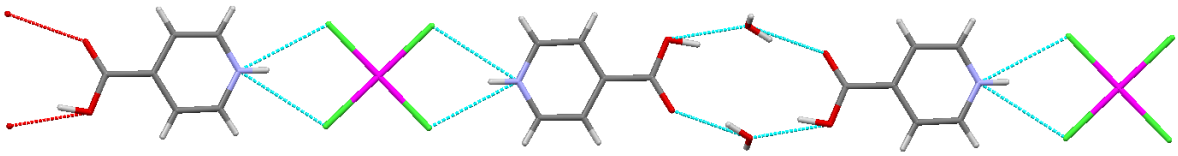

Figure 4.14: One-dimensional hydrogen bonded organic-inorganic ribbon.

Analogous to the ribbon that also forms in the previous structure, it is observed that the carboxylic acid group of the isonicotinic acid moiety does not form the typical hydrogen bonded carboxylic acid dimer, instead neutral solvate molecules act as bridging units between neighbouring cations (Figure 4.14) via hydrogen bonding between the carboxylic acid groups resulting in a one-dimensional ribbon.

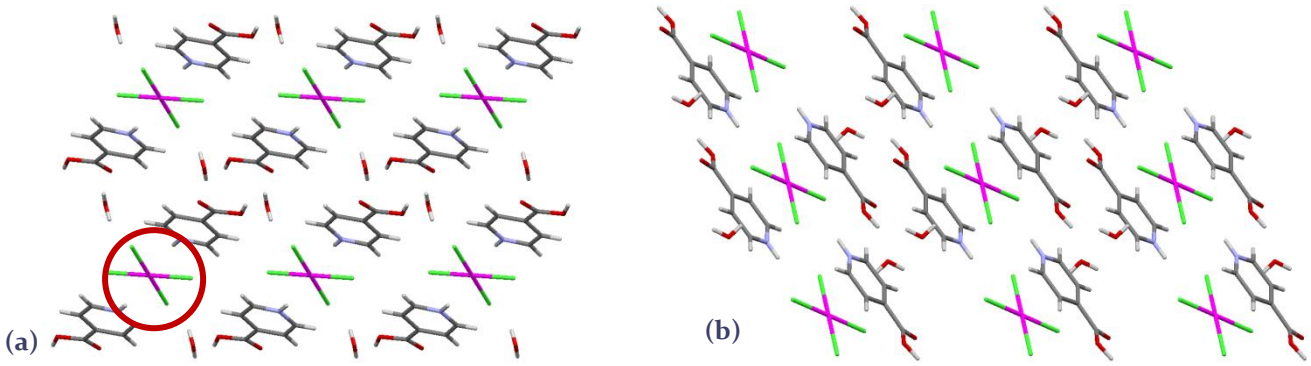

Figure 4.15: Packing of structure I viewed along the (a) a-axis and (b) b-axis. An isolated inorganic anion is circled.

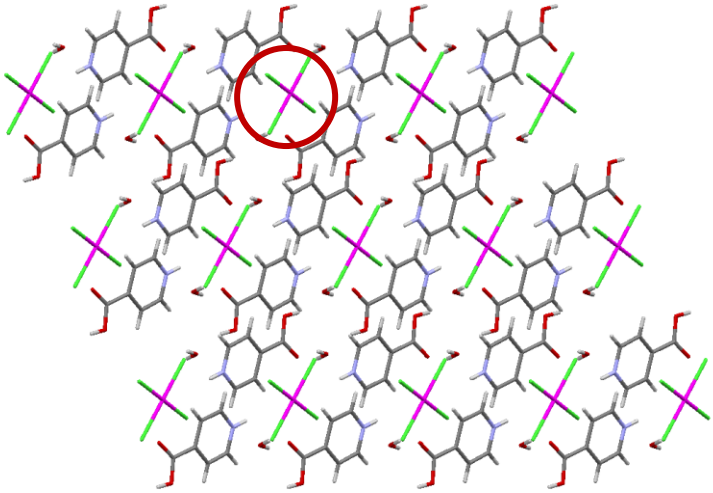

Figure 4.16: Packing of structure viewed along the c-axis. An isolated inorganic anion is circled.

Hydrogen bonding interactions between the nitrogen atom on 4-carboxypyridinium anion and two chloro ligands occur at distances (N—H···Cl) of 2.63 Å and 2.44 Å respectively, and make angles (N—H···Cl) of 130.04° and 145.21°. In addition, H-bonding occurs between the water molecule and the carboxylic acid groups at distances of (O—H···O) 1.740 Å and 1.898 Å while two coordinated chloro ligands also act as acceptor atoms for hydrogen bonds (O—H···Cl) with H-bonding distances of 2.770 Å and 2.635 Å.

J: bis(4-carboxypyridinium) tetrachloropalladate dihydrate, (Adams, et al., 2006), (CSD Refcode: XECFIV)

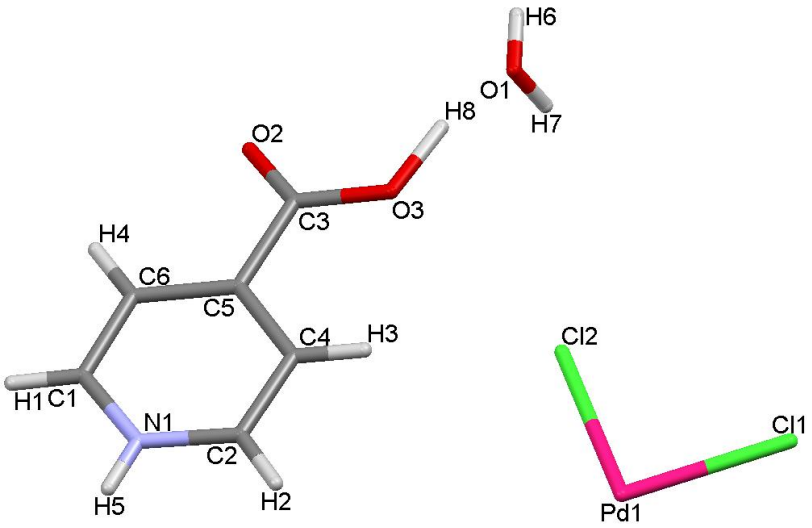

Figure 4.17: Asymmetric Unit of compound J:

Structure J is isostructural to structures H and I, and will not be discussed in detail. Figures showing the hydrogen bonding interactions as well as the packing of the molecules are included for clarity.

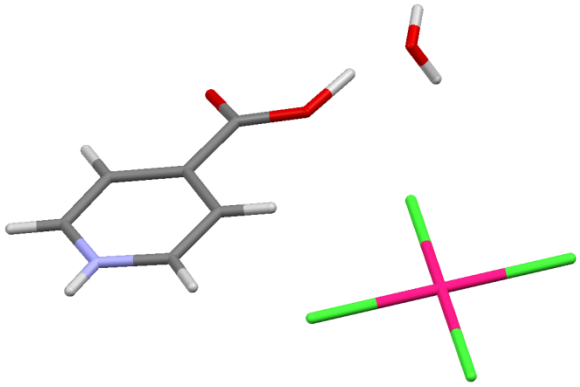

Figure 4.18: Molecular geometry of compound J.

The perhalometallate anion consists of a palladium atom that coordinates to four chloro ligands and has a slightly distorted square planar geometry. The chloro ligands have very similar bonding distances (Pd—Cl) of 2.307 Å and 2.309 Å to the palladium atom and make angles (Cl—Pd— Cl) 90.46° and 89.54° with respect to the metal atom producing a slight distortion in the geometry.

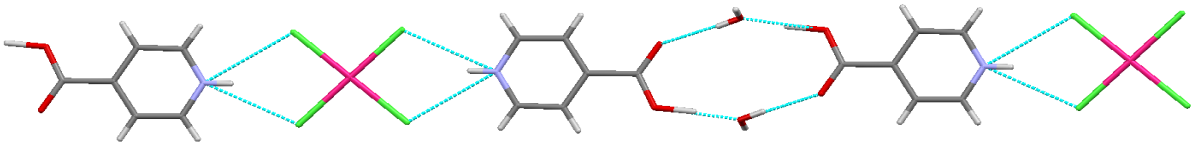

Figure 4.19: One-dimensional hydrogen bonded organic-inorganic ribbon.

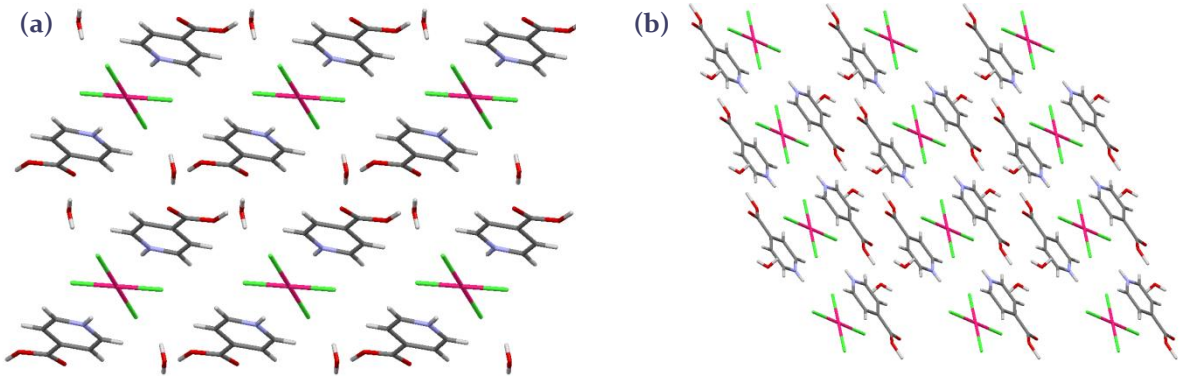

Figure 4.20: Layered packing of structure J viewed along the (a) a-axis and (b) b-axis.

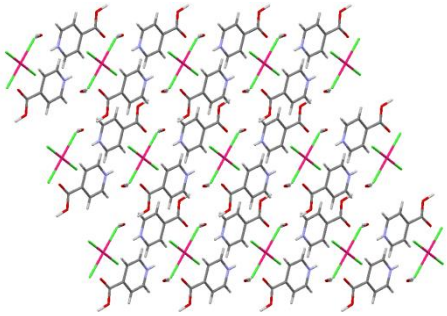

Figure 4.21: Packing of structure J viewed along the c-axis.

Hydrogen bonding interactions between the nitrogen atom on the 4-carboxypyridinium cation and two chloro ligands occur at distances (N—H···Cl) of 2.485 Å and 2.661 Å and make angles (N—H···Cl) of 146.21° and 134.76°. H-bonding also occurs between the carboxylic acid groups and water molecules at distances of (O—H···O) 1.433 Å and 1.949 Å while two coordinated chloro ligands also act as hydrogen bonding acceptor atoms (O—H···Cl) with H-bonding distances of 2.776 Å and2.583 Å.

K: bis(4-carboxypyridinium) tetrachloroplatinate, (Adams, et al., 2006), (CSD Refcode: XECCUE)

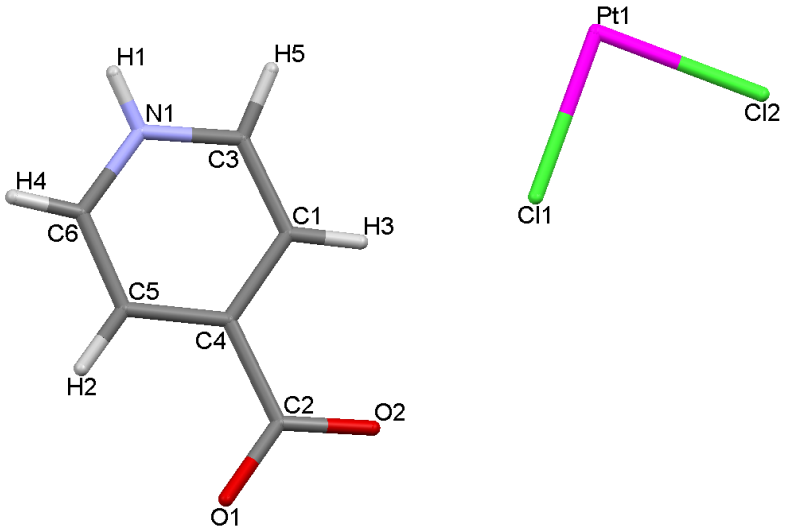

Figure 4.22: Asymmetric Unit of compound K:

The asymmetric unit of structure K contains 4-carboxypyridinium cation, with protonation occurring on the pyridine ring nitrogen atom of the isonicotinic acid molecule, and a platinum atom that coordinates to two chloro ligands. The platinum atom has a site occupancy factor of 0.25 and is positioned on a centre of inversion, and the rest of the molecule is generated by the symmetry operator (-x, -y, -z). The authors reported that the carboxylic acid hydrogen atoms were disordered, and as a result they are not shown in the Figures. Unlike what was observed in previously discussed 4-carboxypyridinium containing perhalometallate structures, no water molecules are incorporated into the structure. In the organic cation, the carboxylic acid functional group makes a dihedral angle of 6.11° with the aromatic ring plane. The platinum atom is situated in the corner of the unit cell, and the rest of the square planar anion is generated through symmetry. The unit cell contains two asymmetric units.

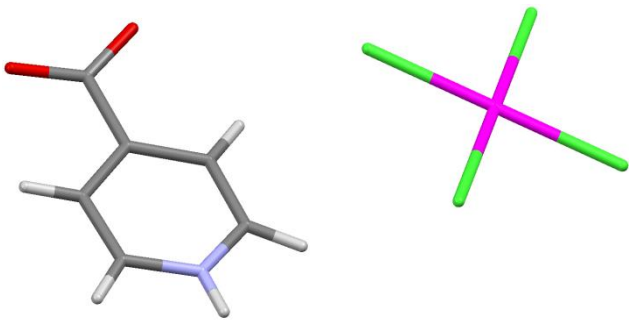

Figure 4.23: Molecular geometry of compound K.

The perhalometallate anion consists of a platinum atom that coordinates to four chloro ligands and has a slightly distorted square planar geometry. The chloro ligands exhibit bonding distances of (Pt—Cl) of 2.305 Å and 2.311 Å to the platinum atom and make angles (Cl—Pt— Cl) of 90.44° and 89.56° with respect to the metal atom, hence resulting in a slight deviation from ideal square planar geometry.

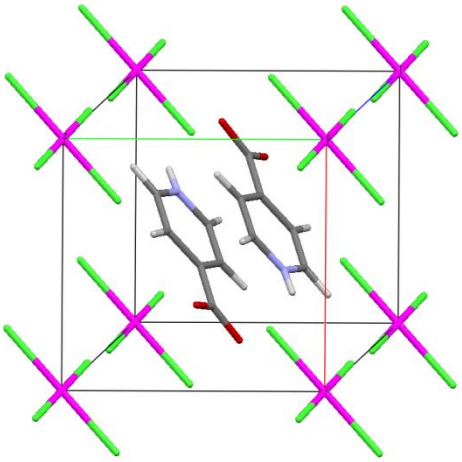

Figure 4.24: Illustration showing the unit cell and its constituents.

Figure 4.24 above illustrates the packing of the perhalometallate anion. The platinum atom occupies the corner of the unit cell while the cationic isonicotinic acid molecules are situated within the unit cell.

A layered structure is observed for compound K. In this structure a bi-layer of organic cations alternate with single layers of isolated, square planar inorganic anions, as illustrated in Figure 4.25. In the organic bi-layer, the organic cations pack parallel with their carboxylic acid groups pointing towards each other while the protonated pyridine group faces in the direction of the inorganic layer.

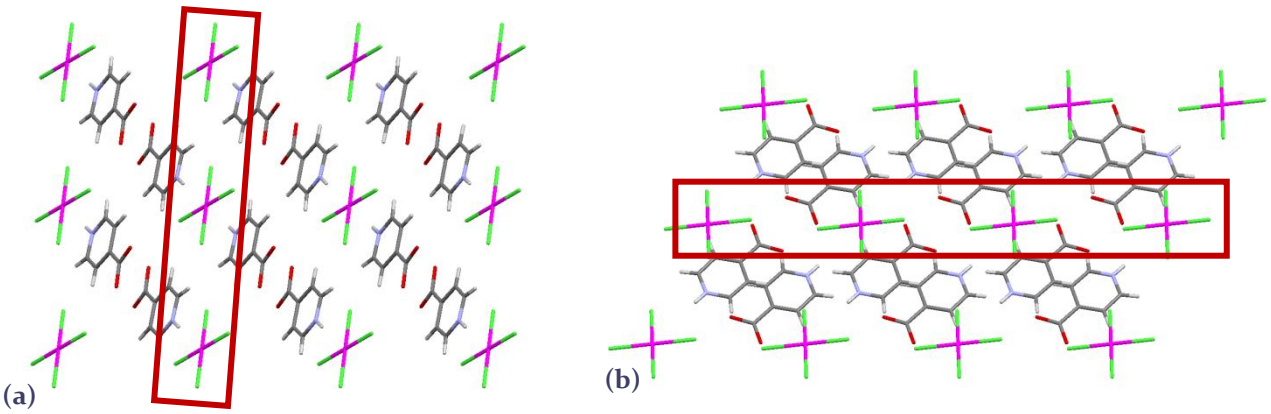

Figure 4.25: Packing of structure K viewed along the (a) a-axis and (b) b-axis. Inorganic layers, consisting of isolated anions, are illustrated within the blocks.

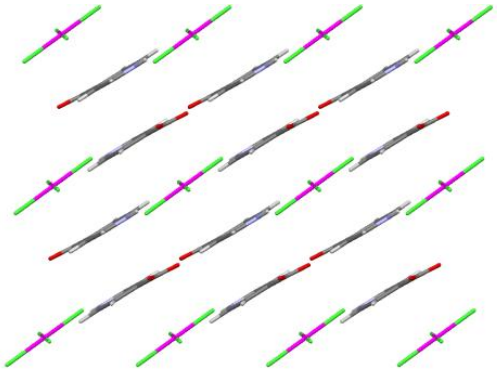

Figure 4.26: Packing of structure K viewed along the c-axis.

Bifurcated hydrogen bonding interactions occur between the pyridine nitrogen atom and the inorganic anion. In addition, a carboxylic acid dimer is formed between neighbouring carboxylic acid functional groups. Hydrogen bonding between the protonated nitrogen atom on the isonicotinic acid unit and two chloro ligands occur at distances (N—H···Cl) of 2.565 Å and 2.450 Å and make angles (N—H···Cl) of 137.78° and 141.13°. These interactions link the ions into a one-dimensional hydrogen bonded ribbon, as illustrated in Figure 4.28. Each hydrogen-bonded ribbon is observed to lie in parallel succession and forms a two-dimensional layer produced by extensive hydrogen bonding between anionic and cationic moieties.

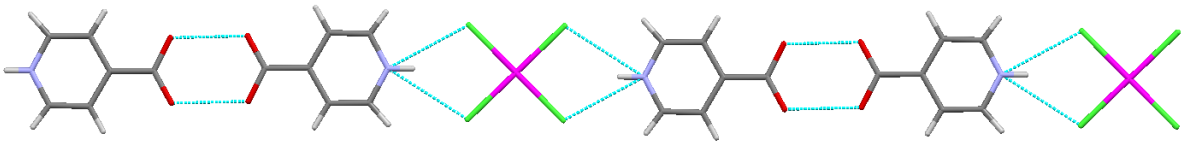

Figure 4.28: One-dimensional hydrogen bonded organic-inorganic ribbon.

Results

Structural investigation of novel compounds

A total number of ten novel ionic structures containing organic cations and perhalometallate anions have been determined in this investigation. These include four ionic structures containing the 4-carboxyanilinium cation, one structure containing the 4-carboxypyridinium cation, and five structures containing the protonated 4-aminobenzamide cation (also known as the 4-ammoniumbenzamide cation. The salt structure of 4-carboxypyridinium bromide was also determined. Note that no other ionic structures containing 4-ammoniumbenzamide have been reported in the literature, hence the current investigation makes a significant contribution to the knowledge regarding these types of structures.

Tables 4.2 to 4.4 below list the novel structures obtained in this study together with the structures reported in the literature, to form a matrix or family of compounds for each specific organic constituent. Note that the novel structures are numbered using uppercase Roman numerals in order to distinguish them from the structures reported in the literature. Table 4.5 and 4.6 lists the crystallographic parameters for the novel structures. Crystallographic information files (CIF) of all the novel structures are included on the accompanying CD.

Table 4.2: 4-Ammoniumbenzamide Family.

Metal	Cl	Br
Zn	**VI: Novel Structure (Inclusion structure)**	**VIII: Novel Structure (Isolated tetrahedron)**
Cd	-	**IX: Novel Structure (Isolated tetrahedron)**
Hg	**VII: Novel Structure (Isolated tetrahedron)**	**X: Novel Structure (Inorganic polymer)**

Table 4.3: 4-Carboxyanilinium Family.

Metal	Cl	Br	Cl/Br
Zn	**XI: Novel Structure (Poor data)**	**XII: Novel Structure (Two types of organic layers)**	-
Cd	G: WUGHIZ (Wang, et al., 2002)	**XIII: Novel Structure (Two types of organic layers)**	**XIV: Novel Structure (Halide solid-solution)**

Table 4.4: 4-Carboxypyridinium Family.

Metal	Cl	Br
	-	**XV: Novel Structure (Ionic salt)**
Hg	-	**XVI: Novel Structure (Complex sheet)**
Cu	H: PAQLOJ (Kumar, et al., 2005)	-
Pt	I: QIDLIY & K: XECCUE (Adams, et al., 2006)	-
Pd	J: XECFIV (Adams, et al., 2006)	-

It should be noted that hydrogen bonding distances refer to donor acceptor distances unless stated otherwise, and the terms ”structure X” and “compound X” are used interchangeably.

Table 2.5: Crystallographic data of novel compounds containing 4-carboxypyridinium, 4-carboxyanilinium and 4-ammoniumbenzamide cations.

Compound	VI	VII	VIII	IX	X
Empirical Formula	$2(C_7H_9ON_2)^+[ZnCl_4]^{2-}$ $.2H_2O$	$2(C_7H_9ON_2)^+[HgCl_4]^{2-}$ $\cdot H_2O)$	$2(C7H9ON2)^+[ZnBr_4]^{2-}$ $.H_2O$	$2(C_7H_9ON_2)^+[CdBr_4]^{2-}$ $.H_2O$	$(C_7H_9ON_2)^+[HgBr_3]^-$ $.H_2O$
M_r(g/mol)	545.51	1000.02	445.30	499.33	592.47
Crystal system	Monoclinoic	Monoclinic	Monoclinic	Monoclinic	Monoclinic
Space group	*C*2/c	*C*m	*C*m	*C*m	$P2_1/c$
Z	4	2	2	2	4
a/Å	19.0640(2)	6.9513(1)	7.0956(7)	7.0764(8)	12.980(4)
b/Å	15.0654(1)	21.528(3)	21.853(2)	22.008(2)	14.916(5)
c/Å	7.2630(6)	6.8809(1)	6.9276(7)	7.0176(8)	6.898 (2)
α/°	90.00	90.00	90.00	90.00	90.00
β/°	96.7660(1)	103.404(2)	103.964(2)	104.044(2)	97.923(4)
γ/°	90.00	90.00	90.00	90.00	90.00
V (Å^3)	2071.46(3)	1001.7 (3)	1042.45(2)	1060.2 (2)	1322.8 (7)
F(000)	1048	848	422	465	1060
D_c (g cm^{-3})	1.653	3.316	1.419	1.564	2.975
μ (mm^{-1})	1.73	30.68	6.91	6.66	20.68
R-Factor (%)	3.6	2.4	5.8	2.4	6.4
Diffractometer	Siemens P4 Bruker 1k CCD	Siemens P4 Bruker 1k CCD	Siemens P4 Bruker 1k CCD	Siemens P4 Bruker 1k CCD	Siemens P4 Bruker 1k CCD
T (k)	293	293	293	293	293
λ(Mo Kα) (Å)	0.71073	0.71073	0.71073	0.71073	0.71073
Reflections collected	5570	2675	2696	2866	6725
Unique reflections	1986	1147	1789	1241	2477
Parameters	143	126	126	126	138
$R[F^2>2\sigma(F^2)]$	0.036	0.024	0.058	0.024	0.064
$wR(F^2)$	0.102	0.064	0.136	0.062	0.179
Δp_{max} & Δp_{min} (e Å^{-3})	0.54 and -0.31	1.31 and -1.04	2.91 and –0.96	0.55 and -0.62	2.95 and - 3.31

$R=\sum||F_0|-|F_c||)/\sum|F_c|$
$wR=[\sum w(F^2_0-F^2_c)^2/\sum w(F^2_0)$

Table 4.6: Crystallographic data of novel compounds containing 4-carboxypyridinium, 4-carboxyanilinium and 4-ammoniumbenzamide cations.

Compound	XI	XII	XIII	XIV	XV	XVI
Empirical Formula	$2(C_7O_2N)2(C_7O_2N)^+$ $[ZnCl_4]^{2-}\cdot H_2O$	$2(C_7H_8O_2N)^+[ZnBr_4]^{2-}$ $\cdot H_2O$	$2(C_7H_8O_2N)^+[CdBr4]^{2-}$ $\cdot H_2O$	$(C_7H_8O_2N)^+$ $[CdBr_4H_2O]^-$	$(C_6H_6O_2N)^+[Br]^-$	$2(C_6H_6O_2N)^+$ $[Hg_6Br_{14}]^{2-}$
M_r(g/mol)	743.51	499.46	564.24	155.43	204.02	2570.38
Crystal system	Triclinic	Monoclinic	Monoclinic	Monoclinic	Monoclinic	Triclinic
Space group	*Cc*	*P*2/c	*P*2/c	*P*2/c	*P*2/n	*P*1
Z	4	4	4	2	2	1
a/Å	13.3054(1)	7.0537(5)	7.1578(1)	12.0977(1)	7.3127(6)	7.4390(8)
b/Å	7.3719(6)	45.732(3)	45.919(8)	5.8974(5)	7.3395(6)	10.5049(1)
c/Å	33.553(3)	6.6183(5)	6.6341(1)	15.0241(1)	13.5279(1)	13.7390(2)
α/°	90.00	90.00	90.00	90.00	90.00	73.126(2)
β/°	92.508(1)	100.1960(1)	100.172(3)	100.1120(1)	94.3710(1)	78.584(2)
γ/°	90.00	90.00	90.00	90.00	90.00	70.873(2)
V (Å^3)	3287.9 (5)	2101.2(3)	2146.22	1055.24	723.95	964.41
F(000)	1592	976	1040	140	458	584
D_c (g cm^{-3})	1.567	1.579	1.746	0.489	2.084	2.247
μ (mm^{-1})	1.130	4.99	8.44	0.99	5.61	16.24
R-Factor (%)	8.19	7.47	10.8	3.9	3.1	5.4
Diffractometer	Siemens P4 Bruker 1k CCD	Siemens P4 Bruker 1k CCD	Siemens P4 Bruker 1k CCD	Siemens P4 Bruker 1k CCD	Siemens P4 Bruker 1k CCD	Siemens P4 Bruker 1k CCD
T (k)	293	293	293	293	293	293
λ(Mo Kα) (Å)	0.71073	0.71073	0.71073	0.71073	0.71073	0.71073
Reflections collected	6826	11376	10581	5465	3770	5239
Unique reflections	3415	5739	3936	2000	1378	4028
Parameters	419	490	231	141	109	255
$R[F^2>2\sigma(F^2)]$	0.0819	0.074	0.108	0.039	0.031	0.054
$wR(F^2)$	0.2223	0.085	0.276	0.117	0.080	0.170
Δp_{max} & Δp_{min} (e Å^{-3})	2.65 and -1.81	0.70 and -0.56	9.34 and -2.16	1.18 and -0.50	0.59 and -0.38	3.12 and -2.56

$R=\sum||F_0|-|F_c||)/\sum|F_c|$
$wR=[\sum w(F^2_0-F^2_c)^2/\sum w(F^2_0)$

Novel 4-Ammoniumbenzamide containing perhalometallate structures

A total of five novel structures containing the 4-ammoniumbenzamide cation have been determined in this study. As mentioned previously, these structures will make a large contribution to the understanding of this system since no structures containing this cation combined with a perhalometallate anion have been reported in the literature.

VI: (4-ammoniumbenzamide) tetrachlorozincate dihydrate

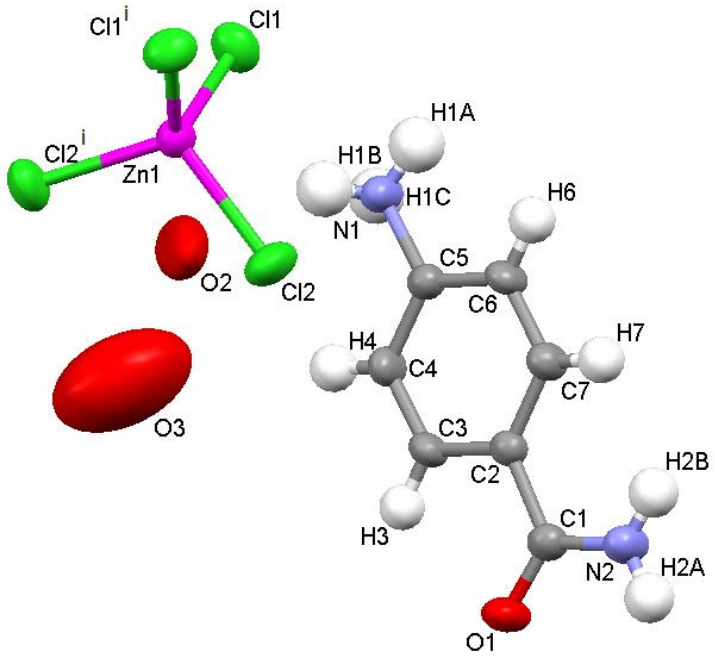

Figure 4.29: Asymmetric unit of compound VII: Ellipsoids are drawn at the 50% probability level. (Symmetry operator i: -x, y, ½ - z).

The asymmetric unit of structure VI consists of half an inorganic anion, in which a zinc atom is coordinated to two chloro ligands, as well as an isolated, amine protonated 4-ammoniumbenzamide cation. In addition there are two isolated solvate water molecules in the asymmetric unit. Both water molecules display disorder, with one water molecule being significantly more disordered than the other. The hydrogen atoms on the disordered oxygen atoms of the water molecules could not be placed. The disordered oxygen atom O2 lies on the special position (0, 0, 0.5), with a site occupancy of 0.5. The zinc atom is located on a special position (0, 0.755886, 0.25), and lies both on a mirror plane and a two-fold rotation axis, with a fractional occupancy of 0.5, and as a result the rest of the isolated inorganic anion is generated by symmetry. The unit cell comprises four asymmetric units.

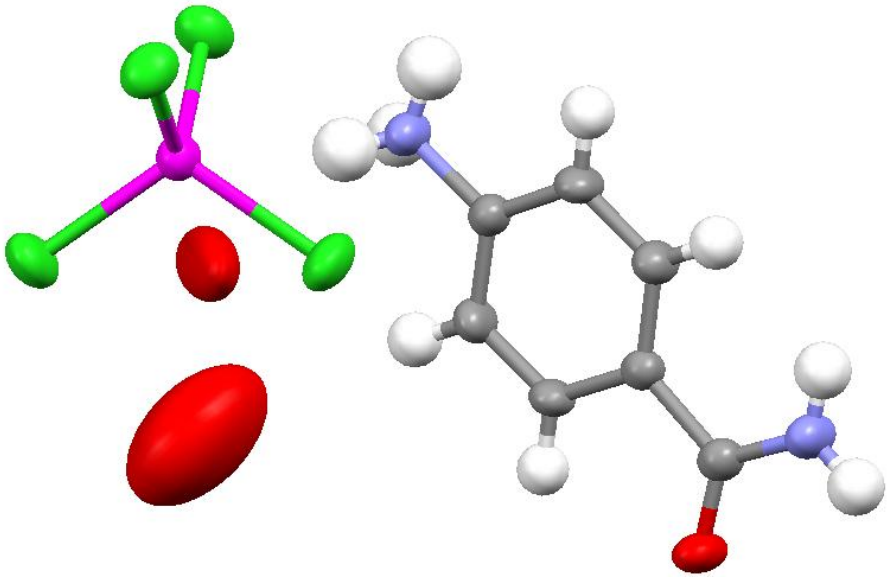

Figure 4.30: Molecular geometry of compound VII.

Figure 4.30 illustrates the geometry of the two ions. The isolated perhalometallate anion consists of a zinc atom that coordinates to four chloro ligands and produces a slightly distorted tetrahedral geometry. The coordination distances of the chloro ligands with the metal atom (Zn–Cl) are measured to be 2.2616(7) Å and 2.2553(7) Å respectively. The angles that are generated between the metal atom and the coordinated chloro ligands vary, and are observed to range from 108.91(4)° to 109.04(3)°, values which also hint at the slight geometrical distortion from an ideal tetrahedral geometry. The organic cation is observed to be planar.

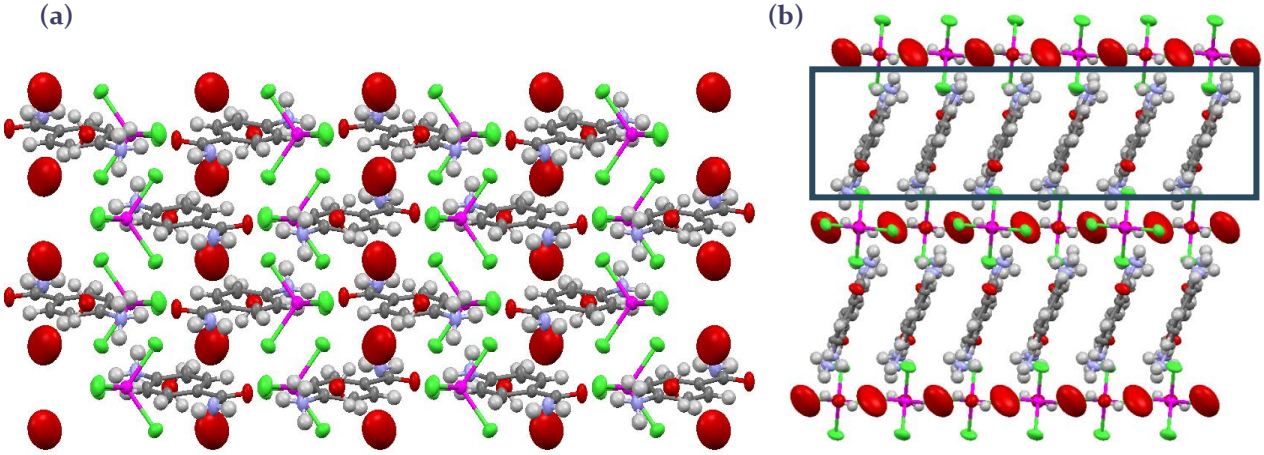

Figure 4.31: Packing of structure VI viewed along the (a) a-axis and (b) b-axis. The block indicates the organic layer in Figure (b).

Figures 4.31 illustrate the packing of molecular ions in the structure. A layered structure, with layers extending parallel to the ab-plane, is formed in which the 4-ammoniumbenzamide cations comprise the organic layer, while the isolated tetrachlorozincate anions form the inorganic layer. The water molecules also form part of the inorganic layer, with the highly disordered water molecules packing on the corners of the unit cell. Layers of organic cations alternate with layers containing water molecules and inorganic anions. All the species present interact via hydrogen bonding interactions. It is observed that in the organic layer the cationic species alternate in their orientation relative to the inorganic.

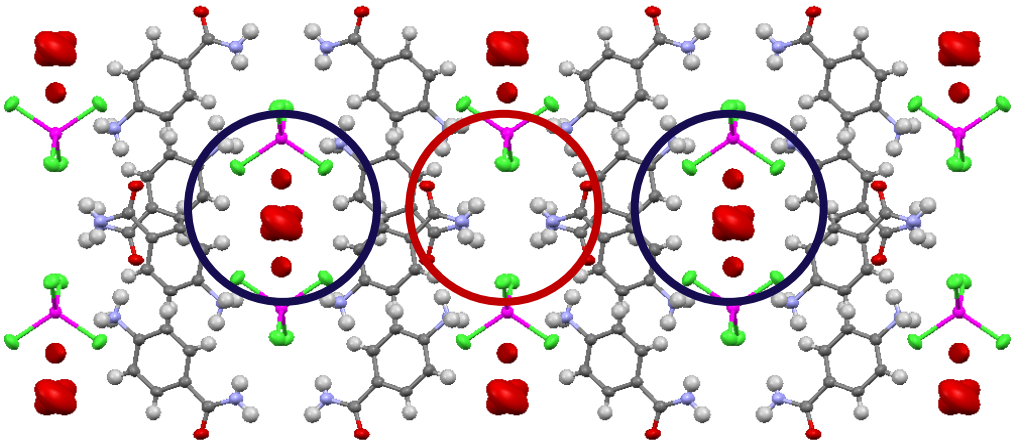

Figure 4.32: Packing of structure VI viewed along the c-axis. Circles indicate the channels that are generated in the structure.

Figure 4.32 illustrates packing of the species as viewed along the c-axis and shows the inclusion of solvate water molecules into channels in the structure. This compound may be viewed as an inclusion compound. These channels are generated by cations and anionic species that are linked via hydrogen bonds between the protonated amine groups and the inorganic anions. The section of the channel wall formed by the aromatic rings is hydrophobic, while the part of the channel wall formed by the anions is hydrophilic.

It is observed that two types of channels are generated; one that incorporates the water molecules and another smaller channel that contains no water molecules. The second, smaller channel, indicated by a red circle in Figure 4.32 is formed by the NH_2 groups of the amide functional groups and the tetrachlorozincate anions, which interact through hydrogen bonding. The distinction arises from the steric hindrance that is generated by the amide group, and as a result, reduces the dimensions of the channels.

Water molecules are incorporated into the larger channels, indicated by the blue sircles, but show disorder. When viewed down the c-axis, as shown in Figure 4.32, it is evident that in each channel the water molecules pack in rows, with three different rows of water molecules extending into the channels in the c-direction.

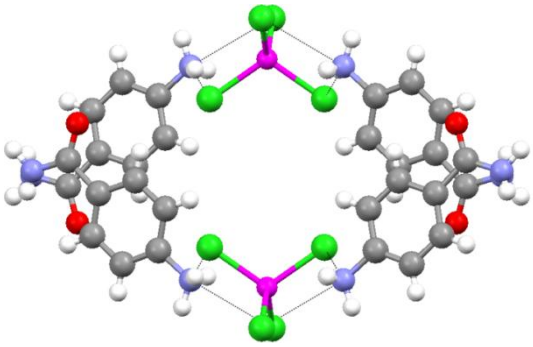

Figure 4.33: Hydrogen bonding interactions between ammonium groups and tetrachlorozincate anions which result in the formation of a channel.

The severe disorder of the water molecule located in the centre of the channel, hence the middle row of water molecules, may be due to the fact that this water molecule cannot form or accept hydrogen bonds, of suitable strength, to or from the channel wall, hence it cannot be anchored well.

Each channel comprises a limited number of chlorine atoms within their walls, towards which strong hydrogen bonds from water molecules are possible, hence the two water molecules neighbouring the channel wall can form hydrogen bonds to the chloro ligands, and hence be more anchored than the central water molecules, resulting in less disorder. The water molecules in the centre of the channel can only form hydrogen bonds to the water molecules on the ends, which are anchored to the channel wall, but which are also disordered, thus causing the position of the water molecules to vary in the channel.

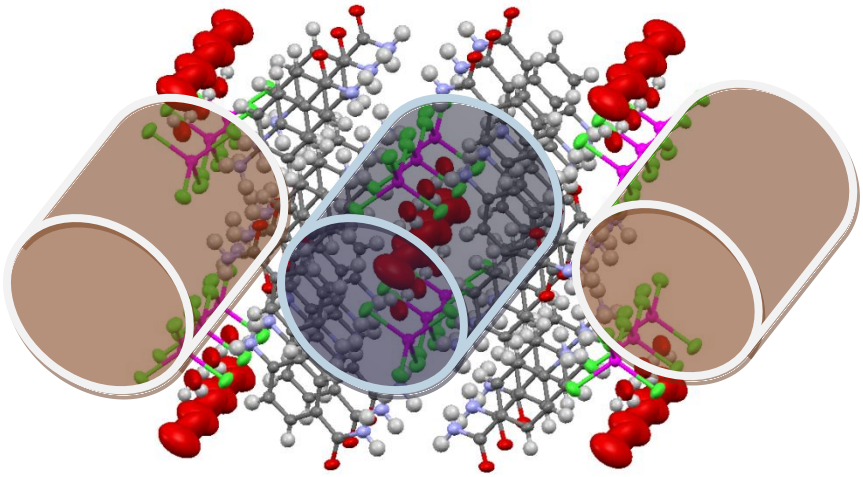

Figure 4.34: Three-dimensional representation of the channels that are generated within the structure.

The cations partake in extensive intermolecular hydrogen bonding interactions with the anionic species via the amine portion of the amide group, and the ammonium groups and, as a consequence, produce a two dimensional hydrogen bonded organic-inorganic structure. Hydrogen bonding parameters are listed in Table 4.7.

The nitrogen atom of the ammonium group undergoes extensive hydrogen bonding, exemplified by a bifurcated hydrogen bond that exist, linking the nitrogen atom with a chloro ligand (N1—H1B···Cl1) and an oxygen atom (N1—H1B···O2) at distances 3.499(3) Å and 2.928(4) Å respectively. In addition, hydrogen bonds occur towards another chloro ligand (N1—H1C···Cl2) at a distance of 3.355(3) Å and towards the oxygen atom on the amide group (N1—H1A···O1) with a distance of 2.696(3) Å. The nitrogen atom on the ammonium group forms hydrogen bonds with coordinated chloro ligands on neighbouring zinc atoms at distances of (N2—H2A···Cl1) 3.450(2) Å and (N2—H2B···Cl1) 3.370(2) Å. Hydrogen bonding parameters are listed in Table 4.7, and the resulting two-dimensional hydrogen bonding network parallel to the bc-plane is illustrated in Figure 4.35.

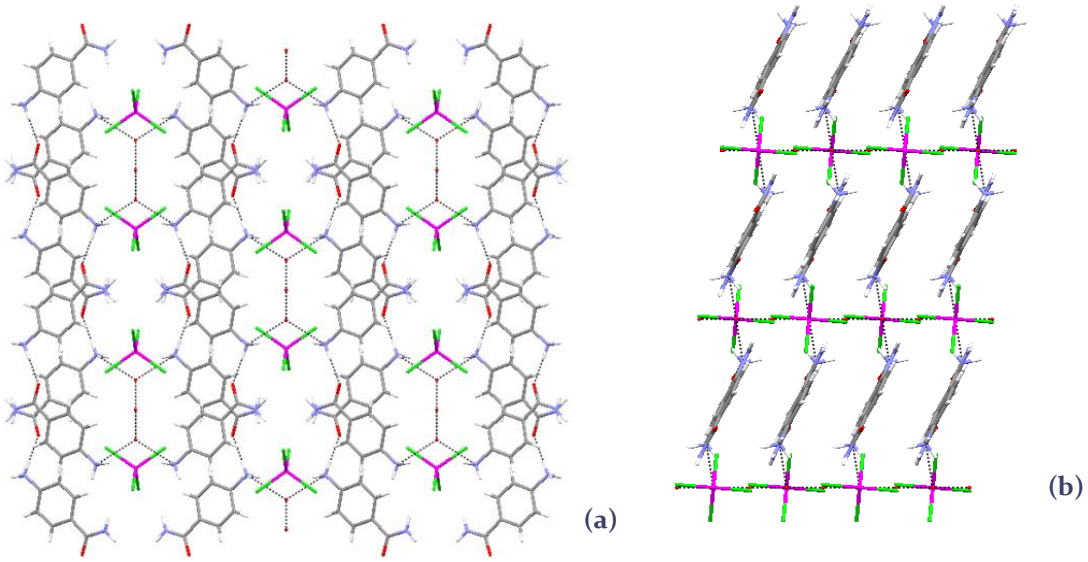

Figure 4.35: Hydrogen bonding interactions are shown as black dotted lines. Please note that only the oxygen atoms of the water molecules are shown, and it is assumed that they participate in hydrogen bonding.

Table 4.7: Hydrogen-bond geometry, (Å, °).

Compound V				
D—H···A	D—H	H···A	D···A	D—H···A
N1—H1A···O1 [i]	0.89	1.81	2.696(3)	176.2
N1—H1B···O2	0.89	2.24	2.928(4)	133.7
N1—H1B···Cl1	0.89	2.83	3.499(3)	133.5
N1—H1C···Cl2 [ii]	0.89	2.49	3.355(3)	165.6
N2—H2A···Cl1 [iii]	0.86	2.60	3.450(2)	171.1
N2—H2B···Cl1 [iv]	0.86	2.61	3.370(2)	147.6

Symmetry codes: (i) –x+1/2, y- 1/2, -z+3/2; (ii) x, y, z+1; (iii) x+1/2, y+1/2, z: (iv) –x+1/2, -y+3/2, -z+1.

The aromatic rings lie in extreme parallel displacement relative to each other with a centroid-to-centroid distance of 5.55 Å which separates neighbouring parallel aromatic rings.

VII: (4-ammoniumbenzamide) tetrachloromercurate hydrate

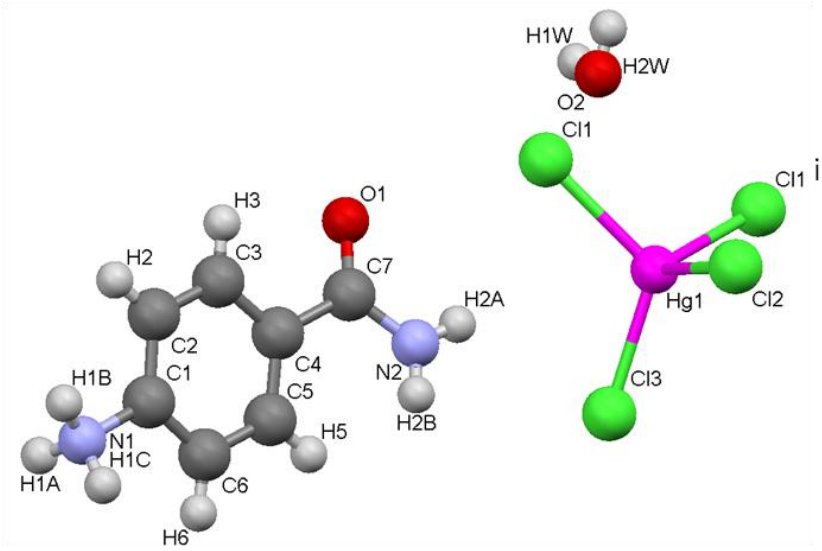

Figure 4.36: Asymmetric unit of compound VII: Ellipsoids are drawn at the 50% probability level. (Symmetry operator i: x, -y, z).

The asymmetric unit of novel structure VII contains a 4-ammoniumbenzamide cation, which is protonated on the amine portion to form an ammonium group opposite the amide functional group, an inorganic unit comprising a mercury atom coordinated to three chloro ligands, as well as an isolated water molecule, as shown in Figure 4.36. The mercury atom lies on a mirror plane with a site occupancy of 0.5, and the rest of the anion is generated across the mirror plane. The water molecule also lies on a mirror plane. The amide group of the cation makes an intersecting angle of 18.13° with the plane generated by the aromatic ring. The unit cell comprises two asymmetric units.

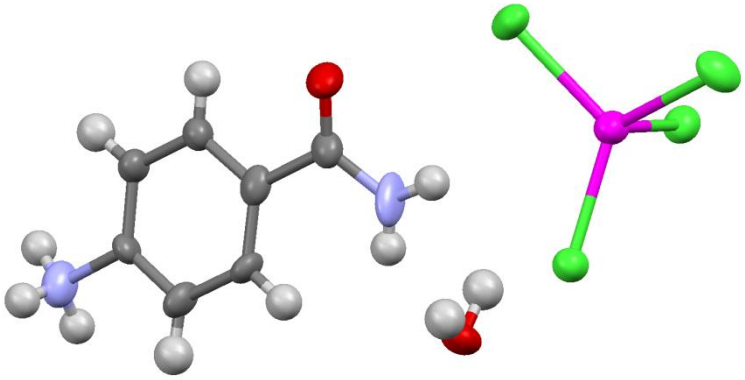

Figure 4.37: Molecular geometry of compound VII.

The complete tetrachloromercurate anion is shown in Figure 4.37. This perhalometallate anion consists of a mercury atom that coordinates to four chloro ligands and produces an anion with a distorted tetrahedral geometry. The coordination distances of the chloro ligands with the metal atom are measured to be 2.423(3) Å and 2.596(3) Å while two other chloro ligands share an equivalent distance of 2.477(2) Å.

The Cl—M—Cl angles that are generated by the ligands vary, and are observed to range from 102.60(7)° to 118.44(7)° which is indicative of the geometrical distortion of the tetrahedron. The discrete perhalometallate anions produce a one-dimensional chain as shown below, but the contact between the potential bridging halogeno ligand and the neighbouring mercury atom is too long, at approximately 4.48 Å, to be considered a coordination bond, hence the anions are considered to be isolated. However, this long M-Cl...M contact may be weakly stabilising.

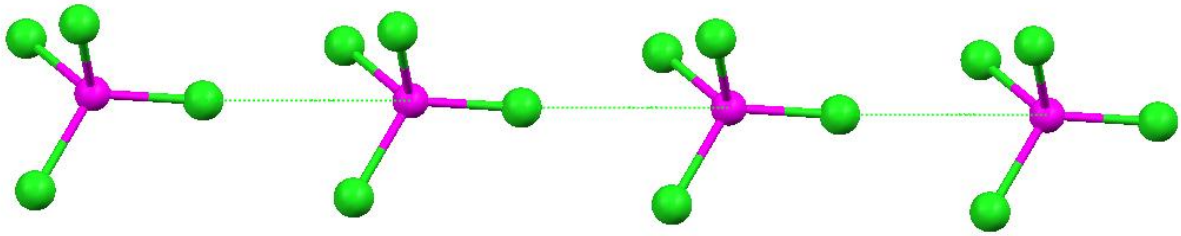

Figure 4.38: Long M—Cl···M contact in structure VII.

As can be observed in Figure 4.39 translation of the unit cell gives a layered structure, parallel to the bc-plane, consisting of an inorganic two-dimensional layer of isolated inorganic units and water molecules. Secondly, the structure contains layers of the organic constituent, which alternate successively with the anionic layer. In this case, the 4-ammoniumbenzamide cations interact non-covalently with the inorganic units and water molecule through hydrogen bonding via both the amide and ammonium groups. It is observed from Figure 4.39 and 4.40 that the inorganic layers lie in parallel succession with the organic layer. The aromatic rings of the organic cations are stacked in an approximately parallel sequence, and alternate in orientation when viewed down the c-axis. This irregularity in terms of non-parallel aromatic rings may be attributed to the steric hindrance brought on by both the ammonium group and the amide group, and may cause the organic molecules to rotate in orientation.

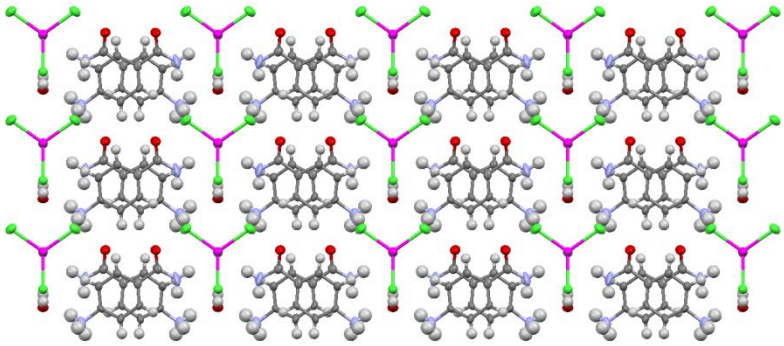

Figure 4.39: Packing of structure VII viewed along the a-axis.

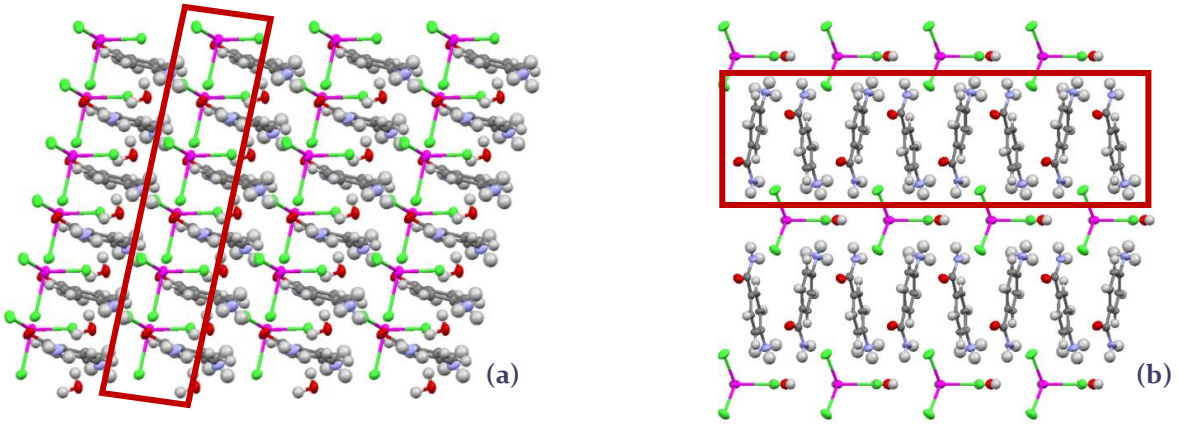

Figure 4.40: Packing of structure VII viewed along the (a) b-axis and (b) c-axis. The inorganic layer and organic layers are shown within the blocks.

Extensive hydrogen bonding interactions are present between all the species comprising the structure. The nitrogen atom on the ammonium group is surrounded with, and forms hydrogen bonds to a chloro ligand (N1—H1A···Cl1) at a distance of 3.234(8) Å, a water molecule (N1—H1B···O2) at a distance of 3.013(1) Å and an oxygen atom from the amide group (N1—H1C···O1) at a distance of 2.813(1) Å. The nitrogen on the amide group forms hydrogen bonds with two chloro ligands (N—H···Cl) at distances 3.424(8) Å and 3.767(9) Å. All hydrogen bonding parameters are listed in Table 4.8, and Figure 4.41 illustrates the complex hydrogen bonding network, parallel to the ac-plane.

Table 4.8: Hydrogen-bond geometry of structure VII, (Å, °).

Compound V				
D—H···A	D—H	H···A	D···A	D—H···A
N1—H1A···Cl1 ^{i}	0.89	2.37	3.234(8)	164.5
N1—H1B···O2 ^{ii}	0.89	2.15	3.013(1)	162.7
N1—H1C···O1 ^{iii}	0.89	1.99	2.813(1)	153.2
N2—H2A···Cl2 ^{iv}	0.86	2.67	3.424(8)	146.9
N2—H2B···Cl1 ^{v}	0.86	2.92	3.767(9)	168.7
O2—H2W···Cl2 ^{vi}	0.743(2)	2.643(3)	3.38(2)	172.4(1)
O2—H1W···Cl3 ^{vi}	0.812(2)	2.618(3)	3.429(19)	176.4(1)

Symmetry codes: (i) x-1/2, -y+1/2, z+1; (ii) x+1/2, y+1/2, z+1; (iii) x+1/2, -y+1/2, z+1; (iv) x-1, y, z; (v) x, y, z+1; (vi) x-1, y, z-1.

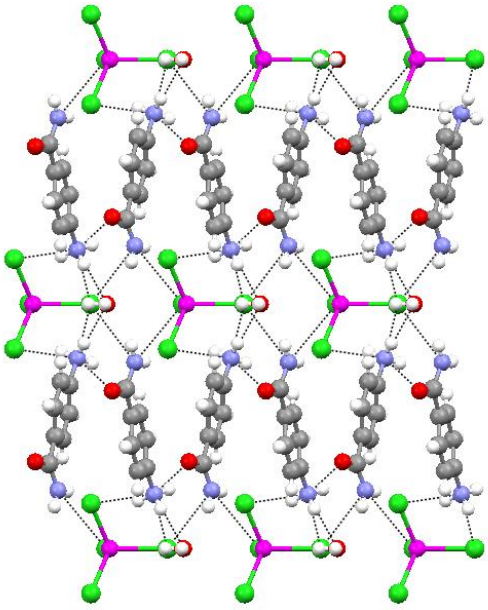

Figure 4.41: Two-dimensional hydrogen bonding network parallel to the ac-plane.

The aromatic rings of the organic constituents lie in planes that are approximately parallel to one another. There is no direct overlap between the rings and it is observed that the rings exhibit slipped displacement relative to each other. The distance between the centres of the parallel rings is 3.748 Å (centroid-to-centroid distance) which corresponds to the distance found in attractive aromatic interactions. The angle of the ring normal and the vector through the ring centre is 21.98° which is similar to the expected angle of 20° which is often observed for π-π interactions according to Janiak (2000).

VIII: (4-ammoniumbenzamide) tetrabromozincate hydrate

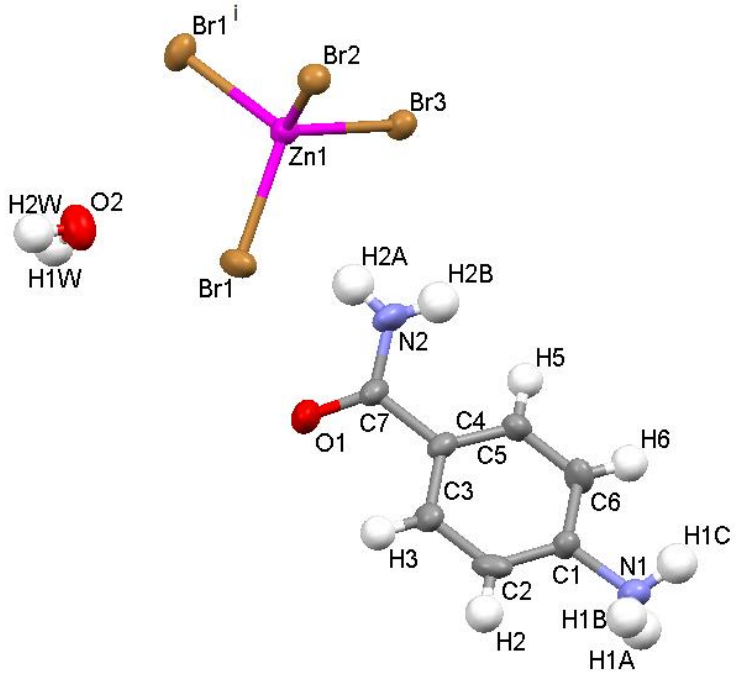

Figure 4.42: Asymmetric unit of compound VIII: Ellipsoids are drawn at the 50% probability level. (Symmetry operator i: x, -y, z).

Structure VIII is isostructural to structure VII, and only selected structural features will be highlighted, and relevant Figures included. In the organic cation, the amide functional group makes an intersecting angle of 21.98° with the plane generated by the aromatic ring. The unit cell is made up of two asymmetric units where both the zinc atom and the oxygen atom of the water molecule is positioned on the mirror plane on the face of the unit cell and have a site occupying factor of 0.5.

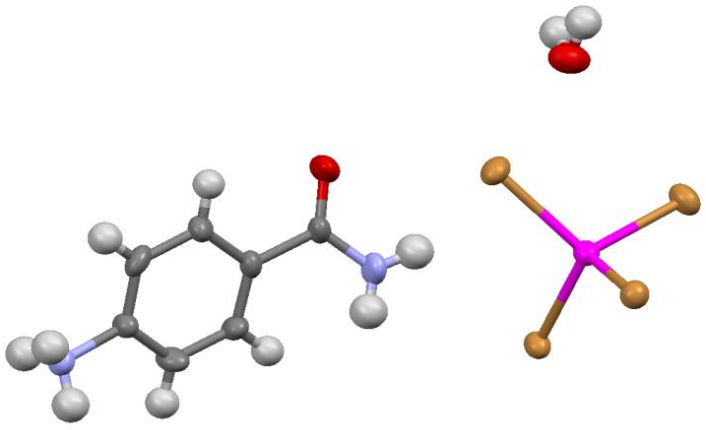

Figure 4.43: Molecular geometry of compound VIII.

Figure 4.43 shows the geometry of the anion. In the tetrahedral perhalometallate anion the coordination distances of the bromo ligands to the metal atom are 2.3923(15) Å and 2.4402(16) Å while two other bromo ligands bond at the equivalent distance of 2.4091(10) Å.

Figure 4.44 illustrates how the discrete $[ZnBr_4]^{2-}$ perhalometallate anions pack in a one-dimensional chain while the cationic species forms an organic layer and balance out the charge. Similar to the previous structure, the inorganic tetrahedral units display no interactions between neighbouring anions while the 4-carboxyanilinium cation partakes in extensive intermolecular interactions with the anionic species, consequently producing a two-dimensional hydrogen bonded network.

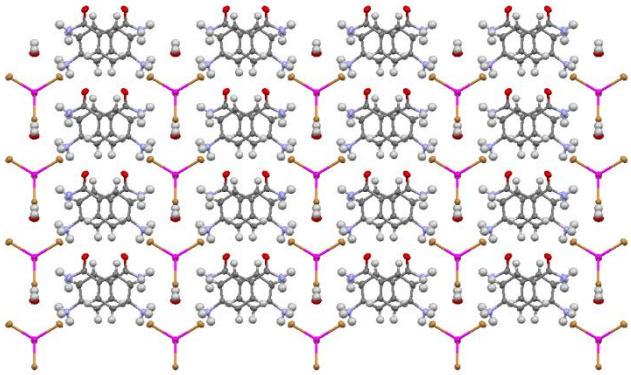

Figure 4.44: Packing of structure VIII viewed along the a-axis.

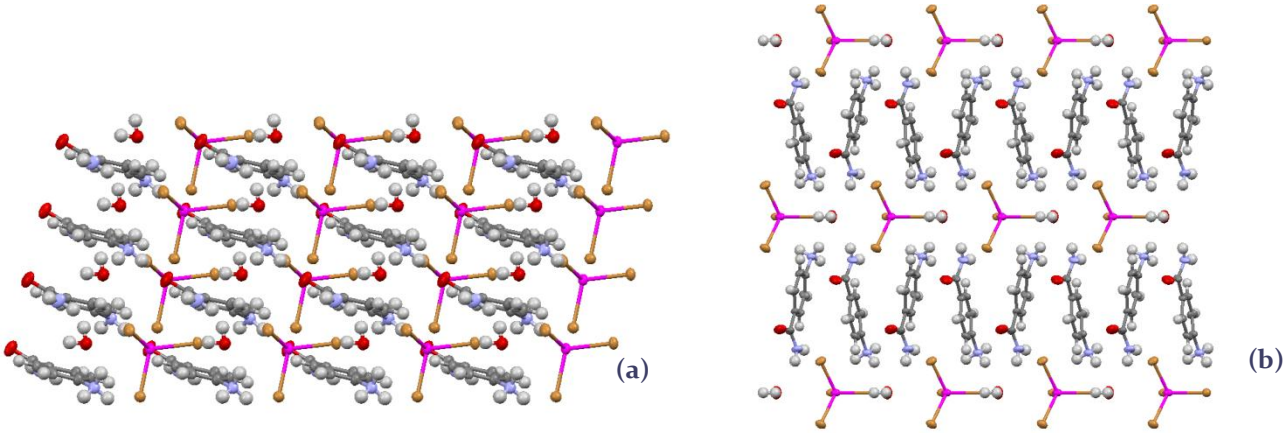

Figure 4.45: Packing of structure VIII viewed along the (a) b-axis and (b) c-axis.

As observed in the previous structure extensive intermolecular hydrogen bonding occurs between the anionic and cationic constituents within the structure, while the solvate water molecule shows significant linking that aggregate organic and inorganic building blocks. The nitrogen atom on the ammonium group forms hydrogen bonds with a bromo ligand (N1—H1A···Br1) 3.414(7) Å, a water molecule (N1—H1B···O2) at 3.046(9) Å and an oxygen atom from the amide group (N1—H1C···O1) at 2.819(1) Å. The nitrogen atom on the amide group forms a bifurcated hydrogen bond with two bromo ligands (N—H···Br) at distances of 3.587(8) Å and 3.420(8) Å. Hydrogen bond parameters are listed in Table 4.9.

Table 4.9: Hydrogen-bond geometry of structure VIII, (Å, °).

Compound V				
D—H···A	D—H	H···A	D···A	D—H···A
N1—H1A···Br1 [i]	0.89	2.59	3.414(7)	155.2
N1—H1B···O2 [ii]	0.89	2.19	3.046(9)	160.4
N1—H1C···O1 [iii]	0.89	1.96	2.819(1)	160.8
N2—H2A···Br2 [iv]	0.86	2.86	3.587(8)	143.7
N2—H2A···Br3	0.86	3.03	3.420(8)	110.0
N2—H2B···Br1 [v]	0.86	3.07	3.909(8)	165.9
O2—H2W···Br2 [vi]	0.827(9)	2.6544(1)	3.469(1)	169.0(7)
O2—H1W···Br3 [vi]	0.822(1)	2.6873(1)	3.509(1)	179.2(7)

Symmetry codes: (i) x-1/2, -y+1/2, z+1; (ii) x+1/2, y+1/2, z+1; (iii) x+1/2, -y+1/2, z+1; (iv) x-1, y, z; (v) x, y, z+1; (vi) x-1, y, z-1.

The aromatic rings of the organic constituents pack in an approximately parallel fashion. The centroid-to-centroid distance between the centre of parallel rings are 3.829 Å indicating the presence of aromatic interactions. The angle produced by the ring normal and the vector through the ring centre is 22.09° which is similar to the expected angle of 20° often observed for aromatic interactions, as reported by Janiak, (2000).

IX: (4-ammoniumbenzamide) tetrabromocadmate hydrate

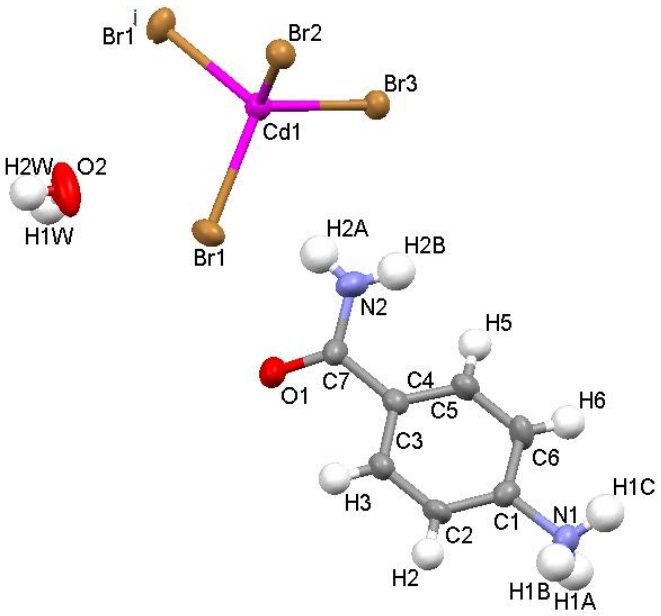

Figure 4.46: Asymmetric unit of compound IX: Ellipsoids are drawn at the 50% probability level. (Symmetry operator i: x, -y, z).

Structure IX is isostructural to compounds VII and VIII above. Only the main structural characteristics will be discussed below, and relevant Figures included. The amide group forms a dihedral angle of 22.54° with the plane of the aromatic ring. The cadmium atom has a site occupancy factor of 0.5 while the oxygen atom comprising the water molecule also has a site occupancy factor of 0.5

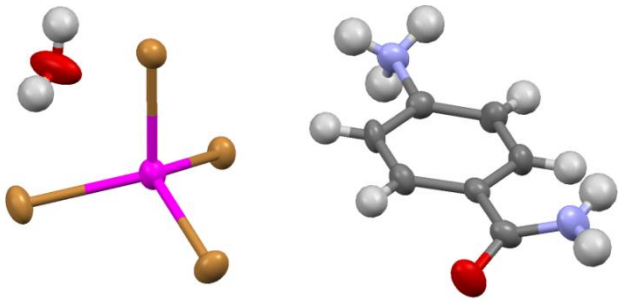

Figure 4.47: Molecular geometry of compound IX.

The anion geometry and the molecular geometry of the cation indicating the twist of the amide group relative to the aromatic plane are shown in Figure 4.47. The Cd—Br bonding distances are 2.5768(7) Å, 2.5634(10) Å and 2.6281 (11) Å. The angles that are generated by the ligands vary, and are observed to range from 104.87(2)° to 113.70(2)° which indicates the geometrical distortion of the anion. The amide group is rotated 22.51° relative to the plane of the aromatic ring. Figures 4.48 to 4.49 illustrates the layered packing of the species constituting the structure and hydrogen bonding interactions are listed in Table 4.10.

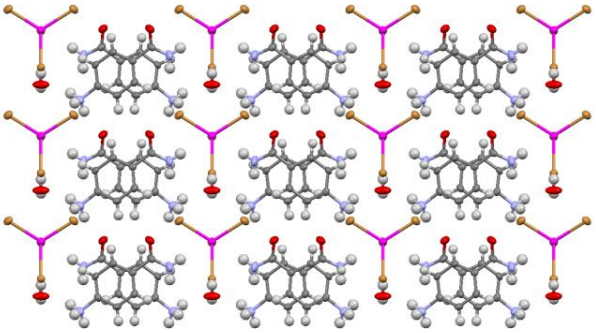

Figure 4.48: Packing of structure IX viewed along the a-axis.

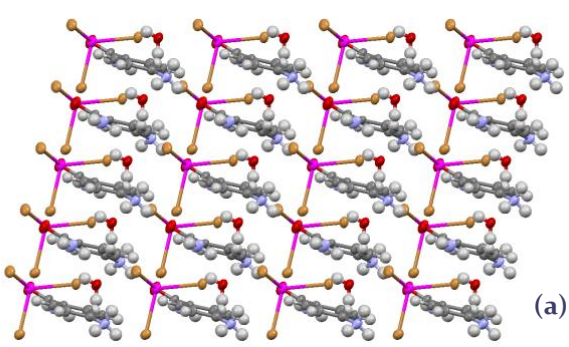

(a)

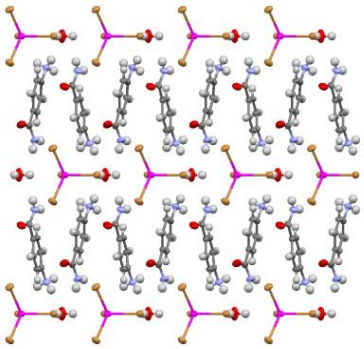

(b)

Figure 4.49: Packing of structure viewed along the (a) b-axis and (b) c-axis.

The nitrogen atom on the ammonium group forms hydrogen bonds to a bromo ligand (N1—H1A···Br1) at a distance of 3.426(6) Å, a water molecule (N1—H1B···O2) at a distance of 3.102(8) Å and an oxygen atom from the amide group (N1—H1C···O1) at a distance of 2.850(8) Å. The nitrogen on the amide group also forms a hydrogen bond with a bromo ligand (N2—H2A···Br2) at a distance of 3.557(6) Å and (N2—H2B···Br1) 3.928(7) Å.

Table 4.10: Hydrogen-bond geometry of structure IX, (Å, °)

Compound V				
D—H···A	D—H	H···A	D···A	D—H···A
N1—H1A···Br1 [i]	0.89	2.59	3.426(6)	156.8
N1—H1B···O2 [ii]	0.89	2.24	3.102(8)	163.3
N1—H1C···O1 [iii]	0.89	2.00	2.850(8)	158.4
N2—H2A···Br2 [iv]	0.86	2.80	3.557(6)	148.4
N2—H2B···Br1 [v]	0.86	3.09	3.928(7)	165.6
O2—H2W···Br2 [vi]	0.766(8)	2.72	3.483(8)	172.0(6)
O2—H1W···Br3 [vi]	0.808(8)	2.69	3.497(8)	178.0(5)

Symmetry codes: (i) x-1/2, -y+1/2, z+1; (ii) x+1/2, y+1/2, z+1; (iii) x+1/2, -y+1/2, z+1; (iv) x-1, y, z; (v) x, y, z+1; (vi) x-1, y, z-1.

The centroid-to-centroid distance between aromatic rings is 3.832 Å indicating the presence of aromatic interactions. The angle produced by the ring normal and the vector through the ring centre is 22.57°.

X: (4-ammoniumbenzamide)-(μ₂-bromo)-tetrabromomercurate hydrate

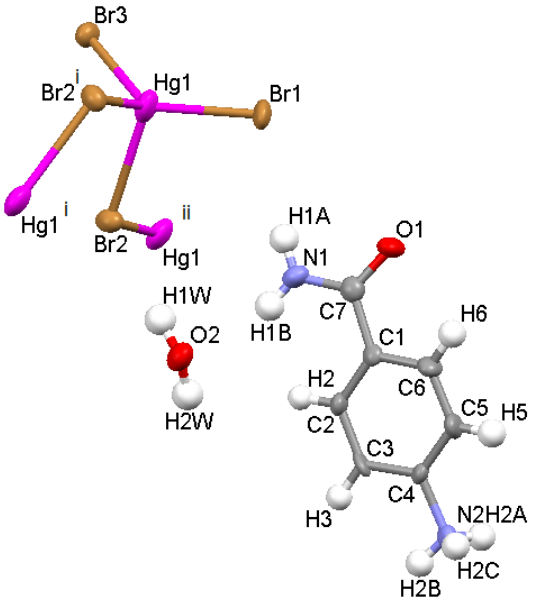

Figure 4.50: Asymmetric unit of compound X. Ellipsoids are drawn at the 50% probability level. (Symmetry operator i: x, 1.5 – y, -0.5 +z; symmetry operator ii: x, 1.5 – y, 0.5 + z).

In the structure of compound X, the asymmetric unit, which is illustrated in Figure 4.50., contains a 4-ammoniobenzamide cation and a mercury atom that is coordinated to three bromo ligands. In addition a water molecule is also present in the asymmetric unit. In the organic cation the amide group is rotated by an angle of 14.90° with respect to the aromatic ring. The unit cell consists of four asymmetric units.

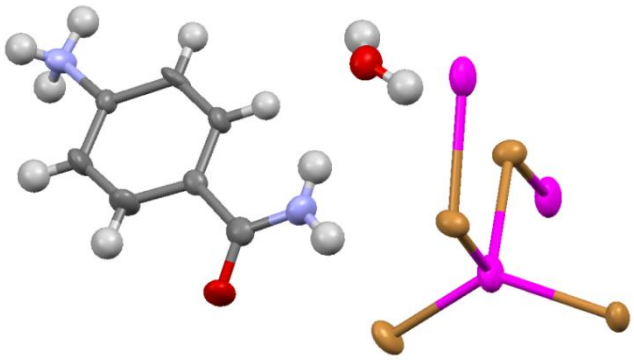

Figure 4.51: Molecular geometry of compound X.

Figure 4.51 illustrates the geometries of the molecular ions. As can be seen in this Figure, the perhalometallate anion consists of a mercury atom that coordinates to four bromo ligands in a tetrahedral fashion. Two of the bromo ligands are shared between metal atoms, to bridge neighbouring metal atoms on opposite sides of the metal atom. This corner sharing of tetrahedral results in the formation of a corrugated, one-dimensional anionic polymer in

which Hg—Br bonding distances are observed to be 2.5153(14) Å and 2.7751 (16) Å while the bridging bromo distances are observed to be (Hg—μ_2Br) 2.5384 (15) Å and 2.6745(15) Å.

The Br-Hg-Br angles in the anion range from 100.46(5)° to 127.08(5)° which indicates slight distortion of the inorganic tetrahedron. Figure 4.52 illustrates how the bridging perhalometallate anions produce an infinite one-dimensional inorganic polymer. The amide group is rotated by 14.90° relative to the plane of the aromatic ring.

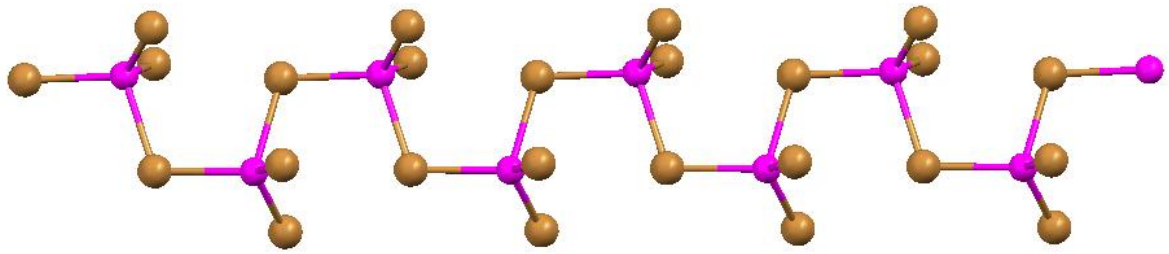

Figure 4.52: One-dimensional polymeric perhalometallate anion, which illustrates the sharing of edges of tetrahedra to form a corrugated polymer.

A layered structure parallel to the ab-plane is formed, with the packing of chemical species shown in Figures 4.53 to 4.54. In this structure the one-dimensional perhalometallate anionic polymer and isolated water molecules pack in the inorganic layer which alternates with the organic layer. The cationic species pack in a separate layer to form this organic layer. When viewed down the c-axis, it can be seen that in the organic layer pairs of cations adopt approximately the same orientation, and neighbouring pairs of cations display opposite orientations, but still form single layer of aromatic rings.

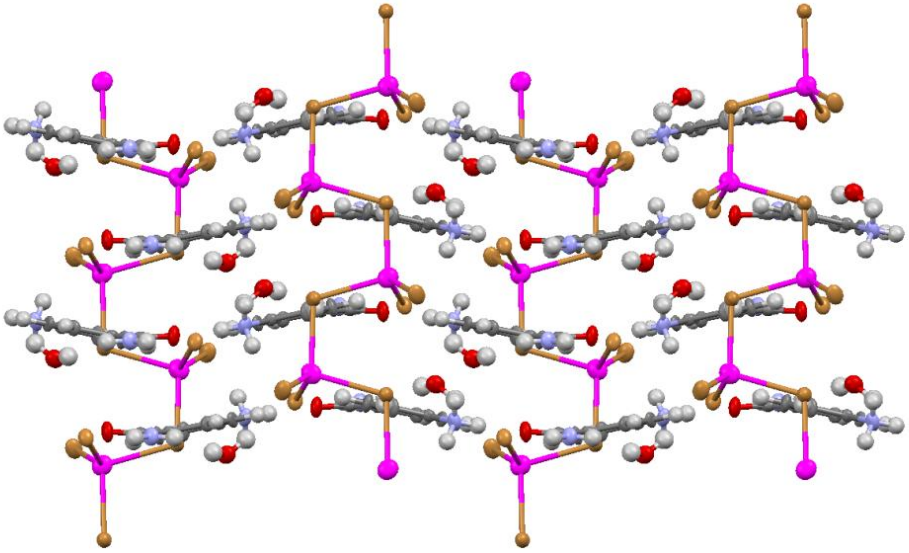

Figure 4.53: Packing of structure X viewed along the a-axis.

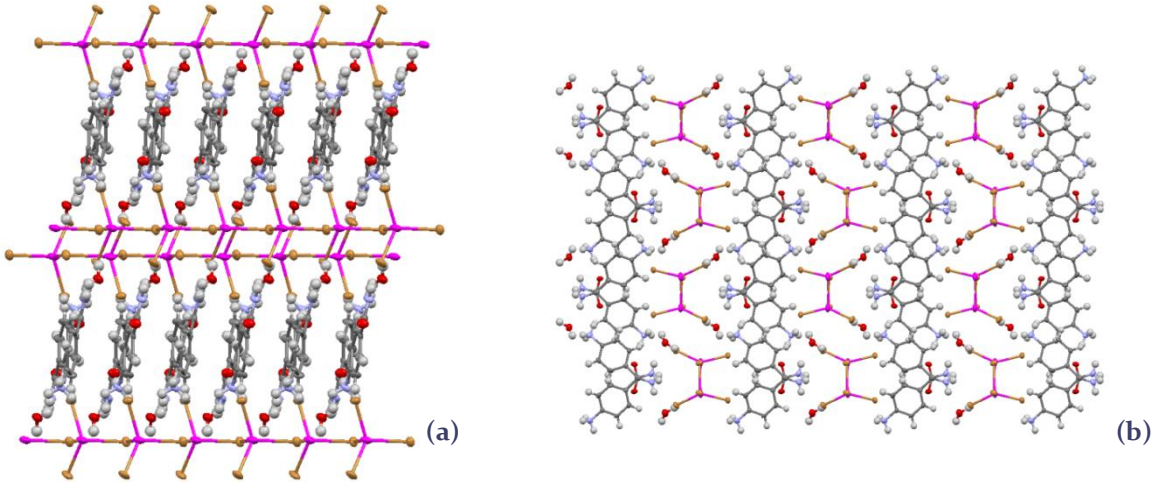

Figure 4.54: Packing of structure X viewed along the (a) b-axis and (b) c-axis.

Translation of the unit cell demonstrates the expansion of the inorganic polymer throughout the structures (Figure 4.54). The inorganic polymers are linked to the cations through extensive hydrogen bonding that occurs via the solvate water molecules and as a result, a complex hydrogen bonding network is generated.

In the structure the nitrogen atom on the ammonium group is surrounded by hydrogen bonding acceptors and forms hydrogen bonds with two bromo ligands at distances of (N2—H2A···Br3) 3.443(1) Å and (N2—H2A···Br1) 3.389(1) Å, as well as with a water molecule (N2—H2C···O2) at a distance of 2.786(2) Å and an oxygen atom of the amide group (N2—H2B···O1) at a distance of 2.693(1) Å. The nitrogen atom on the amide group forms a hydrogen bond with a bromo ligand (N1—H1A···Br1) at a distance of 3.576(1) Å and with the oxygen atom on the water molecule (N1—H1B···O2) at 3.042(2) Å. Hydrogen bonding parameters are listed in Table 4.11, and Figure 4.55 illustrates the resulting complex, two-dimensional hydrogen bonding network.

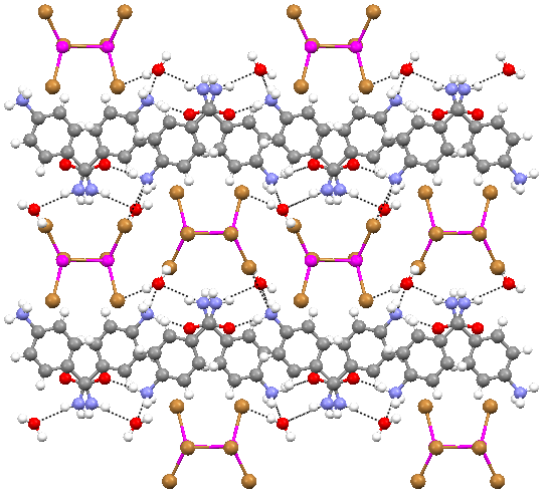

Figure 4.55: Complex hydrogen bonding network parallel to the bc–plane. Hydrogen bonding interactions are indicated as black dotted lines.

Table 4.11: Hydrogen-bond geometry of structure X, (Å, °).

	Compound V			
D—H···A	**D—H**	**H···A**	**D···A**	**D—H···A**
O2—H2W···Br3 [i]	0.958(10)	2.4022(14)	3.360(1)	179.9(6)
N1—H1A···Br1	0.86	2.73	3.576(1)	168.8
N1—H1B···O2	0.86	2.22	3.042(2)	159.2
N2—H2A···Br3 [ii]	0.89	2.60	3.443(1)	157.9
N2—H2A···Br1 [i]	0.89	2.97	3.389(1)	110.4
N2—H2B···O1 [i]	0.89	1.80	2.693(1)	175.6
N2—H2C···O2 [iii]	0.89	1.93	2.786(2)	159.9

Symmetry codes: (i) -x+1, y-1/2, -z+1/2; (ii) x, -y+3/2, z+1/2; (iii) -x+1, -y+1, -z.

The aromatic rings of the organic constituents lie in planes that are not parallel to one another and the planes make an intersecting angle of 23.08°. There is no direct overlap between the rings and it is observed that there exists slipped displacement. The distance between the centre of parallel rings is 3.624 Å (centroid-to-centroid distance) which indicates the presence of aromatic interactions. The angle produced by the ring normal and the vector through the ring centre is 48.48° which is dissimilar to the approximate expected angle of 20°, and as a result, no strong π-π interactions can be expected to exist.

Novel 4-Carboxyanilinium containing perhalometallate structures

A total of four novel structures containing the 4-carboxyanilinium cation combined with a perhalometallate anion have been determined in this study.

XI: bis(4-aminobenzoic acid) bis(4-carboxyanilinium) tetrachlorozincate hydrate

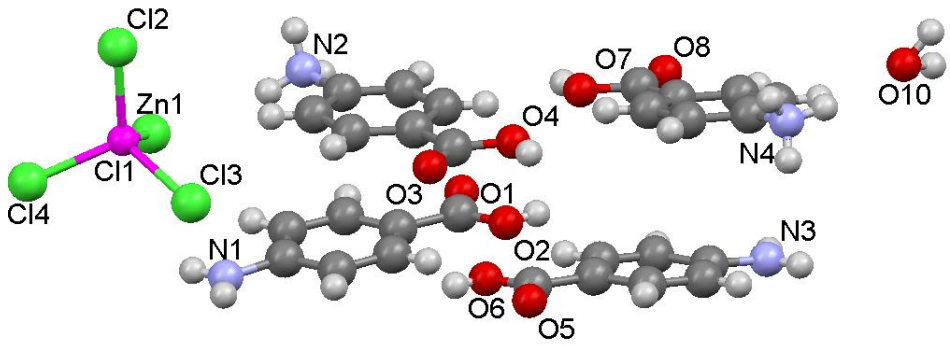

Figure 4.56: Asymmetric unit of compound XI: Ellipsoids are drawn at the 50% probability level. Certain atom labels were excluded to simplify the Figure.

The asymmetric unit of compound XI is illustrated in Figure 4.56, and consists of two neutral, crystallographically independent 4-aminobenzoic acid molecules and two crystallographically independent 4-carboxyanilinium cations, where protonation occur on the nitrogen atom of the amine group. There exists a zinc atom that coordinates to four chloro ligands in an isolated, tetrahedral fashion to form a ($ZnCl_4^{2-}$) anion. Within the asymmetric unit, a water molecule is also present. The unit cell consists of four asymmetric units. The organic components that are protonated were identified in the Fourier difference map and distinguished from the neutral organic molecules

The Zn—Cl bonding distances are observed to be 2.271(3) Å, 2.264(3) Å, 2.273(3) Å and 2.256(3) Å for the isolated zinc tetrahedron. The angles that are generated by the ligands (Cl—Zn—Cl), vary, and range from 105.8(1)° to 112.9(1)°, values which indicate a slight distortion from the ideal tetrahedral geometry. This tetrahedral geometry is typically observed for zinc complexes.

A two-dimensional layered structure, parallel to the ac-plane, is formed as illustrated in Figure 4.57. The inorganic layer consists of discrete $ZnCl_4^{2-}$ anions and water molecules, while the organic layer comprises neutral cations and organic molecules that pack to form a bi-layer, with their carboxylic acid functional groups facing each other.

In the structure the organic bi-layer and inorganic layer alternates. The cations and neutral organic molecules both bond, non-covalently, to the inorganic units via the protonated nitrogen atom of the ammonium group or the amine group of the 4-aminobenzoic acid molecules. Hydrogen bonding interactions occur between the carboxylic acid functional groups of the organic molecules in the bi-layer, resulting in the formation of a hydrogen bonded carboxylic acid dimer.

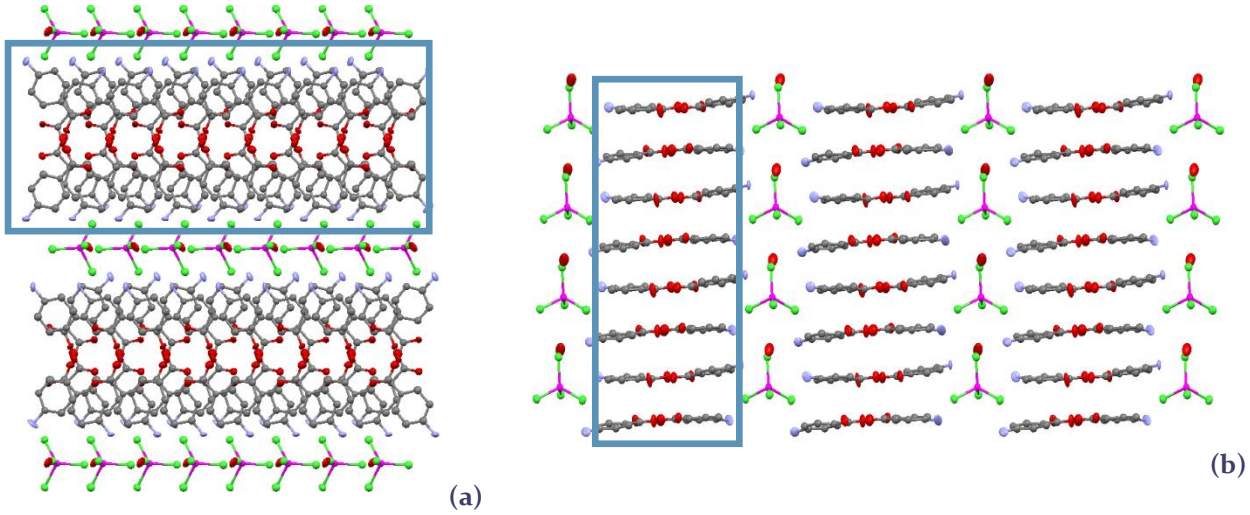

Figure 4.57: Packing of structure XI viewed along the (a) a-axis and (b) b-axis. The organic bi-layer is shown in the block.

Between the neutral PABA molecules, hydrogen bonded dimers exist, and the hydrogen bonding lengths asscociated with these interactions are observed to be (O6—H6A···O1) 2.625(1) Å and (O2—H2···O5) 2.633(1) Å. The hydrogen bonded dimers that exist between the 4-carboxyanilinium cations have hydrogen bonds with lengths (O4—H4···O8) 2.628(1) Å and (O7—H7···O3) 2.614(1) Å. It is observed that between a nitrogen atom on the ammonium group and a nitrogen atom on the amine group hydrogen bonds are generated, with distances (N2—H2A···N1) 2.915(2) Å and (N4—H4B···N3) 2.881(2) Å.

Table 4.12 below illustrates the extent of hydrogen bonding that occurs in the structure. The water molecule is observed to play a significant role in the linking between the inorganic and organic layers. A hydrogen bond exists between the water oxygen atom and a nitrogen atom of the ammonium group, with a distance (N4—H4C···O10) of 2.862(2) Å while two additional hydrogen bonds exist between the water oxygen atom and chloro ligands with distances (O10—H2W···Cl3) 3.563(1) Å and (O10—H1W···Cl2) 3.383(1) Å.

Table 4.12: Hydrogen-bond geometry of structure XI, (Å, °).

	Compound V			
D—H···A	**D—H**	**H···A**	**D···A**	**D—H···A**
O2—H2···O5 [i]	0.82	1.82	2.633(1)	169.4
N1—H1A···Cl2 [ii]	0.86	2.63	3.377(1)	146.0
N1—H1B···N2 [iii]	0.86	2.50	2.915(2)	110.2
O6—H6A···O1 [iv]	0.82	1.82	2.625(1)	167.1
N3—H3B···Cl4 [v]	0.86	2.90	3.411(1)	119.7
O4—H4···O8 [vi]	0.82	1.82	2.628(1)	166.7
N2—H2A···N1 [vii]	0.89	2.11	2.915(2)	150.5
N2—H2B···Cl1	0.89	2.75	3.620(1)	165.6
N2—H2C···Cl3 [viii]	0.89	2.78	3.418(1)	130.0
O7—H7···O3 [viii]	0.82	1.80	2.614(1)	169.6
N4—H4A···Cl4 [ix]	0.89	2.44	3.317(1)	167.6
N4—H4B···N3 [x]	0.89	2.04	2.881(2)	156.8
N4—H4C···O10	0.89	1.98	2.862(2)	170.8
O10—H1W···Cl2 [xi]	0.979(1)	2.575(3)	3.383(1)	139.9(6)
O10—H2W···Cl3 [xii]	0.970(1)	2.593(3)	3.563(1)	179.9(8)

Symmetry codes: (i) x, y+1, z; (ii) x+1/2, y+1/2, z; (iii) x+1/2, y-1/2, z; (iv) x, y-1, z ; (v) x, -y+1, z+1/2; (vi) x, y-1, z; (vii) x-1/2, y+1/2, z; (viii) x, y+1, z ; (ix) x, -y, z+1/2 ; (x) x-1/2, y-1/2, z ; (xi) x, -y+1, z+1/2; (xii) x-1/2, -y+1/2, z+1/2.

The distorted aromatic rings of the four crystallographically independent organic units lie in planes that are approximately parallel to one another. The majority of the organic moieties demonstrate no direct overlap between their rings and exist in extremely displaced positions relative to one another. There are however cations that have their rings in a slightly offset position relative to one another where their centroid-to-centroid distance are measured to be 3.825 Å. For this interaction the angle between the normal to the aromatic plane and the vector between the centroids is measured to be 22 °, which is similar to the angle given in the literature for the most common in π-π interactions.

XII: bis(4-carboxyanilinium) tetrabromozincate hydrate

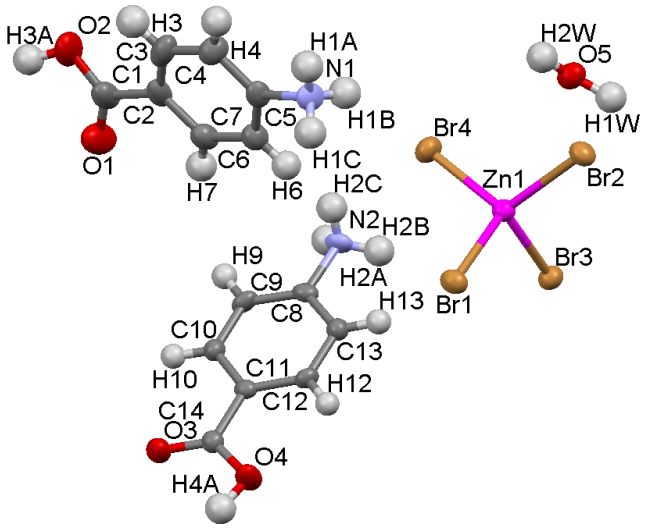

Figure 4.58: Asymmetric Unit of compound XII. Ellipsoids are drawn at the 50% probability level.

The asymmetric unit of structure XII is illustrated in Figure 4.58 and consists of two crystallographically different 4-carboxyanilinium cations and a zinc atom that coordinates to four bromo ligands and adopt a tetrahedral geometry. A solvent water molecule is also present in the unit. The unit cell is comprised of four asymmetric units.

The bonding distances that the bromo ligands make with the zinc atom (Zn1—Br) are 2.4054(9) Å, 2.447(1) Å, 2.382(1) Å and 2.4470(9) Å while the angles that the ligands produce (Br—Zn1—Br) range from 103.47(3)° to 115.15(4)°. These values indicate that the tetrahedral are slightly distorted from the ideal tetrahedral geometry in both cases.

A layered structure is formed with layers extending parallel to the ac-plane as illustrated in Figure 4.59, but this structure exhibits features not observed in related structures. Firstly the isolated inorganic anions and water molecules form the inorganic layer. In this structure two different types of organic layers alternate with the inorganic layer.

Firstly an interdigitated organic layer is present, in which the organic units pack to form a single layer of aromatic rings, and both ends of the organic cation participates in hydrogen bonding interactions with the neighbouring inorganic layers. In this organic layer, cations pack with their aromatic planes approximately parallel, but the cations alternate in relative orientation when viewed down the a-axis. This organic layer contains only one of the crystallographically independent cations, namely the cation containing atom N1.

A second type of organic layer is present in which the organic cations pack in a bi-layer arrangement. In this layer the ammonium groups of the two rows of organic cations constituting the bi-layer interact with inorganic layers through hydrogen bonding, while their neighbouring carboxylic acid functional groups interact via hydrogen bonding interactions to form a carboxylic acid dimer. In this layer the aromatic planes of the cations are parallel.

The organic cations in consecutive bi-layers alternate in their relative orientation, as shown in Figure 4.59. Each bi-layer contains only the cation containing atom N2. And this cation constitutes a hydrogen bonded dimer.

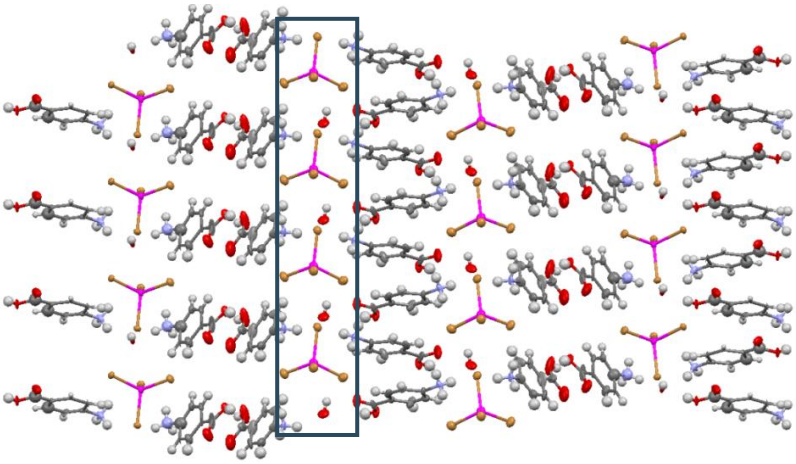

Figure 4.59: Packing of structure XII viewed along the a-axis. The inorganic layer is shown in the block.

The long b-unit cell parameter of 45.732(3) Å is as a result of the different types of organic layers.

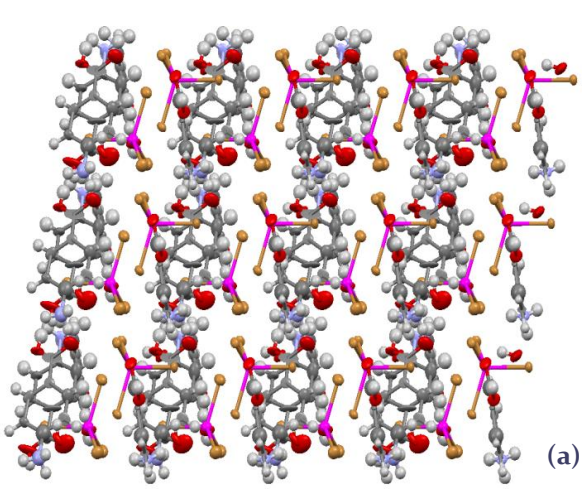

(a)

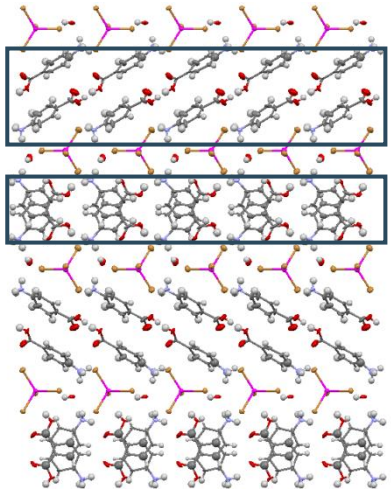

(b)

Figure 4.60: Packing of structure XII viewed along the (a) b-axis and (b) c-axis. The organic layer and organic bi-layer is illustrated in the blocks.

Hydrogen bonding interactions are listed in Table 4.13. The water molecule is observed to undergo extensive hydrogen bonding and as a consequence links the inorganic and organic layers. A hydrogen bond exist between an oxygen atom of the water molecule and a nitrogen atom of the ammonium group of the 4-carboxyanilinium cations of both organic layers, with distances (N1—H1C···O5) of 2.844(7) Å and (N2—H2A···O5) 2.861(7) Å. Additionally, two hydrogen bonds exist between the water oxygen atom and two bromo ligands with distances (O5—H1W···Br1) 3.389(5) Å and (O5—H1W···Br2) 3.578(5) Å.

Table 4.13: Hydrogen-bond geometry of structure XII, (Å, °).

	Compound V			
D—H···A	**D—H**	**H···A**	**D···A**	**D—H···A**
O5—H1W···Br1 ^{i}	0.985(5)	2.42	3.389(5)	169.2(3)
O5—H1W···Br2	0.985(5)	3.35	3.578(5)	95.2(3)
N1—H1A···Br4 ^{ii}	0.89	2.67	3.552(6)	169.6
N1—H1B···O1 ^{i}	0.89	2.60	3.106(9)	116.6
N1—H1B···Br4	0.89	2.83	3.602(6)	145.8
N1—H1C···O5 ^{iii}	0.89	2.01	2.844(7)	155.7
N2—H2A···O5 ^{iii}	0.89	1.98	2.861(7)	170.8
N2—H2B···O3 ^{iv}	0.89	2.04	2.896(7)	161.9
N2—H2C···Br1 ^{v}	0.89	2.47	3.333(5)	164.5
O4—H4A···Br3 ^{vi}	0.950(4)	2.54	3.354(5)	143.2(3)
O4—H4A···Br1 ^{viii}	0.950(4)	2.96	3.556(5)	121.9(3)
O2—H3A···O1 ^{vii}	0.977(5)	1.855(6)	2.672(7)	139.2(4)
N1—H1B···O1 ^{i}	0.89	2.60	3.107(9)	116.7
O4—H4A···Br3 ^{vi}	0.950(4)	2.54	3.354(5)	143.2(3)

Symmetry codes: (i) x+1, y, z; (ii) x, y, z-1; (iii) x-1, y, z; (iv) x+1, -y+1/2, z+1/2; (v) x, y, z-1; (vi) x-1, -y+1/2, z-3/2; (vii) -x-2, -y, -z; (viii) -1, -y+1/2, z-1/2.

Within the single organic layer, aromatic rings of the organic constituents lie in parallel planes. It is observed that there is no direct overlap between the rings and the rings are stacked in a parallel displacement. The distance between the centre of the parallel rings is 3.566 Å (centroid-to-centroid distance) which falls within the cut-off distance for aromatic interactions. In this interaction the angle produced by the ring normal and the vector through the ring centre is 21.86° which is similar to the expected angle of 20° which is commonly observed for π-π interactions.

Within the organic bi-layer it is observed that the planes generated by the aromatic rings are also stacked in parallel succession, however they demonstrate extreme parallel displacement, exemplified by their centroid-to-centroid distance of 5.020 Å. Additionally, the angle produced by the ring normal and the vector through the ring centre is 46.77° which is also in contrast with to the usual angle of 20° expected for π-π interactions.

XIII: bis(4-carboxyanilinium) tetrabromocadmate hydrate

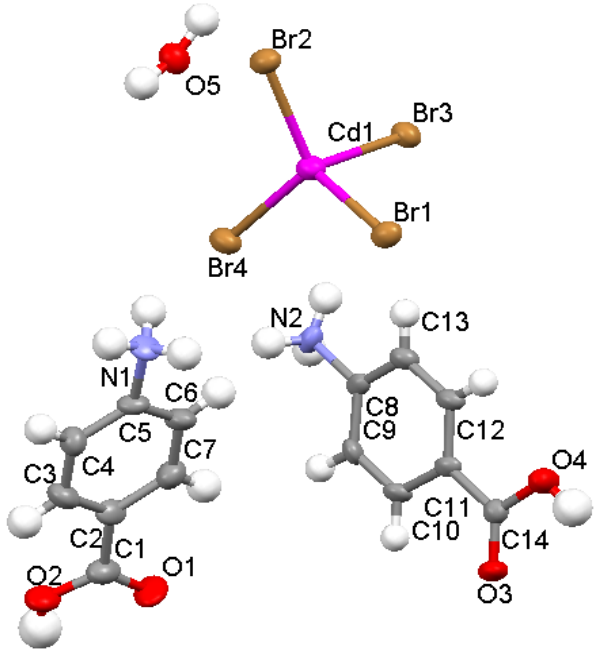

Figure 4.61: Asymmetric Unit of compound XIII: Ellipsoids are drawn at the 50% probability level.

The asymmetric unit of compound XIII is illustrated in Figure 4.61., and contains two crystallographically independent 4-carboxyanilinium cations and a cadmium atom that coordinates to four bromo ligands and has an isolated tetrahedral coordination geometry. In addition an isolated water molecule is present in the unit cell. Compound XIII is observed to be isostructural to compound XII.

The perhalometallate anion has a distorted tetrahedral geometry and the bond lengths that form between the bromo ligands and the cadmium atom (Cd1—Br) are 2.620(2) Å, 2.581(2) Å, 2.651(2) Å and 2.562(2) Å respectively. The Br—Cd—Br angles range from 100.22(7) ° to 117.95(7)° and illustrates the slight distortion observed in the geometry of the anion. The carboxylic acid functional groups make dihedral angles of 11.02° and 5.34° with respect to the aromatic planes in the two crystallographically independent cations. The planes through the aromatic rings of the two independent cations intersect at an angle of 76.68°. The unit cell is comprised of four asymmetric units.

The perhalometallate anions exist as discrete units and pack in layers parallel to the ac-plane. The cationic molecules are observed to pack in organic layers that alternate with the inorganic layers, and undergo extensive hydrogen bonding with the anionic species via the protonated nitrogen atom of the amine group.

It is observed that two types of organic layers are formed (Figure 4.62), similar to those observed in structure XII, and can be seen to alternate with the inorganic layers and this results in a large b-unit cell parameter of 45.191(8) Å.

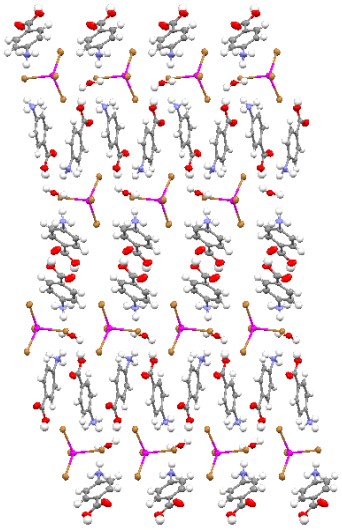

Figure 4.62: Packing of structure XIII viewed along the a-axis.

The first type of organic layer that forms is a bi-layer and is generated by the formation of a dimer between the carboxylic acid functional groups on neighbouring cationic constituents. The second type of layer that is produced is a single organic layer and occurs as a result of stacking of the organic units. Figure 4.63(b) illustrates how the single layer organizes into a stacked arrangement and may be as a result of the aromatic interactions that take place between the benzene rings.

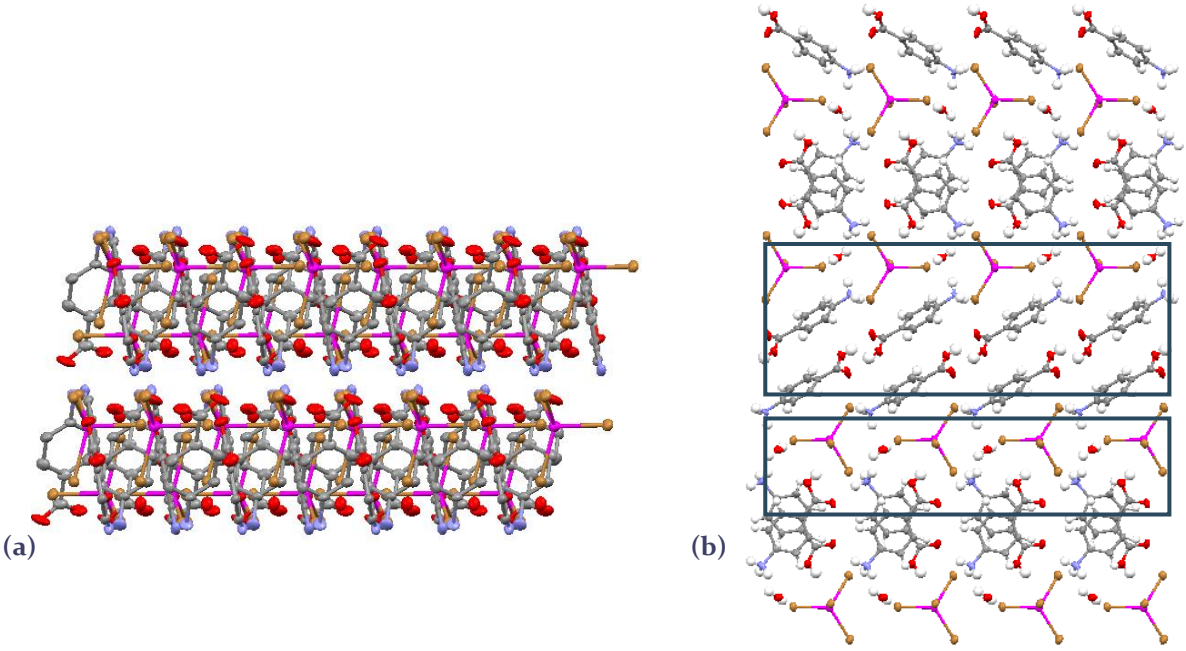

Figure 4.63: Packing of structure XIII viewed along the (a) b-axis and (b) c-axis. The two types of organic layers are indicated within the block.

Hydrogen bonding interactions are listed in Table 4.14. Between the carboxylic acid functional groups of the cations a cyclic dimer is generated forming the organic bi-layer. The hydrogen bond associated with the dimer (O2—H3A···O1) demonstates a donor to acceptor distance of 2.678(2) Å.

The water molecule is observed to link the inorganic and organic layers. A hydrogen bond exists between an oxygen atom of the water molecule and a nitrogen atom of the ammonium group of the 4-carboxyanilinium cations of both organic layers, with distances (N1—H1C···O5) of 2.900(2) Å and (N2—H2A···O5) 2.877(2) Å. Additionally, two hydrogen bonds exist between the water oxygen atom and two bromo ligands with distances (O5—H1W···Br1) 3.420(1) Å and (O5—H1W···Br2) 3.517(1) Å.

Table 4.14: Hydrogen-bond geometry of structure XIII, (Å, °).

	Compound V			
D—H···A	**D—H**	**H···A**	**D···A**	**D—H···A**
O5—H1W···Br1 ^{i}	0.954(1)	2.4656(2)	3.420(1)	179.5(7)
O5—H1W···Br2	0.954(1)	3.3706(2)	3.517(10)	90.9(6)
N1—H1A···Br4 ^{ii}	0.89	2.70	3.586(1)	173.1
N1—H1B···O1 ^{i}	0.89	2.59	3.083(2)	115.7
N1—H1B···Br4	0.89	2.80	3.581(1)	147.3
N1—H1C···O5 ^{iii}	0.89	2.06	2.900(2)	155.8
N2—H2A···O5 ^{iii}	0.89	2.00	2.877(2)	169.5
N2—H2B···O3 ^{iv}	0.89	2.03	2.901(2)	164.3
N2—H2C···Br1 ^{v}	0.89	2.50	3.334(1)	155.8
O4—H4A···Br3 ^{vi}	0.892(1)	2.4948(1)	3.316(1)	153.4(8)
O4—H4A···Br1 ^{viii}	0.892(1)	3.1147(1)	3.580(1)	114.7(8)
O2—H3A···O1 ^{vii}	1.004(1)	1.866(1)	2.678(2)	135.7(8)
N1—H1B···O1 ^{i}	0.89	2.59	3.084(2)	115.7

Symmetry codes: (i) x+1, y, z; (ii) x, y, z-1; (iii) x-1, y, z; (iv) x+1, -y+1/2, z+1/2; (v) x, y, z-1; (vi) x-1, -y+1/2, z-3/2; (vii) -x-2, -y, -z; (viii) -1, -y+1/2, z-1/2.

It is observed that within the single organic layer, aromatic rings of the organic constituents lie in parallel planes. It is observed that there is no direct overlap between the rings and they are stacked in a parallel displacement. The distance between the centre of parallel rings are 3.574 Å (centroid-to-centroid distance) which corresponds to the distance found in aromatic interactions. The angle produced by the ring normal and the vector through the ring centre is 21.87° which is similar to the expected angle of 20° which is observed with π-π interactions.

Within the organic bi-layer it is observed that the planes generated by the aromatic rings are also stacked in parallel succession, however they demonstrate extreme parallel displacement, exemplified by their centroid-to-centroid distance of 5.022 Å. Additionally, the angle produced by the ring normal and the vector through the ring centre is 40.62° which also contrasting to the usual angle of 20° expected for π-π interactions.

XIV: 4-carboxyanilinium trans-diaquatetrabromocadmate

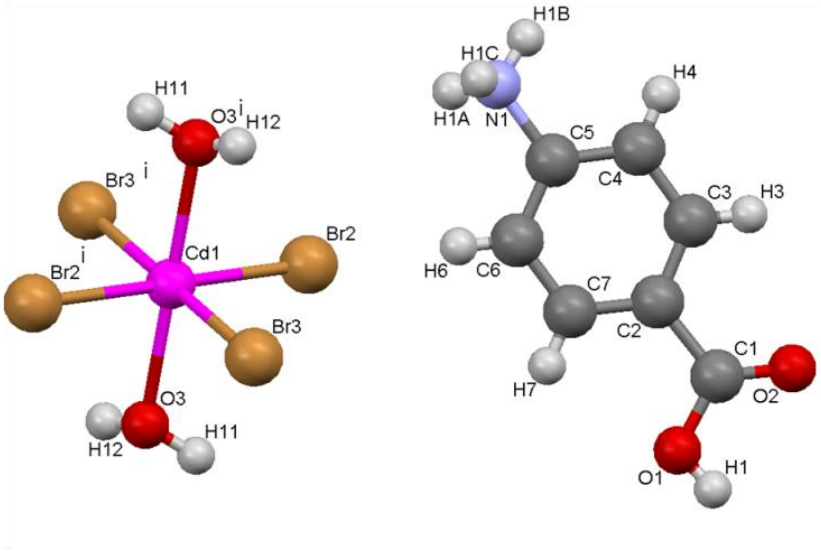

Figure 4.64: Asymmetric Unit of compound XIV. Ellipsoids are drawn at the 50% probability level. (Symmetry operator i: -x,- y, 1-z).

This structure is isostructural to the literature structure G with the CSD reference code WUGHIZ. In WUGHIZ all the ligands coordinated to the cadmium metal atom of the perhalometallate anions are chloro ligands. However, in the current structure bromo ligands are coordinated to the metal atom.

The asymmetric unit of novel structure XIV consists of an isolated 4-carboxyanilinium cation and a cadmium atom that coordinates to two halogeno ligands and a water (aquo) ligand. The cadmium atom is positioned on the corner of the cell axis and has a site occupying factor of 0.25. The rest of the octahedral anion is generated by symmetry. The unit cell is comprised of two asymmetric units.

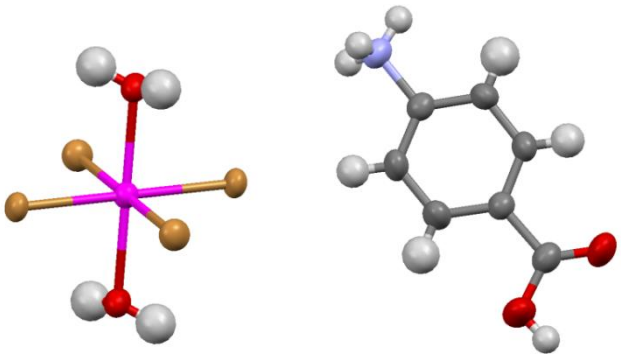

Figure 4.65: Molecular geometry of compound XIV.

The full anion as well as the cation geometry is shown in Figure 4.65. The perhalometallate anion consists of an octahedral cadmium metal atom that coordinates to two water molecules and four halogeno ligands. The four halogeno ligands are coordinated along the equatorial plane, producing a square planar geometry and the Cd—Br bond distances distances are at 2.6001(6) Å and 2.5995(7) Å respectively.

The two water molecules are coordinated trans to each other in the axial positions and are observed to have bonding distances of 2.3782(26) Å from the cadmium atom (Cd-OH_2). The inorganic octahedral geometry is slightly distorted with angles between ligands and the cadmium atom not varying far from the ideal 90° angle. The isolated organic unit has a planar geometry.

In the structure the ions pack in layers parallel to the bc-plane. A single organic layer, in which neighbouring organic cations display alternating orientations, alternates with an inorganic layer which contains the isolated octahedral anions. When viewed down the a-axis it can be seen that the orientation of the octahedral anions alternate in consecutive inorganic layers.

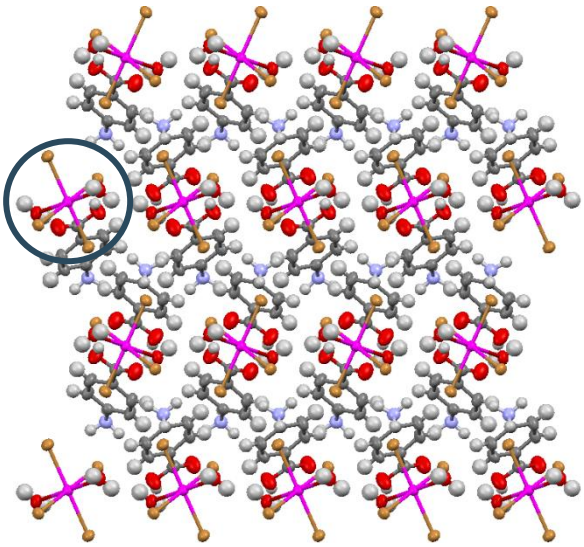

Figure 4.66: Packing of structure XIV viewed along the a-axis. The isolated octahedron is illustrated within the circle.

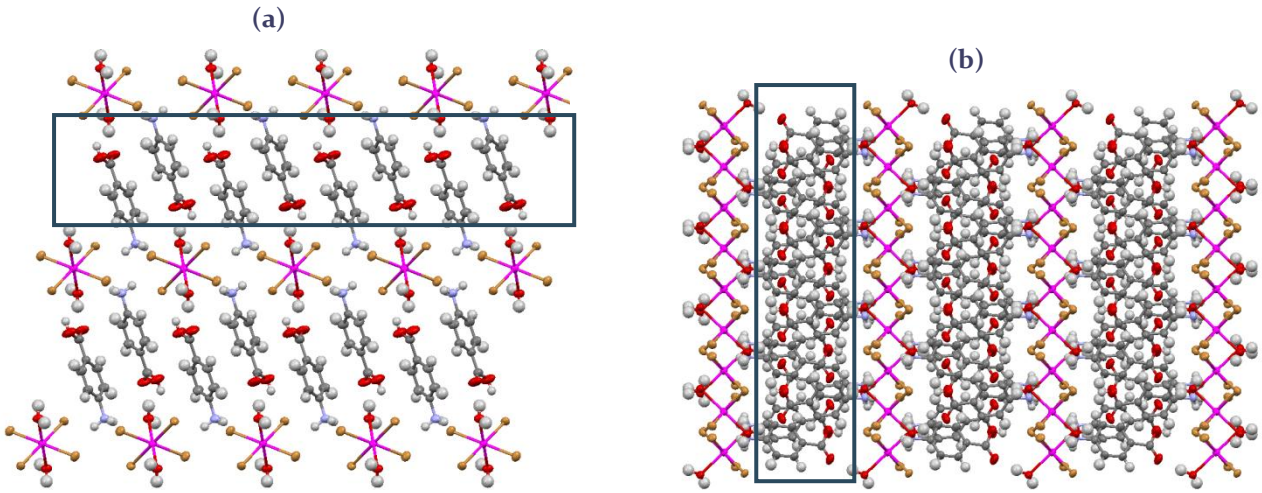

Figure 4.67: Packing of structure XIV viewed along the (a) b-axis and (b) c-axis. The organic layer is shown in the blocks.

There are no aromatic interactions present in this structure as benzene rings in the organic constituents lie in planes that are not parallel to one another and subsequently provide no opportunity for overlapping of orbitals.

Hydrogen bonding interactions are listed in Table 4.15. A hydrogen bond exist between the protonated nitrogen atom of the ammonium group and three halogeno ligands at donor to acceptor distances of 3.261(3) Å, 3.205(4) Å and 3.258(4) Å. Hydrogen bonding occurs between the carboxylic acid functional group and a halogeno ligand at a distance (O1—H1···Br1) of 3.079(3) Å as well as between the coordinated water molecule and an oxygen of the carboxylic acid functional group (O3—H2W···O2) with a distance 2.759(4) Å. Figure 4.68 shows the complex two-dimensional hydrogen bonding network parallel to the bc-plane that results from these interactions.

Table 4.15: Hydrogen-bond geometry of structure IV, (Å, °).

Compound V				
D—H···A	D—H	H···A	D···A	D—H···A
O3—H1W···Br1 [i]	0.80(5)	2.49(5)	3.266(3)	164(5)
O3—H2W···O2 [ii]	0.95(7)	1.82(7)	2.759(4)	169(6)
N1—H1A···Br2 [iii]	0.89	2.39	3.261(3)	166.1
N1—H1B···Br2 [iv]	0.89	2.39	3.205(4)	152.6
N1—H1C···Br2 [v]	0.89	2.41	3.258(4)	158.7
O1—H1···Br1 [ii]	0.82	2.28	3.079(3)	164.5

Symmetry codes: (i) x, y-1, z; (ii) -x+1, -y+1, -z+1; (iii) x, -y+1/2, z-1/2; (iv) x, -y+3/2, z-1/2; (v) -x, -y+1, -z+1.

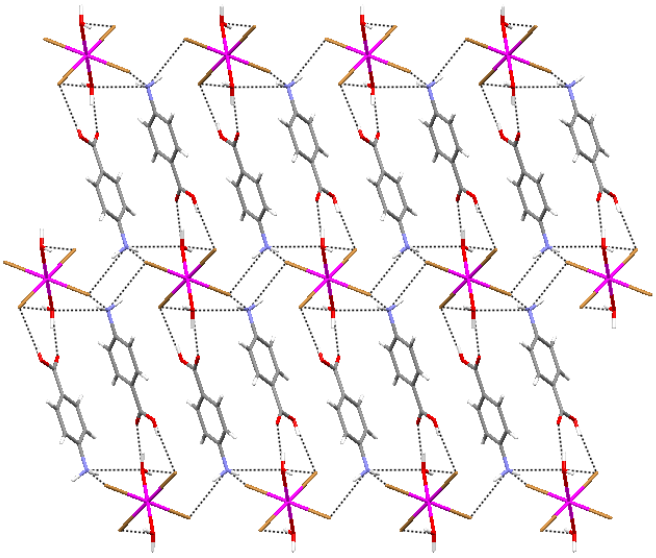

Figure 4.68: Two-dimensional hydrogen bonding network extending parallel to the bc-plane.

XV: 4-carboxypyridinium bromide

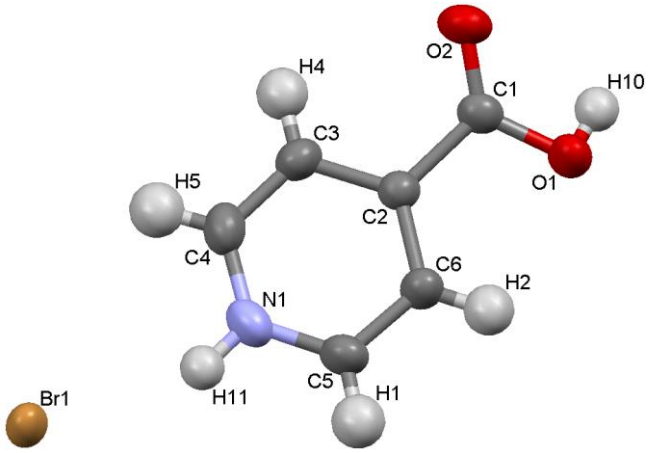

Figure 4.69: Asymmetric Unit of compound XV:

The crystal structure of 4-carboxypyridinium bromide was determined during the course of this study. This bromide salt formed during an attempt to crystallize a perhalometallate salt. We also became aware that this crystal structure has also recently been published in the literature by another group (Wang, 2010), but at that stage the structure was already written up in detail, hence the inclusion of the structure in the dissertation. Note that only the main structural features will be discussed below. If more detail is required the reader is referred to the paper in the literature.

The asymmetric unit consists of a 4-carboxypyridinium cation and a single bromide anion existing as a discrete constituent. The unit cell comprises two asymmetric units. The cation demonstrates a non-planar geometry, by reason of the carboxylic acid group that generates a dihedral angle of 17.84° with the plane of the aromatic ring.

Hydrogen bonds, via both the protonated nitrogen atom and the carboxylic acid groups, are formed and generate a one-dimensional hydrogen bonded chain.

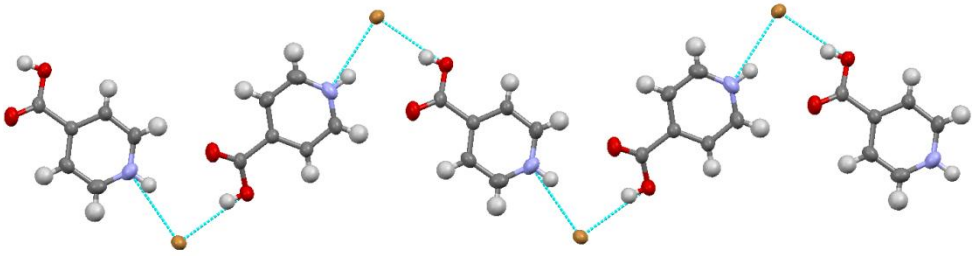

Figure 4.70: Expansion of the asymmetric unit producing a one-dimensional zigzag chain.

Figure 4.71 illustrates the formation of alternating organic and inorganic layers parallel to the ab-plane. The organic layer comprises 4-carboxypyridinium cations that are stacked in parallel layers while the inorganic layer is comprised of discrete bromide anions. The orientation of the cations is observed to alternate in successive layers along the b-axis.

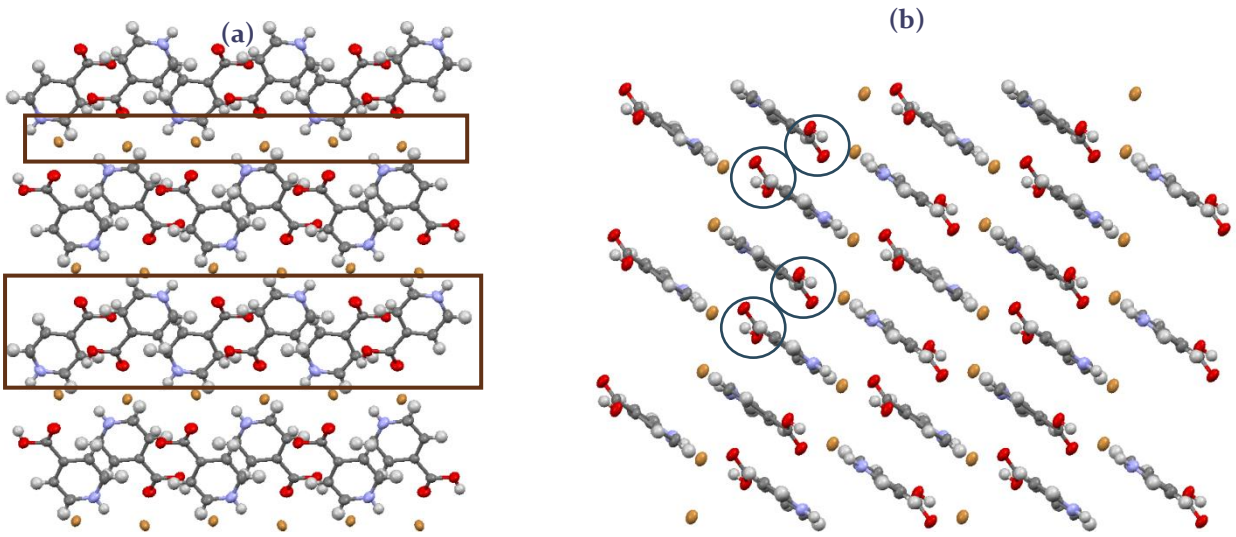

Figure 4.71: Packing of structure XVI viewed along the (a) a-axis and (b) b-axis. The inorganic and organic layers are illustrated in the block.

Strong, charge assisted, hydrogen bonds occur between the pyridinium group and the bromide anion (N—H^+···Br^-) and has a distance of 3.246 (2) Å. The hydroxyl group produces a hydrogen bond with another bromide anion (O—H···Br) at a distance of 2.364 Å. The functionality of the cation's quality to generate hydrogen bonds on both ends is exemplified by the formation of the zigzag organic-inorganic one-dimensional chain. It is observed that that hydrogen bonds link the organic and inorganic layers.

Within the organic layer it is observed that the planes generated by the aromatic rings are stacked in parallel succession, however they demonstrate extreme parallel displacement, exemplified by their centroid-to-centroid distance of 4.199 Å. Additionally, the angle produced by the ring normal and the vector through the ring centre is 58.39° which also contrasting to the usual angle of 20° expected for π-π interactions.

Novel 4-Carboxypyridinium containing perhalometallate structures

Only one crystal structure containing a protonated isonicotinic acid molecule was determined in the current investigation.

XVI: bis(4-carboxypyridinium)-[hexakis(μ_2-bromo)-mono(μ_3-bromo)-hepta-bromo-hexamercurate)]

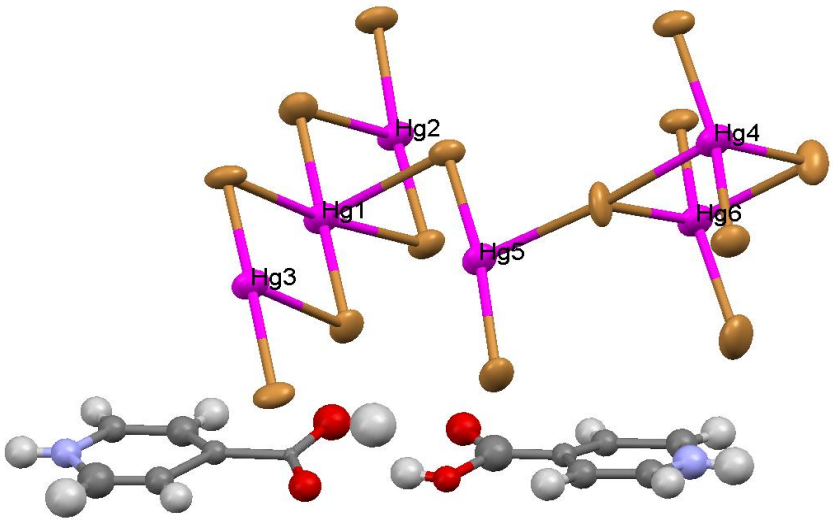

Figure 4.72: Asymmetric Unit of compound XVI. Ellipsoids are drawn at the 50% probability. Only mercury atoms are labelled for clarity.

The diffraction data collected for compound XVII is not of exceptionally good quality, most probably due to the large heavy atom content. Nevertheless, due to the extraordinary structural aspects of the structure, and the fact that the structural characteristics are still evident, the structure was included in the dissertation. The unit cell is comprised of one asymmetric unit.

In this structure all the heavy atoms were refined anisotropically, but the light atoms, namely carbon, hydrogen and nitrogen, were only refined isotropically.

The asymmetric unit of structure XVI consists of two crystallographically independent 4-carboxypyridinium cations, six mercury atoms and fourteen bromo ligands, as illustrated in Figure 4.72. The cations display non-planar geometry as the carboxylic acid groups are rotated by 9.96° and 7.20° relative to the aromatic planes. A complex perhalometallate anion is formed through bridging of the metal atoms by the bromo ligands. Mercury atoms (Hg4 and Hg6) have tetrahedral geometries and each mercury atom coordinates to two terminal bromo ligands and two bridging bromo ligands (a μ_2-bromo and a μ_3-bromo). It is observed that two other mercury atoms (Hg1 and Hg3) have octahedral geometries and each coordinates to four bridging μ_2-bromo ligands and two bridging μ_3-bromo ligands.

Mercury atoms (Hg2 and Hg5) have square-pyramidal geometries and each mercury atom coordinates to three bridging μ_3-bromo ligands and a bridging μ_2-bromo ligand and a terminal bromo ligand.

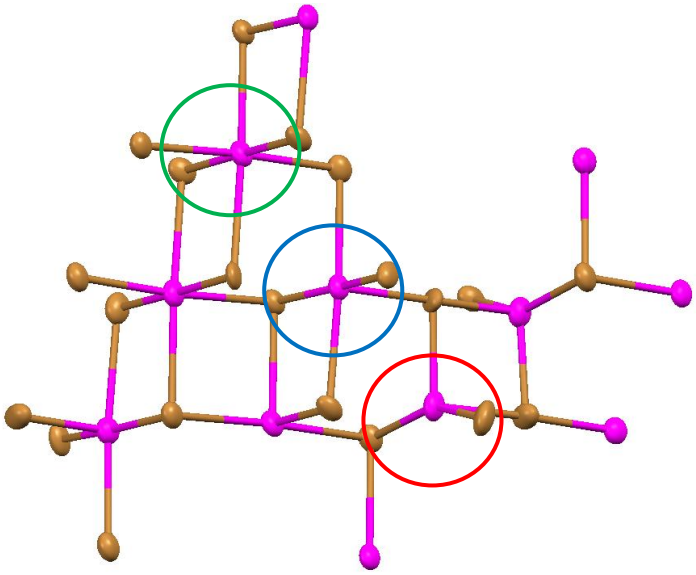

Figure 4.73: The complex two-dimensional inorganic sheet. Different coordination geometries are circled, with an octahedral geometry shown in green, a square pyramidal geometry shown in blue and a tetrahedral geometry shown in red.

The complex two-dimensional perhalometallate sheet that is formed is illustrated in Figure 4.73 and Figure 4.74. A very interesting feature of this sheet is the fact that the mercury atoms demonstrate different coordination geometries in the same two-dimensional anion and Figure 4.73 illustrates the varying geometries exhibited by mercury atoms. The coordination geometries range and alternate between octahedral, square-pyramidal and tetrahedral. It is observed that within the inorganic sheet, gaps or holes are generated. These voids may manifest as a result of the crystallographic arrangement attempting to accommodate the close packing of the varying coordination geometries.

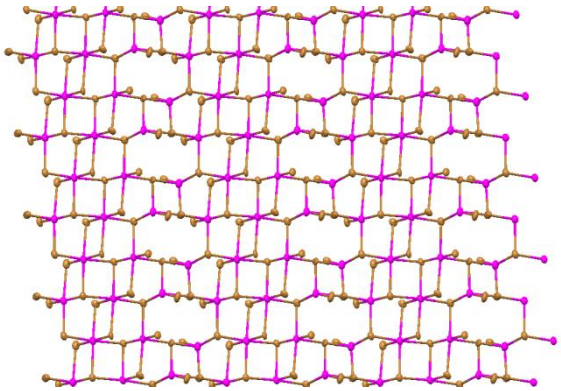

Figure 4.74: The inorganic perhalometallate anion viewed along b-axis. Holes are present throughout the structure.

To our knowledge this type of sheet structure has never been reported previously. The two-dimensional perovskite sheet structure, discussed in the literature section, is commonly found for alkylammonium perhalometallates, but in the perovskite sheet, only one coordination geometry is displayed by the metal atoms.

Another unique aspect of this structure is the fact that, even though a layered structure is displayed parallel to the ab-plane, the layers are stepped as shown in Figure 4.75, unlike the layers reported for the rest of the novel structures. In addition, unlike what was observed in the rest of the structures, the organic cations pack parallel to the layer plane, instead of adopting an approximately perpendicular orientation as was observed in the other structures. Figure 4.75 illustrates the step-wise manner in which the inorganic perhalometallate sheet packs along the ac-plane. The "holes" in the sheet correspond to the steps.

The organic layer is generated by a cyclic dimer that forms between the carboxylic acid groups of the cations. The parallel organic dimer is sandwiched between and alternates with the stepped inorganic layer. It is observed that the organic layer effectively terminates at each inorganic step. The organic dimer shows a perfect fit in the steps created by the inorganic sheet. The organic dimer is anchored to the "pocket" formed by the inorganic sheet through hydrogen bonds involving the pyridine nitrogen atom.

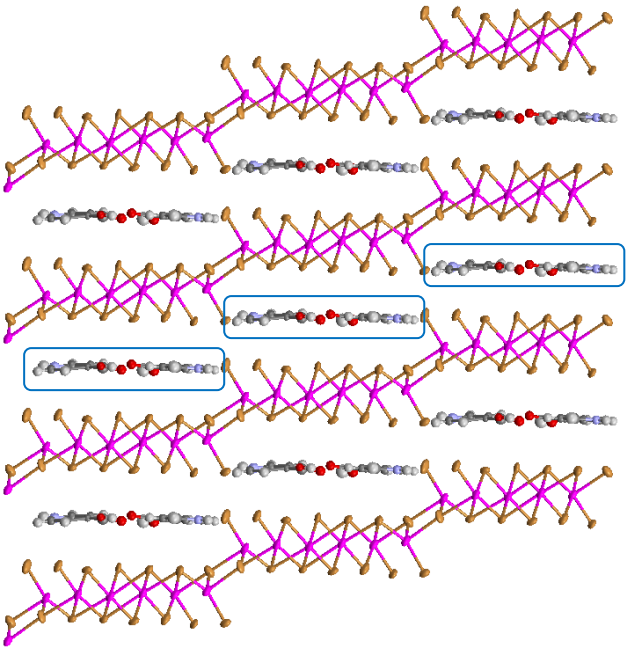

Figure 4.75: Packing of structure XVII viewed along a-axis. The dimers are shown in the blocks.

Figure 4.75 illustrates the packing of both the organic and the inorganic layers and it is shown that the two-dimensional sheets expand to infinity.

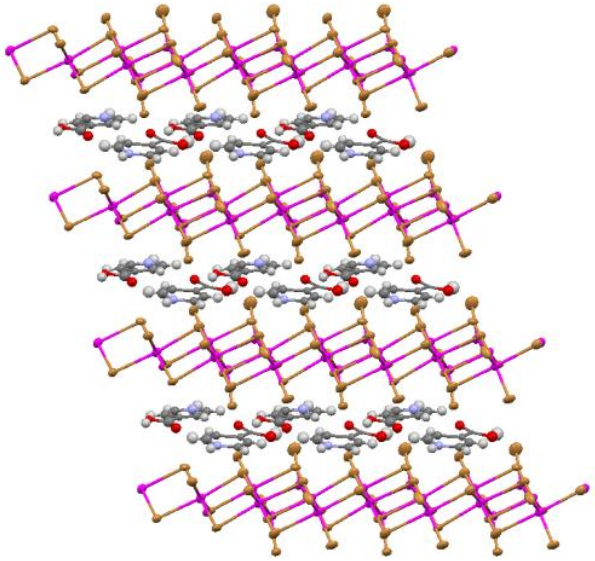

Figure 4.76: Packing of the structure XVII viewed along c-axis.

Hydrogen bonding interactions occur between the carboxylic acid groups of the cations and the pyridine nitrogen atom of the cation and the perhalometallate anion. The hydrogen bonds generate a cyclic dimer between the carboxylic acid functional groups of the 4-carboxypyridinium cations (O—H···O) and have donor-acceptor bonding distances of 2.72(4) Å and 2.62(4) Å. Hydrogen bonds exists between the protonated nitrogen of the pyridinium groups and terminal coordinated bromo ligands (N—H···Br) and have bonding distance of 3.55(3) Å and 3.22(3) Å.

Table 4.16: Hydrogen-bond geometry of structure XVI, (Å, °).

Compound V				
D—H···A	D—H	H···A	D···A	D—H···A
N1-H1A...Br13 [i]	0.86	2.39	3.22(3)	161.3
O2-H2...O4	0.82	1.91	2.72(4)	173.2
O3-H1...O1	0.82	1.88	2.62(4)	151.3
N2-H1B...Br7 [ii]	0.86	2.85	3.55(3)	140.8

Symmetry codes: (i) x-1, y, z-1; (ii) x+1, y-1, z.

Comparison Study

This section aims to compare the structural features and trends in the novel ionic hybrid structures, and to compare these features with those of the literature structures where relevant.

One structure containing a 4-carboxyanilinium cation and a perhalometallate anion has been reported in the literature (structure G), and four novel structures of this family were determined in the current study (structures XI, XII, XIII and XIV), bringing to five the number of structures available for comparison. It is observed that G and XIV are isostructural.

A total number of four literature structures that contain the 4-carboxypyridinium cation and a perhalometallate anion were located (structures H, I, J and K, where H, I and J are isostructural), and a further structure was determined in the current study (structure XVI) hence five structures are available for comparison.

In the 4-ammoniobenzamide group, no structures have been reported in the literature, but five novel structures have been determined in this investigation (structures VI, VII, VIII, IX and X, where VII, VIII and IX are isostructural), again allowing for the comparison of five structures that contain a 4-ammoniobenzamide cation and a perhalometallate anion.

Structure Type

Figures 4.77 to 4.79 illustrate the packing diagrams for both the literature structures and the novel structures employed in the comparison. A common structural feature is the fact that layered structures are formed. In all the structures the anion packs in what is termed the inorganic layer. The water molecules typically pack in the inorganic layer, as observed in structures G, VI, VII, VIII, X, XI and XII. An exception is structure H, I and J where the water molecules occur in the organic layer.

The anion geometry is not important in the formation of a layered structure, and this structure type is observed for isolated tetrahedral, isolated octahedral, isolated square planar and one-dimensional polymeric anions and two-dimensional sheet anions. In all the structures the layers are parallel, but one exception is structure XVI, which displays a stepped layer. In all the structures, except structure XVI, the organic cations pack either perpendicular or slightly tilted relative to the inorganic layer. However, in structure XVI the cations pack parallel to the inorganic layer.

The cations may form a single, interdigitated organic layer, as observed in structures G, XIV, VI, VII, VIII, IX and X, or may form an organic bi-layer, as seen in structures XI, H, I, J and K. In the structures where a bi-layer is formed, the carboxylic acid functional groups link molecules into hydrogen bonded dimers. Structures XII and XIII are interesting due to the fact that they display both single organic layers and organic bi-layers.

Not all the cations that contain carboxylic acid functional groups pack to form organic bi-layers. In the case of the 4-carboxyanilinium containing structures, both single and bi-layers are present, and two of the structures display both types of layers as mentioned previously. For the 4-ammoniumbenzamide cation containing structures, only single organic layers are present, hence the formation of a dimer linked through the amide group is not observed in any of the structures. In the family containing the 4-carboxypyridinium cations, only carboxylic acid dimers are formed in all the structures, even in structure XVI, where the cations pack parallel to the inorganic layer.

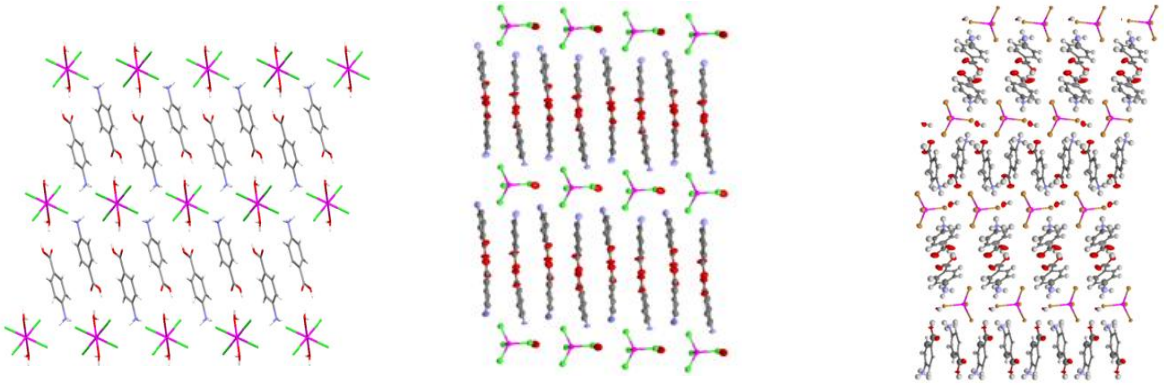

(a) (b) (c)

Figure 4.77: Packing diagrams showing structural features in 4-carboxyanilinium containing structures (a) structure G (also representative of structure XIV) (b) structure XI (c) structure XII (also representative of structure XIII).

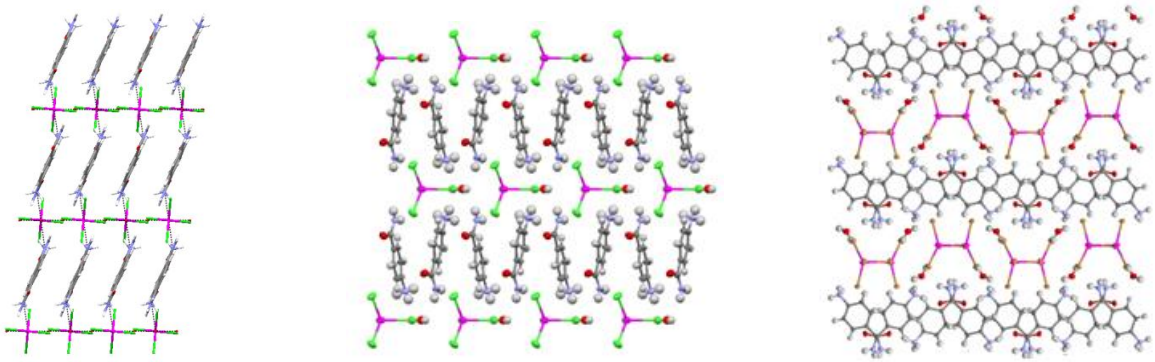

(b) (c)

Figure 4.78: Packing diagrams showing structural features in 4-ammoniumbenzamide cation containing structures (a) structure VI (b) structure VII (also representative of structures VIII and IX (c) structure X.

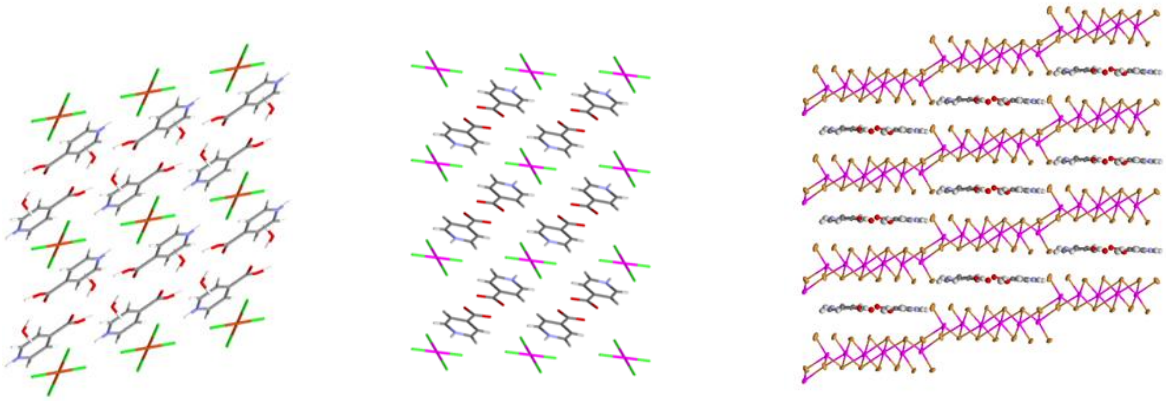

(b) (c)

Figure 4.79: Packing diagrams showing structural features in 4-carboxypyridinium containing structures (a) structure H (also representative of structures I and J) (b) structure K (c) structure XVI.

Water inclusion into structures

Water molecules were available to be included in all the novel structures determined in this study, due to the fact that diluted acid was used in the preparation of the ionic hybrids. It was found that eight out of the ten novel structures contain water molecules incorporated as solvent molecules, and these molecules are always included into the inorganic layer. One of the novel structures, structure XIV (isostructural to structure G) contains water in the form of ligands coordinated to the metal atom. Only one of the novel structures, the exceptional structure XVI, does not contain any water molecules.

Anion Geometry

A number of anion geometries are observed in novel structures determined in the current study. The isolated tetrahedral geometry is by far the most common geometry adopted by the anion (Figure 4.80(a)). This geometry is observed for seven out of the ten novel structures, namely structures VI, VII, VIII, IX, XI, XII and XIII. The anions that adopt this geometry all contain the d10 metal atoms Zn, Cd or Hg, and chloro or bromo ligands, and are $ZnCl_4^{2-}$, $HgCl_4^{2-}$, $ZnBr_4^{2-}$, $CdBr_2^{2-}$ and $HgBr_4^{2-}$.

One novel structure, structure X, exhibits a one-dimensional polymeric anion in which neighbouring tetrahedra share edges to form a corrugated polymer consisting of mercury atoms and bridging bromo ligands (Figure 4.80(b)). An isolated octahedral geometry was observed in the case of structure XIV, due to the coordination of two water (aquo) ligands to a square planar $CdBr_2$ unit. This same anion was present in the isostructural literature structure G. In both these structures the central metal of the anion is cadmium (Figure 4.80(c)).

All the literature structures that contain the 4-carboxypyridinium cations show isolated square planar geometries (Figure 4.80(d)), but the metal atoms studied are different from those in the current study, namely Cu, Pt and Pd, and the square planar anion geometry is common for these metals.

In the novel 4-carboxypyridinium containing structure, structure XVI, a very unique, two-dimensional anion is observed (Figure 4.80(e)). This type of anion has, to our knowledge, never been reported for any combination of metal and halogen atom. In this polymeric sheet anion, three different metal coordination geometries are observed, namely octahedral, tetrahedral and square pyramidal, and corner- and edge-sharing between the mercury atoms occur through bridging bromo ligands.

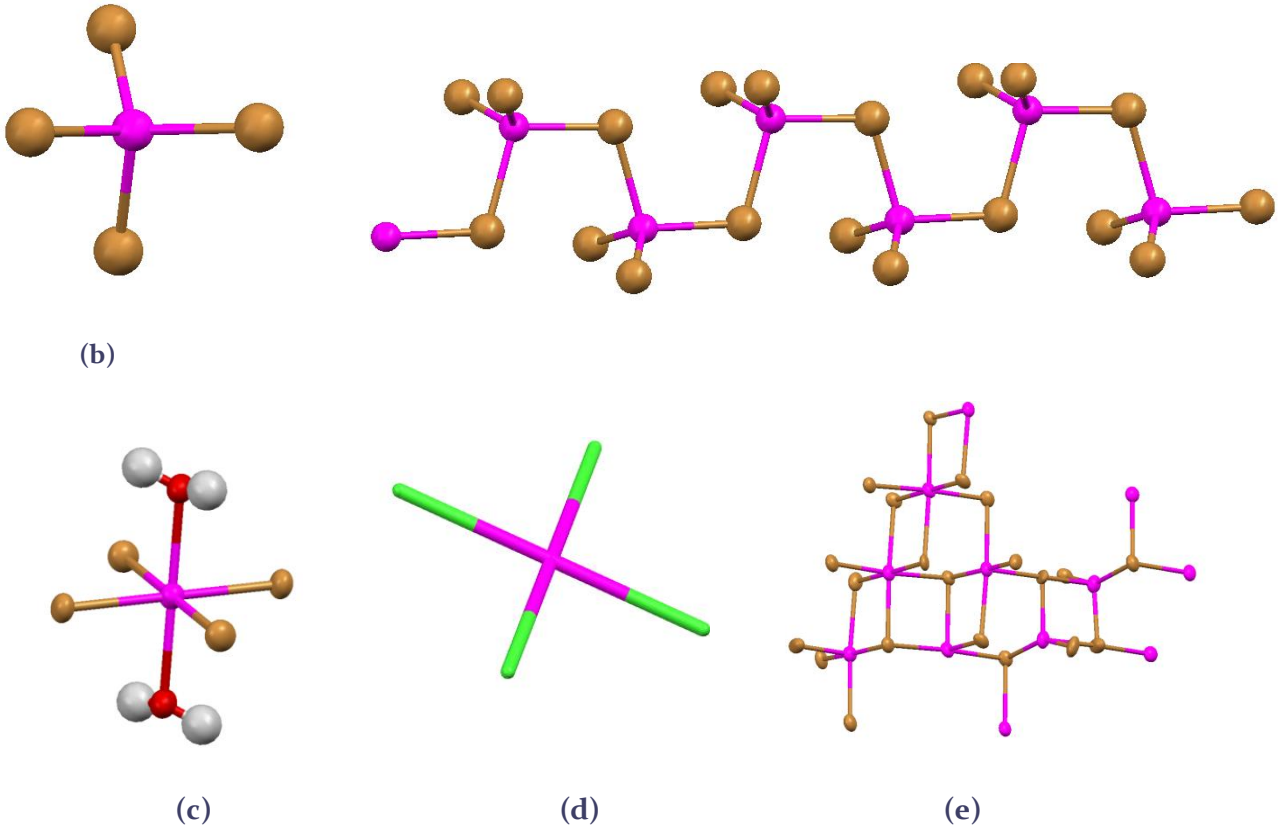

Figure 4.80: Anion geometries observed in the novel and literature structures (a) isolated tetrahedral geometry present in structures VI, VII, VIII, IX, XI, XII and XIII (b) one-dimensional polymeric anion occurring in structure X (c) isolated octahedral geometry observed in structure G and XIV (d) isolated tetrahedral geometry present in structures H, I, J and K (e) isolated anionic sheet observed in structure XVI.

Cation Geometry

It is observed that the cationic species exhibit a variety of geometries, whereby the carboxylic functional groups, or amide group in the case of 4-aminobenzamide cation, are either planar to the aromatic ring or twisted out of the plane. Table 4.17 below shows a comparison of all the geometries that are demonstrated by the cationic species in the structures. The geometries are characterized as either planar or twisted.

Table 4.17: Comparison of the cationic geometries in the ionic hybrid compounds.

Structure	Cation Geometry	Rotation angle (°)	Organic Cation	Structure	Cation Geometry	Rotation angle (°)	Organic Cation
G	Twisted	3.47	PABA	**VIX**	Twisted	22.54	4-ABA
H	Twisted	8.15	INA	**X**	Twisted	14.90	4-ABA
I	Twisted	10.39	INA	**XI**	Planar	-	PABA
J	Twisted	10.13	INA	**XII**	Planar	-	PABA
K	Twisted	6.11	INA	**XIII**	Twisted	11.02	PABA
VI	Planar	-	4-ABA	**XIV**	Planar	-	PABA
VII	Twisted	18.13	4-ABA	**XV**	Twisted	17.84	INA
VIII	Twisted	21.98	4-ABA	**XVI**	Twisted	9.96/7.20	INA

The abbreviations used in Table 4.17 (PABA, 4-ABA and INA) are the protonated 4-carboxyanilinium, 4-ammoniumbenzamide and 4-carboxypyridinium cations.

It is observed that 25% of the cationic species demonstrate planar geometries, where three of those structures belong to the 4-carboxyanilinium family except for structure VI. The 4-ammoniumbenzamide cationic family showed the most extreme cases of twisting of the amide functional group while 4-carboxypyridinium showed moderate twisting of the carboxylic group.

Isostructurality

Despite the fact that only small changes were made to the composition of the materials under investigation in each of the families (4-carboxyanilinium, 4-ammoniumbenzamide and 4-carboxypyridinium), isostructurality between structures was not as common as might have been expected. For the family of ionic 4-ammoniumbenzamide containing structures, it was found that three out of the five structures were isostructural while the 4-carboxyanilinium family demonstrated isostructurality between two structures. Since only one ionic structure was determined in the isonicotinic acid family, it is impossible to comment on the occurrence of isostructurality in this family.

The family of 4-ammoniumbenzamide containing ionic compounds all exhibit isolated tetrahedral geometries, where only structure X forms an inorganic chain and all the structures have water molecules that are incorporated into their structures. Figure 4.81 below shows the crystal structures of those 4-ammoniumbenzamide containing compounds that are observed to be isostructural.

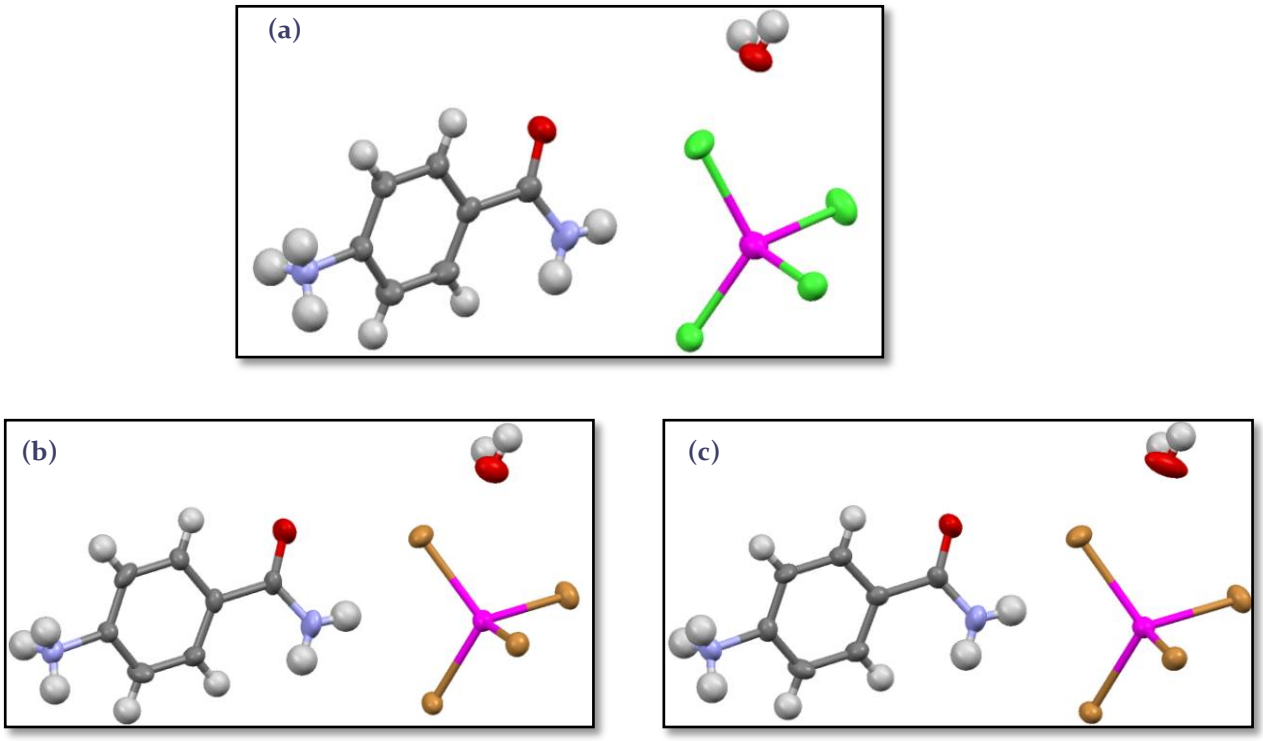

Figure 4.81: Crystal structures of isostructural 4-ammoniumbenzamide containing ionic compounds: (a) VII, (b) VIII and (c) IX.

Unit cell paramaters and I(v) values for the set of isostructural compounds are listed in Table 4.18.

Table 4.18: Unit cell parameters of the 4-ammoniumbenzamide containing isostructural ionic compounds.

Com-pound	Space Group	a(Å)	b(Å)	c(Å)	α/°	β/°	γ/°	I(v)	
VII	*Cm*	6.9513(10)	21.528(3)	6.8809(10)	90.00	103.404(2)	90.00	85.6	**VIII**
VIII	*Cm*	7.0956(7)	21.853(2)	6.9276(7)	90.00	103.964(2)	90.00	86.8	**IX**
IX	*Cm*	7.0764(8)	22.008(2)	7.0176(8)	90.00	104.044(2)	90.00	83.8	**VII**

In the 4-ammoniumbenzamide VII and VIII structures, an increase in all the unit cell parameters is observed. Even though the metal atom decreases in size, from mercury in structure VII to zinc in structure VIII, the ligand size inceases, from the chloro to the larger bromo ligand. The fact that each anion contains one metal atom and four ligands explains the increasing trend in unit cell parameters. The b and c unit cell parameters increase in going from structure VII to IX due to the increase in metal atom size from zinc to cadmium.

The family of 4-carboxyanilinium containing ionic compounds exhibit isolated tetrahedral geometries, except for structure XIV which demonstrates an octahedral geometry. These stuctures incorporate water molecules in their structures except for structure XIV which has a aqua ligand that coordinates to its cadmium metal centre. Figure 4.82 below shows the two structures that are observed to be isostructural.

(a) 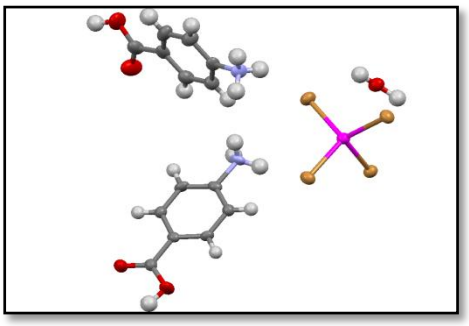 (b) 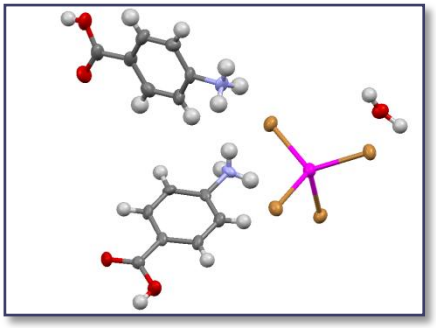

Figure 4.82: Crystal structures of isostructural 4-carboxyanilinium containing ionic compounds: (a) XII and (b) XIII.

Table 4.19: Unit cell parameters of the 4-carboxyanilinium containing isostructural ionic compounds.

Com-pound	Space Group	a(Å)	b(Å)	c(Å)	α/°	β/°	γ/°	I(v)
XII	*P*2/c	7.0537(5)	45.732(3)	6.6183(5)	90.00	100.1960(10)	90.00	**94.5**
XIII	*P*2/c	7.1578(13)	45.919(8)	6.6341(12)	90.00	100.172(3)	90.00	

It is observed that the unit cell parameters increase with increasing metal size (from XII to XIII). The I(v) value for the comparison of structure XII and XIII is high and indicates a good correlation of the atomic coordinates.

Protonation Behaviour

The protonation of the organic component employing a suitable mineral acid, HX where X = Cl, Br or I, is a requirement for the formation of an ionic material. In this study, as well as for the structures reported in the literature it was observed that for all three organic components, namely isonicotinic acid, 4-aminobenzoic acid and 4-aminobenzamide, protonation occurs on the amine or pyridine nitrogen atom, as illustrated in Scheme 4.3. This is expected for the isonicotinic acid and 4-aminobenzoic acid molecules because the protonation of the carboxylic acid oxygen atom is unlikely.

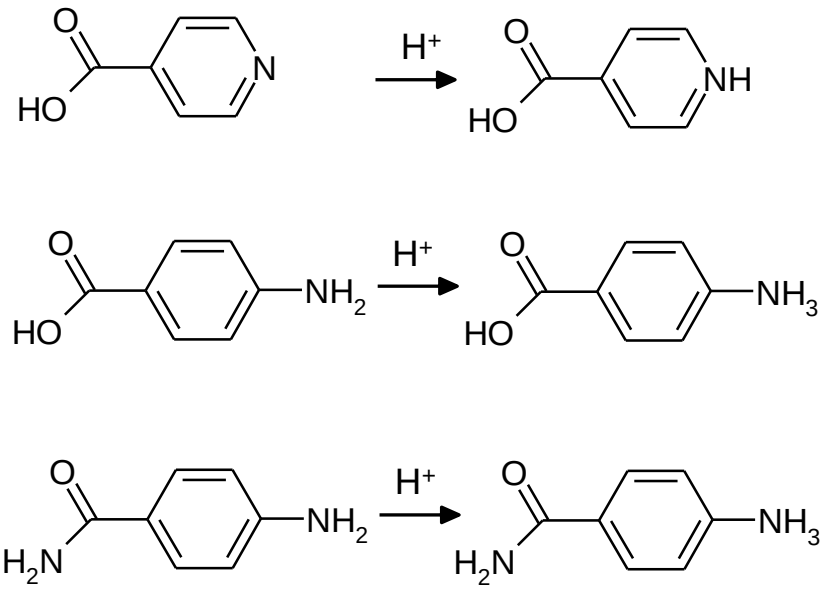

Schematic 4.3: Experimentally observed protonation sites of organic component.

In the case of 4-aminobenzamide, protonation may theoretically occur on either the amine group or the nitrogen atom or oxygen atom of the amide group. If only the amide group is considered, resonance would suggest the protonation of the oxygen atom in preference to the nitrogen atom, as indicated in the scheme below.

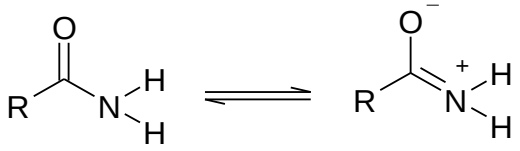

Schematic 4.4: Resonance structures of the amide functional group indicating that, in the absence of any other functional groups, the oxygen atom is the most likely protonation site in the amide functional group.

However, the experimental results confirm that the amine group is protonated in the case of the 4-aminobenzamide molecule, which is an indication of the fact that this nitrogen atom is more basic than any of the atoms of the amide group.

Aromatic Interactions

All the organic cations under investigation may potentially form aromatic interactions with neighbouring cations due to the presence of an aromatic ring in the molecular ion. In this section the packing of organic cations is analysed for each of the structures in order to identify stacking trends, which are discussed at the end of this section.

Structure XI

The structure contains distorted cationic species with four crystallographically independent organic units which lie in planes that are approximately parallel to one another. The aromatic rings demonstrate no direct overlap and exist in a slightly offset position relative to one another where their centroid-to-centroid indicate aromatic interactions. The angle between the normal to the aromatic plane and the vector between the centroids is measured to be 22°. The stacking of aromatic rings for each of the layers is shown in Figure 4.83.

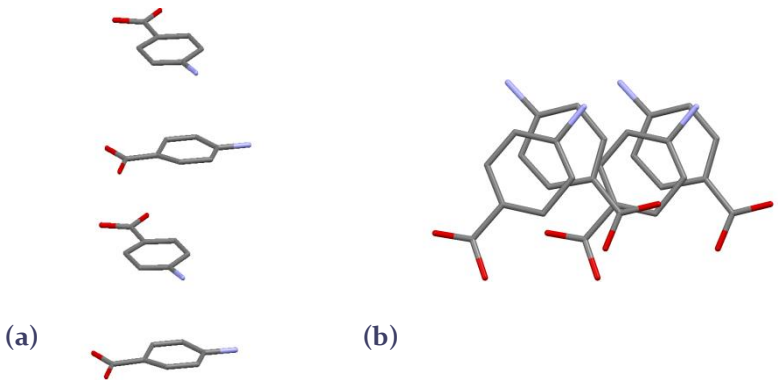

Figure 4.83: (a) Stacking of aromatic rings in the organic bi-layer; (b) View perpendicular to aromatic plane Hydrogen atoms are omitted for clarity.

Structure XII

This structure contains two crystallographically independent cations in the asymmetric unit. Pairs of these cations pack in a parallel fashion. As mentioned previously, the structure contains three types of organic layers, namely two single layers that contain only one crystallographically independent cation each, and a bi-layer that contains the other two cations. The stacking of aromatic rings for each of the layers is shown in Figure 4.84.

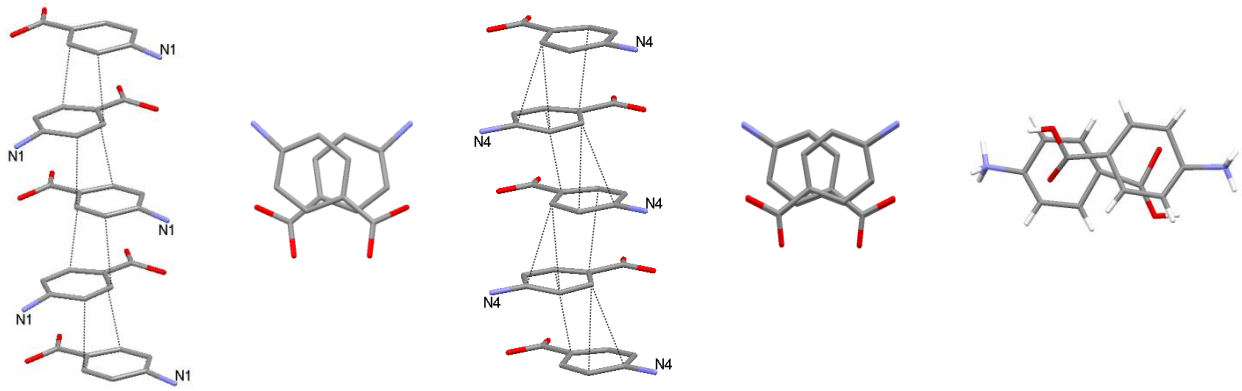

(a) (b) (c) (d) (e)

Figure 4.84: (a) Stacking of aromatic rings in the single organic layer containing cation with atom N1; (b) View perpendicular to the aromatic plane; (c) Stacking of aromatic rings in single organic layer containing cation with atom N4; (d) View perpendicular to the aromatic plane; (e) Perpendicular view of cation pair in organic bi-layer. Hydrogen atoms are omitted for clarity.

Structure XIII

This structure contains two crystallographically independent cations in the asymmetric unit. The cations pack in a parallel fashion in both the single and organic bi-layer. In the organic bi-layer, pairs of the cations stack in an extreme parallel displacement while in the single layer pairs of cations stack in a slight parallel displacement. The stacking of aromatic rings for each of the layers is shown in Figure 4.85.

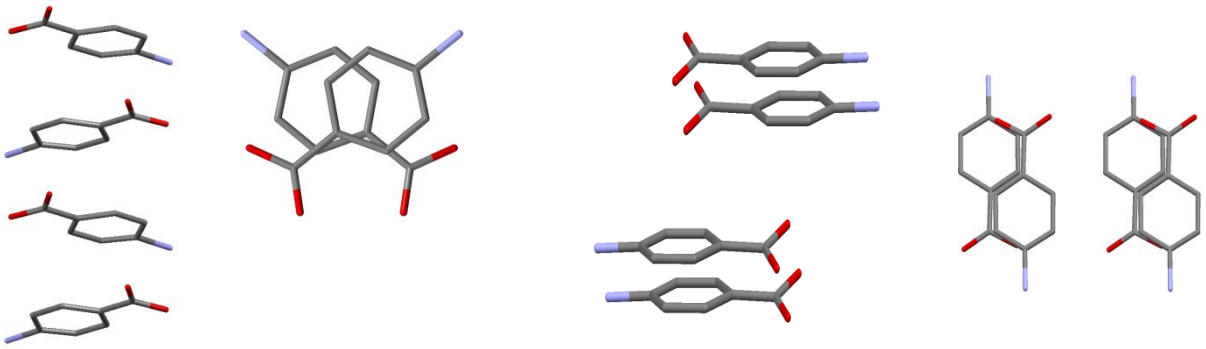

(a) (b) (c) (d)

Figure 4.85: (a) Stacking of aromatic rings in single organic layer; (b) View perpendicular to the aromatic plane; (c) Stacking of aromatic rings in the organic bi-layer; (d) View perpendicular to aromatic plane. Hydrogen atoms are omitted for clarity.

Structure VI

In the single organic layer, it observed that cations, immediately stacked over one another, alternate in orientation (Figure 4.86(a)) and do not lie in parallel planes, however every alternate cation lies on parallel planes. Cations are stacked in an extreme displacement, exhibiting no direct overlap of aromatic rings (Figure 4.86(b)).

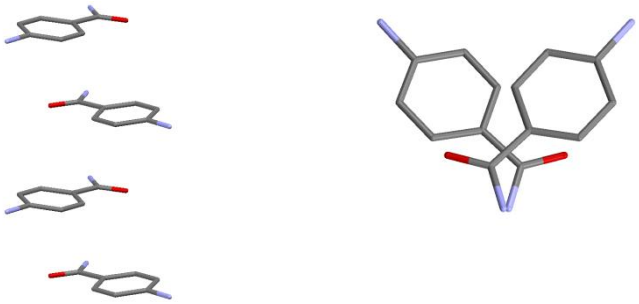

(a) (b)

Figure 4.86: (a) Stacking of cations in organic layer of structure VI; (b) View approximately perpendicular to aromatic plane. Hydrogen atoms are omitted for clarity.

Structure VIII

Only one cation is present in the structure of the isostructural set of structures 4-ammoniumbenzamide structures. In the organic the aromatic planes of neighbouring cations are not parallel, and the cations alternate in the relative orientations, as can be seen in Figure 4.87(a). When viewed approximately perpendicular to the aromatic planes of the stack, it can be observed in Figure 4.87(b) that, in a stack, partial overlap of the aromatic groups occur. Neighbouring cations pack with the ammonium groups one the same side in a stack, while the amide groups pack on the opposite side, while the cations maintain an alternating orientation.

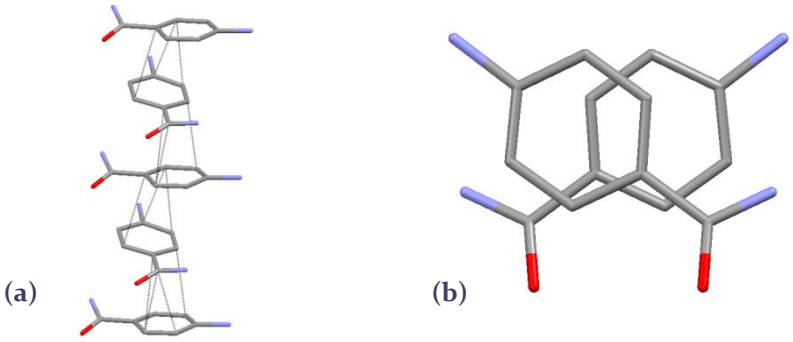

(a) (b)

Figure 4.87: (a) Stacking of cations in organic layer of structure VIII, representative of stacking in isostructural structures VII, VIII and IX (b) View approximately perpendicular to aromatic plane. Hydrogen atoms are omitted for clarity.

Comparison between families of structures showed that stacking of the cations in the organic layer always resulted in cations alternating in their relative orientations (Figure 4.88(a)). An exception however is observed for structure XIII where the cations pair up and stack parallel and each pair shows similar orientation (Figure 4.88(b)).

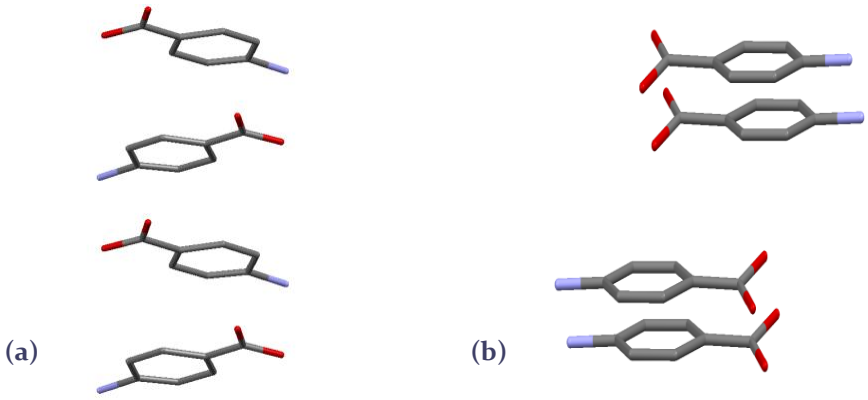

(a) (b)

Figure 4.88: (a) Predominantly observed stacking arrangement of cations with their alternating orientation; (b) stacking arrangement observed for structure XIII, where cations of similar orientation pair up.

Additionally, it is observed that the same relative orientations of cations are exhibited across families by the $ZnBr_4^{2-}$ containing structures XIII (Figure 4.89(a)) and VII (Figure 4.89(b)) which is representative of stacking in isostructural structures VII, VIII and IX.

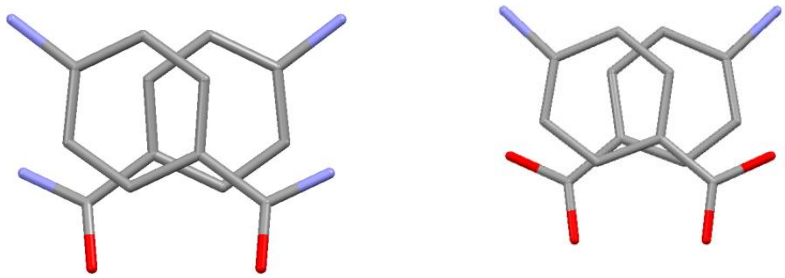

(a) (b)

Figure 4.89: Similar orientations of cations across cationic families: (a) the 4-carboxyanilinium containing XIII structure and, (b) the 4-ammoniumbenzamide containing VII structure.

A common stacking pattern is observed in structures XIII and VI, containing both 4-carboxyanilinium and 4-ammoniumbenzamide cations, as illustrated in Figure 4.89. In this pattern, cations have their ammonium groups on the same side of the stack, while neighbouring cations are rotated 180°. This stacking is expected to minimize steric hindrance between functional groups.

Hydrogen Bonding Interactions and Functional Group Recognition

In all of the novel structures (structures VI to XVI) the cations have two functional groups, on opposite sides of the cation. One end of the cation contains a nitrogen atom as potential hydrogen bond donor. This atom is a protonated pyridine nitrogen atom in the case of the 4-carboxypyridinium cation, and an ammonium nitrogen atom in the case of the 4-carboxyanilinium and 4-ammoniumbenzamide cations. The opposite end of the cation contains a functional group that can act as both a hydrogen bond donor or acceptor, namely a carboxylic acid functional group which is present in the 4-carboxypyridinium and 4-carboxyanilinium cations, while an amide group is present in the 4-ammoniumbenzamide cation. A perhalometallate anion is present in all the structures as hydrogen bond acceptor, while water molecules, which may be hydrogen bonding donors or acceptors occur in a large percentage of the novel structures.

As indicated in Chapter 1, a rule which is often employed for the prediction of the type of hydrogen bonding network which may result in a structure, is the assumption that the strongest hydrogen bonding donor will hydrogen bond to the strongest hydrogen bonding acceptor (Etter, 1990). In the novel structures, the strongest hydrogen bonding donor is the protonated nitrogen atom (protonated pyridine or ammonium group), while the strongest hydrogen bond acceptor is a halogeno ligand on the charged anion. This hydrogen bond donor and acceptor combination will result in the formation of strong, charge assisted hydrogen bonds, as a result of the charge carried by both the cation and the anion.

The combination of the second strongest hydrogen bond donor and acceptor would result in the formation of a dimer between the carboxylic acid group or the amide group in the relevant structures. In these functional groups the donor and acceptor atoms are not charged, and this would result in the formation of weaker hydrogen bonds compared to the charge assisted hydrogen bonds described above.

The prediction of "functional group recognition" by employing the strength of the resulting hydrogen bonds is obeyed only for the structures in which an organic bi-layer is formed, since this type of packing results in the interaction of the charged nitrogen atom with the anion, and the formation of a dimer between uncharged functional groups. As discussed previously, the formation of an organic bi-layer exclusively, is only observed in the novel structure XI, and the literature structures H, I, J and K. The novel structures XII and XIII display both an organic bi-layer and a single organic layer. This means that "recognition" through hydrogen bonding occurs in certain layers, but not in others. In the rest of the structures, G, XIV, VI, VII, VIII, IX and X, the protonated nitrogen atom, the anion, and the amide/carboxylic acid group all interact in the same hydrogen bonding network.

In all of the 4-carboxypyridinium cation containing structures, the strongest hydrogen bonding donor interacts with the strongest hydrogen bonding acceptor, as predicted, but this happens only in certain 4-carboxyanilinium cation containing structures. This "rule" is not applicable to any of the structures in the 4-ammoniumbenzamide cation family.

This means that the rule of combination of the strongest hydrogen bond donor with the strongest hydrogen bond acceptor is not strictly applicable to all the families of structures under investigation. However, a closer inspection of the hydrogen bonding networks formed in the structures that do not show "recognition" reveal that some degree of recognition is still present. It is found that, in these structures, a primary hydrogen bonding network is often formed between the strong protonated nitrogen atom and the strong hydrogen bond acceptor, the anion. Secondary hydrogen bonding interactions then further anchor the weaker donor/acceptor atoms to this primary network. Thus, hydrogen bonding interactions between the strongest donor and strongest acceptor are present, but not exclusively – a weaker donor may also interact with the strongest acceptor (the anion).

The incorporation of water molecules into the hydrogen bonding network may be due to the formation of a more stable hydrogen bonding network, or to fulfil the space filling requirements of close packing in the structure, or both.

With the exception of structure XVI, a two-dimensional hydrogen bonding network is observed in all the structures, as a result of the layered packing of the different molecular ions, as well as the fact that the cations pack approximately perpendicular to the inorganic layer.

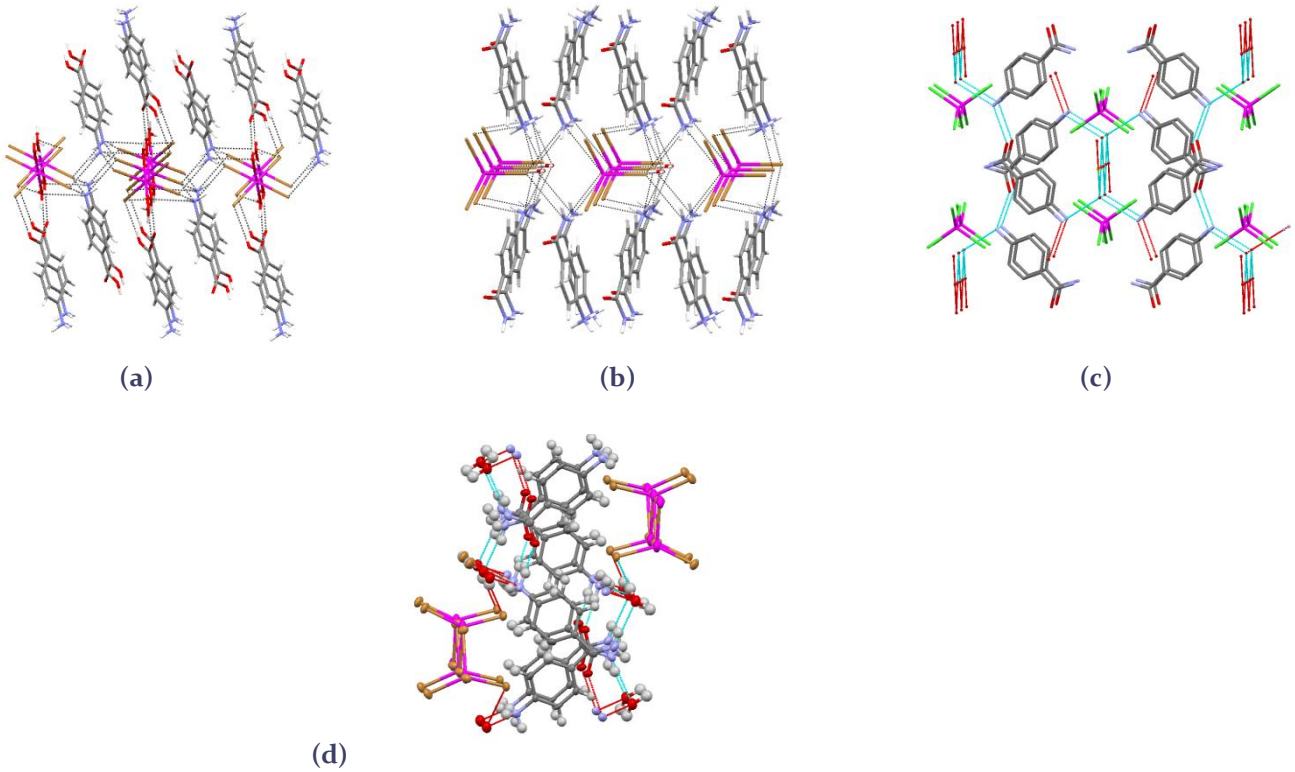

Figure 4.90: Two-dimensional hydrogen bonding networks in structures with a single organic layer. (a) Structure XIV (also representative of structure G; (b) structure VII (also representative of structures VIII and IX; (c) structure VI and; (d) structure X.

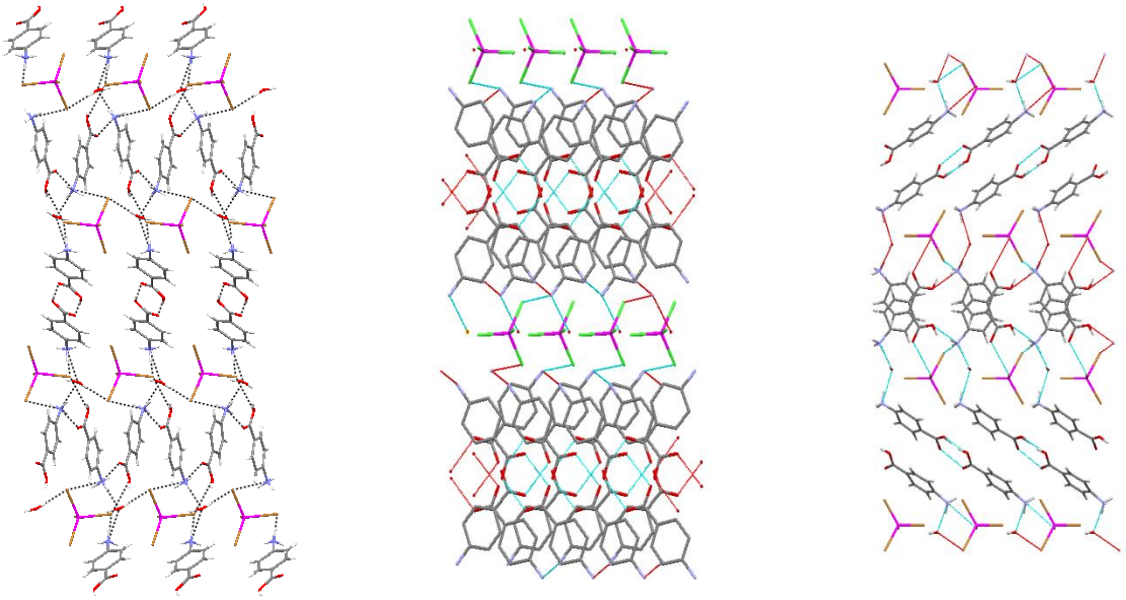

(a) (b) (c)

Figure 4.91: Two-dimensional hydrogen bonding networks in structures with an organic bi-layer. (a) Structure XIII; (b) structure XI and; (c) structure XII.

Crystal Engineering Synthons

The identification of robust synthons in the novel structures may aid in the prediction of structural characteristics of related structures. The software programme Mercury (version 2.2, Macrae, at al., 2008) was employed to investigate the structures for the occurrence of common zero-dimensional hydrogen bonding synthons between the constituents.

A detailed study of the synthons occurring in the literature structures H, I, J and K has been carried out and reported in the literature (Orpen, et al., 2010), and these structures will not be discussed here.

A relatively large number of novel ionic structures, namely seven out of the ten novel structures (structures VI, VII, VIII, IX, XI, XII and XIII), contain an isolated tetrahedral anion, an isolated water molecule(s) and a 4-carboxyanilinium or 4-ammoniumbenzamide organic cation in the asymmetric unit. The only difference between the 4-carboxyanilinium or 4-ammoniumbenzamide cation is the replacement of the carboxylic functional group in the 4-carboxyanilinium cation with an amide functional group in the 4-ammoniumbenzamide cation. These seven structures present a logical starting point in the search of robust crystal engineering synthons due to the similarity of their components. Note that the following structures in the category are isostructural: structures VII, VIII and IX, and structures XII and XIII. Each set of isostructural structures represent a structural type.

Figure 4.92(a) illustrates the zero-dimensional synthons observed in the structures containing an isolated anion. As can be seen in Figure 4.92 (a), (c), (e) and (g), a synthon common to all the structures consists of two cations, an isolated tetrahedral anion and a water molecule. In the case of structures VII, VIII, IX, XII and XIII, which contain the anions $HgCl_4^{2-}$, $ZnBr_4^{2-}$, $CdBr_4^{2-}$, $ZnBr_4^{2-}$ and $CdBr_4^{2-}$ respectively, this synthon is similar.

In the Figures showing this synthon the orientation of the anion at the top of the Figure is the same for all of the synthons, with the top and bottom ligands of the tetrahedron pointing out of the page, while the other two ligands point into the page. In the synthon the two halogeno ligands pointing into the page act as hydrogen bonding acceptors from two different hydrogen atoms of each ammonium group.

Of interest is the fact that this same synthon is observed for the 4-ammoniumbenzamide cation containing structures and two 4-carboxyanilinium cation containing structures. In the case of the 4-ammoniumbenzamide cation structures the synthon is centrosymmetric, but it is non-centrosymmetric in the 4-aminobenzoic acid cation structures. Another notable point is that this synthon occurs for anions containing larger metal atoms (Cd or Hg), or when the smaller zinc metal atom is combined with larger bromo ligands.

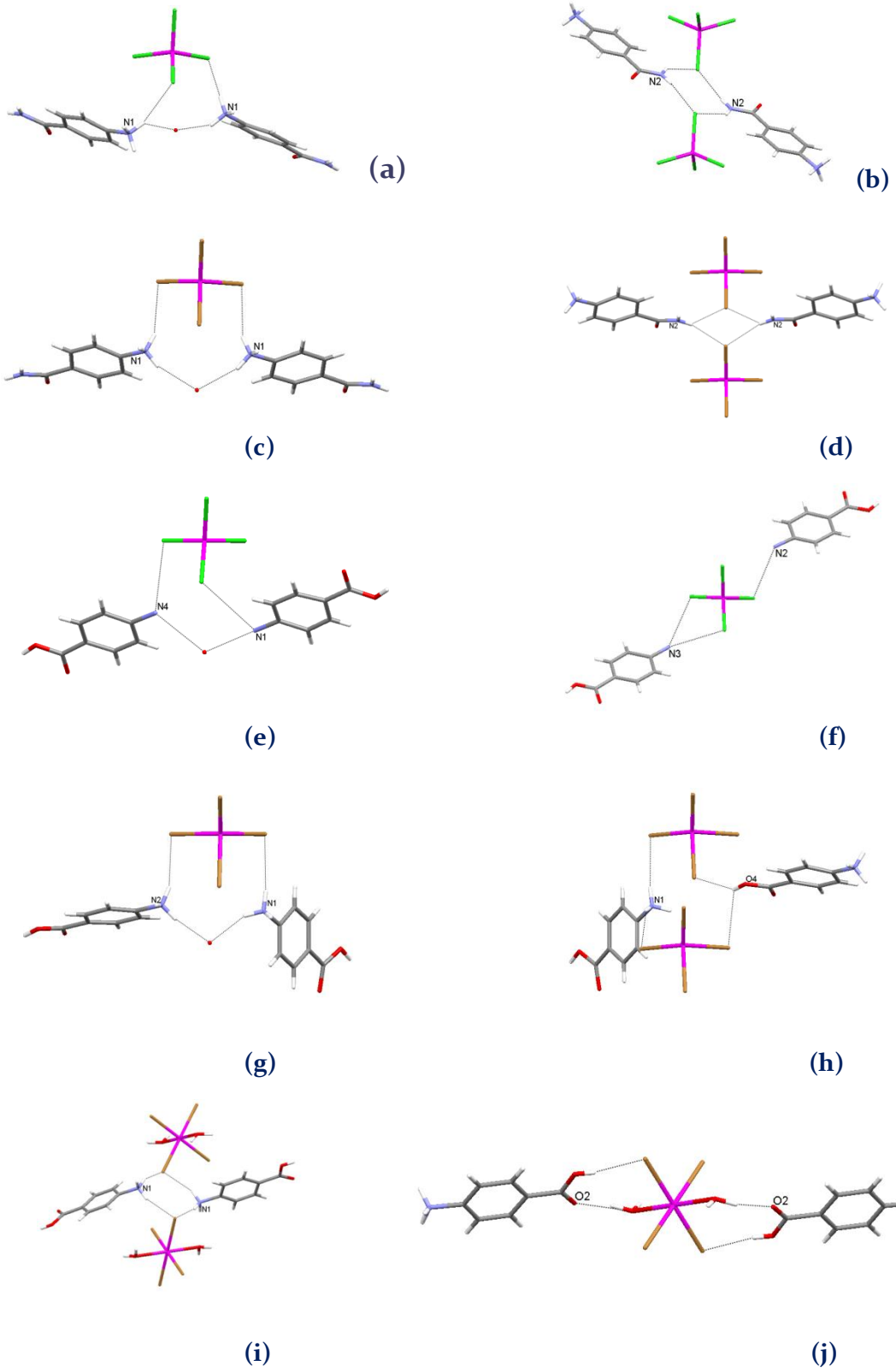

Figure 4.92: Zero-dimensional synthons in (a), (b) structure VI (c), (d) structure VIII (also representative of structures VII and IX) (e), (f) structure XI (hydrogen atoms on nitrogen atoms omitted) (g), (h) structure XIII (also representative of structure XI) (i), (j) structure XIV.

In the $ZnCl_4^{2-}$ containing structures VI and XI, a different halogeno ligand acts as hydrogen bonding acceptor, compared to the rest of the structures, as shown in Figure 4.92(a) and Figure 4.92(e). This synthon also consists of two cations, one water molecule and an isolated tetrahedral anion, and is non-centrosymmetric. In this synthon one forward facing and one backward facing ligand act as hydrogen bonding acceptors, which is different from what was observed in the other structures. It should be noted that this synthon is only observed in structures containing the small metal atom zinc combined with the small chloro ligands.

As shown in Figure 4.92 (b), (d) and (f), a second synthon is observed in the 4-ammoniumbenzamide cation containing structures VI, VII, VIII and IX. In this centrosymmetric synthon a hydrogen bonded tetramer is formed between two anions and the amide groups of two cations. One hydrogen atom of the amide nitrogen on each cation forms a bifurcated hydrogen bond to two different halogeno-ligand acceptors on two different anions. In this synthon two forward facing ligands act as hydrogen bonding acceptors. Even though structure VI is not isostructural to structures VII, VIII and IX, and different anions occur in the structures, the amide groups form the same synthon.

A third type of synthon is present in structure XI, as shown in Figure 4.92(f), comprised of one anion and two 4-carboxyanilinium cations. In this synthon the nitrogen atom N3 forms a bifurcated hydrogen bond to the anion, while the N2 atom only forms a single hydrogen bond to the anion. This synthon is similar to that reported for the isonicotinic acid cation containing structure K which possesses a square planar $PtCl_4^{2-}$ cation. Note that the carboxylic acid dimer synthon also occurs in the 4-aminobenzoic acid cation containing structures. The hydrogen bonded synthons present in structure XI link the ions into one-dimensional hydrogen bonded chains, similar to what was observed in structure K, as shown in Figure 4.92(c) and (d).

A second synthon observed in structure XIII is shown in Figure 4.92(h). In this synthon a tetramer consisting of four anions and two cations is formed. What makes this synthon unique is the fact that it contains different hydrogen bonding donors, namely both an ammonium group and a carboxylic acid functional group. In all the other synthons identified in this study the two cations in the synthon interact through the same functional group.

In structure XIV, and the isostructural literature structure G, a synthon which is similar to that shown in Figure 4.92(b) and (d) is observed, as illustrated in Figure 4.92(i). Even though in this case the anion adopts an octahedral geometry, the similarity is striking. A similar synthon was also reported for structures containing aryl- or alkylammonium cations and isolated tetrahedral tetrahalometallate anions (Rademeyer et al., 2011). A second synthon present in this structure consists of two cations and one ion, to form a centrosymmetric synthon linked by four hydrogen bonds between carboxylic acid functional groups and the anion

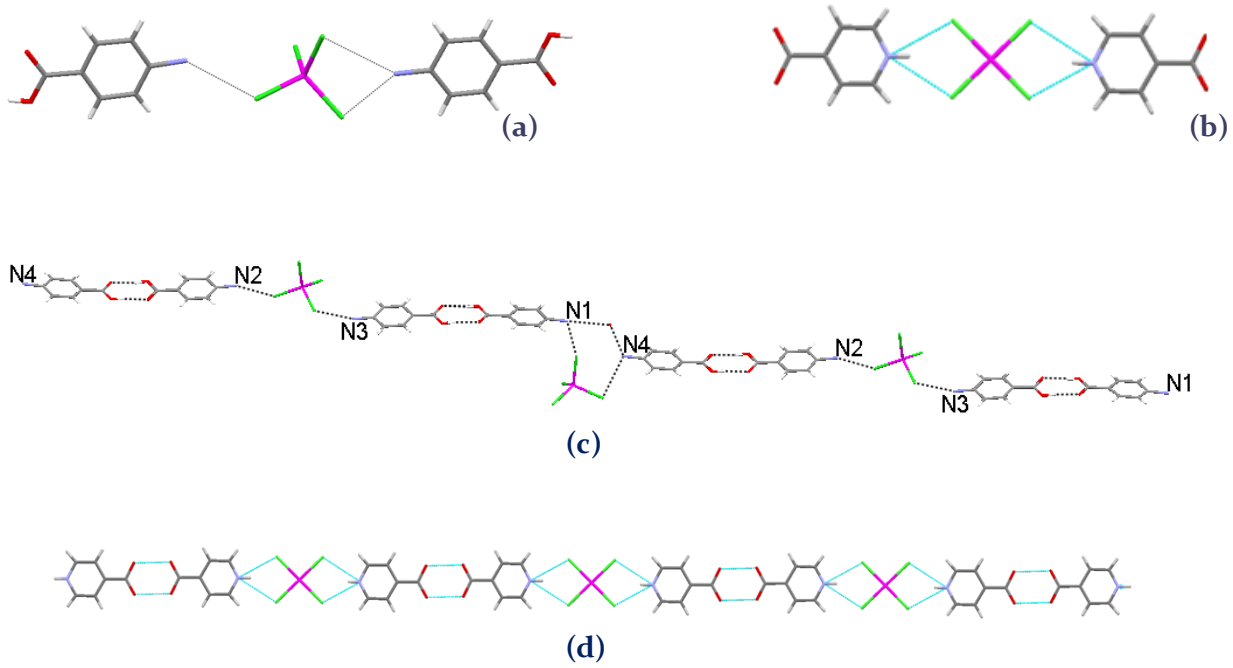

Figure 4.93: (a) Hydrogen bonding synthon observed in structure XI (b) Similar hydrogen bonding synthon observed in literature structure K (c) One-dimensional hydrogen bonded ribbon formed in structure XI (d) Related one-dimensional hydrogen bonded ribbon formed in structure K.

In all of the structure types containing isolated anions the synthons link neighbouring ions into one-dimensional hydrogen bonded ribbons, as illustrated in Figure 4.93(c), and Figure 4.93(a) –(d).

In structures VI, VII, VIII, IX and XI the two synthons alternate and share organic cations, as illustrated in Figure 4.94(a), (b) and (d). However, in the 4-carboxyanilinium cation containing structures a more complex sequence of synthons are present in the one-dimensional hydrogen bonded ribbon, as shown in Figure 4.94(c) and (c). In structure XI carboxylic acid dimers are present between the two types of alternating synthons. If the water containing synthon is denoted a, the carboxylic acid dimer is indicated by the symbol b and the third synthon is given the symbol c, the sequence of synthons linking the ions is: b-c-b-a-b-c-b. Thus a b synthon appears between alternating a and c synthons.

In structures XII and XIII the synthon sequence is different, as shown in Figure 4.94 (c). If the same symbols as above are employed, the sequence is a-b-c-a-b-c.

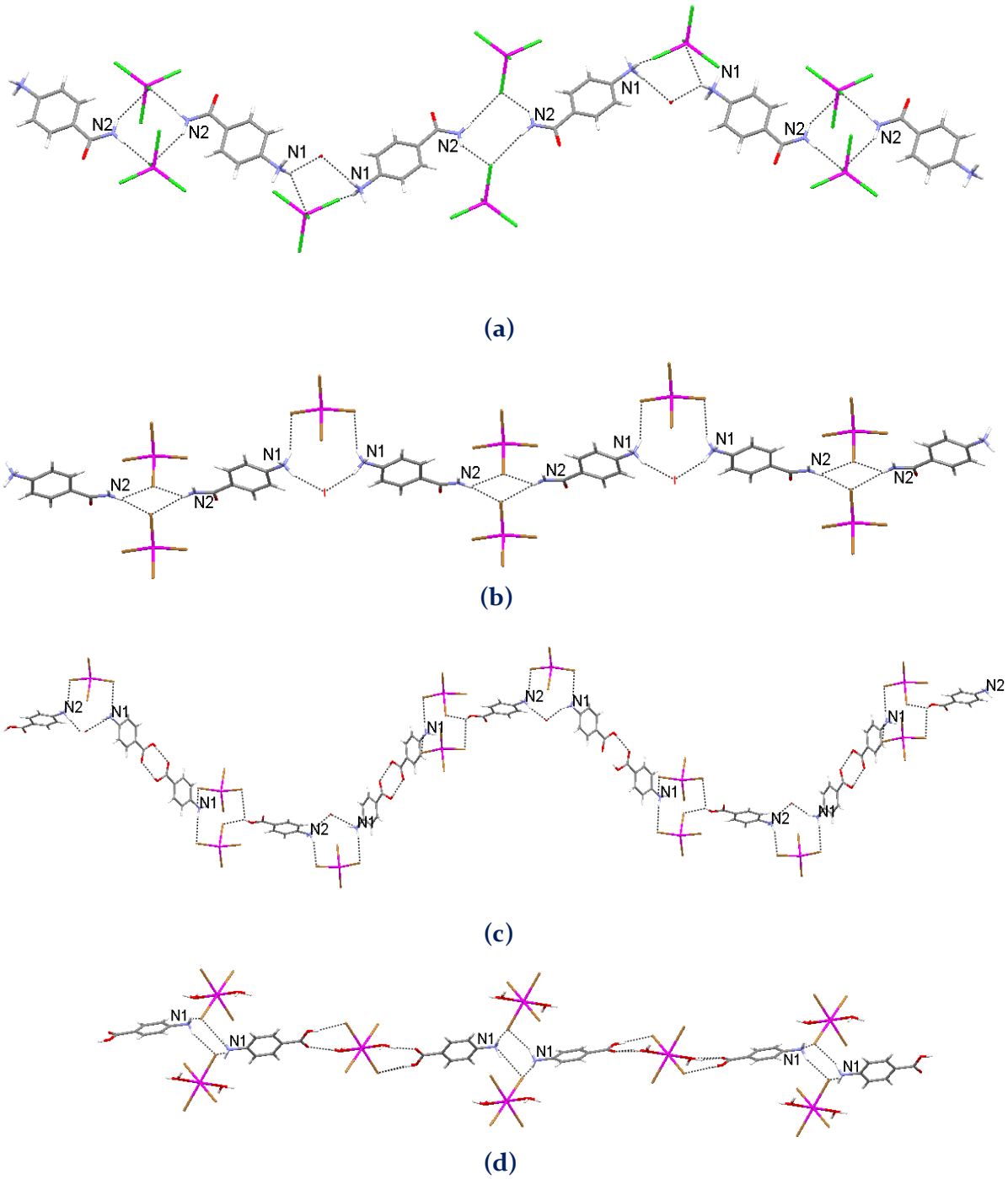

Figure 4.94: Hydrogen bonded chains in (a) structure VI (b) structure VIII (c) structure XIII (d) structure XIV.

Due to the complexity of the structures, and the fact that one- and two-dimensional anions are formed, respectively, in structures X and XVI, and the fact that these structures are not related to any other structures in these families determined in this study, or in the literature, the crystal engineering synthons in these structures have not been investigated further.

Powder X-Ray Diffraction

The mechanochemical synthesis of the ionic hybrid compounds proved to be problematic in many cases. It was found that even during grinding, some of the samples attracted water from the atmosphere to yield a paste that could not be analysed by PXRD. In addition, when complete reaction between the components did not occur the metal halide component reacted with the aluminium sample holder employed.

Tables 4.20 to 4.22 shows the analysis of PXRD results for ionic compounds. Each powder product was compared to the powder patterns of the starting materials, and by using this "fingerprinting" technique, it could be determined whether or not reagents were still present in the sample and whether a product had formed.

Table 4.20: Powder XRD analysis of products obtained during grinding synthesis of the 4-carboxyphenylammonium chloride/bromide hybrid salts and varying metal halides. (Organic salt : Metal halide)

Reactants		**PXRD Analysis**		
Metal-halide	Ratio	Organic Molecule	Metal-halide	Product
$MnCl_2$	1:1	-	-	X
$MnCl_2$	1:2	-	-	X
$MnCl_2$	2:1	X	-	X
$MnBr_2$	1:1	X	-	X
$MnBr_2$	1:2	X	-	X
$MnBr_2$	2:1	X	-	X
$CuBr_2$	1:2	X	X	-
$CuCl_2$	1:2	X	X	-

Table 4.21: Powder XRD analysis of products obtained during grinding synthesis of the 4-ammoniumbenzamide chloride/bromide hybrid salts and varying metal halides. (Organic salt : Metal halide)

Reactants		**PXRD Analysis**		
Metal-halide	Ratio	Organic Molecule	Metal-halide	Product
$MnBr_2$	1:2	-	X	X
$MnBr_2$	2:1	-	-	X
$CuBr_2$	1:1	-	X	X
$CuBr_2$	1:2	-	X	X
$CuCl_2$	1:2	-	-	X
$CuCl_2$	2:1	-	-	X
$ZnCl_2$	1:1	-	-	X
$ZnCl_2$	2:1	-	-	X

Table 4.22: Powder XRD analysis of products obtained during grinding synthesis of the *4-Carboxy-pyridinium chloride*/bromide hybrid salts and varying metal halides. (Organic salt : Metal halide)

Reactants		**PXRD Analysis**		
Metal-halide	Ratio	Organic Molecule	Metal-halide	Product
$MnCl_2$	1:1	X	X	-
$MnCl_2$	1:2	X	X	-
$MnCl_2$	2:1	X	X	-
$MnBr_2$	1:1	X	-	X
$MnBr_2$	1:2	X	-	X
$MnBr_2$	2:1	X	-	X
$CuBr_2$	1:1	X	-	X
$CuBr_2$	1:2	-	X	X
$CuBr_2$	2:1	X	-	X
$CuCl_2$	1:1	-	X	X

In the cases where a product was formed, as indicated in Tables 4.20 to 4.22, none of the products obtained via grinding corresponded to the products obtained via solution crystallization. A possible reason is the fact that most of the solution crystallized samples contained water, and water was not available during the grinding experiment. Figure 4.96 below is an example of such a comparison and no overlap of the peaks can be observed. It should be noted that the term 4-ABA$^+$Cl$^-$ refers to the 4-ABA chloro salt that was synthesized and used during this study.

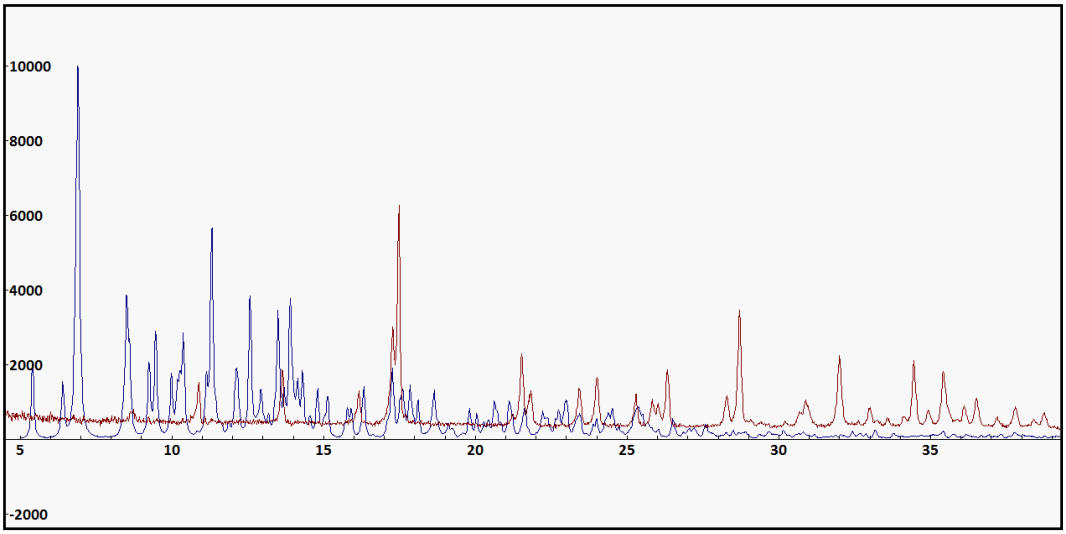

Figure 4.96: Comparison of PXRD result of 4-ABA$^+$Cl$^-$ + $ZnCl_2$ (red) with calculated SCD result (blue).

Differential Scanning Caloriometry

The DSC analysis of the ionic materials could not be performed successfully due to the release of corrosive acid vapours upon heating. Corrosion of the instrument occurred after only a few samples were scanned, and it was decided to terminate the study when it was realised that even when applying a high N_2 gas flow to purge the instrument, corrosion still occurred.

Photoluminescence

The photoluminescence spectrum of compound X was measured and is shown in Figure 4.95.

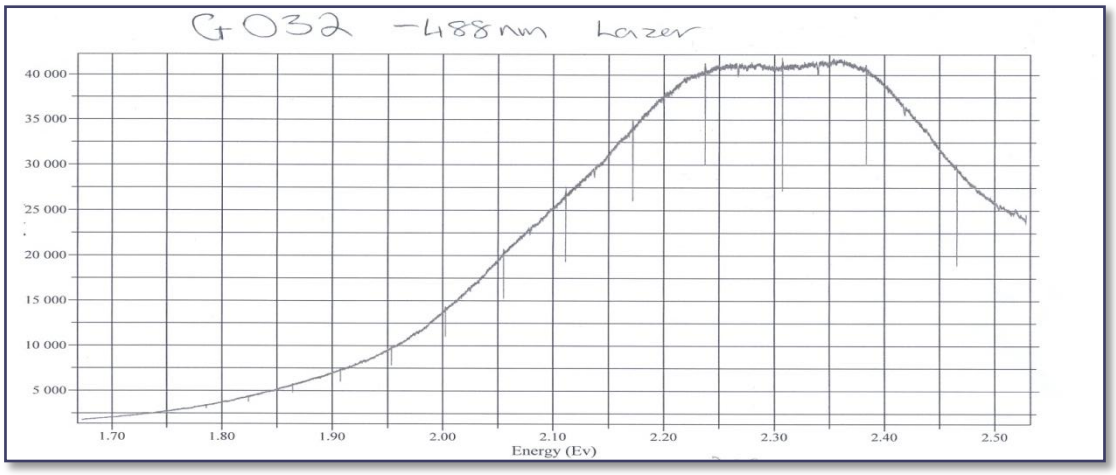

Figure 4.95: Photoluminescence scan of compound X.

The wavelength of the laser beam employed is 488nm and the result indicate that the band gap approximately falls between 2.2 and 2.4 eV. This is an indication of semi-conducting behaviour.

Electric conductance

As part of the preliminary study towards the electrical conductivity of novel compounds, measurements was carried out using two probe DC analysis on the compounds X (Figure 4.97) and XVI (Figure 4.98). Please see Figure 4.50 and Figure 4.72 for the asymmetric units of compounds X and XVI on pages 149 and 167 respectively.

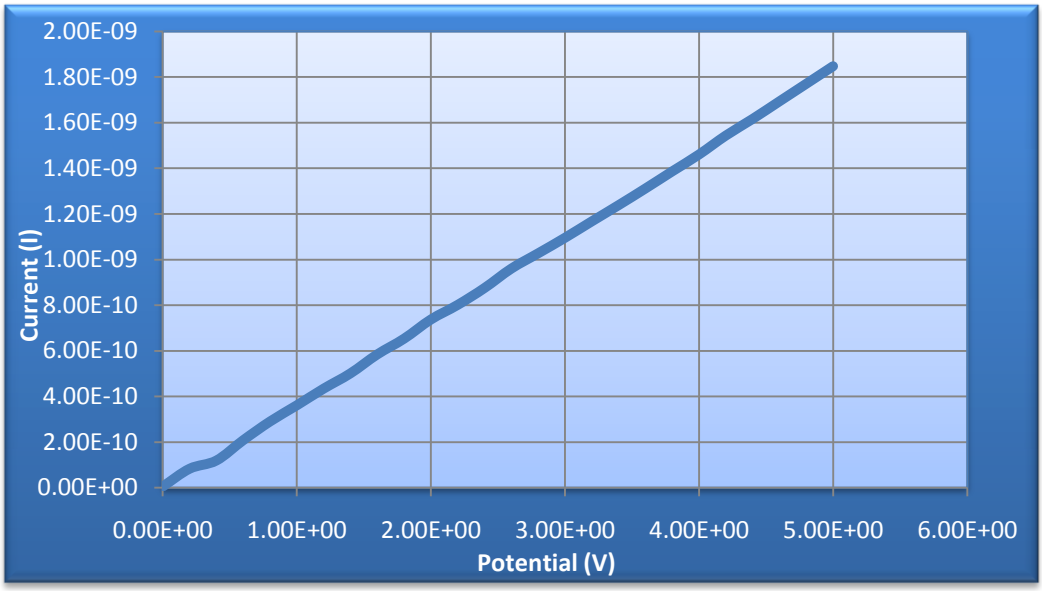

Figure 4.97: Two probe DC scan of compound X:

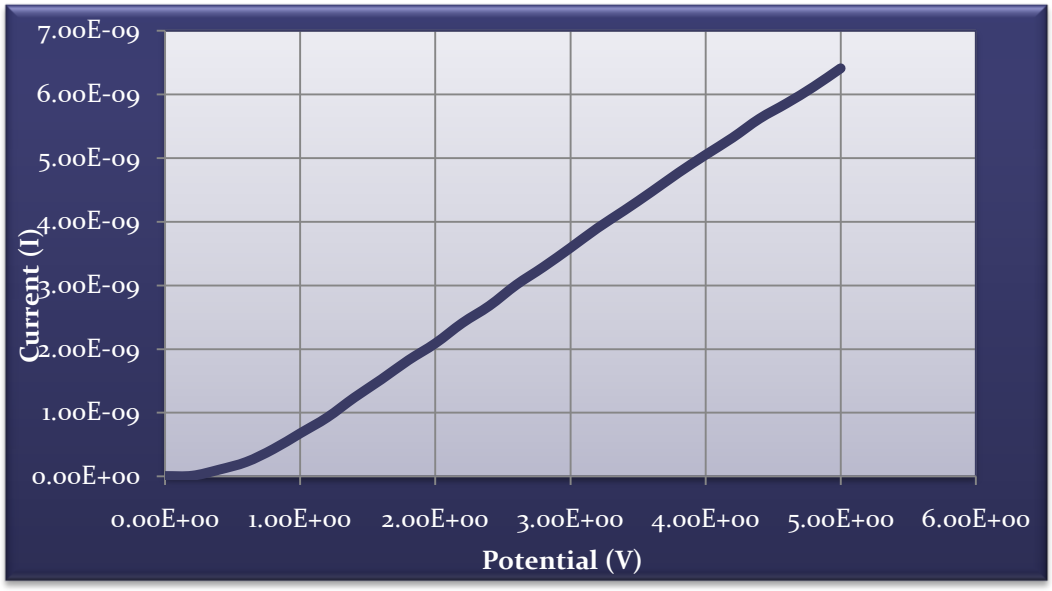

Figure 4.98: Two probe DC scan of compound XVI:

Unlike the semi-conducting behaviour observed for the coordination compound IV, compound X demonstrate ohmic behaviour. However, compound XVI shows semi-conducting behaviour. Similar to the previous measurements, values for the current is low and occur as a result of the crystal-electrode electrical contacts.

Chapter 5

Conclusion and Prospective Studies

Summary

The combination of organic and inorganic constituents to form novel materials is a topic that currently enjoys significant attention in the field of materials science. The resulting materials may combine the desired properties of both the organic and inorganic components, or may exhibit novel properties, depending on the mechanism of combination of the two units. When combined as ions, properties of the constituents are often retained, while the combination through covalent bonds is expected to alter the properties of the constituents to a certain degree.

In the current study the combination of aryl-containing organic components with divalent inorganic metal halides is of interest. Related materials have been reported to have sought-after properties, including photoluminescence, semi-conducting, conducting or magnetic properties. In order to be able to control the properties of the materials the relationship between the structure and the properties of a material needs to be understood. At an even more fundamental level it is necessary to understand the structural characteristics of the materials, as this knowledge may ultimately enable the control of the structure as well as the properties of the material.

In the current study the structural characteristics of a range of ionic and coordination materials were studied with the aim of identifying structural trends and robust synthons using the approach of crystal engineering. Small changes were made to the components that constitute the material, namely the organic component, the metal atom or the halogeno ligand, and the effect of the change on the structure was noted.

Ionic and coordination organic-inorganic hybrid materials formed between the divalent metal halides of Cu, Mn, Zn, Cd and Hg and the organic components 4-aminobenzamide, 4-aminobenzoic acid and isonicotinic acid were structurally characterised.

Five novel coordination structures were determined in this study. The combination of 4-aminobenzoic acid with $ZnCl_2$ and $HgCl_2$ respectively (structures I and II) resulted in isostructural tetrahedral zero-dimensional coordination complexes, while a square planar zero-dimensional complex was obtained for the combination of this organic component with $CuCl_2$ (structure III) through coordination bonds. Of specific interest is the one-dimensional coordination polymer obtained by the combination of 4-aminobenzoic acid and $HgBr_2$ (structure IV) in which mercury octahedra share edges. The combination of $MnBr_2$ and isonicotinic acid (structure V) yielded a unique coordination polymer of a type that has never been reported. In this structure coordination of the ligand occurs through a carboxylate group. This carboxylate group is most probably created by zwitter-ion formation in which the hydrogen atom of the carboxylic acid functional group protonates the basic pyridine nitrogen atom.

In all the novel zero-dimensional 4-aminobenzoic acid containing coordination compounds coordination occurs through the amine group, and the carboxylic acid group link the molecules into hydrogen bonded ribbons through hydrogen bonded carboxylic acid dimers.

This structural motif is common to all these structures regardless of the fact that they are not all isostructural, and that the anion geometry varies between tetrahedral or square planar.

In the polymeric structure of 4-aminobenzoic acid and $HgBr_2$ (structure IV) neighbouring polymers are also linked by hydrogen bonded carboxylic acid dimers, resulting in a structure that is remarkably similar to that observed for the isolated coordination compounds.

For all the coordination structures, except structure V, a parallel, slipped stacking of aromatic groups occur. In the case of structure V the aromatic planes of neighbouring ligands are not parallel.

Hydrogen bonded carboxylic acid dimers are formed in all the 4-aminobenzoic acid coordination compounds. In addition, hydrogen bonds between the coordinated amine groups and halogeno ligands are present in all of the structures.

Ten novel ionic hybrid materials were structurally characterised in this study. It was found that in all of the organic molecules employed, namely 4-aminobenzamide, 4-aminobenzoic acid and isonicotinic acid, protonation occurs on the pyridine or amine nitrogen. Seven out of the ten structures displayed isolated tetrahedral anions, MX_4^{2-}, and isolated water molecules in combination with the protonated organic constituent (structures VI, VII, VIII, IX, XI, XII and XIII). Less common anionic forms that were observed in this study include one isolated octahedral $MX_4(OH_2)_2^{2-}$ anion (structure XIV), one corrugated one-dimensional polymer in which the metal atom adopts a tetrahedral geometry and one bridging ligand is present (structure X), and an exceptional two-dimensional sheet anion with several metal coordination geometries (structure XVI).

The combination of 4-aminobenzamide and $ZnCl_2$ in acidic medium (structure VI) resulted in a unique inclusion structure that contains channels of disordered water molecules. Ionic compounds of 4-aminobenzamide and $HgCl_2$, $ZnBr_2$ and $CdBr_2$ are isostructural (structures VII, VIII and IX), while the combination of this organic part with $HgBr_2$ (structure X) gives an ionic structure containing a one-dimensional polymeric anion.

In the ionic 4-aminobenzoic acid family the combination with $ZnBr_2$ and $CdBr_2$ are isostructural (structures XII and XIII), but different from the structure obtained from the combination with $ZnCl_2$ (structure XI). All three structures contain isolated anions and water molecules in addition to their organic components.

Undoubtedly, the most intriguing structure obtained in this study is the ionic compound formed between isonicotinic acid and $HgBr_2$ (structure XVI). This unique structure displays a number of structural characteristics that differ significantly from the rest of the structures determined in this study and reported in the literature. Interesting aspects include the formation of a very complex, stepped, two-dimensional anion in which the metal atoms display three different coordination geometries, namely tetrahedral, square pyramidal and octahedral, and the fact that, unlike what is observed in all the other structures, the cations pack parallel to the inorganic layer, and fit into a “pocket” formed by the stepped anions.

A crossed, alternating stacking mode of cations occurs in both the 4-aminobenzoic acid ionic family and the 4-aminobenzamide ionic family. Robust zero-dimensional crystal engineering synthons were identified for the ionic structures containing isolated anions, and it was found that a common one-dimensional hydrogen bonded motif is the linking of ions into hydrogen bonded ribbons through alternating synthons.

A comparison of all the ionic and coordination structures reveals that a common structural trend is the formation of a layered structure consisting of alternating organic and inorganic layers. This structure type is formed irrespective of the type of organic component (ligand or isolated cations) and anion (isolated or polymeric). With the exception of one structure, the organic components, whether ionic or coordinated ligands, pack in a tilted arrangement relative to the inorganic layer plane. Organic bi-layers in which organic ligands are linked through hydrogen bonded carboxylic acid dimers are ubiquitous in coordination compounds of 4-aminobenzoic acid, but they are not found exclusively in the analogous ionic compounds. Single organic layers occur in all of the 4-aminobenzamide ionic structures, as well as in the coordination compound formed between isonicotinic acid and $MnBr_2$.

Even though one of the initial aims of the study was to investigate the thermal behaviour of the materials, this aspect of the investigation was terminated when it was realised that the release of corrosive acid vapours on heating of the materials was resulting in corrosion of the DSC instrument.

Preliminary investigations of the electronic conducting behaviour of a selected number of materials, both ionic and coordination materials, were performed. These studies indicated that certain materials fall in the semi-conductor category, and confirmed that future investigation of this property is warranted. A preliminary photoluminescence experiment confirmed that the bandgap of one of the ionic compounds fall within the semi-conductor range, confirming the electronic conductance behaviour identified by the conductance measurements.

Prospective Studies

Future work includes the completion of the structural characterization of all the materials, both ionic and coordination materials, in the three families of materials. Once this has been done, a more statistically significant comparison of the structures is possible, allowing for the identification of structural trends, and crystal engineering synthons to be employed in the areas of structure prediction and control.

As indicated by the preliminary property investigations performed in this study, particular materials show semi-conductor behaviour. In order to fully understand the relationship between the structure of the material and its electronic conducting characteristics, detailed investigations of these properties will be performed employing photoluminescence for band-gap determination and current-voltage measurements. These results will be correlated with the structural characteristics of the materials.

A powerful tool available to the materials scientist is the use of computational chemistry to predict material properties. This involves the quantum mechanical determination of the electronic structure of the material, with the single crystal structure as starting point, through the use of suitable approximations. Once the electronic structure has been determined, a number of physical properties may be calculated, for example band gap and magnetic properties. Specialised software to perform these types of calculations is available, and the modelling of these materials will form a prospective study. The calculated material properties will be compared with the experimentally measured properties mentioned in the previous paragraph. The validation of the calculated parameters by means of comparison with experimental values is an essential step in this process.

Bibliography

Aakeröy, C.B., Seddon, K.R., 1993, The Hydrogen Bond and Crystal Engineering, *Chemical Society Reviews*, 22, 397-407.

Adams, C.J., Angeloni, A., Orpen, A.G., Podesta, T.J., Shore, B., 2006, Crystal Synthesis of Organic-Inorganic Hybrid Salts Based on Tetrachloroplatinate and –palladate Salts of Organic Cations: Formation of Linear, Two-, and Three-Dimensional NH···Cl Hydrogen Bond Networks, *Crystal Growth & Design*, 6, 2,411–422.

Adams, C.J., Kurawa, M.A., Orpen, A.G., 2010, Coordination chemistry in the solid state: Synthesis and interconversion of pyrazolium salts, pyrazole complexes, and pyrazolate MOFs, *Dalton Transactions*, 39, 6974–6984.

Adams, C.J., Kurawa, M.A., Orpen, A.G., 2010, Coordination Chemistry in the Solid State: Reactivity of Manganese and Cadmium Chlorides with Imidazole and Pyrazole and Their Hydrochlorides, *Inorganic Chemistry*, 49, 22, 10475–10485.

Allendorf, M.D., Bauer, C.A, Bhakta, R.K., Houk, R.J.T., 2009, Luminescent metal–organic frameworks, *Chemical Society Reviews*, 38, 1330–1352.

Amo-Ochoa, P., Castillo, O., Alexandre. S.S., Welte, L., de Pablo, P.J., Rodríguez-Tapiador, M.I., Gómez-Herrero, J., Zamora F., 2009, Synthesis of Designed Conductive One-Dimensional Coordination Polymers of Ni(II) with 6-Mercaptopurine and 6-Thioguanine, *Inorganic Chemistry*, 48, 7931–7936.

Angeloni, A., Paul, C., Crawford, A., Orpen, G., Podesta, T.J., Shore, B.J., 2004, Does Hydrogen Bonding Matter in Crystal Engineering? Crystal Structures of Salts of Isomeric Ions, *Chemistry – A European Journal*, 10, 3783-3791.

Angeloni, A., Orpen, A.G., 2001, Control of hydrogen bond network dimensionality in tetrachloroplatinate salts, *Chemical Communications*, 4, 343–344.

Antonio, L., Jon, S., Oscar, C., & Pascual, R., 2001, Crystal packing and physical properties of pyridium tetrabromocuprate(II) complexes assembled via hydrogen bonds and aromatic stacking interactions, *New Journal of Chemistry*, 25, 1208-1214.

Arnby, C.H., Jagner, S., Dance, I., 2004, Questions for crystal engineering of halocuprate complexes: concepts for a difficult system, *Crystal Engineering Communications*, 6, 46, 257-275.

Arunan, E., Desiraju, G.R., Klein, R.A., Sadlej, J., Scheiner, S., Alkorta, S., Clary, D.C., Crabtree, R.H., Dannenberg, J.J., Hobza, P., Kjaergaard, H.G., Legon, A.C., Mennucci, B. and Nesbitt, D.J., 2010, Definition of the Hydrogen Bond, *Pure and Applied Chemistry* 26, 2, 1-7.

Atkins, P., Overton, T., Rourke, J., Weller, M., Armstrong, F., 2006, *Shriver & Atkins: Inorganic Chemistry*, 4th ed., Oxford University Press, 87-88.

Atkins, P., de Paula, J., 2006, *Atkins' Physical Chemistry*, 8th ed., Oxford Universiy Press, 42.

Batten, S.R., Neville, S.M., Turner, D.R, 2009, *Coordination Polymers: Design, Analysis and Application*, RSC Publishing, Cambridge, UK, 6-10, 295-297, 144-155, 172-173, 330-338, 9-10.

Bell, N.A., Gelbrich, T., Hursthouse, M.B., Light, M.E., Wilson, A., 2000, Reactions of trichlorovinylmercurials with potential non-chelating bidentate ligands. Crystal structures of [$(C_2Cl_3)_2Hg$ (4,4'-bipyridyl)], [C_2Cl_3Hg(2-pyridyl thiolate)] and polymeric $HgBr_2$(2,2'-dipyridyl disulfide), *Polyhedron 19*, 2539–2546.

Bertani, R., Sgarbossa, P., Venzo, A., Lelj, F., Amati, M., Resnati, G., Pilati, T., Metrangolo, P., Terraneo, G., 2010, Halogen bonding in metal–organic–supramolecular networks, *Coordination Chemistry Reviews*, 254, 677–695.

Braga, D., Grepioni, F., 2005, Making crystals from crystals: a green route to crystal engineering and polymorphism, *Chemical Communications*, 29, 3635–3645.

Braga, D., Grepioni, F., Desiraju, G.R., 1998, Crystal Engineering and Organometallic Architecture, *Chemical Reviews*, 98, 1375-1405.

Braga, D., Crystal Engineering, Where from? Where to?, 2003, *Chemical Communications*, 2751.

Braga. D., Giaffreda, S.L., Grepioni, F., Pettersen, A., Maini, L., Curzi, M., Polito, M., 2006, Mechanochemical preparation of molecular and supramolecular organometallic materials and coordination networks , *Dalton Transactions,* 10, 1249–1263.

Brammer, L., Swearingen, J.K., Bruton, E.A., Sherwood, P., 2002, Hydrogen bonding and the perhalometallate ions: A supramolecular synthetic strategy for new inorganic materials, Procedings of the National Academy of Sciences of the United States of Americ*a*, 99, 4956-4961.

Brammer, L., Vitorica-Yrezabal. I.J., Sullivan, R.A., Purver, S.L, Curfs, C., Tang, C.C., 2010, Synthesis and polymorphism of (4-ClpyH)$_2$[$CuCl_4$]: solid–gas and solid–solid reactions, *Crystal Engineering Communications,* 13, 3189-3196.

Brammer, L., Espallargas, G.M., van de Streek, J., Fernandes, P., Florence, A.J., Brunelli, M., Shankland, K., 2010, Mechanistic Insights into a Gas–Solid Reaction in Molecular Crystals: The Role of Hydrogen Bonding, *Angewandte Chemie International Edition*, 49, 8892 –8896.

Brammer, L., Espallargas, G.M., Florence, A.J., van de Streek, J., 2011, Different structural destinations: comparing reactions of [$CuBr_2$(3-Brpy)$_2$] crystals with HBr and HCl gas, *Crystal Engineering Communications,* Advance Article.

Brinck, T., Murray, J.S., Politzer, P., 1992, An overview of halogen bonding, *International Journal of Quantum Chemistry,* 44, 19, 57-64.

Bruker, 2001, SMART, SAINT and SADABS, Bruker AXS Inc., Madison, Wisconsin, USA.

Bruno, I. J., Cole, J. C., Edgington, P. R., Kessler, M., Macrae, C. F., McCabe, P., Pearson, J., Taylor, R., 2002, Mercury CSD 2.0-new features for the visualization and investigation of crystal structures, *Acta Crystallography*, B58, 389–397.

Cambridge Structural Database, Retrieved 2011, from http://www.ccdc.cam.ac.uk

Chadwick, K., Davey, R., Cross, W., 2007, How does grinding produce co-crystals? Insight from the case of benzophenone and diphenylamine, *Crystal Engineering Communications*, 9, 723-734.

Chandrasekhar, V., Senapati, T., 2010, Trapping two different $CdCl_2$ 1D-layered structures by a cyclocarbophosphazene-based ligand, *Crystal Engineering Communications*, 2010, 12, 682–684.

Cheetham, A.K., Rao, C.N.R., Feller, R.K., 2006, Structural diversity and chemical trends in hybrid inorganic–organic framework materials., *Chemical Communications*, 46, 4780-4795.

Clark, J., 2004, Chemguide, The Acid-Base Behaviour of Amino Acids, Retrieved 2011, from http://www.chemguide.co.za/organicprops/aminoacids/acidbase.html#top

Daintith, J., 2004, *A Dictionary of Chemistry*, 5th ed. Oxford University Press, 89, 255, 594.

Daintith, J., 2004, *A Dictionary of Chemistry*, 5th ed. Oxford University Press, 187, 150, 454.

Desiraju, G.R, 1997, Designer crystals: Intermolecular interactions, network structures and supramolecular synthons, *Chemical Communications*, 16, 1475-1482.

Desiraju, G.R., 1996, *Review of General Principles, in Comprehensive Supramolecular Chemistry*, eds. MacNichol, D.D., Toda, F., Bishop, R., Pergamon, Oxford, 6, 4-9.

Desiraju, G. R., 1995, Self-Assembly of Nanometer-Scale Secondary Building Units into an Undulating Two-Dimensional Network with Two Types of Hydrophobic Cavity, *Angewandte Chemie Internationsl Edition*, 34, 2311-2327.

Desiraju, G. R., 1996, *The Crystal as a Supramolecular Entity*; John Wiley & Sons, Ltd., 55.

Douglas, B.E., McDaniel, D.H., Alexander, J.J., 1994, *Concepts and Models of Inorganic Chemistry*, John Wiley and Sons, Inc., 3rd ed, 272.

Dugald, J., MacDougall, J., Morris, J., Noll, B.C., Henderson, K.W., 2005, Use of alkali metal aggregates in controlling network assembly, *American Crystallographic Association*, Etter Transactions, Vol 1.

Dutrow, B.L., (Louisiana State University), Clark, C.M.,(Eastern Michigan University), 2009, Geochemical Instrumentation and Analysis, X-ray Powder Diffraction (XRD),Retrieved April, from: http://serc.carleton.edu/research_education/geochemsheets/techniques/XRD.html

Drichko, N., Petrov, B., Semkin, V.N., Vlasova, R.M., Bogdanova, O.A., Zhilyaeva, E.I., Lyubovskaya, R.N., Olejiniczak, I., Kobayashi, H., Kobayashi, A., 2004, A comparative mid-infrared study of superconductor $BETS_4Hg_2.Br_8$ and metal $BETS_4Hg_3Cl_8$, *J. Phys. IV. France,* 114, 305-307.

Eddaoudi, M., Kim, J., Vodak, D., Wachter, J., O'Keeffe, M., Yaghi, O.M., 2002, Systematic Design of Pore Size and Functionality in Isoreticular MOF's and Their Application in Methane, *Storage, Science*, 295, 5554, 469-472.

Etter, M.C., 1990, Encoding and Decoding Hydrogen Bond Patterns of Organic Compounds, *Accounts of Chemical Research*, 23, 4, 120-126.

Englert, U., 2010, Halide-bridged polymers of divalent metals with donor ligands – structures and properties, *Coordination Chemistry Reviews,* 254, 537–554.

Fabian, L. and Kalman, A., 1999, Method for the computational comparison of crystal structures, *Acta Crystallography*, B55, 1099-1108.

Farrugia, L.J., 1997, WinGX suite for small-molecule single-crystal crystallography, *Journal of Applied Crystallography,* 30, 565.

Farrugia, L.J., 1999, WinGX suite for small-molecule single-crystal crystallography, *Journal of Applied Crystallography*, 32, 837-838.

Férey, G., 2008, Hybrid porous solids: past, present, future, *Chemical Society Reviews*, 37, 191-214.

Fleischer, H., Hardt, S., Schollmeyer, D., 2006, Structural Diversity within Analogous Compounds: Synthesis and Studies of $M(SCH_2CH_2NH_2)Cl$ (M=Zn, Cd, Hg). *Inorganic Chemistry*, 45, 8318-8325.

Garay, A.L., Pichon, A., James, S.L., 2007, Solvent-free synthesis of metal complexes, *Chemical Society Reviews*, 36, 846–855.

Goher, M.A.S., Mak, T.C.W., 1985, Crystal Structure of a Polymeric 2:1 Complex of Nicotinic Acid with Copper(I) Chloride, *Inorganic Chimica Acta*, 101, 27.

Gracin, S., Rasmuson, A.C., 2004, Polymorphism and Crystallization of p-Aminobenzoic Acid, *Crystal Growth & Design*, 4, 5, 1013–1023.

Haddad, P.R., Jackson, P.E., 1990, Ion chromatography: Principles and applications, *Journal of Chromatography*, 46, 306-308.

Hamilton, W. C., Ibers, J. A., 1968, *Hydrogen Bonding in Solids*, Benjamin, W.A., Inc., New York, 86.

Herringer, S.N., Longendyke, A.J., Turnbull, M.M., Landee, C.P., Wikaira, J.L., Jameson, G.B., Telfer, S.G., 2010, Synthesis, structure, and magnetic properties of bis(monosubstituted-pyrazine)dihalocopper(II), *Dalton Trans*actions, 39, 2785-2797.

Höhne, G., Hemminger W., Flammersheim, H.J., 1996, *Differential Scanning Calorimetry: An Introduction for Practitioners*, Springer-Verlag Berlin Heidelberg, 15-20.

Hu, C., Kalf, I., Englert, U., 2007, Pyridine complexes of mercury(II)halides: Implications of a soft metal center for crystal engineering, *Crystal Engineering Communications*, 9, 603–610.

Hu, C., Li, Q., Englert, U., 2003, Structural trends in one and two dimensional coordination polymers of cadmium(II) with halide bridges and pyridine-type ligands, *Crystal Engineering Communications*, 5, 94, 519–529.

Jacoby, M., 2008, *Heading to Market with MOFS*, C&EN, Chemical & Engineering News, Metal-Organic Frameworks, 86, 34, 13-16.

Janaik, C., 2000, A critical account on π-π stacking in metal complexes with aromatic nitrogen-containing ligand., *Dalton Trans*actions, 3885-3896.

Janaik, C., 2003, Engineering coordination polymers towards applications, *Dalton Trans*actions, 2781-2804.

Jeffrey, P., X-ray Data Collection Course, 2006, v0.6, Accessed online: March 2010 from http://xrayo.princeton.edu/~phil/Facility/Guides/XrayDataCollection.html

Klein, C., 2002, *Mineral Science*, 22nd ed., John Wiley & Sons, INC., 87-88.

Knorr, M., Pam, A., Khtyr, A., Strohmann, C., Kubicki, M.M., Rousselin, Y., Aly, S.M., Fortin, D., Harvey, P.D., 2010, Reactivity of CuI and CuBr toward Et_2S: a Reinvestigation on the Self-Assembly of Luminescent Copper(I) Coordination Polymers, *Inorganic Chem*istry, 49, 5834-5844.

Koutselas, B., Ducasse, L., Papavassiliou, G.C., 1996, Electronic properties of three- and low-dimensional semi-conducting materials with Pb halide and Sn halide units, *Journal of Physics: Condensed Matter, 8*, 1217-1227.

Knight, D.A, 2005, *Anion and solvent influences on The Self-Assembly of Copper(I) Coordination Solids*, A Dissertation presented to The Faculty of the Graduate School, University of Missouri-Columbia.

Knutson, J.L, Martin, Martin, J.D., 2005, Tuning the Band Gap in Hybrid Tin Iodide Perovskite Semiconductors Using Structural Templating, *Inorganic Chemistry*, 44, 13, 4699–4705.

Kraus, W., Nolze, G., PowderCell for Windows, Version 2.4, 8.03.2000, Federal Institute for Materials and Research and Testing, Rudower Chaussee 5, 12489, Berlin, Germany.

Kumar, D.K., Ballabh, A., Jose, D.A., Dastidar, P., Das, A., 2005, Nonpolymeric Hydrogelator Derived from N-(4-Pyridyl)isonicotinamide, *Crystal Growth & Design,* 5, 2, 10413-10418.

Le Fur, Y., Masse, R., 1996, Bis(p-aminobenzoic acid-N)dichlorocadmium(II), *Acta Crystallography, Sect.C: Cryst.Struct.Commun*., 52, 2183.

Lehn, J. –M., 1995, Supramolecular Chemistry, VCH, Weinheim, 74.

Li, X., Zhen, L., Fan, Y., Fan, X., Zeng,. Q., 2007, Crystal Engineering Based on Polymeric Hydrogen-Bonded Supramolecules by Self-Assembling of 9, 10-Bis(3,5-dihydroxyphenyl) anthracene and 2,2′ ,4,4′ -Tetrahydroxybenzophenone with Bipyridines, *International Journal of Molecular Sci*ence, 8, 241-258.

Liu, B., Yuan, Q., 2005, Two novel linear arrangement hexamers with isonicotinic acid: Structures, blue luminescent and semi-conducting properties, *Inorganic Chemistry Communications 8*, 1022–1024.

Loots, L.A., 2009, *Investigation of the Co-crystallization of N-heterocycles*, Thesis, Stellenbosch University.

Kumar, D.K., Ballabh, A., Jose, D.A., Dastidar, P., Das, A., 2005, How Robust Is the N-H···Cl2-Cu Synthon? Crystal Structures of Some Perchlorocuprates, *Crystal Growth & Design*, 5, 2, 651–660.

Macrae, C.F., Bruno, I. J. Chisholm, J. A. Edgington, P. R. McCabe, P. Pidcock, E. Rodriguez-Monge, L. Taylor, R. van de Streek J. Wood, P. A., 2008, Mercury CSD 2.0 - new features for the visualization and investigation of crystal structures *Journal of Applied Crystallography*, 41, 466-470.

Maddox, 1988, Crystals from first principles, *J. Nature*, 335, 201.

Maitland, G. C., Rigby, E. B., Smith, E. B., Wakeham, W. A., 1981, *Intermolecular Forces: Their Origin and Determination*, Oxford University Press, Oxford, 62.

McNaught, A.D., & Wilkinson, A., 1997, IUPAC. Compendium of Chemical Terminology, 2nd ed. (the "Gold Book"), Blackwell Scientific Publications, Oxford, Accessed Online: 2011 from http://goldbook.iupac.org

Mateo-Marti, E., Welte, L., Amo-Ochoa, P., Miguel, P.J.S., Gomez-Herrero, J., Martin-Gago, J.A., Zamora, F., 2008, Direct evidence of nanowires formation from a Cu(I) coordination polymer, *Chemical Commun*ications, 945, 893–1024.

Mercier, Louvain, Bi, 2009, Structural diversity and retro-crystal engineering analysis of iodometalate hybrids**,** *Crystal Engineering Communications*, 11, 720-734.

Mercier, N., Riou, A., 2004, An organic-inorganic hybrid perovskite containing copper paddle-wheel cluster linking perovskite layers: $[Cu(O_2C\text{-}(CH_2)_3\text{-}NH_3)_2]PbBr_4$, *Chemical Commun*ications, 844-845.

Minguez, G., Brammer, L., 2005, Halogen Bonds in Inorganic Crystal Design, *Acta Crystallography*, 61, 362.

Mitzi, D.B., 1999, A Layered Solution Crystal Growth Technique and the Crystal Structure of $(C_6H_5C_2H_4NH_3)_2PbCl_4$, *Journal of Solid State Chemistry*, 145, 694-704.

Mitzi, D.B., 2001, Templating and structural engineering in organic-inorganic perovskites, *Dalton Transactions*, 1-12.

Mitzi, D.B., 2000, Organic-Inorganic Perovskites Containing Trivalent Metal Halide Layers: The Templating Influence of the Organic Cation Layer, *Inorganic Chemistry*, 39, 6107-6113.

Mitzi, D.B., Dimitrakopoulos, C.D., Kosbar, L.L., 2001, Structurally Tailoring Organic-Inorganic Perovskites: Optical Properties and Solution-Processed channel Materials for Thin-Film Transistors, *Chemistry of Materials*, 13, 3728-3740.

Mitzi, D.B., Chondroudis, K., Kagen, C.E., 1999, Design, Structural, and Optical Properties of Organic-Inorganic Perovskites Containing an Oligothiophene Chromophore, *Inorganic Chemistry*, 38, 6246-6256.

Mitzi, D.B., Medeiros, D.R., DeHaven, P.W., 2002, Low-Temperature Melt Processing of Organic–Inorganic Hybrid Films, *Chemistry of Materials*, 14, 2839-2841.

Mitzi, D. B., Chondroudis, K., Kagan, C. R., 2001, Organic–inorganic electronics, IBM *J. RES. & DEV.* 45, 29 – 45.

Mitzi, D.B., 2001, Templating and structural engineering in organic-inorganic perovskites, *J. Chem. Soc., Dalton Transactions*, 1-12.

Mitzi, D.B., 2004, Solution-processed inorganic semiconductors, *Journal of Materials Chem*istry, 14, 2, 355–2365.

Molecular Expressions™, *"Diode Lasers", Optical Microscopy Primer: Physics of Light and Colour*, Accessed Online (2011), From: http://micro.magnet.fsu.edu/primer/java/lasers/diodelasers/index.html

Morsali, A., Masoomi, M.Y., 2009, Structures and properties of mercury(II) coordination polymers, *Coordination Chemistry Reviews* 253, 1882–1905.

Moulton, B., Zaworotko, M.J., 2001, From Molecules to Crystal Engineering: Supramolecular Isomerism and Polymorphism in Network Solids, *Chemical Reviews*, 101, 1629-1658.

Nandhini, M.S., Krishnakumar, R.V., Sivakumar, K., Natarajan, S., catena-Poly[[cadmium(II)]-μ-β-alanine-di-μ-chloro], *Acta crystallographica C*, 58, 6, 307.

Orpen, A.G., Angeloni, A., 2001, Control of hydrogen bond network dimensionality in tetrachloroplatinate salts, *Chemical Communications*, 343–344.

Orpen, A.G., Adams, C.J., Gillon, A.L., Lusi, M., 2010, Towards polymorphism control in coordination networks and metallo-organic salts, *Crystal Engineering Communications*, 12, 4403–4409.

Orpen, A.G., Adams, C.J., Haddow, M.F., Lusi, M., 2010, Crystal synthesis of 1,4-phenylenediamine salts and coordination networks, *Crystal Engineering Communications*, Advance Article.

Papavassilou, G.C., Mousdis, G.A., Raptopoulou, C.P., Terzis, A., 2000, Some New Luminescent Compounds Based on 4-Methylbenzylamine, *Zeitschrif für Naturforsch*, 55 b, 536-540.

Politzer, P., Lane, P., Concha, M.C., Ma, Y., Murray, J.S., 2007, An overview of halogen bonding, *Journal of Molecular Modelling*, 13, 305-311.

Qin, Z., Jennings, M.C., Puddephatt, R.J. Muir, K.W., 2002, Self-Assembly of Polymer and Sheet Structures in Palladium(II) complexes Containing Carboxylic Acid Substituents, Inorgorganic Chemistry, 41, 5174.

Rademeyer, M., Tsouris, C., Billing, D.G., Lemmerer, A., Charmant, J., 2011, Robust motifs in 2-phenylethylammonium and related tetrahalometallates, *Crystal Engineering Communications*, 13, 3485.

Rademeyer, M., Overbeek, G.E., Liles, D.,2010, Bis(4-aminobenzoic acid-κN)dichloridozinc(II). *Acta Crystallography*, B66, 634.

Ramanathan, E., 2005, *Dictionary of Chemistry*, 1st ed., Sura Books (PVT, LTD., 211.

Rather, E., 2004, *Supramolecular Metal-Organic and Organic Materials*, Dissertation, College of Arts and Sciences, University of South Florida.

Rawlinson, C., 2006, *Differential Scanning Caloriometry: "Cooking with Chemicals*". School of Pharmacy, University of Bradfort, EYP.

Roswell, J.L.C., Yaghi, O.M., 2004, Metal-Organic frameworks: a new class of porous materials., *Microporous and Mesoporous Materials*, 73, 3-14.

Reynolds, K., Willett, R.D., Twamley, B., 2003, (b-Alanine)dibromolead(II), *Acta Crystallography*, 59, 402-404.

Sanchez, C., Julian, B., Bellville, P., Popell, M., 2005, Applications of hybrid organic–inorganic nanocomposites , The Royal Society of Chemistry 2005, *Journal of Materials Chemistry*, 15, 3559–3592.

Schreuer, J., Haussuhl, S., 1993, Crystal structure of catena-(trimethylammoniumacetato) tetrachloro-aqua-dimanganese, $((CH_3)_3NCH_2COO)\ Cl_4(H_2O)Mn_2$, *Zeitschrif für Naturforsch*, 205, 313.

Sheldrick, G.M., University of Goettingen, Germany, Release, 97-2.

Sheldrick, G. M., (2008). *Acta Crystallography*, B64, 112–122.

Solomon, T.W.G., Fryhle, G.B., *Organic Chemistry*, 8th ed., (Editors), John wiley & Sons, 681.

Steiner, T., 2002, The whole palette of hydrogen bonds, The Hydrogen Bond in the Solid State, *Angewandte Chemie International Edition*, 41, 48-76.

Sanchez, C., Julian, B., Bellville, P., Popell, M., 2005, Applications of hybrid organic–inorganic nanocomposites, *Journal of Materials Chemistry*, 15, 3559–3592.

Scott, B.M.T., 2008, From small molecules to nano-scale architectures – A supramolecular approach, An Abstract of a dissertation, Kansas State University, Manhattan, Kansas.

Serway, R.A., *Physics for Scientists & Engineers with Modern Physics*, 3rd ed., Saunders Golden Sunburst Series, Saunders College Publishing, 748-749.

Spek, A. L., 2009, Structure validation in chemical crystallography, *Acta Crystallography*, B65, 2, 148–155.

Threfall, T.L., 1995, Analysis of organic polymorphs. A review., *Analyst*, 120, 2435-2460.

Trask, A.V., Shan, N., Motherwell, W.D.S., Jones, W., Feng, S., Tan, R.B.H., Carpenter, K.J, 2005, Selective polymorph transformation via solvent drop grinding, *Chemical Communications*, 880-882.

Urbina, J.F., 2005, Design, Synthesis, and Crystal Engineering of Versitile Supramolecular Reagents, Dissertation, Department of Chemistry, College of Arts and Sciences, KANSAS STATE UNIVERSITY, Manhattan, Kansas.

Wang, R., Hong, M., Luo, J., Cao, R., Shi, Q., Weng, J., 2002, Syntheses and Crystal Structures of Five Cadmium(II) Complexes Derived from 4-Aminobenzoic Acid, *European Journal of Inorganic Chemistry*, 2904-2912.

Wells, A.F., *Structural Inorganic Chemistry*, Oxford, Clarendon Press, 4th ed., 195.

Welte, L., Calzolari, A., Di Felice, R., Zamora, F., Gómez-Herrero, J., 2010, Highly conductive self-assembled nanoribbons of coordination polymers, *Nature Nanotechnology*, 5, 110-115.

Wyckoff, R.W.G., 1960, *Crystal Structures*, Interscience, New York, Vol1, 272.

Wojdyr, M., 2010, Fityk: a general-purpose peak fitting program, *Journal of Applied Crystallography*, 43, 1126-1128.

Wang, Y., 2010, 4-Carboxypyridinium bromide, *Acta Crystallography*, B66, 1553.

Wang, W., Qiao, J., Wang, L., Duan, L., Zhang, D., Yang, W., Qiu, Y., 2007, Synthesis, Structures, and Optical Properties of Cadmium Iodide/Phenethylamine Hybrid Materials with Controlled Structures and Emissions, American Chemical Society, *Inorganic Chemistry*, 46, 24, 10252.

Xu, Z., Mitzi, D.B., 2003, $[CH_3(CH_2)_{11}NH_3]SnI_3$: A Hybrid Semiconductor with MoO_3-type tin(II) Iodide Layers, *Inorganic Chemistry*, 42, 21, 6589–6591.

Xu, Z., Mitzi, D.B., Dimitrakopoulos, C.D., Maxcy K.R., 2003, Semi-conducting Perovskites $(2\text{-}XC_6H_4C_2H_4NH_3)_2SnI_4$ (X=F, Cl, Br): Steric Interactions between the Organic and Inorganic Layers, *Inorganic Chemistry*, 42, 2031-2039.

Zhang, P., Niu, Y.Y., Zhang, Z.P., Zhang, H.Y., Li, Z.J., Niu, C.Y., Wu, B.L., Hou, H.W., 2008, Synthesis, crystal structure and characterization of a 1D chain coordination polymer of zinc (II) with aroylamide, $[Zn(H_2bpb)Cl_2]n{\cdot}CH_3OH$, (H2bpb=1,2-bis(3-pyridylcarboxamide) benzene)), *Journal of Coordination Chemistry*, 61, 2, 285–293.

Appendix :

Full tables of solution synthesis for SCD.

Table A1: Stoichiometric ratios of metal halide to organic component used in the synthesis of coordination compounds.

		PABA (1g)			4-ABA (0.2g)			INA (0.5g)		
	Mr (g/mol)	2:1	1:2	1:1	2:1	1:2	1:1	2:1	1:2	1:1
$CdCl_2$	183.32	2.68	0.67	1.34	0.55	0.14	0.27	1.50	0.38	0.75
$CdCl_2.2.5H_2O$	228.36	3.33	0.83	1.67	0.69	0.17	0.34	1.87	0.47	0.94
CdI_2	366.21	5.35	1.34	2.67	1.10	0.27	0.55	3.00	0.75	1.50
$CdBr_2.4H_2O$	344.3	5.03	1.26	2.51	1.03	0.26	0.52	2.82	0.71	1.41
$ZnBr_2$	225.19	3.29	0.82	1.64	0.68	0.17	0.34	1.85	0.46	0.92
$ZnCl_2$	136.28	1.99	0.50	0.99	0.41	0.10	0.20	1.12	0.28	0.56
ZnI_2	319.2	4.66	1.17	2.33	0.96	0.24	0.48	2.62	0.65	1.31
$HgCl_2$	271.5	3.96	0.99	1.98	0.81	0.20	0.41	2.23	0.56	1.11
$HgBr_2$	360.41	5.26	1.32	2.63	1.08	0.27	0.54	2.96	0.74	1.48
HgI_2	454.4	6.63	1.66	3.32	1.36	0.34	0.68	3.73	0.93	1.86
$CuCl_2.2H_2O$	170.48	2.49	0.62	1.24	0.51	0.13	0.26	1.40	0.35	0.70
$CuCl_2$	134.45	1.96	0.49	0.98	0.40	0.10	0.20	1.10	0.28	0.55
CuI_2	190.44	2.78	0.70	1.39	0.57	0.14	0.29	1.56	0.39	0.78
$CuBr_2$	223.36	3.26	0.82	1.63	0.67	0.17	0.34	1.83	0.46	0.92
$MnCl_2.4H_2O$	197.91	2.89	0.72	1.44	0.59	0.15	0.30	1.62	0.41	0.81
$MnBr_2$	214.76	3.14	0.78	1.57	0.64	0.16	0.32	1.76	0.44	0.88
$PbCl_2$	331.2	4.84	1.21	2.42	0.99	0.25	0.50	2.72	0.68	1.36
CoI_2	312.74	4.57	1.14	2.28	0.94	0.23	0.47	2.56	0.64	1.28
$CoBr_2$	218.75	3.19	0.80	1.60	0.66	0.16	0.33	1.79	0.45	0.90
AgI_2	361.7	5.28	1.32	2.64	1.09	0.27	0.54	2.97	0.74	1.48
$AgNO_3$	169.87	2.48	0.62	1.24	0.51	0.13	0.25	1.39	0.35	0.70

Table A2: Stoichiometric ratio of metal halide to organic chloride salt employed in the synthesis of ionic hybrid compounds.

		$(PABA)^+Cl^-$ (0.5g)			$(4\text{-}ABA)^+Cl^-$ (0.2g)			$(INA)^+Cl^-$ (0.5g)		
	Mr(g/mol)	2:1	1:2	1:1	2:1	1:2	1:1	2:1	1:2	1:1
CdCl2	183.32	1.10	0.27	0.55	0.44	0.11	0.22	1.17	0.29	0.59
CdCl2.2.5H2O	228.36	1.37	0.34	0.69	0.55	0.14	0.27	1.46	0.37	0.73
ZnCl2	136.28	0.82	0.20	0.41	0.33	0.08	0.16	0.87	0.22	0.44
HgCl2	271.5	1.63	0.41	0.81	0.65	0.16	0.33	1.74	0.43	0.87
CuCl2.2H2O	170.48	1.02	0.26	0.51	0.41	0.10	0.20	1.09	0.27	0.55
CuCl2	134.45	0.81	0.20	0.40	0.32	0.08	0.16	0.86	0.22	0.43
PbCl2	331.2	1.10	0.27	0.55	0.79	0.20	0.40	2.12	0.53	1.06
MnCl2.4H2O	197.91	-	-	-	0.47	0.12	0.24	1.27	0.32	0.63

Table A3: Stoichiometric ratio of metal halide to organic bromide salt employed in the synthesis of ionic hybrid compounds.

		$(PABA)^+Br^-$ (0.5g)			$(4\text{-}ABA)^+Br^-$ (0.2g)			$(INA)^+Br^-$ (0.5g)		
	Mr(g/mol)	2:1	1:2	1:1	2:1	1:2	1:1	2:1	1:2	1:1
$CdBr_2.4H_2O$	344.3	1.58	0.40	0.79	0.69	0.17	0.34	1.72	0.43	0.86
$ZnBr_2$	225.19	1.04	0.26	0.52	0.45	0.11	0.23	1.13	0.28	0.56
$HgBr_2$	360.41	1.66	0.41	0.83	0.72	0.18	0.36	1.80	0.45	0.90
$CuBr_2$	223.36	1.03	0.26	0.51	0.45	0.11	0.22	1.12	0.28	0.56
$MnBr_2$	214.76	0.99	0.25	0.49	0.57	0.14	0.29	1.43	0.36	0.72
$CoBr_2$	218.75	1.01	0.25	0.50	0.44	0.11	0.22	1.09	0.27	0.55